The Modulation of Apoptosis by Poxviruses

by

Ninad Mehta

A thesis submitted in partial fulfillment of the requirements for the degree of

Doctor of Philosophy

in

Virology

Department Of Medical Microbiology and Immunology

University of Alberta

ABSTRACT

Apoptosis serves as a powerful defense against damaged and unwanted cells. The family of Bcl-2 proteins plays a key role in the regulation of apoptosis at the mitochondria. Members of the Bcl-2 family include pro- and anti-apoptotic members that collectively determine the state of the cell. Apoptosis is an effective defense against viral infection, and many viruses, including poxviruses, encode proteins to prevent or delay apoptosis. In this thesis, we demonstrate that ectromelia virus, the causative agent of lethal mousepox, encodes an inhibitor of apoptosis, EVM025. EVM025 is the orthologue of VACV F1, previously shown to inhibit apoptosis. EVM025 contains a large N-terminal repeat and a C-terminal domain that is essential for localization to the mitochondria. Cells infected with ECTV lacking EVM025 undergo apoptosis, highlighting the importance of the anti-apoptotic activity of EVM025. We further demonstrate that expression of EVM025 is crucial to prevent apoptosis triggered by various stimulations. Expression of EVM025 prevents the activation of Bak and Bax and maintains mitochondrial membrane integrity upon infection with ECTV. Our virulence studies have established that ECTVΔ025 is highly attenuated in mice, with virus only being detected in the draining lymph node (D-LN) following footpad inoculation. ECTVΔ025 was unable to escape the D-LN and replicate in other organs such as spleen, kidney and liver. Our studies show that the T cell response is required to limit the spread of the virus beyond the D-LN.

The vaccinia virus Copenhagen (VACV) E3 protein is essential for virus replication in a wide range of cells. E3 dampens various innate immune responses

by inhibiting PKR, thus maintaining efficient protein translation over the course of a virus infection cycle. In addition to being an inhibitor of PKR, E3 has also been associated with the inhibition of cellular apoptosis. In this thesis we confirmed that infection with VACVΔE3L triggers the intrinsic apoptotic pathway, and leads to the cleavage of Caspase-3 and eventual cell death. However, our data suggest that E3 does not directly inhibit the intrinsic apoptotic pathway; instead, it suppresses apoptosis indirectly, by promoting the accumulation of the VACV anti-apoptotic F1 protein. F1 mRNA is present in cells infected VACVΔE3L but the protein product does not detectably accumulate, suggesting a block at the translational level. F1 expression is restored by ectopic expression of E3 or by knocking out PKR, reversing the pro-apoptotic phenotype of VACVΔE3L.

ACKNOWLEDGMENT

I would like to thank my initial supervisor, Dr. Michele Barry, for accepting me into her laboratory. I would like to thank members of the Barry Lab for all the wonderful memories. I would like to thank Dr. John Thibault for all the funny memories. You are deeply missed. I would like to thank Dr. Bettina Lehman; we have been through a lot together. Furthermore, I would like to thank Dr. Stephanie Stefura for training me in the Barry Laboratory. In addition, I would like to thank Dr. Emeka Enwere and Dr. Ryan Noyce for all the support. I would also like to thank all the member that went through the Barry Lab.

I am very grateful to my current supervisor, Dr. Jim Smiley. I cannot thank Dr. Smiley enough for welcoming me into his lab, and for all the support and guidance. I really enjoyed working in your laboratory, and the freedom I got during this time helped me develop and grow as a Scientist. I would also like to thank Holly Bandi for all her support and help. In addition, I would like to thank Dr. Brett Duguay, Dr. Bianca Dauber, Ulrike Strunk and Theodore Dos Santos for making my time in the Smiley Lab a lot of fun.

I also want to acknowledge the guidance offered from my supervisory committee members: Dr. Thomas Simmen and Dr. David Evans. Thank you, Dr. David Evans and the Evans Lab for all the helpful discussion, the reagents and help that you all provided during my thesis. I would like to specially thank Dr. Chad Irwin for all this help and just for being a wonderful person. Also, I want to show my great appreciation for the continual support provided by the Anne Giles, Debbie Doudiet, Tabitha Vasquez, and Michelle Zadunayski.

A simple “thanks” would never be enough for Dr. Judy Gnarpe. Thank you for being a great mentor and friend. I have learned a lot from being a teaching assistant for you, and I am a better person because of that.

I would like to thank my mom, Kalyani Mehta, my uncle and aunt (Chetan Mehta and Shilpa Mehta), and my family. I could not have done this without your support, at both the best and worst of times. I am so lucky to be a part of our family.

Lastly, I lovingly thank my wife, Megha. I am incredibly blessed to have met her many years ago and even more fortunate that she agreed to follow me across the world to Alberta. We have shared so many ups and downs and through them all she has always been there for me. Words will never fully express my gratitude to her.

Table of Contents

List of Figures

Chapter-1- Introduction

Chapter-3- Ectromelia virus encodes an anti-apoptotic protein

Chapter-4- Ectromelia virus encodes an anti-apoptotic protein

Chapter-5- Expression of the vaccinia virus anti-apoptotic F1 protein is blocked by PKR in the absence of the viral E3 protein

List of Tables

LIST OF ABBREVIATIONS AND SYMBOLS

AIF – apoptosis-inducing factor
ATP – adenosine triphosphate
Bad – Bcl-2 antagonist of cell death
Bak – Bcl-2 antagonist/killer
Bax – Bcl-2-associated x protein
Bcl-2 – B-cell lymphoma/leukaemia 2
Bcl-xL – Bcl-2-like protein x large isoform
Bcl-xS – Bcl-2-like protein x small isoform
Bcl-w – Bcl-2-like protein w
Bcl-2A1 – Bcl-2-like protein A1
BGMK – Buffalo green monkey kidney
BH – Bcl-2 homology
Bid – BH3-interaction domain death agonist
Bik – Bcl-2-interacting killer
Bim – Bcl-2-interacting mediator of cell death
BimEL – Bim extra-long isoform
BimL – Bim long isoform
BimS – Bim short isoform
Bmf – Bcl-2 modifying factor
BMH – 1,6-bismaleimidohexane
BMK – baby mouse kidney
bp – base pairs
CrmA – cytokine response modifier A
CTL – cytotoxic T-lymphocyte
Da – Dalton
DAPI – 4’6-diamino-2-phenylindole
DMEM – Dulbecco’s modified Eagle medium
DMF – dimethylformamide
DMSO – dimethylsulfoxide
DNA – deoxyribonucleic acid
dsDNA – double-stranded deoxyribonucleic acid
dsRNA – double-stranded ribonucleic acid
DTT – dithiothreitol
EBV – Epstein-Barr virus
ECL – enhanced chemiluminescence
EDTA – ethylenediaminetetraacetic acid
EGFP – enhanced green fluorescent protein
EMCV – encephalomyocarditis virus
ER – endoplasmic reticulum
EV – enveloped virus
FACS – fluorescence activated cell sorting
FADD – FAS-associated death domain
FAS – apoptosis-stimulating fragment

FASL – apoptosis-stimulating fragment ligand
g – gram
GAPDH – glyceraldehyde-3 phosphate dehydrogenase
GDP – guanosine diphosphate
GTP – guanosine triphosphate
hrs – hour
hpi – hrs post-infection
Hrk – harakiri
HRP – horseradish peroxidase
IAP – inhibitor of apoptosis
IFN – interferon
IP – immunoprecipitation
IPTG – isopropyl -D-1 thiogalactopyranoside
IRF – interferon regulatory factor
IV – immature virus
k – kilo-
l – litre
LB – Luria-Bertani broth
LMH – chicken leghorn male hepatocellular carcinoma
LMP – low melting point
Mcl-1 – myeloid cell leukaemia sequence 1
Mcl-1s – Mcl-1 short isoform
MAC – mitochondrial apoptosis-induced channel MOAP-1 – modulator of apoptosis 1
MCMV – murine cytomegalovirus
MEF – mouse embryo fibroblasts
min – minute
MOI – multiplicity of infection
MOM – mitochondrial outer membrane
MOMP – mitochondrial outer membrane permeabilisation
mRNA – messenger ribonucleic acid
MV – mature virus
MV – measles virus
MVA – modified vaccinia virus Ankara
n – nano-
NF-κB – nuclear factor kappa B
NK – natural killer cell
NTP – nucleoside triphosphate
OAS – 2'-5' oligoadenylate synthetase
ORF – open reading frame
PAGE – polyacrylamide gel electrophoresis
PARP – poly (ADP-ribose) polymerase
PBS – phosphate-buffered saline
PCR – polymerase chain reaction
PFU – plaque forming units
PKR – dsRNA-dependent protein kinase
PTPC – permeability transition pore complex

Puma – p53-upregulated modulator of apoptosis
PVDF – polyvinylidine fluouride
RNA – ribonucleic acid
RNAi- ribonucleic acid interference
RT-PCR – real-time polymerase chain reaction
SDS – sodium dodecyl sulfate
SMAC – second mitochondrial-derived activator of caspases
SSC – saline sodium citrate
STS – staurosporine
TAE – tris acetate EDTA
TBST – tris-buffered saline plus Tween 20
TK – thymidine kinase
TLR – toll-like receptor
TM – transmembrane
TMRE – tetraethylrhodamine ethyl ester
TNF – tumour necrosis factor
TNFR – tumour necrosis factor receptor
TRADD – TNFR-associated death domain
vBcl-2 – virus Bcl-2-like protein
VDAC – voltage dependent anion channel
WB – Western blot
WT – wild-type
WV – wrapped virus
x g – times gravity
X-gal – 5-bromo-4-chloro-3-indolyl-D-galactopyranoside
XIAP – x-linked inhibitor of apoptosis
zVAD.fmk – carbobenzoxy-valyl-alanyl-aspartyl-[O-methyl]- fluoromethylketone

Chapter -1- Introduction

1.1. Poxviruses

Smallpox is a contagious, disfiguring, and often deadly disease that has affected humans for thousands of years. It has been responsible for multiple pandemics throughout the history of humanity. It is responsible for killing more humans in recorded history than all other infectious diseases combined. A successful vaccination campaign lead by the World Health Organization (WHO) was responsible for the eradication of the disease with the last reported case of small pox in the US occurring in 1949[1]. The last naturally acquired case in the world was reported in 1977 in Somalia[2-5]. In 1980, the WHO certified that the world was free of smallpox; thus making smallpox an extinct human disease[6]. Variola virus is the causative agent of smallpox, and therefore the most infamous member of the Poxviridae family. Poxviridae comprises viruses identified by a single, linear double-stranded DNA (dsDNA) genome, and for their ability to replicate exclusively in the cytoplasm of infected cells. The earliest classification of poxviruses was based on the disease symptoms and gross pathology. In addition to Variola virus (Orthopoxvirus), molluscum contagiosum virus (Molluscipoxvirus) is capable of directly infecting humans. The members of Orthopoxvirus, Molluscipoxvirus, Parapoxvirus, and Yatapoxvirus genera can infect humans, though most natural infections have occurred through zoonosis[7]. As mentioned earlier, the poxvirus family is most well known for being the causative agent of smallpox, though many members of the family are currently being used in the studies of vaccine development, gene therapy and oncolytics.

1.1.1. Poxvirus Classification

Based on their hosts, the Poxviridae are classified into two subfamilies: the Entomopoxvirinae, virus that infect invertebrates, and the Chorodopoxvirinae, virus that infect vertebrates[8,9]. The Chorodopoxvirinae sub-family is further divided into ten genera based on their genetic makeup and host range similarity: orthopoxviruses, yatapoxviruses, leporipoxviruses, capripoxviruses, cervidpoxviruses, suipoxviruses, parapoxviruses, molluscipoxviruses, crocodylipoxviruses and avipoxviruses. An outstanding feature of the viruses belonging to the chordopoxviruses, is their range of host species[8,10,11]. In fact, the host range varies drastically even between closely related species within a single genus. Among the orthopoxviruses, variola virus was stringently human specific, whereas monkeypox and cowpox viruses naturally infect a wide variety of mammalian species.

1.1.2. Orthopoxviruses

The Orthopoxvirus genus is comprised of some of the best-studied poxviruses and the genomes of many of its members have been completely sequenced[7,12]. In addition to the variola virus (VARV), there are other well-known and well-studied poxviruses. One well-studied poxvirus is the Vaccinia virus (VACV), which was used in the vaccine against smallpox. Another well-known member of poxviruses is monkeypox (MPXV), which has been responsible for multiple zoonotic outbreaks of poxvirus in the United States and Africa. In addition to these viruses, other orthopoxviruses include ectromelia virus (ECTV), camelpox virus (CMLV), taterapox virus (TATV), rabbitpox virus (RPXV), horsepox virus (HSPV) and different cowpox virus (CPXV) species[7].

Orthopoxviruses are closely related to each other antigenically and these antigenic similarities result in cross-reactivity and cross-protection against recurrent orthopoxvirus infection. These features have also allowed for the development of a successful vaccine against VARV[13].

1.1.3. Poxvirus Morphology and Genome

Poxviruses have virion size of approximately 360 x 270 x 260 nanometers (nm). Poxviruses are typically described as being barrel- or brick- shaped and have a characteristically uneven surface (Fig. 1.1 A)[14]. The overall morphology of poxviruses is consistent throughout the Chorodopoxvirinae family. Poxvirus virions are found in various morphologically distinct states during the infection process, all of which contain a proteinaceous core that houses their genomic material. Poxvirus virions come in two infectious forms: the mature virion (MV, also known as intracellular mature virus, IMV) and the enveloped virion (EV; also known as extracellular enveloped virus, EEV)[15,16]. The MV is the basic infectious unit that is enveloped by a single lipid membrane, while the EV is an MV encased by an additional membrane[15-18]. Poxviruses also have a complex, asymmetrical, internal, dumbbell-shaped, nucleoprotein core which is flanked by heterogeneous protein aggregates in concavities called 'lateral bodies'. This core houses the dsDNA genome along with all of the enzymes required for early mRNA transcription (Fig. 1.1 B)[14].

The poxvirus genome is a single, linear, covalently closed molecule of dsDNA. The dsDNA genome is held within the core of the virion by a nucleoprotein structure[12]. Poxvirus genomes range in size from 134 kbp in Parapoxviruses to over 350 kbp in

Avipoxviruses, and contain on an average around 200 open reading frames, about ninety of which are conserved among all chordopoxviruses[19]. Chordopoxvirus genomes have an extremely consistent genome organization. The central region of their genome consists of highly conserved genes. This region includes genes required for essential functions like replication, mRNA synthesis, protein processing, virion assembly, and structural components. In contrast, genes involved in immune evasion or host-specific interactions are found immediately flanking the central conserved region. The two end regions are more variable among genera and species, differing in both gene content and nucleic acid content (Fig. 1.1 C)[20,21]. These genes are largely involved in pathogenicity, host range, and immune system modulation. The poxvirus genomes contain inverted terminal repeats (ITRs), which form hairpin loops to connect the two strands of DNA. The naming convention for VACV genes was created using HindIII restriction endonuclease fragment letters, followed by the open reading frame number (ORF) within the fragment, then L or R depending on the transcriptional direction of the gene[21,22].

1.1.4. Poxvirus Life Cycle

1.1.4.1. Virus Entry

As mentioned earlier, two types of infectious vaccinia virus particles exist: the MVs and the EVs. The MV extracellular virions have an additional membrane envelope derived from the cellular trans-golgi membrane or the cellular endosomal cisternae. This membrane is made by the insertion of multiple viral proteins[23,24]. Previous work has

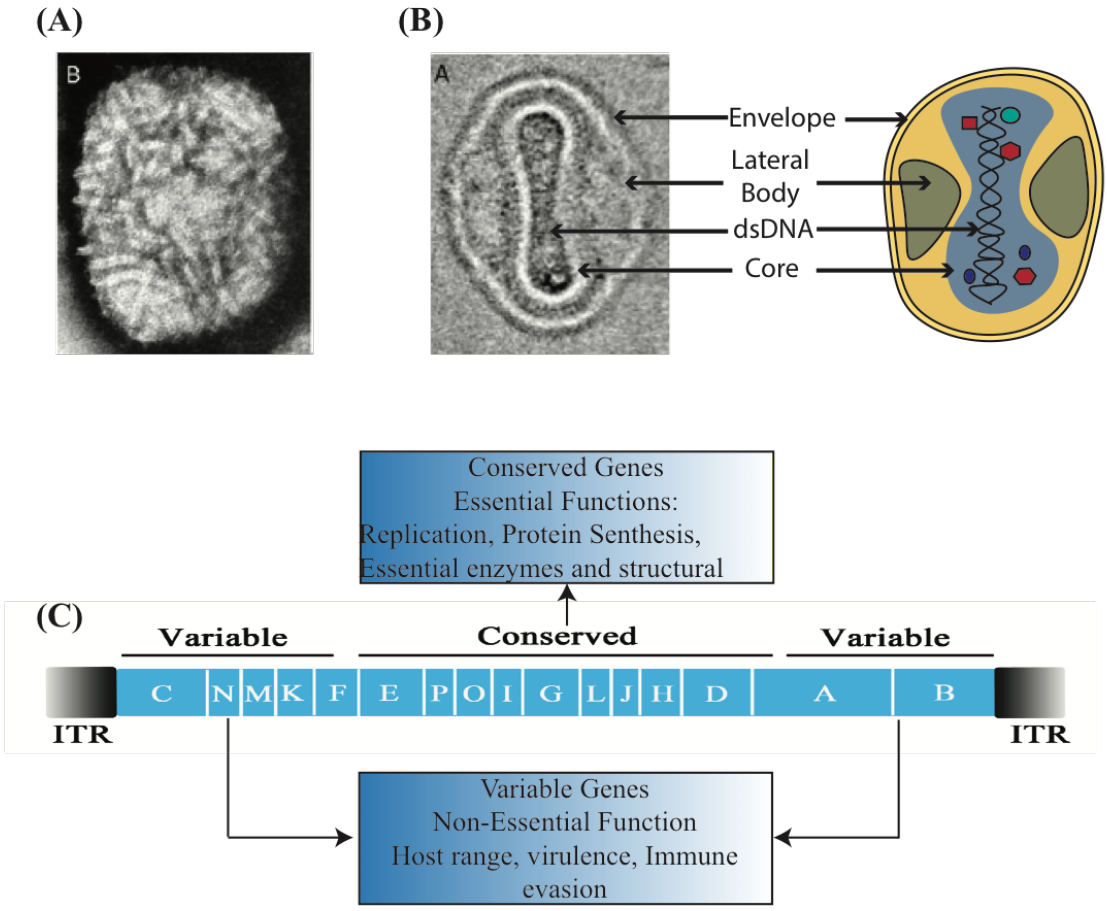

Figure 1.1. Poxvirus structure and genome. (A) An electron micrograph of a single VACV. (B) A VACV viron electron micrograph cross-section compared to the schematic diagram of the virus. (C) Schematic diagram of the VACV genome.

Source: Condit, R. C., Moussatche, N., & Traktman, P. (2006). In A Nutshell: Structure and Assembly of the Vaccinia Virion (Vol. 66, pp. 31–124)

shown that MV can use a variety of cellular molecules including chondroitin sulfate, heparin sulfate, glycosaminoglycans, and laminins as entry receptors[10,15,24]. Studies have shown that receptor used by the MV depends on the cell type, virus strain and experimental condition. During a VACV infection of cells, MVs are observed inside vesicles and seen fusing with the cellular plasma membrane. These events are followed by release of the core into the cytoplasm[15,17]. For EV entry, the outermost membrane must first be disrupted to expose the entry-fusion complex. The exact events that lead to the disruption of the membrane are yet to be understood. There is evidence suggesting a pH-dependent manner or that direct fusion can occur at the plasma membrane following macropinocytosis of the virion (Fig 1.2)[17,25].

1.1.4.2. Virus Uncoating, Gene Expression and DNA Replication

Following the removal of the MV membrane or both the membranes of the EV, the core of the virus makes it way deeper into the cytoplasm using the host's microtubule machinery. As mentioned earlier, the viral core consists of viral structural proteins, a compacted DNA, and transcriptional enzymes required for immediate gene transcription[21]. These viral cores accumulate near the perinuclear region of the cell, and the viral genomes are partially uncoated to enable the viral DNA-dependent RNA polymerase to transcribe immediate early genes into mRNAs. Poxviral gene expression is temporally regulated; early genes of the virus encode immune evasion proteins, a DNA-dependent DNA polymerase, and proteins involved in viral DNA replication. Early transcripts can be detected within the first 20 minutes post infection[26]. Termination of the early transcription phase coincides with core disassembly, when exposure of viral

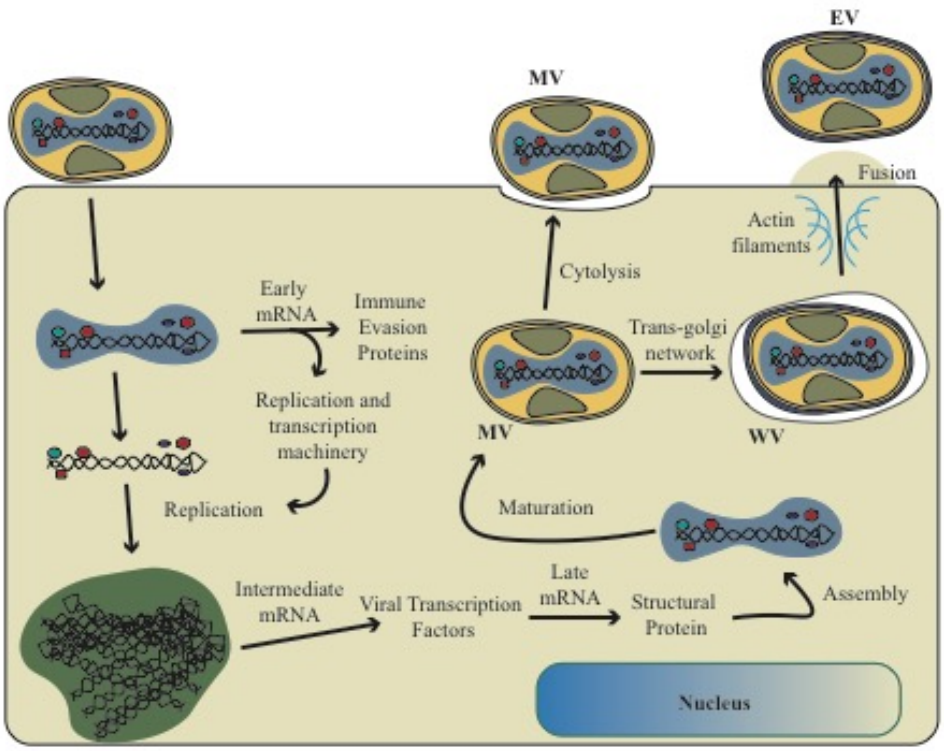

Figure 1.2. Poxvirus Life Cycle. Mature virus (MV) binds to cellular receptor leading to the fusion of the virus to the cell's plasma membrane. This fusion event leads to the release of the viral core into the cytoplasm and the early transcription begins. Early viral mRNAs encode proteins that are involved in immune evasion, viral replication and intermediate mRNA transcription. Viral replication takes place in discrete DNA-rich cytoplasmic sites known as viral factories. Intermediate genes encode transcription factor (TFs) for late gene expression. Late mRNA encodes structural protein and early TFs that get packaged in newly synthesized virions. Virus assembly begins with the formation and acquisition of crescent-shaped members that surrounds the genome-containing cores to produce MV, which are released by cytolysis. In addition to release, some MVs may also get in the trans-Golgi network to produce the wrapped (WV). The WV attaches to the plasma membrane to lose one of its three membranes to form the EV. The EV uses actin filaments to propels itself towards the neighbouring cell.

genomes to the cytoplasm initiates the DNA replication phase. Replication of viral genomic DNA and transcription of viral genes occurs in cytoplasmic regions termed "viral factories". Following the replication of viral DNA, intermediate genes are then expressed. These intermediate genes encode transcription factors that facilitate late gene expression[27]. The intermediate genes transcription is followed by the transcription of late genes. Poxvirus late proteins consists of structural proteins and proteins that aid virion assembly[28]. Following late protein synthesis, virion morphogenesis begins in the viral factory (Fig 1.2)[21,26].

1.1.4.3. Virion Morphogenesis and Egress

Poxvirus virion morphogenesis and egress consists of a series of complex steps, which are yet to be completely understood. During the late stages of infection, membrane crescents made of lipids and viral core proteins form. These viral structures are stabilized by the activity of viral scaffolding proteins. The origin of the lipid membranes remains uncertain. However, recent studies have suggested that these membranes might be derived from the cellular endoplasmic reticulum (ER)[15,29]. As the infection progresses, the membranes completely close around the viral core proteins. At this stage, the virions are called immature virions (IV)[30]. Encapsidation of the dsDNA in the IVs, followed by the proteolytic cleavage of the core proteins, leads to the maturation of the IVs to the MVs. A majority of the progeny virus are MVs and they get released upon cell lysis. A small percentage of progeny MVs are transported along microtubules away from the virus factory. Additional double membranes that originate from the trans-Golgi cisternae or endosomal membranes further wrap these MVs, resulting in a wrapped

virion (WV)[31]. These wrapped viruses are transported to the cell periphery along actin filaments where they fuse with the plasma membrane and lose their outermost membrane, leading to the release of the virus into the extracellular space. These viruses are now known as EVs[18]. Some of the exocytosed EVs may remain attached to the plasma membrane of infected cells as cell-associated EV (CEV). Viral proteins induce the formation of actin projectiles, propelling the CEV towards surrounding uninfected host cells. This phenomenon is responsible for the cell-to-cell spread of the virus within an infected host and is an efficient method of cell-to-cell spread for the virus to avoid the host immune system (Fig 1.2)[15,18,32].

For the purpose of this thesis, two Orthopoxvirus family viruses are will be considered further: 1. vaccinia virus (VACV) and 2. ectromelia virus (ECTV)

1.1.5. Vaccinia Virus

VACV was used as the vaccine strain used to immunize humans against the deadly VARV[9]. As such, VACV does not normally cause a human disease, but as previously mentioned, is antigenically similar enough to VARV to provide long-term immunity. This, combined with the high stability of the vaccine strains, aided in the immense, unparalleled success of the WHO vaccination program[1]. While the natural host for VACV is currently unknown, the virus is capable of infecting a wide variety of hosts. In humans, VACV produces a localized benign lesion and the virus is rapidly cleared by the immune system of healthy individual with the lesion eventually healing[1,9,13]. Formerly believed to have originated from either HSPV or CPXV, VACV has been cultivated primarily by human-to-human passage or growing the virus in tissue culture.

Due to the long passage history of the virus, it has been well adapted to grow in tissue culture. VACV has been extensively used to study virus-host interactions, poxviral life cycle and poxviral gene expression[9,13]. In addition, VACV is also being pursued as a vector for a number of vaccines including HIV, Hepatitis B and Hepatitis C[33]. Furthermore, VACV possesses oncolytic activity, and thus, is being studied for possible use in cancer therapeutics. As VACV is not naturally selective for cancerous cells, to make it more specific to actively replicating cancer cells[34,35].

1.1.6. Ectromelia Virus

Ectromelia virus (ECTV) is the etiological agent of the disease mousepox, a disease specific to susceptible strains of mice. Infectious ECTV was identified in 1930 when the mouse was first introduced as an experimental small animal model for poxvirus infection[36-38]. It is believed that wild populations of mice and other rodents in Europe are susceptible to natural infection. ECTV and VARV are genetically similar, and this similarity has led to the use of ECTV as a model of smallpox and exanthematous diseases in mice[38,39]. ECTV manifests as a foot lesion followed by swelling of the foot and lesions on the liver and spleen in addition to the foot, indicating that infectious ECTV is a systemic infection. Mice that survive the acute phase of the disease, recovered weight steadily and a rash is observed at the site of infection [38-41]. Thus, ECTV has been a good model to improve our understanding of a native poxvirus infection in the small animal model. Since 1930, multiple ECTV strains have been isolated from outbreaks in Europe and the USA, with differences in pathogenicity. ECTV strain Moscow (ECTV-Mos) isolated by V. Sololiev is the most virulent strain isolated yet. ECTV strain Naval

(ECTV-Nav) manifests a fatal disease in BALB/c mice and a mild disease with mild morbidity and mortality in CD-1 mice. The genomes of ECTV-Nav and ECTV-Mos have been sequenced and are approximately 208 to 210 kbps in size[38,42,43]. The sequence alignment shows that the two viruses are about 99.5% similar.

1.1.6.1. Mousepox Infection

The natural route of infection of ECTV is believed to be through the skin. The virus is transmitted through direct contact with an infected animal or through fomites[36,41]. In addition, the spread of the virus through the respiratory route has also been observed. Micro-abrasions provide the virus with direct entry to the lower layers of the dermis, where the virus initiates infection (Fig 1.3)[36,38]. The initial replication occurs in the epidermis at the site of infection. The viral progeny released from the initial site of infection results in spread to the lymph nodes. At high doses the virus reaches the draining lymph node (D-LN) within the first 12 hrs of infection, and infects the spleen, liver and bone marrow 3 or 4 days after the initial infection[41,44]. When infected spleens were studied, majority of the lymphocytes were found to be infected with the ECTV. The phagocytic Kupffer cells are the first infected cells that appear in the liver. Here, the virus spreads from the Kupffer cells to the parenchymal cells. Necrosis of the infected organs leads to the releases the virus in the blood. At a low infectious dose about 80-90 % of

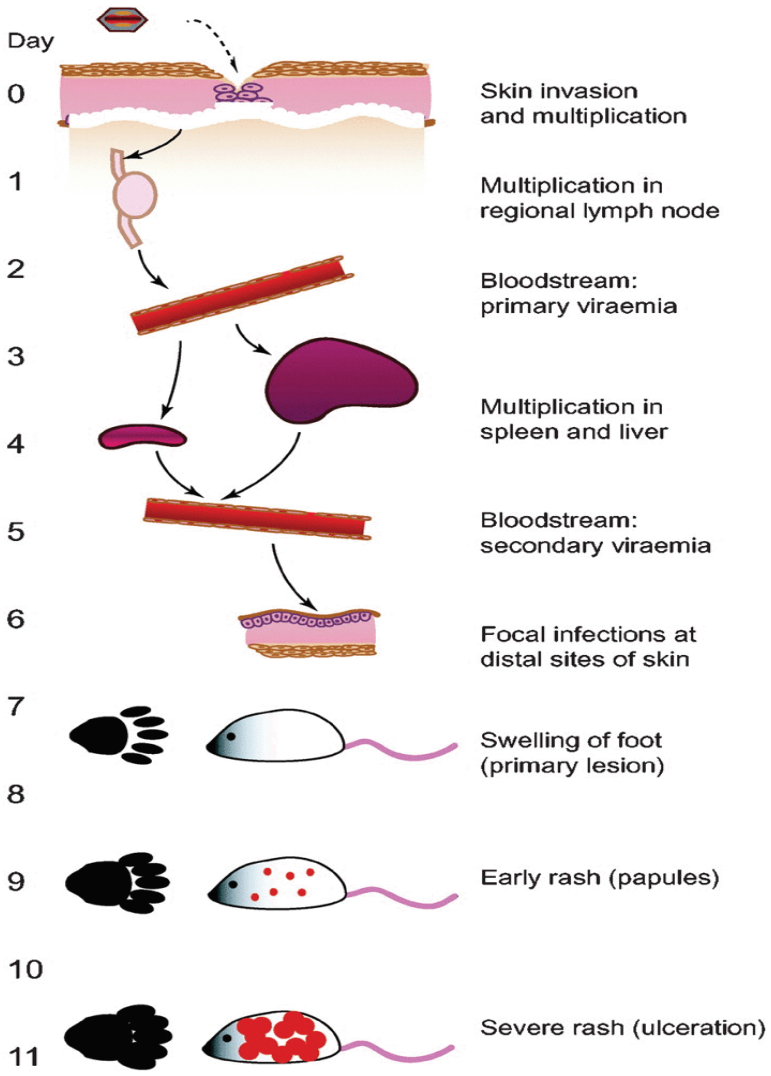

Figure 1.3- Mousepox Infection. A figure representing the sequence of events during the course of ECTV infection in a susceptible mouse.

Source - Esteban, D. J., & Buller, R. M. L. (2005). Ectromelia virus: the causative agent of mousepox. The Journal of General Virology, 86(Pt 10), 2645–2659
Copyright Conformation Number: 11590063

highly susceptible mouse strains like BALB/c, A, and DBA/2 will succumb by day 7-8 post infection[38]. Most mice will perish from the infection due to severe necrosis of the liver and spleen[41]. Mice that survive the mousepox infection or susceptible mice that are infected with avirulent strains may show the following clinical signs after about 10 days of infection: ruffled fur, hunched posture, facial edema, swelling of limbs, conjunctivitis, cutaneous pustules and ulceration (Fig. 1.3)[38,45]. Conversely, in resistant mice such as the C57BL/6, the systemic infection has few clinical signs and results in a less severe infection[46]. Disease progression, severity and outcome depend on virus strain, dose and route of infection. In addition to these, the disease also depends on the genetic background of the mice.

1.1.6.2. The Role of Genetics in Mousepox Susceptibility and Resistance

The genetic background of mice plays an important role in their susceptibility to a mousepox infection. Various studies have identified the genetic determinants that play an important role in determining the genetic susceptibility and resistance to an ECTV infection. By crossing susceptible stains with resistant strains, the gene loci responsible for the resistance to the mousepox infection were identified. These regions were termed as resistance to mousepox (rmp) loci[40,47]. Four different rmp loci have been identified. The rmp-1 is located on chromosome 6. This region maps to the NK gene complex NKR-P1, a region that is responsible for the signal transduction and activation of NK cells[48]. The rmp-2 locus is on chromosome 2 and maps near the complement component C5 gene. Delayed or impaired recruitment of the complement system has been shown to delay the recruitment of circulating leukocytes to the site of infection [38,49]. The rmp-3

locus is gonad-dependent and is linked to the MHC (H-2)[47,49]. The rmp-4 locus maps to the selectin gene complex. The members of this gene complex are involved in encoding type II membrane proteins, which are involved in leukocyte recruitment[49]. In addition to the above-mentioned rmp, studies have also elucidated the importance of the cytokine-inducible nitric oxide synthase (NOS2) gene, and the IFN-γ responses[38,49,50]. Thus the severity of ECTV depends on a balance between the swiftness of virus replication and spread in the host and the swiftness and strength of the immune response, and this balance is affected by the genetic background of the mouse.

1.1.7. Poxvirus and Immunity

As mentioned earlier, smallpox was a devastating disease. If a previously unexposed population is exposed to smallpox, the death rate was estimated to be 50% or greater amongst the very young and those over 40 years in age. However, it was observed that the individuals that recovered from smallpox were resistant to subsequent exposure of the diseases[9,13,42]. Edward Jenner made similar observations in that milkmaids who acquired cowpox were resistant to smallpox infection. Edward Jenner's observations lead to the development of the smallpox vaccine. As described earlier, the vaccine used in the eradication of smallpox consisted of a VACV strain, although Jenner initially used a CPXV strain[9]. Later studies have revealed that orthopoxviruses are closely related and can elicit a cross reacting immune response. As the eradication of VARV occurred prior to modern advances in biological sciences, there is a deficiency in our understanding of the immune responses during a smallpox infection. A majority of our understanding

about the immune responses and immune evasion strategy of the orthopoxviruses comes from the study of viruses such as VACV, ECTV, CPVX and MPVX[4,7,38,51,52].

1.1.7.1. Immune Responses against Poxvirus

Both the innate and adaptive immune responses are involved in controlling the poxvirus infection. The adaptive arm of the immune response involves the cell mediated cytotoxic T-lymphocyte (CTLs) and the humoral immunity (B-cells). Vaccinia virus induces a strong $CD4^+$ and $CD8^+$ T cell response[13,53,54]. A strong $CD8^+$ T cell response was usually detected by 7 days post infection. A strong $CD8^+$ T cell (CD8 T cells) is detected with in the first 30 days of exposure[55]. Similar to the $CD8^+$ response, vaccinia virus-specific $CD4^+$ T-cell responses also peak at about 7 days post infection. Recent studies have also shown that most effector $CD4^+$ T cells (CD4 T cells) produced high amounts of IFN-γ and IL-12, and these cytokines are crucial in controlling virus infection[56]. Previous studies have shown that the smallpox vaccine induces a strong humoral response. Not a lot is known about the B-cell response in the case of a poxvirus infection in humans, but recent work has demonstrated that vaccinia specific antibodies persist for decades post immunization[54]. In addition to the adaptive arm of the immune response, poxvirus inhibits a wide array of innate immune responses including apoptosis, the PKR pathway, the NF-κB pathway, interferon responses, inflammasomes and production of inflammatory cytokines[57-59]. For this thesis, we will revisit apoptosis and the PKR pathway in greater detail in the later sections.

1.1.7.2. Immune Responses against Ectromelia Virus

Like VACV, both the innate and adaptive immune responses are involved in limiting the lethality of ECTV. One of the major strengths of the ECTV model is the ability to study the pathogenesis and immunobiology of acute poxvirus infection in this natural host[38]. The immune response against ECTV depends on the route of infection. The natural route of infection is believed to be skin abrasion[36]. The micro abrasion allows access to the lower layers of epidermis and dermis. The abrasion would cause an injury and lead to the release of cytokines such as interleukin (IL)-1β, IL-18 and other growth factors[60]. ECTV has to overcome this response to establish itself at the site of infection. In the infected cells, toll like receptors recognise the virus infection and this leads to the production of IFN and the activation other innate anti-viral genes [61]. Knock-out studies have shown that TLR-9 and MyD88 are required for the protection against ECTV infection[62]. An interferon response is crucial in clearing an ECTV infection. It acts as a first line of defense against an ECTV infection. Studies have shown that type-1 interferons (IFNα/β) are required to protect B6 mice against ECTV infection[38,63]. In addition to the activation of the type-1-interferons, the virus is also able to activate the NFκB pathway[64]. ECTV encodes multiple inhibitors to help it overcome the multitude of cell intrinsic defense mechanisms[64,65]. Once ECTV has established itself at the primary site of infection, it spreads to the primary D-LN. Type-1 interferons are detected in the D-LN before the virus is detected in the D-LN. Similarly, the upregulation of interferon and NFκB stimulated genes is detected as early as 12 hrs post infection in B6 mice[46,66,67]. Studies using B6 mice have shown that early activation of innate responses are crucial in resistance of these mice [46].

In addition to above mentioned response, NK cells play a pivotal role in the innate response to ECTV infection in resistant strains. An appropriate NK cell response is crucial in limiting the spread of the virus in resistant strains[44,48]. In B6 mice, the NK cell population starts expanding approximately 24 hrs post infection in the primary draining lymph-node. A similar trend was observed in other tissues like spleen and liver were NK cell population levels increased within the first four days of infection[66]. BALB/c mice are unable to mount an appropriate NK cell response, allowing the virus spread beyond the D-LN[38]. In addition to this, the resistant strains that are deficient in complement C5 and NOS are also unable to prevent the early spread of the virus[50,68]. These knock-out mice studies helped demonstrate the importance of a functional complement and NOS response during an ECTV infection. During an ECTV infection NK cell secrete IFN- γ in the D-LN, suggesting a role in establishing a Th1 response[46]. In addition, granzymes A and B are required for recovery from a mousepox infection[45,69]. Thus, a strong cell mediated and innate immune response is required for the resistance to mousepox infection.

A wide array of work has shown that CD8 and CD4 T-cells are essential for resistance to primary ECTV infection. As the ECTV virus spreads from the D-LN to the spleen and liver of B6 mice, the virus generates a robust T-helper type 1 (Th1) response. The early activation of NK cells, macrophages, dendritic cells, and monocytes produce the IFN-γ, IL-2 and TNF that aids in the robust Th1 response to ECTV[63]. The appropriate Th-1 response is crucial in giving rise to a cytotoxic T cell response. The importance of a cytotoxic T-cell response to protect against ECTV infection is demonstrated in mice that are either missing or depleted in their CD8 T cells[56,70], or are knock out of granzyme A[69].

An expansion of T-cells is observed after 4-5 days of infection of resistant strains with ECTV[46]. The role of B-cells and antibodies produced by them during the primary infection is yet to be completely understood. As mentioned earlier, poxviruses encode a wide range of proteins that help the virus to avoid the immune responses.

1.1.7.3. Poxvirus and evasion of immune system

Viruses are obligate intracellular pathogens, and thus must contend with the host cellular, innate and adaptive immune responses. As mentioned earlier, poxviruses have large coding capacity and thus have an expansive diversity of proteins to interfere with host anti-viral responses. Poxviruses encode proteins that inhibit both the adaptive and innate arms of the immune response. In addition to this, they also encode proteins that interfere with cell responses such as the NFκB pathway, inflammasomes, apoptosis and the PKR pathway. In this thesis we will discuss the inhibition of apoptosis by ECTV and the inhibition of PKR pathway by VACV. Poxviruses encode numerous proteins that inhibit apoptosis and the PKR pathway, and thus ultimately the outcome of many immune responses.

1.2. Apoptosis

Apoptosis is a genetically programmed mechanism of triggered cell death found in all multi-cellular life forms. Apoptotic mechanisms play crucial roles during embryonic development, tissue and organ homeostasis and removal of dead or aberrant cells[71,72]. Apoptosis also acts as a defence mechanism against pathogens, and cancerous cells. Cells undergoing apoptosis display a number of characteristic morphological changes which include: cell shape change, mitochondrial dysfunction, condensation of

the chromatins, fragmentation of the nuclear DNA, and plasma membrane blebbing[73,74]. As apoptosis progresses the dying cell produces small membrane-bound fragments, known as apoptotic bodies, that are engulfed by phagocytic immune cells[75,76].

1.2.1. Caspases

Regardless of the trigger that initiates apoptosis, it always ends with the activation of a group of protein known as caspases. Caspases are a group of highly specific cysteine aspartate proteases that cleave target proteins after the aspartic acid residue in the tetrapeptide motif X-X-X-Asp (where X differs for each caspase)[77,78]. In healthy cells, the caspases are present in an inactive pro-enzyme from. The pro-enzyme must undergo proteolytic processing to form an active enzyme, often an active hetero-tetramer[77,78]. In mammals, the caspase family consists of 14 members. Seven of these fourteen caspases are associated with apoptosis. The activation of the apoptotic pathways can trigger the dimerization and auto-activation of the "initiator" caspases-2, -8, -9, and -10. The activated initiator caspases cleave and activate the "executioner" caspases-3, -6, and -7. The executioner caspases cleave hundreds of cellular proteins[71,77,79,80]. The events that lead to the activation of the initiator caspases can be divided into two cellular signaling pathways: the extrinsic apoptotic pathway and the intrinsic apoptotic pathway.

1.2.2. Extrinsic Apoptotic Pathway

Extrinsic apoptosis gets triggered in response to extracellular cues provided by "death ligands" to their associated transmembrane receptors (Fig. 1.4). The activation of

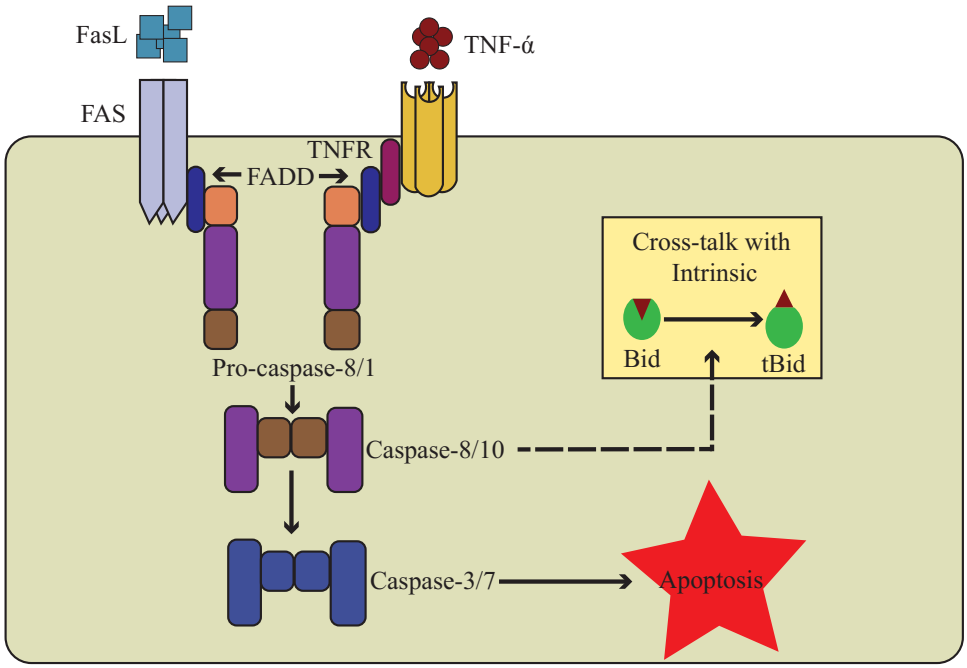

Figure 1.4 - The extrinsic apoptotic pathway. The extrinsic apoptotic pathway begins with the trimerisation of a death receptor (FAS/TNFR) by the binding of death ligands (FAS/TNF-ά). The adaptor protein TRADD and/or FADD recruit the initiator caspases pro-caspase-8 or -10, which become auto-catalytically activated and go on to cleave a variety cellular substrate proteins.

death receptors such as tumor necrosis factor receptor (TNFR) by TNF-α or apoptosis stimulating fragments (FAS) by FAS ligand (FasL)[81-83] leads to the activation of the extrinsic apoptotic pathway. The activation of TNFR and FasL leads to the trimerisation of these receptors. The trimerisation of FAS results in the recruitment of FAS ligand associated death domain (FADD). Once activated, TNFR recruits FADD through a TNFR-associated death domain (TRADD). FADD also possesses a "death effector domain" (DED) that interacts with a similar domain in the pro-caspases-8/10[81,84]. Upon activation caspases-8/10 goes on and cleaves effector caspases-3 and 7. These caspases will start cleaving the cellular target proteins (Fig. 1.4)[78,82,85,86].

1.2.2. Intrinsic Apoptotic Pathway

Mitochondria play a crucial role in the intrinsic pathway (Fig. 1.5)[87]. The mitochondrion maintains a pool of proteins, such as cytochrome *c* (Cyto *c*), Second mitochondrial-derived activator of caspase (Smac/Diablo), and apoptosis inducing factor (AIF) which when released in the cytoplasm activates caspases[88,89].The release of these molecules into the cytoplasm is due to a change in mitochondrial outer membrane permeability (MOMP) [90]. Upon a change in MOMP, Cyto *c* is released from the intermembrane space of the mitochondria to the cytoplasm, where it activates a signaling cascade that results in caspase activation. Cyto *c* binds to apoptotic protease-activating factor 1 (APAF1) and promotes a conformational change in APAF1 that results in its oligomerisation and the ATP-dependent assembly of a heptameric complex known as the apoptosome[91-93]. The apoptosome undergoes activation, and it recruits pro-caspase-9 [71,94].

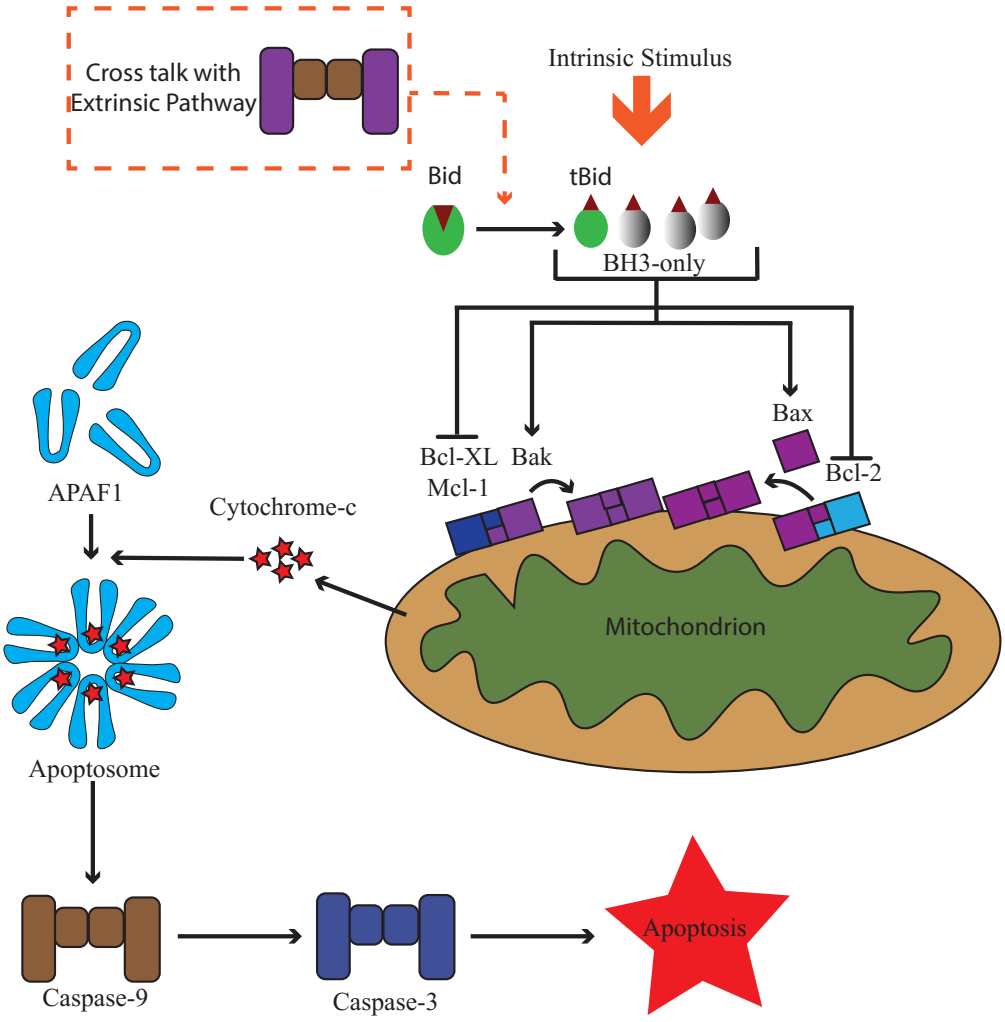

Figure 1.5 - The Intrinsic Apoptotic Pathway. The intrinsic apoptotic pathway is triggered by intracellular stress that leads to the activation of one or multiple BH3- only proteins. Once activated, BH3- only proteins inhibit the anti-apoptotic Bcl-2 family members and/or directly activate Bak and Bax. Once activated, Bak and Bax form homo-oligomers that destabilize the integrity of the outer mitochondrial membrane (OMM) and this results in the release of cytochrome c. Cytochrome c complexes with APAF1 to form the apoptosome, which activates caspase-3. The intrinsic pathway is bisected by the extrinsic pathway with the caspase-8-mediated cleavage of the BH-3 only protien Bid, which, once cleaved into its active form, tBid, can induce Bak and Bax activation (Fig. 1.3).

Activated caspase-9 activates caspases-3 and 7, there by committing the cell to apoptotic death.

The induction of Cyto *c* induced apoptosis can be inhibited by the cellular protein known as X-linked inhibitor of apoptosis(XIAP). To counteract the activity of XIAP, Smac/Diablo is also released from the dysfunctional mitochondria. Smac/Diablo binds to XIAP and prevents its function[88,95,96]. In addition, AIF and endonuclease G are also released form the intermembrane space upon MOMP. These proteins facilitate apoptosis by contributing to DNA cleavage[97].

Mitochondrial integrity is extremely crucial in preventing or triggering apoptosis. The mitochondrial integrity is tightly governed by the Bcl-2 family of proteins, all of which are united by the presence of one or more Bcl-2 homology (BH) domains. Bcl-2 members contain both activators (pro-apoptotic proteins) and inhibitors (anti-apoptotic proteins) (Fig. 1.6)[98]. A delicate balance exists between the anti-apoptotic and pro-apoptotic proteins, and tipping of the scale can trigger apoptosis. The proteins Bak and Bax are considered to be the gatekeepers of mitochondrial cell death[98-100]. In viable cells, the pro-apoptotic proteins Bax and Bak, which share homology in BH domains 1-3, exist as non-activated monomers. Bax is cytoplasmic and Bak is directly associated with the outer mitochondrial membrane (OMM)[101]. Upon apoptotic stimuli, a conformational change in Bax exposes its C-terminal hydrophobic transmembrane tail region, thus facilitating its integration into the OMM. Homotypic interactions between the pro-apoptotic proteins Bak and Bax leads to the loss of mitochondrial membrane integrity, which lead to the release of pro-apoptotic factors[101-104]. Bak and Bax are crucial proteins in this process due to the fact that Bak or Bax alone are sufficient to enable the

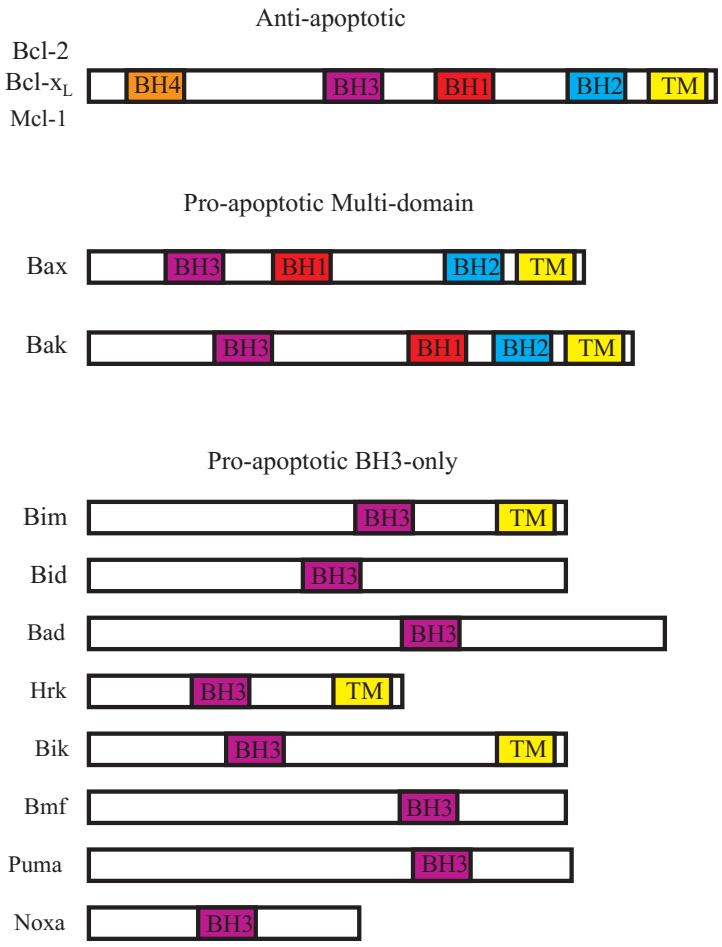

Figure 1.6 - The Bcl-2 Family. The Bcl-2 family of proteins can be separated into two classes: (1) the anti-apoptotic multi-domain proteins, which typically possess all four BH domains (BH1-4); (2) the pro-apoptotic multi-domain proteins (Bak and Bax), which contain BH1, 2, and 3 domains; and the BH3-only proteins, which possess only the BH3 domain, and certain members possess a transmembrane tail (TM) for mitochondrial localization.

release of cyto *c*; and both proteins must be disabled to alleviate apoptotic events[105]. The activation of Bak and Bax requires an additional set of Bcl-2 proteins, the BH3-only proteins (Bim, Bid, Bad, Bmf, Noxa, Puma, Hrk and BNIP3)[98]. BH3-only proteins can induce apoptosis via two distinct methods. Bim and Bid are capable of directly activating Bak and Bax; Bad and Noxa act by indirectly activating Bak and Bax by antagonizing the anti-apoptotic proteins such as Bcl-2, Bcl-xL and Mcl-1 [106,107] Anti-apoptotic Bcl-2 members such as Bcl-2, Bcl-xL, Bcl-w, Bfl-1 and Mcl-1 are required keep Bak and Bax inactive in healthly cell (Fig. 1.5). These anti-apoptotic proteins are distinguished by the presence of homology in all four BH domains. These proteins are generally in the OMM, however, they have also been shown to reside within the cytosol and at the ER membrane[86,98,108].

Cross-talk exists between the extrinsic and intrinsic pathways. A triggered apoptotic pathway activates the effector caspases-8, which in turn can cleave a BH3-only protein Bid. The cleaved form of Bid is known as tBid[42,104,109,110]. At the mitochondria, tBid interacts with other Bcl-2 proteins to facilitate the release of cytochrome c, which then results in the activation of caspases. Cross-talk exists between the extrinsic and intrinsic pathway in type-2 cells. In type 2 cells, the activation of the extrinsic pathway leads to the activation of the feedback loop by the cleavage of Bid, that leads to the release of cytochrome-c. HeLa cells is an example of type-2 cells. No such cross talk exists in type-1 cells[104,109-111].

1.2.3. Virus and Apoptosis

In higher vertebrates, apoptosis is a key defense mechanism to eliminate viral infections. Thus, not surprisingly, viruses have evolved mechanisms to either inhibit, or

delay apoptosis depending on the life cycle stage. The first clue about viral proteins blocking apoptosis came from a Human Adenovirus[112]. Years of research on virus-host interaction revealed that viruses have evolved mechanisms to interfere at several key regulatory points in the apoptotic pathway. One mechanism by which viruses interfere with apoptosis is by inhibiting or altering the function of cellular protein p53. p53 stimulates the transcription of Fas receptors, Bax and other proteins that are involved in death signal propagation through the mitochonria[72,113]. In addition, p53 downregulates the expression of Bcl-2, an anti-apoptotic protein that antagonises the function of Bax and Bak[114]. Human papillomavirus E6[115], and adenovirus E1B-55K[116] facilitate the degradation of p53. Hepatitis B virus pX protein complexes with p53 and thus inhibits the expression of p53 dependent genes[114]. As previously mentioned, caspases play a crucial role in apoptosis. Thus, viruses encode orthologues of cellular inhibitor of apoptosis protein (IAPs)[117]. IAPs are a group cellular protein that bind to caspases and inhibit their function[88,96]. Cowpox virus-encoded cytokine response modifier A (CrmA), also known as Spi-2, inhibits both Fas ligand and tumor necrosis factor (TNF) induced apoptosis by inhibiting the activity of caspase 1 and caspase 8[118,119]. Viruses have multiple strategies to modulate the TNF receptor (TNFR) superfamily. Neutralization of TNF by soluble decoy receptors is one of the most commonly observed strategies. TNFR orthologues have been found all throughout the genomes of lepri- and orthopoxviruses[120]. Human CMV contains a TNFR ortholog encoded by the UL144 orf[121]. Adenovirus E3 region encodes proteins that function by removing the FAS, TRAILR1 and TRAILR2 from the surface of the cell[114]. In addition to the above mentioned strategies, multiple viruses encode orthologs of cellular anti-apoptotic Bcl-2 proteins, and is one of the most

widely used strategies. Adenovirus E1B-19k is similar in function and structure to cellular Bcl-2[112,122,123]. This protein has been shown to block apoptosis and thereby promote viral replication by interacting and sequestering the pro-apoptotic proteins Bak and Bax[122,123]. Furthermore, human cytomegalovirus (hCMV) encodes a well-characterized protein known as the viral mitochondrial inhibitor of apoptosis (vMIA) that is capable of preventing cell death by recruiting Bax to the mitochondria and preventing the formation of Bax oligomers[124,125]. Interestingly, vMIA functions by preventing apoptosis despite sharing limited sequence similarity to members of the Bcl-2 family[125,126]. Notably, many poxviruses code for viral Bcl-2 proteins (v-Bcl-2) which despite limited sequence similarity to Bcl-2 members, fold like Bcl-2 and exert anti-apoptotic functions known as [127,128]. M11L, an anti-apoptotic protein from myxoma virus, contains limited sequence homology to Bcl-2 proteins, yet also interacts with both Bak and Bax and prevents mitochondrial membrane permeabilization. Other anti-apoptotic proteins include FPV039 from fowlpox virus, DPV002 from deerpox virus, SPPV014 from sheeppox virus[129-133]. Furthermore, VACV contains another anti-apoptotic protein with limited sequence homology yet folds in a similar fashion with Bcl-2, known as F1 [134,135].

1.2.4. Vaccinia Virus F1

The observation that VACV-infected cells are resistant to apoptosis prompted the search for an anti-apoptotic protein in VACV. Using a series of vaccinia virus containing large deletion mutations, the anti-apoptotic activity was mapped on to the F1 ORF by our

laboratory. Based on the elucidated x-ray structure, it is believed that F1 adopts a domain-swapped Bcl-2 like fold, even though there is no primary sequence similarity (Fig. 1.7 A)[136]. F1 is an anti-apoptotic protein that localizes to the outer mitochondrial membrane and protects the cell against a variety of apoptotic stimuli[134,137,138]. Studies performed have convincingly shown that F1 can block the release of Cyto c and prevent the loss of mitochondrial membrane potential (MOMP)[138]. F1 also inhibits the activation of pro-apoptotic activity of Bax and Bak. F1 is capable of interacting with Bak and this interaction prevents the oligomerization of Bax[138-140]. The Barry lab had also shown that F1 is able to interact with Bak using the divergent BH3 domain; this kind of interaction is similar to the ones observed in the case of Mcl-1 (Fig. 1.7 B)[141]. F1 indirectly inhibits the activation and oligomerization of Bax. It is probable that F1 is able to inhibit Bax activation by interacting with BH3 only protein Bim[136,139] or Noxa[142]. Thus in a virus infected cell F1 can functionally replace the cellular Mcl-1 to act as an anti-apoptotic modulator. In addition to the inhitbiton of apoptosis, F1 is also shown to inhibit the activity of inflammasomes[143]. The orthologues of F1 can be observed in other orthopoxvirus family members.

In chapter 3 and 4 of this thesis we will study EVM025, the orthologue of F1 protein in ECTV. The natural host for VACV is currently unknown. Thus, it is not possible to study F1's role in virulence in an appropriate animal model. However, the mouse is the natural host of ECTV. This provides an excellent opportunity to study the role of an anti-apoptotic protein in its natural host-pathogen role. Therefore, I set out to characterize the EVM025 protein in tissue culture, and understand the role of the protein during virus infection. In chapter 5 we wanted to understand why VACV devoid of E3

(A)

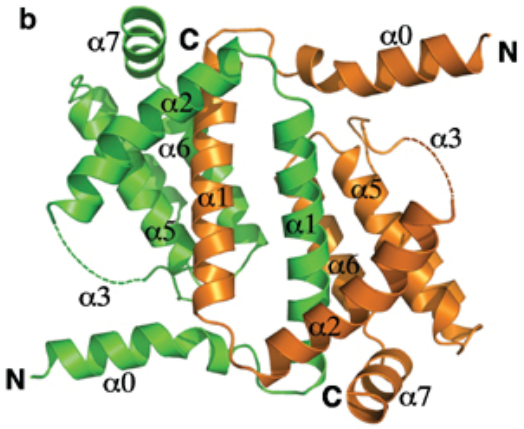

(B)

Figure 1.7 - F1L adopts a Bcl-2 like fold. (A) A ribbon digarm of F1L from MVA. F1L forms a helical bundle highly reminiscent of Bcl-2 family members. F1L forms a domain swapped dimer; a helix, α1, of one monomer is swapped into the structure of the second monomer. (B) The schematic diagram of F1L depicts the location of the transmembrane domain (TM) and the location of the BH domains.

Source- Kvansakul, M., Yang, H., Fairlie, W. D., Czabotar, P. E., Fischer, S. F., Perugini, M. A., et al. (2008). Vaccinia virus anti-apoptotic F1L is a novel Bcl-2-like domain-swapped dimer that binds a highly selective subset of BH3-containing death ligands. Cell Death and Differentiation, 15(10), 1564–1571.

triggers apoptosis upon infection. Published literature has shown that MVA missing the E3 ORF triggers apoptosis in a manner that is similar to the virus that is missing F1 ORF. This led to the question, why would VACV encode two anti-apoptotic proteins that function to inhibit apoptosis at the same point. This would thus lead us to question the mechanism underlying the anti-apoptotic activity of VACV E3.

1.3. Response to Double-Stranded RNA

1.3.1. Viral dsRNA

One major source of dsRNA is a viral infection. RNA viruses with a dsRNA genome trigger the innate immune response through their genome itself. ssRNA and DNA viruses produce dsRNA molecules during replication, or produce ssRNA that anneal to form dsRNA. As previously described VACV is a dsDNA virus, and VACV genes are expressed in a temporal manner[26,27]. VACV infection produces dsRNA during the transcription of the intermediate and late genes. Poxvirus intermediate and late gene transcripts are heterogeneous at their 3' ends[144,145]. Thus, transcripts from one DNA strand often run through into regions of the VACV genome that are transcribed from the opposite strand. This would result in the formation of complementary RNA, which would anneal to form dsRNA which can elicit an innate response in infected cells[146].

1.3.2. dsRNA-induced Translational Block

dsRNA induces a wide variety of responses in the host cell. One such host response is activation of mechanisms that inhibit the translation process. In mammalian cells, dsRNA activates distinct proteins that block translation: the dsRNA-activated

protein kinase(PKR) (Fig. 1.8) and the 2′-5′-Oligoadenylate synthetase 1(2′-5′OAS) (Fig 1.9).

1.3.2.1. The PKR pathway

PKR protein is constitutively expressed at low levels in the cell cytoplasm in an unphosphorylated state; a very small amount of PKR is also present in the nucleus[147-149]. dsRNA strands shorter than 30bp does not bind stably to the PKR and is not an effective activators of the pathway. As a result, a minimal dsRNA of 30bp is required for the activation of the PKR pathway[150]. Upon the binding of an appropriate dsRNA to the PKR, it undergoes a conformational change which exposes the domain for autophosphorylation of the protein[148,151]. The phosphorylated PKR, can subsequently phosphorylate multiple substrates. One important and well characterized substrate of phosphorylated PKR is eukaryotic initiation factor 2α (eIF-2α)[147]. The phosphorylation of eIF-2α at serine 51, results in the binding of the eIF-2α to the Eukaryotic initiation factor 2B (eIF-2B). The "frozen" eIF-2α prevents the initiation of future translational events, resulting in the block of cellular translational processes[152,153]. Studies have shown that as little as 20% of eIF-2α being phosphorylated is sufficient for the inhibition of translation[148]. Thus, activated PKR leads to protein synthesis inhibition and confers an antiviral state in the cell. In addition to the phosphorylation of eIF-2α, PKR phosphorylates IκB via the IKK complex leading to the activation of NF-κB pathway[154]. Furthermore, PKR can activate cellular apoptosis pathway by activating NF-κB pathway. Studies have shown that the activation of PKR stimulates the expression of Fas, Bax and p53[147,153].

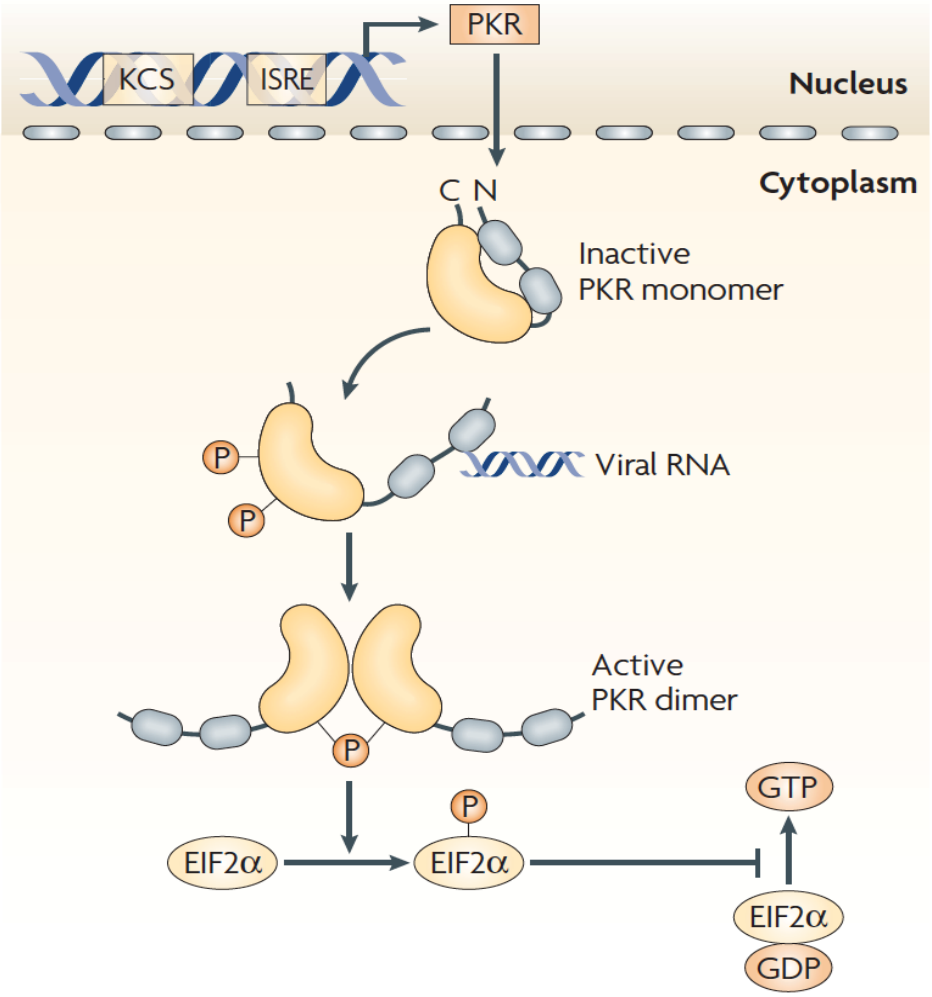

Figure 1.8 - Mechanism of action of PKR. PKR is constitutively expressed, and is also induced by type-1 interferon. PKR accumulates in the cytoplasm and the nucleus of the cell in an inactive monomoric form. The protein is activated directly by viral RNA. Following activation, PKR monomers are phosphorylated and dimerise to form the active enzyme. Actived PKR regulated a multitude of pahtways. A crucial function of PKR in viral defence is the inhibitition of translation by phosphorylation of eIF-2α.

Source: Sadler, A. J., & Williams, B. R. G. (2008). Interferon-inducible antiviral effectors. Nature Reviews Immunology, 8(7), 559–568.
Copyright Conformation Number: 3947891235451

1.3.2.2. 2′-5′-Oligoadenylate synthetase 1 (2′-5′OAS) Pathway

2'-5' OAS is an interferon inducible gene in mammalian cells. This enzyme is activated by dsRNA strands that are larger than 15bp. In the presence of dsRNA with secondary structures OAS undergoes a conformational change which leads to its activation[155]. Activated 2'-5' OAS catalyzes the oligomerization of cellular ATP to 2' ,5'-linked oligoadenylate (pppA) ranging from dimers to oligomers up to 30-mers[155,156]. These pppA in turn can bind to the inactive RNase L and activate the enzyme. Activated RNase L degrades both viral ssRNA and cellular mRNA that is present with in the cells, resulting in the drop in protein synthesis[157]. The mechanism operates using a positive feedback loop. As the viral infection proceeds, there is an increasing amounts of viral dsRNA consequently activates additional RNase L[156,158]. Thus a viral dsRNA overload leads to the dysregulation of the cellular translation pathway to the extent that apoptotic pathway could be triggered.

1.3.2. dsRNA-activated pathways in transcriptional response

In mammalian cells Toll-like receptors recognize components of pathogens and trigger an innate immune response. Toll-like receptor 3 (TLR3) is a major mediator of cellular response to viral infection as it is capable of detecting dsRNA that is produced during virus infection[154,159]. TLR3 in turn initiates NF-κB signaling, and also induces phosphorylation of the transcription factors IRF3 and IRF7 which are normally sequestered in the cytoplasm. Phosphorylation of IRF3/7 leads to their nuclear translocation, and initiates transcription of type I interferons[154,160]. Activation of both NF-

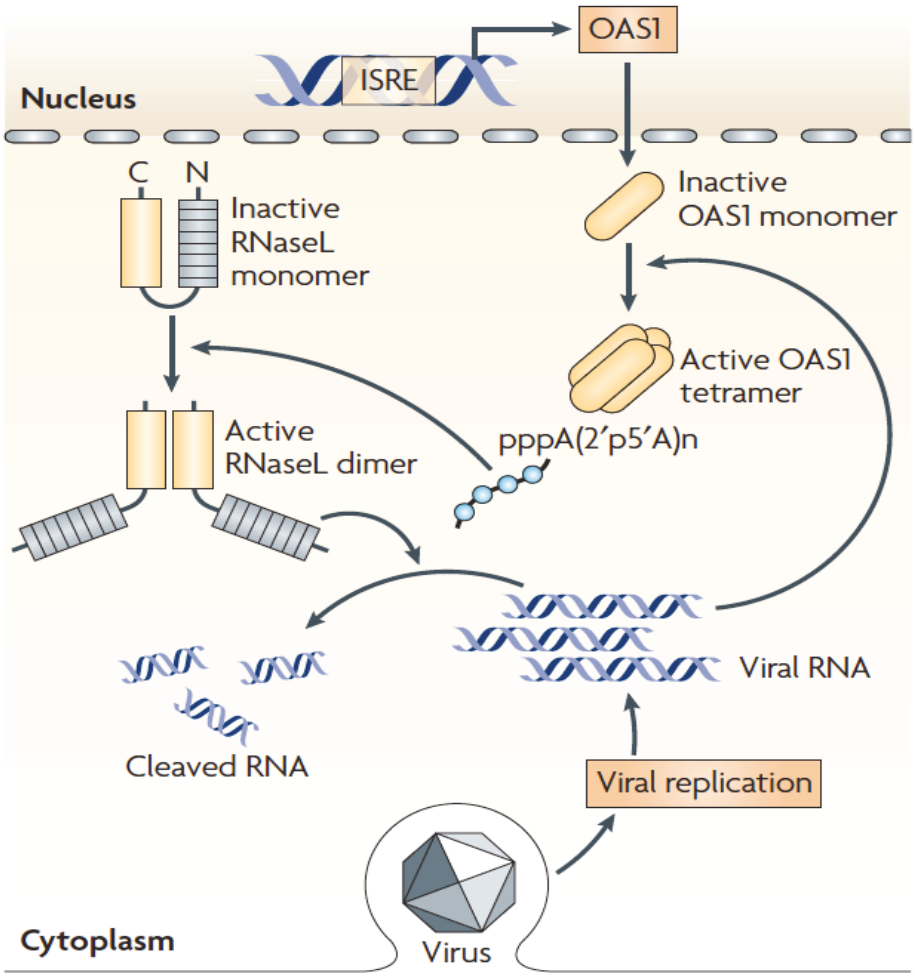

Figure 1.9 - 2'-5' OAS - RNaseL Pathway. 2'-5' OAS is expressed constitutively at low levels and is upregulated by type-1 interfereons. 2'-5' OAS protein is present in an inactive monomeric form in the cytoplasm. Following activation by viral dsRNA, the enzyme oligomerizes to form a tetramer. The tetramer leads to synthesis of 2' ,5'-linked oligoadenylate(pppA). The pppA inturn activates the constitutively present RNaseL. The activated RNaseL forms dimers, and this leads to the clevage of viral RNA.

Source: Sadler, A. J., & Williams, B. R. G. (2008). Interferon-inducible antiviral effectors. Nature Reviews Immunology, 8(7), 559–568.
Copyright Conformation Number: 3947891235451

κB and interferon pathways by infection leads to a second round of cellular responses: NF-κB signaling initiates expression of cytokines such as TNFα and IL-6, which are regarded as "pro-inflammatory" because they initiate localized inflammation at the site of infection or tissue damage. The type I interferons, which include IFNα and IFNβ, induce expression of a range of interferon-stimulated genes, and mediate other responses that are particularly important in dealing with viral infections[156,158,161].

1.3.3. Viral evasion of cellular dsRNA response

PKR pathway is a very potent inhibitor of virus replication, and this is highlighted by the observation that all classes of virus encode proteins that target the PKR pathway. As previously mentioned, in order for PKR pathway to get activated, PKR must bind to dsRNA. Thus, many viruses encode proteins that inhibit the activation of PKR by sequestering the dsRNA. One such protein is the HSV protein US11 that consists of a dsRNA binding domain which can sequester dsRNA, and is also able bind PKR[162]. In addition, VACV encodes E3[163], Influenza A NS1[164], Ebola Virus encodes VP35[165] and Rotavirus encodes sigma3[166] that are all capable of sequestering dsRNA and preventing the activation of PKR pathway. Another strategy adopted by viruses to prevent the activation of the PKR pathway is to encode proteins that act as substrate of the activated PKR. One such protein is K3 encoded by VACV. K3 shares 30% amino acid homology with eIF-2α. Activated PKR phosphorylates the K3L in place of the cellular eIF-2α, allowing the cellular translation to continue[146,167,168]. Viruses can also target phosphorylated eIF-2α for dephosphorylation. HSV produces an early protein ICP34.5

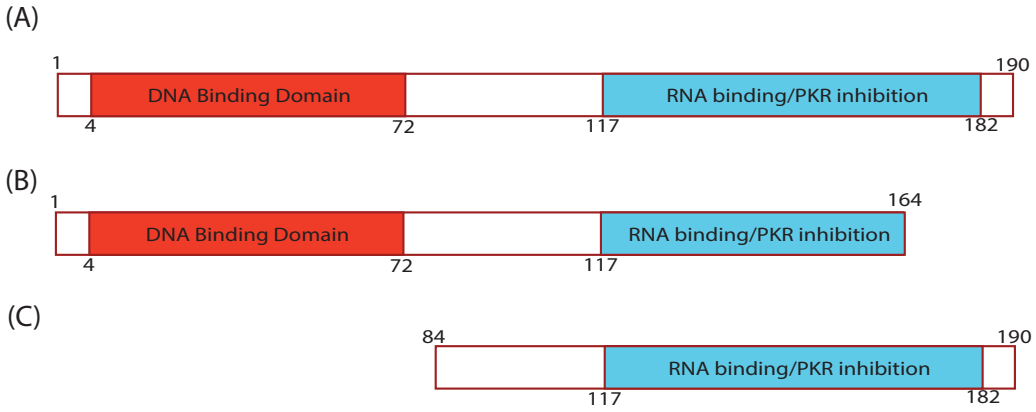

Figure 1.10 - Schematic Diagram of VACV E3L and E3L mutants. (A) A schematic diagram of the 190 animo acid E3L protein encoded by VACV. The protein possecess a C-terminus RNA binding domain and a N-terminus z-DNA binding domain. (B) Schematic diagram of the VACV-E3LΔ26C mutant virus. (C) Schematic diagram of VACV-E3LΔ83N mutant virus.

which recruits protein phosphatase 1 alpha, which in turn dephosphorylates eIF-2α[169,170]. Human Papilloma Virus 18 encodes E6 that also dephosphorylates eIF-2α[171]. In addition, to inactivating the PKR pathway, viruses also inhibit the activation of RNase L. RNase L is activated by the binding of dsRNA to 2′-5′OAS. Thus, any virus protein that sequesters dsRNA will also inhibit the RNase L activation. Another unique mechanism adapted by viruses is to inhibit the activity of PKR by expression dsRNA homologues that bind directly to PKR. Adenovirus encodes the virus-associated RNAs I (VAI), Epstein Barr Virus (EVB) EBER1 and HCV IRES all consists of extensive secondary RNA structures. These structures mimic dsRNA and bind to PKR and impede its function[172]. For the purpose of this thesis VACV E3 protein is important, and is discussed in the next section.

1.3.4. Vaccinia Virus E3

The vaccinia virus E3 protein is essential for virus replication in a wide range of cells [173]. E3 suppresses the interferon response by inhibiting PKR, thus maintaining efficient protein translation over the course of a virus infection cycle. E3 also suppresses interferon induction in some cells by inhibiting phosphorylation of IRF3 and IRF7. E3 is a 190-amino-acid protein with well-conserved N-terminal DNA-binding and C-terminal RNA-binding domains (Fig. 1.10 A). Many early *in vitro* studies suggested that the C-terminal RNA-binding domain is necessary and sufficient for PKR inhibition and virus replication [163,174,175]. These studies were based on observations that vaccinia virus lacking E3 (ΔE3L) and mutant virus lacking only the RNA-binding domain of E3 (E3LΔ26C) (Fig. 1.10 B) are interferon-sensitive and replication-defective in many cell lines. In

contrast, a mutant virus retaining the RNA-binding domain, but lacking the amino-terminal DNA-binding domain (E3LΔ83N) is interferon-resistant and replicates normally (Fig. 1.10 C). Nevertheless, several lines of evidence point to an essential role of the E3 protein in viral pathogenesis. The E3LΔ83N virus causes considerable mortality in susceptible mice as compared to the ΔE3L virus, though it is still attenuated with respect to the wildtype virus [176,177]. In HeLa cells, VACV E3L masks virtually all dsRNA synthesized by the viruses[178]. The deletion of E3 in MVA (Modified Vaccinia Ankara) results in defective late protein synthesis. Viral early transcripts are detected, while intermediate transcripts are being accompanied with r-RNA degradation[178,179]. Previous work suggests that vaccinia virus E3 can act as an inhibitor of apotosis[180]. In this thesis we try to understand the mechanism underlying this observation.

1.4. Thesis Objective

Published work has shown that VACV protein F1 acts as an important inhibitor of apoptosis during infection in the tissue culture model[134,138,140,141]. A single study has also shown that VACVΔF1L virus is less virulent then its parent wild type strain[143]. As we have previously mentioned, the natural host of VACV is unknown. Hence, a high infectious dose of virus is required to observe mortality. Thus, VACV infection of mice does not provide an appropriate model to study the importance of the poxvirus anti-apoptotic gene during viral pathogenicity. In the first part of the thesis, we examined the orthologue of F1 in ECTV. Since ECTV is a natural pathogen of mice, it provides an excellent model to study the importance of an anti-apoptotic gene during viral infection. This research is divided into two objectives:

Chapter. 3: To characterize EVM025, the F1 orthologue in ECTV. Based on the sequence similarity we hypothesized that EVM025 like F1 will be able to inhibit apoptosis by inhibiting the activity of Bak and Bax.

Chapter. 4: In chapter 1, we describe data showing that EVM025 functions in a manner similar to F1. Based on this we hypothesized that EVM025 is a virulence factor. In this chapter we describe the effect of EVM025 deletion on ECTV virulence, and the spread of the virus in the mice. In this chapter we also describe the immune response that mice generate against the ECTVΔ025 mutant.

The second part of the thesis asks a different question. A single study suggests that VACV E3 protein acts an anti-apoptotic protein[180]. Another study shows that E3 deleted MVA mutant triggers apoptosis in a manner that is similar to MVA that is missing the anti-apoptotic protein F1[136]. These published works led me to question the reason behind having two anti-apoptotic proteins that inhibit apoptosis at the same point. In the last chapter (Chapter 5) of this thesis we are attempting to understand the relationship between E3 and F1 during an infection of HeLa cells.

Chapter-2- Methods and Materials

2.1. Buffer Formulas

1X Tris, acetic acid, EDTA (TAE) buffer

40 mM Tris (Invitrogen)

20 mM Sodium acetate trihydrate (EMD)

1 mM Ethylenediaminetetraacetic acid (EDTA) dihydrate (EMD)

5X Protein sample buffer

200 mM Tris-Cl (pH 6.8) 5% (w/v)

Sodium dodecyl sulphate (SDS) (BIORAD)

50% (v/v) Glycerol (Fisher)

1.43 M 2-mercaptoethanol (Sigma)

10X DNA loading dye

100 mM Tris-Cl (pH 8.0)

10 mM EDTA

50% Glycerol

0.02 g (w/v) Bromophenol blue (Sigma)

0.02 g (w/v) Xylene cyanol (Sigma)

2% CHAPS Lysis buffer

2% CHAPS

150mM NaCl

50mM Tris pH 8.0

1X cOmplete (EDTA-free) protease inhibitor cocktail

10X MOPS gel buffer

20mM EDTA

200mM 3-(N-morpholino) propanesulfonic acid (MOP)

50 mM Sodium acetate

Adjust pH to 7.0 using NaOH.

20X SSC Buffer

3M Sodium chloride

0.3M Sodium citrate

Cell Lysis Buffer

1.2% SDS

50mM Tris pH 8.0

4mM EDTA

4mM $CaCl_2$

0.2mg/mL proteinase K (Fermentas)

Church Buffer

1 % (w/v) bovine serum albumin

1 mM EDTA

0.5 M Na_2HPO_4 (pH 7.2)

7% (w/v) SDS

Church Wash 1

2x SSC 50mL

0.1% SDS 2.5mL

Church Wash 2

0.2x SSC

0.2% SDS

Digitonin lysis buffer

1 mM Sodium phosphate monobasic (NaH_2PO_4)

8 mM Sodium phosphate dibasic (Na_2HPO_4)

75 mM NaCl 250 mM Sucrose

190 μg/mL Digitonin (Sigma)

1X cOmplete (EDTA-free) protease inhibitor cocktail (Roche)

Digitonin permeabilization buffer

75nM NaCl

1mM NaH2PO4

250mM sucrose

190µg/mL of digitonin (Sigma-Aldrich)

Luria-Bertani (LB) medium

1% (w/v) Bacto-tryptone (BD)

0.5% (w/v) Yeast extract (BD)

1% (w/v) NaCl

Luria-Bertani (LB)/agar plates

LB medium

15 g/L Agarose

Antibiotic: 50-100 µg/mL ampicillin (Sigma), 30 µg/mL chloramphenicol (Sigma), or 30 µg/mL kanamycin (Sigma)

SOC medium

20mg/mL tryptone,

5mg/mL yeast extract,

0.5mg/mL NaCl,

2.5mM KCl (pH 7.0)

Nick translation reaction buffer

33 mM Tris-Cl (pH 7.9) 10 mM

Magnesium chloride (MgCl2)

50 mM NaCl

33 μM dATP/dGTP/dTTP (Invitrogen)

20 μCi [α-32P]-dCTP (PerkinElmer)

5U Escherichia coli DNA polymerase I (New England Biolabs)

Oligo labelling buffer

44 mM Tris-Cl (pH 8.0) 4.4 $MgCl_2$

9 mM 2-mercaptoethanol

17.6 μM dATP/dGTP/dTTP)

181 mM HEPES (pH 6.6)

20 μCi [α-32P]-dCTP (PerkinElmer)

Phosphate buffered saline (PBS) (pH 7.4)

137 mM NaCl

2.7 mM KCl

8.3 mM Sodium phosphate dibasic ($Na2HPO_4$) (Caledon)

1.7 mM Potassium phosphate monobasic ($KH2PO_4$) (Caledon)

Radioimmunoprecipitation assay (RIPA) buffer

50 mM Tris-Cl (pH 8.0)

150 mM NaCl

1 mM EDTA

1% (v/v) IGEPAL CA-630

0.1% (w/v) SDS

0.5% (w/v) Sodium deoxycholate

1X cOmplete (EDTA-free) protease inhibitor cocktail

Triton-X-100 lysis buffer

25mM Tris pH8.0

0.1% Triton-X-100 (Fisher Scientific)

Resolving gel buffer

375 mM Tris-Cl (pH 8.8)

7.5, 10%, or 12.5% Acrylamide:Bis-Acrylamide (37.5:1) (Fisher)

0.1% (w/v) SDS 0.05% (w/v) Ammonium persulfate

0.05% (v/v) Tetramethylethylenediamine (TEMED) (Sigma)

SDS-PAGE running buffer (pH 8.3)

25 mM Tris 1

92 mM Glycine

0.1% (w/v) SDS

Stacking gel buffer

125 mM Tris-Cl (pH 6.8)

4% Acrylamide:Bis-Acrylamide (37.5:1)

0.1% (w/v) SDS

1% (w/v) Ammonium persulfate

0.1% (v/v) TEMED

Transfer buffer

192 mM glycine,

25 mM Tris-HCl

20% methanol

Urea/SDS buffer

10 mM Tris-C1 (pH 7.8)

7 M Urea (GE)

350 mM NaCl

10 mM EDTA

1% (w/v) SDS

2.2. DNA manipulation methodology

2.2.1. Polymerase Chain Reaction

The polymerase chain reaction (PCR) was used to amplify regions of viral DNA, which were subsequently used for various other downstream steps. PCRs were made up

in a total volume of 50µL and contained the appropriate buffer, 2.5mM $MgCl_2$, 0.2mM of each deoxyribonucleotide triphosphate (dNTP) (Invitrogen), 1 pmole of each forward and reverse primer, and 2.0-2.5 U of *Taq* DNA polymerase (Invitrogen) or LongAmp® Taq DNA Polymerase (New England Bio Labs). PCR reactions were carried out in a Bio-rad C1000 Touch™ Thermal Cycler for 30-40 cycles comprised of a 95°C denaturing step for 30 s, a 55-61°C annealing step for 30 s, and an elongation step which was performed as described in enzyme manufacturers manual. The primers used for this study are listed in Table-2.1.

2.2.2. Restriction Endonuclease (RE) Digestion

All restriction digestions were performed with commercially available enzymes using conditions and buffers recommended by the manufacturer. Double digests were performed simultaneously in a buffer in which the maximum activities of the enzymes were attained. All RE digestion were performed for 1-3 hrs at 37 °C. If DNA purification was required following RE digestion, the product was electrophoresed on a 0.8-1% agarose gel, and the anticipated band was purified using QiaQuick gel extraction kit (Qiagen).

2.2.3. Agarose Gel Electrophoresis, Gel-Purification of DNA

DNA fragments were analyzed by gel electrophoresis. Prior to loading, the DNA was mixed with 10x gel loading dye (Invitrogen) and was then loaded on to a 1X TAE Agarose gel containing 1:15,000 SYBR safe (Invitrogen). The concentration of agarose varied from 0.8-1.2% depending on the size of the amplified/RE digested fragment.

Table 2.1- List of Primers Used

Primer Name	Primer Sequence (5' to 3')	Restriction Site
EVM025koF1	AGAATAGCTCAGCTAATCTAT	None
EVM025koR1	AATGCAGATCTGGATCTACGATATTATA CATAAACATCGA	*BglII*
EVM025koF2	GATCCAGATCTGCATTTCGCATACTATA TGCGATGAT	*BglII*
EVM025koR2	TGGATCCTTATCATATCATGTATTTGAG	*BamHI*
EVM025-Forward	TGAATTCTTATGGACAATAGTATTTTGTCG	*None*
EVM025-Reverse	TGGATCCTTATCATATCATGTATTTGAG	*None*
JRS-968-F2L-Forward	TATGCGGGATCCAGTTTTATGTTCAACATG AATATTAACTCACCAGTT	*BamHI*
JRS-970-F2L-Reverse	GATAGACTCGAGCTATTGTTTATTATCTAA	*Xho-I*
EVM107-Forward	GTAGAACGACGCCAGAATAAGAATA	None
EVM107-Reverse	AGAAGATATCAGACGATCCACAATC	None

GeneRuler 1kb DNA Ladder Plus (Fermentas) was used to approximate the size of the DNA fragments. Following separation by electrophoresis, DNA was visualized using UV light. If additional sensitivity was required, the gels were stained with SYBR Gold (Invitrogen), diluted in 1X TAE buffer for 30 minutes. The gel in this case was visualized using a FLA-5100 imager (Fujifilm).

The required fragment of amplified/RE digested DNA was either gel purified or directly purified, using the QiaQuick gel extraction kit or QiaQuick PCR purification kit respectively. The manufacturer's instructions were used for the purification kit.

2.2.4. Cloning and DNA ligations

Ligation of PCR products and RE digestion products into pGEMT-T was performed using the pGEMT-T Easy Vector Kit (Promega), as per the manufacture's instructions. The ligations were typically carried out at 4 °C overnight. PCR products generated using *Taq* DNA polymerase were directly ligated into intermediate pGEMT-T vector using the pGEM®-T Easy Vector Systems (Promega) or the pJet Vector using the pJet1.2 vector using the CloneJet PCR Cloning Kit (Thermo Fisher Scientific). All ligations were carried out using T4 DNA ligase (NEB) according to NEB's instructions. Ligation reactions were made up in a total volume of 20μL and contained ratios of insert DNA to backbone plasmid DNA of 4:1 or 8:1. These reactions were carried out at 16 °C overnight. Ligations were transformed into *Escherichia coli* DH5α. The transformation protocol is described in section 2.2.5.

2.2.5. Bacterial Transformation

Chemically competent *E. coli* DH5α were prepared using $CaCl_2$ as described [181]. Ligations or plasmids for amplification were transfected into *E. coli* DH5α by the heat shock method. Competent DH5α were incubated with plasmid DNA or ligation mixture on the ice for 30 minutes and then placed at 42 °C for 1 min followed by a 2 minute recovery on ice. The transformed bacteria were allowed to recover in SOC media at 37 °C for 45 minutes. After the recovery period the bacteria were plated on LB agar plates containing 80μg/mL of ampicillin and supplemented with 80μg/mL 5-bromo-4-chloro-3-indolyl-β-D-galactopyranoside (X-gal) (Rose Scientific) and 0.5mM isopropyl β-D-1-thiogalactopyranoside (IPTG) (Rose Scientific) to allow for blue-white selection.

2.2.7. Plasmids

Plasmid DNA was normally isolated from 1.5 mL of overnight bacterial culture using the commercially available High-Speed Plasmid Mini Kit PD100/PD300 (Geneaid). To obtain large quantities of endotoxin free DNA for mammalian transfection, the Qiagen Maxi-Prep Kit (Qiagen) was used. For the maxi-prep 100 mL of overnight bacterial culture was used as the starter culture.

The list of plasmids used and generated for this thesis is outlined in Table 2.2.

2.2.8. Sequence alignments

The following sequences were used: VACVCop F1L (AAA48014), VARV Bangladesh C5L (AAA60773), VARV Garcia E1L (CAB54625), MPXV Zaire C7L (AAY97031), CPXV Brighton Red CPXV048 (NP_619836.1), ECTV strain Moscow EVM025

Table 2.2 – List of plasmids used in this study.

Plasmid Name	Description	Source
pEGFP-C3	EGFP expression vector; CMV promoter	Clontech
pcDNA3	Expression vector; CMV promoter	Invitrogen
pcDNA3.1	Expression vector; CMV promoter	Invitrogen
pEGFP-F1L	EGFP-F1L fusion	
pEGFP-Bcl-2	EGFP-Bcl-2 fusion	
pEGFP-EVM025	EGFP-EVM025 fusion	This Study
pEGFP-EVM025(Δ435-453)	EGFP-EVM025(Δ435-453)	This Study
pEGFP-F1L	EGFP-F1L fusion	
pEGFP-Bcl-2	EGFP-Bcl-2 fusion	
pcDNA3-FLAG-Bak	FLAG-tagged wildtype Bak	G. Shore (184)
pcDNA3-HA-Bak	HA-tagged wildtype Bak	G. McFadden (216)
pcDNA3-Flag-BimL	Flag-tagged wildtype BimL	
pcDNA3.1-F2L	F2L expression vector	This Study
pMX-E3L(Human-Codon)	Synthesised from GeneArt with a human codon bias	Invitrogen
pEGFP-E3L(Human-Codon)	EGFP-E3L fusion with human bias codons	This study
pGMET-EVM025 Knock Out Vector	The vector used to generate the ECTVΔ025 and ECTVΔ025ΔCmrA Mutants	This study

(NP_671543). ClustalW using the BLOSUM32 matrix was used to perform the multiple alignments [182].

2.3. RNA Methodology

2.3.1. RNA extraction

HeLa cells were infected with vaccinia virus (VACV), VACVΔE3L, VACVΔF1L, VACVΔF2L for the indicated times. Post infection, the total RNA was extracted using the RNAzol RT (Sigma) reagent using the manufacturers instructions. The mock infected or infected HeLa cells (2×10^6) were lysed in 1mL of RNAzol RT solution and frozen at -80 °C overnight or for up to one week. The samples where thawed on ice, and RNA was harvested according the manufacturer's instructions. The RNA pellet was resuspended in 50µL of water (Dnase/Rnase Free) (GIBCO).

2.3.2. RNAseq

For the RNAseq experiment HeLa cells were infected with VACV and VACVΔE3L. The cells were lysed in RNAzol RT solution 0.5, 1, 2, 3, 5, and 12 hrs post infection. The RNA was extracted as mentioned earlier. RNA samples were qualified using the Agilent technologies 2100 Bioanalyzer (Total RNA Nano kit), all samples displayed RIN values >9, with the exception of VACdE3L-12-1 and VACdE3L-12-2. These samples displayed obvious 28S and 18S RNA peaks with some limited degradation that interfered with the RIN value calculation. RNA concentration was obtained from duplicate measurements using the Qubit™ platform. All samples

were deemed of high enough quality for library preparation using the Illumina TruSeq Sample Preparation v2 kit. Approximately one 920 ng of RNA was used for library generation following the manufacturer's protocol. After an initial poly-A selection step, the RNA was fragmented for 8 minutes, and converted to cDNA (1st and 2nd strand synthesis). The double-stranded DNA (dsDNA) was purified from the reagent mixture using AMPureXP beads. The dsDNA was then processed to create libraries through a series of steps as follows; end repair (in-line controls added), A-tailing and Adapter ligation, followed by a second clean-up with AMPureXP beads. The samples were then amplified by PCR to enrich for fragments with appropriate ends, and subjected to a third round of purification with AMPureXP beads. The resultant libraries were quantified by Qubit and qualified using the Agilent Bioanalyzer (DNA1000 kit). 10nM stocks of each library were prepared using the average fragment length and concentration for each library. Pooled libraries (25 microlitres at ~2.6 nanograms/microlitre) were submitted for sequencing (2x125bp) on an Illumina HiSeq2500 at The Centre for Applied Genomics (TCAG), Toronto.

2.3.3. Generation of radiolabelled probes for Northern blotting

We generated random-primed probes of VACV-F1L and F2L gene for Northern Blot analysis. The template for F1L was obtained by the digestion of F1L wild-type gene out of the pEGFP-F1L plasmid using the BamHI and XhoI restriction enzymes. Similarly, F2L template was obtained by the digestion of F2L wild-type gene out of the

pcDNA 3.1-F2L plasmid using the BamHI and XhoI restriction enzymes. The template was combined with 2 μg/μL random hexamers, heated at 95°C for five minutes, and then cooled on ice. The template/hexamers were then incubated with oligo labelling buffer, bovine serum albumin (New England Biolabs), and Klenow for 30 minutes at 37°C. The reaction was diluted 1:1 with 1X TAE, phenol/chloroform extracted once, and passed through an illustra NICK column (GE, 17-0855-01). All radiolabelled products were quantitated using a LS6500 scintillation counter (Beckman).

2.3.4. Agarose gel electrophoresis and Northern blot analysis

RNA samples for Northern blots were resuspended in RNase free water. Ten micrograms of RNA samples were combined with 3μL of 10X MOPS buffer, 5μL of 37% formaldehyde, and 15μL of deionized formamide. The samples were heated at 55 °C for 15 minutes and then immediately moved to ice. The samples were then subjected to electrophoresis through a 1% agarose gel containing 6% formaldehyde. Electrophoresis was carried out at approximately 8 V/cm for 2 hrs in 1× MOPS buffer containing 6% formaldehyde. The gel was stained with SYBR Gold (Invitrogen), diluted in 1X MOPS for 30 minutes. The stained gel was visualized using the FLA-5100 imager (Fujifilm). RNA was then transferred to a Zeta-Probe Membrane (Bio-Rad) in 10× SSC, then UV cross-linked using the Auto-crosslink option(Stratalinker 2400; Stratagene).

Church Buffer was used to prehybridize the Zeta-Probe membrane at 65°C in a hybridization oven for 4 hrs. The prehybridization buffer was removed and replaced with 7 mLs of Church buffer. To this 1,000,000 cpm/mL of ^{32}P- labeled probe was added. The probe was allowed to hybridize at 65°C for 13-17 hrs. The membranes were then washed

two times with Church Wash Buffer 1 for 20 minutes each. This was followed by two washes with Church Wash buffer 2 for 20 minutes each. The Zeta-Probe membrane was subjected to autoradiography using Kodak X-OMT AR film.

2.4. Cells

HeLa cells were obtained from the American Type Culture Collection (ATCC), Human embryonic kidney 293T (HEK293T) (ATCC), Baby mouse kidney (BMK) and CV-1 cells (ATCC) were grown in Dulbecco's Modified Eagle's Medium (DMEM) (Life Technologies) supplemented with 10% fetal bovine serum (FBS) (Life Technologies), 2mM L-glutamine (Life Technologies), 50U/mL penicillin (Life Technologies), and 50µg/mL streptomycin (Life Technologies). HeLa PKR KO1 (PKR knock out cells) were kindly provided by Dr. J. Smiley[183]. Wild type and $Bak^{-/-}Bax^{-/-}$ deficient mouse embryonic fibroblasts (provided by Dr. S. Korsmeyer) and Baby hamster kidney fibroblasts (BHK) were cultured in DMEM containing 10% FBS, 2mM L-glutamine, 50U/mL penicillin, 50µg/mL streptomycin and 100µM MEM Non-Essential Amino Acid Solution (Life Technologies). Buffalo green monkey kidney (BGMK) cells were obtained from ATCC and maintained in DMEM containing 10% newborn calf serum (NCS) (Life Technologies), 2mM L-glutamine, 50U/mL penicillin, and 50µg/mL streptomycin. Jurkat cells were maintained in Roswell Park Memorial Institute 1640 medium (RPMI) (Life Technologies) supplemented with 10% FBS, 50U/mL penicillin, 50µg/mL streptomycin, and 100µM β-mercaptoethanol (Bioshop Canada Inc.). Jurkat cells stably expressing Bcl-2 were generated as previously described [184]. African Green Monkey Kidney Fibroblast (BSC40) cells were provided by Dr. D. Evans, and cultured in

media containing MEM containing 5% FBS, 2mM L-glutamine, 50U/mL penicillin and streptomycin. All cells were maintained at 37°C with 5% CO_2.

The cells were propagated in either T75 or T150 flasks in the appropriate media. The monolayers were passaged upon reaching ~90-95% confluence. The cells were washed with phosphate buffered saline (PBS) and treated with 0.25% trypsin (Gibco). The trypsin was inactivated using media containing FBS. The cells were reseeded between 10-20% confluence with the 13 to 20 mLs of appropriate media.

Cell counts were performed using 10µl aliquot of the cells, and mixed with 1:1 volume trypan blue dye (Invitrogen), and cell numbers determined using a hemo-cytometer. The cells were then diluted and desired number of cells was added to the tissue culture plates.

2.5. Viruses

Dr. G. McFadden (University of Florida, Gainesville, Florida) provided vaccinia virus (VACV) strain Copenhagen (VACV), VACV expressing the enhanced green fluorescent protein (EGFP), VACV-EGFP. VACV devoid of E3L (VACVΔE3L) was provided by Dr. B. Jacobs (Arizona State University, Tempe, AZ) [185]. VACV lacking the F1L open reading frame (ORF), was generated in the Barry Lab [138]. Vaccinia virus strain Western Reserve (VACVwr), and mutant strain with the disrupted F2L (VACVwrΔF2L) orf were provided by Dr. D. Evans (University of Alberta, Edmonton, Alberta). All vaccinia viruses except VACVΔE3L were propagated in BGMK cells as described previously [186]. VACVΔE3L was propagated in BHK-21 cells as described previously [185].

Ectromelia virus strain Moscow (ECTV), and ECTVΔCrmA were provided by Dr. M. Buller (St. Louis University, St. Louis, Missouri). All viruses were propagated in L929 cells and purified as previously described [186,187].

2.5.1. Generation of Recombinant Viruses

To generate an ECTV virus lacking EVM025, we cloned enhanced green fluorescent protein (EGFP) under the control of a synthetic poxviral early/late promoter (E/L) with flanking *BglII* sites. The poxviral early/late promoter (pE/L) and EGFP was amplified from pSC66-EGFP using primers E/LSynFor and EGFP (BglII) and the final product was cloned into pGEM-T (Promega). To generate the EVM025 knockout cassette, a region of EVM025 containing 158 base pairs upstream of EVM025 and the first 45 base pairs of the 5' end of EVM025 was amplified using the forward primer EVM025koF1 5'-AGAATAGCTCAGCTAATCTAT-3' and reverse primer EVM025koR1 5'-AATGCAGATCTGGATCTACGATATTATACATAAACATCGA-3'. The downstream region consisting of the last 159 base pairs of EVM025 was amplified using the forward primer EVM025koF2 5'-GATCCAGATCTGCATTTCGCAT ACTATATGCGATGAT-3' and reverse primer EVM025koR2 5'-TGGATCCTTATCATATCATGTATTTGAG-3'. EVM025koR1 and EVM025koF2 both contain an overhanging linker region that encodes a BglII restriction site. The PCR products were included in an overlapping PCR reaction to obtain a continuous fragment of the upstream and downstream fragments of EVM025 separated by the BglII restriction site. The 347 base pair fragment was cloned into a pGEMT vector (Life Technologies). An EGFP cassette under the control of a synthetic early/late poxviral promoter was

inserted using the BglII restriction site between the upstream and downstream EVM025 fragments (pGEMT-EVM025/b-EGFP). This effectively encodes a disrupted non-functional version of EVM025 lacking approximately 80% of the EVM025 ORF. ECTV wild type was used to generate ECTVΔ025 by homologous recombination.

In order to generate a version of ECTV deficient in CrmA and EVM025, we generated an EVM025 knockout using the vector described above in the background strain ECTVΔCrmA. BGMK cells (1×10^6) were infected with ECTV at an MOI of 0.05 and transfected with pGEMT-EVM025/d-EGFP using Lipofectamine 2000. Recombinant viruses were selected by EGFP fluorescence and plaque purified.

2.5.2. Analysis of Recombinant Viruses by PCR

Recombinant virus purity and integrity was confirmed by PCR analysis. HeLa for VACV or L929 cells for ECTV were infected with virus at an MOI of 5 for 18-24 hrs, after which the media was replaced by cell lysis buffer and incubated for 6 hrs in the incubator.

This mixture was extracted with buffer-saturated phenol (Sigma) and centrifuged at 18,000g for 15 minutes. The aqueous layer was transferred to a new tube and the DNA precipitated with ice cold 95 % ethanol (2:1 volume) and 3 M sodium acetate pH 5.2 (1:20 volume), and centrifuged for 30 min at 18,000g. The pellet was washed with 70% ethanol, and the DNA resuspended in H2O. DNA was quantified. PCR reactions using different primer pairs were used to confirm the mutations of each virus. In addition, the PCR products were sequenced to confirm the mutations.

2.5.3. Virus Titration

The virus stocks/samples were serially diluted 10-fold by suspending the virus in PBS or DMEM media. The dilutions were plated in triplicate for the titration of virus stocks, or in duplicate for the titration of virus from experiments. Infected monolayers were incubated for 24-48 hrs. The monolayer was then fixed by methanol overlay for 30 minutes at room temperature. Post fixation, the cellular monolayers were stained with 0.5 % crystal violet.

To determine pfu per mL of ECTV, serial titrations were performed on BSC-40 cells. The virus stocks/samples were serially diluted 10-fold by suspending the virus in PBS. The cells were infected, and one-hour post-infection, 2mL of cell culture media with 1% w/v carboxymethylcellulose (CMC) (Sigma-Aldrich), was added to each well. The plates incubated at 37°C for 4 days. The infected plates were fixed and stained with a crystal violet solution containing 20% v/v ethanol and 0.1% w/v crystal violet by rocking overnight at room temperature.

Visible, isolated plaques were counted and viral titres were calculated by multiplying the number of plaques in one well with the reciprocal dilution factor used to infect that well and then dividing by the volume of medium used to infect that well [(number of plaques)x(1/dilution factor)/volume]. The pfu/mL for duplicate plates was averaged to obtain the titer of each virus stock. For all infections the MOI was calculated by multiplying the number of cells in a monolayer by the desired number of particle forming units per cell and then dividing by the titer of the virus stock [(number of cells)x(pfu)/(virus titer)].

2.5.4. Growth Curves

For the high MOI single-step analysis of virus growth 6 well dishes of nearly confluent cells ($1x10^6$) were infected at a MOI of 5 (~ 1x107 pfu). Following 1 hour of infection the cells were washed with PBS and cell culture media. At indicated times, the virus-cell mixture was harvested by scrapping cells into the medium. Virus was then released from cells by freeze-thaw and titred on BSC-40 cells. The experiments were performed in triplicate.

2.6. Protein Methods and Techniques

2.6.1. Cell Lysis and Sample Preparation

Transfected or infected cells were washed in PBS and lysed in RIPA buffer for 15-20 minutes at 4 °C or on ice. DNA in the lysates was sheared using a 28-gauge hypodermic needle. The lysates were cleared by centrifugation at 20,000g for five minutes at 4 °C. All lysates were mixed with 5X protein sample buffer prior to storage at -20 °C.

2.6.2. SDS-polyacrylamide gel electrophoresis (SDS-PAGE)

Prior to running the SDS-PAGE, the samples were boiled at 98 °C for 20 minutes. The protein samples were separated in 7.5%, 10%, or 12.5% acrylamide gels by SDS-PAGE using the Bio-Rad Mini-PROTEAN Tera Cell system (Biorad). The PageRuler Pre-stained Protein Ladder (Fermentas) was used to approximate the size of the reduced

protein bands. Protein samples were separated at 80-150 V in SDS-Page running buffer until adequate resolution was achieved.

2.6.3. Western blotting

Proteins that were resolved in SDS-PAGE were transferred on to Immobilon-P PVDF membrane (Milipore) via semi-dry transfer apparatuses. The PVDF membrane was activated using methanol for 30 seconds. All filter papers, and gels were incubated in transfer buffer for five minutes. For the semi-dry transfer of protein, the sandwich consisting of filter paper, membrane, and gel were placed in a semi-dry transfer (Tyler) and transferred at 450 mA for 1 hour. Membranes for chemiluminescent detection were blocked in TBST (Tris-buffered saline containing 0.1% Tween-20) containing 5% skim milk powder for one hour at room temperature or overnight at 4 °C. Primary antibodies were incubated with membranes for 1 hour at room temperature or overnight at 4 °C. The blots were subsequently washed with TBST five times, and then stained with horseradish peroxidase-conjugated goat anti-mouse or goat anti-rabbit secondary antibodies for one hour at room temperature. All antibodies were diluted in TBST containing 1% skim milk. Proteins were visualized using ECL Plus (GE Healthcare). All western blots performed in chapter-3 where performed using ECL

For infrared imaging the Immobilon-FL PVDF membrane (Milipore), the membranes for infrared imaging were in 1:1 Odyssey Blocking Buffer (LI-COR):TBST for one hour at room temperature. Primary antibodies were incubated overnight at 4 °C and secondary antibodies (Alexa Fluro 680 goat anti-rabbit (Invitrogen) and secondary antibodies Alexa Fluro 790 goat anti-mouse (Invitrogen)) were incubated for one hour at

room temperature. All antibodies were diluted in TBST. Proteins were detected using Odyssey Infrared Imagining System (LI-COR). The images were analyzed using LI-COR ImageStudio Lite software. All western blots performed in chapter 5 were performed using LI-COR.

The list of antibodies used in this study and their sources are tabulated in Table 2.3

2.6.4. Immunoprecipitations

To detect an interaction between EVM025 and endogenous Bak, BMK cells (5x106) were transfected with 5µg of pEGFP-C3 (Clontech Laboratory Inc.), pEGFP-Bcl-2, or pEGFP-EVM025 using X-tremeGENE HP DNA reagent (Roche Diagnostics). Transfected cells were lysed 16 hrs post-transfection in 2% CHAPS (Sigma-Aldrich) containing 150mM NaCl, 50mM Tris pH8.0 and Complete Protease Inhibitors (Roche Diagnostics). Cell lysates were immunoprecipitated with anti-goat GFP antibody. Immune complexes were isolated using protein A-Sepharose (GE Healthcare). Isolated immune complexes were subjected to Western blot analysis. To study the interaction of Bax and BimL with EVM025, HeLa cells were transfected with 4µg of pEGFP-C3, pEGFP-Bcl-2, or pEGFP-EVM025 and 2µg pcDNA3-HA-Bax or pcDNA3-Flag-BimL using 5µl of Lipofectamine 2000 (Life Techonologies). Transfected cells were lysed 16 hrs post-transfection in 2%CHAPS lysis buffer. Cell lysates were immunoprecipitated with anti-goat GFP antibody. Immune complexes were isolated using protein A-Sepharose. The isolated immune complexes were subjected to Western blot analysis.

Table 2.3- List of Antibodies.

Antibody	Species	Application	Characteristics	Source
anti-β-tubulin	Mouse	Western Blot (1:4000)		ECM Bioscience
anti- β-actin	Rabbit	Western Blot (1:5000)		Sigma-Aldrich
anti-α-actin	Mouse	Western Blot (1:5000)		Sigma-Aldrich
anti-Bak Ab-1	Mouse	Flow cytometry (1:50)	Recognizes active Bak	Oncogene Research Products
anti-Bak NT	Rabbit	Western Blot (1:2000)	Recognizes active Bak	Upstate
anti-Bax 6A7	Mouse	Flow cytometry (1:400)	Recognizes active Bax	BD Biosciences
anti-Cytochrome *c*	Mouse	Western Blot (1:1000)		BD PharMingen
anti-PARP	Mouse	Western Blot (1:2000)		BD PharMingen
anti-EGFP	Goat	Immunoprecipitation (1: 7000)		L. Berthiaume
anti-EGFP	Mouse	Western Blot (1:10000)		Covance
anti-NK1.1 (PK136)	Mouse	Flow cytometry (1:400)		K. Kane
anti-FLAG M2	Mouse	Western Blot (1:5000)		Sigma-Aldrich
anti-HA	Mouse	Microscopy (1:200)	Clone 12CA5	Roche Diagnostics
anti-I3L	Mouse	Western Blot (1:20)	VACV Protein	D. Evans
anti-I5L	Rabbit	Western Blot (1:5000)	VACV Protein	
anti-F2L	Rabbit	Western Blot (1:7000)	Generated by ProSci	This Study
anti-F1L	Rabbit	Western Blot (1:10000)	VACV Protein	Barry Laboratory
Anti-A36R	Rabbit	Western Blot (1:5000)	VACV Protein	D. Evans
Anti-A34R	Rabbit	Western Blot (1:10000)	VACV Protein	D. Evans
Anti-B5R	Mouse	Western Blot (1:10000)	VACV Protein	S. Isaacs
Anti-F4L	Rabbit	Western Blot (1:5000)	VACV Protein	D. Evans
anti-mouse-HRP	Donkey	Western blot (1:25,000)		Jackson Immunoresearch
anti-rabbit HRP	Donkey	Western blot (1:25,000)		Jackson Immunoresearch
PE-conjugated anti-mouse	Goat	Flow cytometry (1:100)	Absorbance at 545nm	Jackson Immunoresearch

2.7. Apoptosis Assays

2.7.1. Loss of Mitochondrial Membrane Potential

Following the apoptotic trigger, cells were stained with 0.3 μM TMRE (Thermofisher) for 30 mins at 37 °C. TMRE positive cells were measured through the FL-2 channel equipped with a 586/15 nm filter and GFP positive cells were measured through the FITC channel equipped with 530/30nm filter. Data was acquired by counting 30,000 cells was performed on a BD LSRFortessa. Dividing the total number of EGFP positive and TMRE negative cells by the total number of EGFP positive cells determined the percentage of cells undergoing mitochondrial dysfunction. Standard deviations were determined from three independent experiments. Statistical significance was calculated using Student's-T-test.

2.7.2. PARP Assay

To study poly-ADP ribose polymerase (PARP) cleavage assay, Jurkat cells ($1x10^6$) or MEF cells were lysed at the indicated time and following the appropriate stimuli in SDS-PAGE sample buffer containing 8M urea. Samples were subjected to SDS-PAGE and immunoblotted with anti-PARP, anti-β-tubulin, and anti-I3L antibody.

2.7.3. Cytochrome c Release Assay

After the STS apoptotic stimuli, cells were permiablized using digitonin permeabilition buffer (5mM NaCl, 1mM NaH_2PO_4, 8mM Na_2HPO_4, 250mM sucrose, and 190μg digitonin/mL (Sigma-Aldrich) for 10 min on ice. Mitochondrial and cytoplasmic

fraction were separated by centrifugation for 10 minutes. The mitochondrial pellet was resuspended in Triton-X-100 lysis buffer containing 25mM Tris pH8.0 and 0.1% Triton-X-100 (Fisher Scientific). Mitochondrial and cytoplasmic fraction were subjected to SDS-PAGE and blotted with anti-cytochrome c antibody.

2.7.4. Detection of DNA fragmentation by TUNEL

Apoptosis was stimulated using 2μM STS for 2 hrs for Jurkat cells, or 3 hrs for MEF cells. To induce apoptosis with UV-light, cells were subjected to 200 mJ/cm^2 of UV-C in PBS without a lid using a Stratalinker UV Crosslinker (Stratagene), supplemented with fresh media and allowed to recover for the indicated times. Post infection, the cells were fixed with 4% PFA. The fixed cells were stained with 25U of TUNEL enzyme per manufacturer's instructions (Roche Diagnostics). Cells were washed with PBS containing 1% (v/v) FBS and analyzed on a BD LSRFortessa flow cytometer. In each experiment 50,000 cells were analyzed. TUNEL positive cells were counted through the FL-2 channel equipped with a 561nm filter (586/15 nm band pass), and data were analyzed with FlowJo (Tree Star, Inc.).

2.7.5. Bak and Bax activation

Post the appropriate apoptotic stimulation, cells were permeabilized using 500μM digitonin and stained with 2μg/mL Bak AB-1 or 3μg/mL Bax6A7 antibody or 2μg/mL of an isotype control antibody specific for NK1.1. The cells were counter stained with a Phycoerythrin-conjugated antibody before analysis on a BD LSRFortessa flow cytometer using the FL-2 channel equipped with a 586/15 nm filter. Phycoerythrin-conjugated

antibody was used to counterstain cells before analysis on BD LSRFortessa using the FL-2 channel equipped with a 586/15 nm filter and 50,000 cells were analyzed using FlowJo (TreeStar, Inc.).

2.8. Microscopy methods and techniques

HeLa cells for live cell imaging growing in chambered coverglass dishes (Nunc) were used for all live cell imaging experiments. The HeLa cells were transfected using Lipofectamine 2000 with 2μg of pEGFP, EGFP-EVM025 and EGFP-EVM025(1-255) for 14 hrs.. Fourteen hrs post transfection, the cells were stained with 50 nM MitoTracker Red CMXRos (Invitrogen) for 30 minutes, washed three times with PBS+2%FBS, and covered with warm HeLa medium containing 20mM HEPES pH-7.4. All images were obtained using the Olympus IX-81 spinning disk confocal microscope. Images were analyzed using Image J software.

2.9. Animal Assays

2.9.1 Animals used in the study

All animal husbandry and experimental procedures were performed in St. Louis University in collaboration with Dr. Mark Buller. The protocols were in accordance with PHS policy, and approved by the St. Louis Institutional Animal Care and Use Committee. The University of Alberta Animal Ethics Committee also approved the protocols in this study as a part of the collaborative work. Six to eight week old female BALB/c, SCID and Nude mice were obtained from Taconic, USA. The animals were housed in filter-

top microisolator cages and fed commercial mouse chow and water, ad libitum. The mice were housed in an animal biosafety level 3 containment area.

2.9.2. Infection of mice

BALB/c mice were infected with 600, 6000 or 10^5 PFU of the indicated viruses subcutaneously (s.c.). These mice were anesthetized with CO2/O2 prior to infection. ECTV was diluted in PBS without Ca2+ and Mg2+ to the required PFU/mL and 10µl was used to infect mice via footpad injection. Nude and SCID mice were infected with 600 PFU s.c.. The mice were monitored daily for signs of mouse pox infection such as coat conditions, body paralysis limb swelling and body weight. Mice were monitored for body weight daily for up to 21 days. Mice that demonstrated a drop in body weight to 70% of their original mass, or mice that exhibited severe disease or signs of extreme distress were euthanized. The mortality was used to calculate the LD-50 and also the virulence of each of the ECTV strain.

2.9.3. Virus titration of organs

BALB/c mice were infected with 600 PFU s.c. as previously mentioned. The mice were euthanized 2, 4, and 7 days post infection for organ and serum collection. Popliteal lymph node (P-LN), spleen, lung, liver, kidney were collected in PBS. The organs were weighed and homogenized for 5 minutes at room temperature using Bullet Blender Homogenizer (STL Scientific). The homogenates were subjected to three rounds of freeze thaw to release the virus. Each tube was then centrifuged at 1000g for 3 minutes,

and the supernatant was used to perform the titration on BSC-1 cells as mentioned in section 2.5.3. Virus levels were reported as pfu/g of organ.

To determine the viral load in the footpad and P-LN, BALB/c mice were infected with 600 PFU s.c. as previously mentioned. Footpad and P-LN were harvested and DNA was extracted using the DNeasy Blood & Tissue Kit (Qiagen). The DNA was quantified, and 1µg of DNA was used for Quantitative PCR (qPCR). qPCR was performed on tissue DNA samples using the Power SYBR Green PCR Master Mix on a 7500 Real Time PCR System (Applied Biosystems, Foster City, CA) [83]. The primers (10 pmol) SP028 (GTAGAACGACGCCAGAATAAGAATA, 5′ at 120627 bp) and SP029 (AGAAGATATCAGACGATCCACAATC, 5′ at 120462 bp) were used to amplify 165 bp of gene EV107. The amplification product cloned into a pGEM-T (Promega) was used as a standard to estimate copies of DNA/1µg of total DNA of the harvested organ. Each sample was assayed in triplicate.

2.9.4. Cytokine Analysis

Serum samples were collected from infected mice at day 4 and 7 post infection. The serum sample were processed according to manufactures' instructions for 32 cytokines simultaneously using a Milliplex array (Millipore). The following cytokines and chemokines were measured: Eotaxin (CCL11), granulocyte colony-stimulating factor (G-CSF), GM-CSF, IFN-γ, interleukin-1α (IL-1α), IL-1β, IL-2, IL-3, IL-4, IL-5, IL-6, IL-7, IL-9, IL-10, IL-12p40, IL-12p70, IL-13, IL-15, IL-17, IFN-γ-inducible protein (IP)-10 (CXCL10), keratinocyte-derived chemokine (KC/CXCL1), LIF, lipopolysaccharide (LPS)-induced chemokine (LIX/CXCL5), MCP-1 (CCL2), M-CSF, mitogen-inducible

gene (MIG/CXCL9), MIP-1α (CCL3), MIP-1β (CCL4), MIP-2 (CXCL2), RANTES (CCL5), tumor necrosis factor alpha (TNF-α), and vascular endothelial growth factor (VEGF). ELISA (R&D) determined samples that were out of range for LPS-induced chemokine (LIX/CXCL5) from multiplex analysis.

2.9.5. Flow-cytometer

Whole blood or splenocytes were harvested at day 7 post infection from mock infected mice, and from mice infected with ECTV, ECTVΔ025 and ECTVΔ025rev virus. Whole blood RBCs were lysed using BD Pharm Lyse (BD Pharmingen). The remaining white blood cells were suspended in PBS with 2% FBS. The spleen tissues were harvested from euthanized mice, and disrupted with a Bullet Blender (STL Scientific) for ~2 minutes at room temperature using the lowest setting in PBS. The cells suspension was filtered and the cells were suspended in PBS with 2% FBS. Cells were stained with Fixable Viability Dye eFluor® 506 (eBioscience). Cells were stained for flow cytometry using Anti-Mouse CD16/CD32 (Fc Block) (eBioscience) and the described antibody cocktail in PBS with 2% FBS for 20–30 minutes on ice. Cells were washed twice with PBS containing 2% FBS then fixed on ice with PBS containing 2% FBS and 1% methanol free formaldehyde. Stained cells were analyzed on a BD LSRII. The antibody cocktail used for this study are in table 2.4.

Table 2.4 – List of Antibody used in Animal Studies

Specificity	Clone	Fluorophore	Source	Catalogue No.
CD4	GK1.5	eFluor450	eBioscience	48-0041
CD8	53-6.7	BV605	BD	563152
CD3 (145-2C11 PerCP-Cy5.5)	145-2C11	PerCP-Cy5.5	eBioscience	45-0031
IL-2	JES6-5H4	PE-Cy7	eBioscience	25-7021
CD49b (NK)	DX5	APC	eBioscience	17-5971
CD44	IM7	AF700	eBioscience	56-0441
IFN-γ	XMG1.2	APC-Cy7	BD	561479

2.10. Statistical Analysis

Statistical analysis of data was performed using Graphpad Prism V6. Analysis of variance (ANOVA) tests with either one-way, or two-way tests were used to compare data comprising multiple viruses or time points. For analyses comparing two groups of data a student's T-test, either paired or unpaired was used. Survival curve comparisons were calculated using the Log-Rank (Mantel-Cox) test built into the software. * $P<0.05$, ** $P<0.01$ and *** $P<0.001$.

Chapter-3-Ectromelia virus encodes an anti-apoptotic protein

Portions of this chapter have been published:
Mehta, N., Taylor, J., Quilty, D., & Barry, M. (2015). Ectromelia virus encodes an anti-apoptotic protein that regulates cell death. *Virology*, *475*(c), 74–87.

The experiments for this chapter were performed under the supervision of Dr. Michele Barry, and the manuscript was reviewed and written under the supervision of Dr. Jim Smiley.
The ECTVΔ025ΔCrmA mutant was generated John Taylor. The initial cloning for the ECTVΔ025 deletion mutant was done by John Taylor and Douglas Quilty. All the experiments presented in this chapter were done by Ninad Mehta. The repeats for section 3.2.8 were performed by Megan Brown, a undergraduate honors student mentored by Ninad Mehta

3.1. Introduction

Ectromelia virus (ECTV) is the causative agent of mousepox and a member of the Orthopoxvirus family that is closely related to VACV and variola virus [38]. Being a member of the Orthopoxvirus family, we suspected that ECTV also encoded an inhibitor of the intrinsic apoptotic pathway. Using genome analysis we identified EVM025. Based on the C-terminal homology between EVM025 and F1, we hypothesized that EVM025 could inhibit apoptosis. Here we report that human and mouse cells infected with ECTV are resistant to staurosporine (STS) and UV-induced apoptosis. We generated a recombinant ECTV lacking a functional EVM025 that replicated efficiently in tissue culture but was unable to protect against staurosporine-induced apoptosis. Expression of EVM025 is critical for maintaining the mitochondrial membrane potential and inhibiting apoptosis during viral infection. EVM025 localizes to the mitochondria through the C-terminal transmembrane domain and prevents Bak activation. EVM025 prevents Bax activation by sequestering the BH3-only protein Bim. Collectively, our data suggest that the ECTV protein EVM025 is a inhibitor of the intrinsic apoptosis pathway, which functions together with other viral anti-apoptotic proteins to prolong the life of an infected cell.

3.2. Results

3.2.1 Ectromelia virus infection inhibits apoptosis

ECTV encodes a known anti-apoptotic protein, CrmA, that inhibits caspase-8 activation following treatment with TNFα or FasL, but CrmA is unable to inhibit the intrinsic apoptotic cascade [118,119]. To determine whether ECTV has the ability to inhibit the intrinsic apoptosis pathway, we treated poxvirus-infected cells with STS (staurosporine), a compound that exclusively triggers induction of the intrinsic apoptosis pathway[188]. Jurkat cells were either mock-infected (Fig. 3.1, panel a, b), infected with VACVCop (Fig. 3.1, panel c, d), or ECTV (Fig. 3.1, panel e, f). Six hrs post infection the cells were treated with 2μM STS to induce apoptosis (Fig. 3.1, panel b, d, f, h). Jurkat cells constitutively expressing Bcl-2 were used as a positive control (Fig. 3.1, panel g, h). Mock-infected Jurkat cells, cells infected with VACVCop or ECTV, and Jurkat-Bcl-2 were left untreated and displayed basal levels of DNA fragmentation indicative of healthy cells (Fig. 3.1, panel a, c, e, and g). Jurkat cells treated with STS exhibited an increase in fluorescence that is characteristic of DNA fragmentation and apoptosis (Fig. 3.1, panel b). Infection with VACVCop inhibited STS induced DNA fragmentation (Fig. 3.1, panel c and d). Additionally, cells infected with ECTV were also protected against STS induced apoptosis (Fig. 3.1, panel d and e).

Since mice are the natural hosts of ECTV, we assessed the ability of ECTV to block cell death in murine cells (MEFs). MEFBak$^{-/-}$Bax$^{-/-}$ cells were used as a positive control since they are resistant to mitochondrial apoptosis [101,189]. Untreated MEF and MEFBak$^{-/-}$Bax$^{-/-}$ cells, as well as MEF cells infected with VACVCop or ECTV were

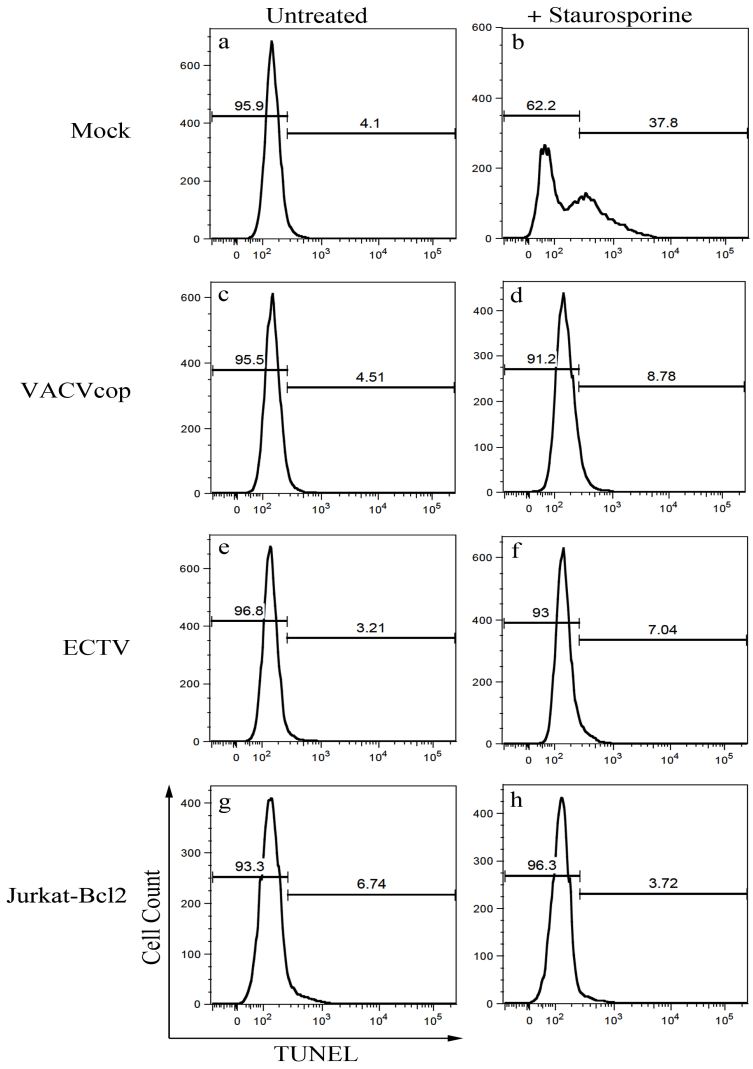

Figure 3.1- ECTV infection inhibits STS induced apoptosis in Jurkat cells. Jurkat cells were either mock-infected (a, b), infected with VACVcop (c, d) or infected with ECTV (e, f) at an MOI of 5. Jurkat cells overexpressing Bcl-2 were also mock-infected (g, h). After 6 hours of infection cells were either treated with 2μM STS for 120 min to induce apoptosis (b, d, e, h) or mock-treated (a, c, e, g). Apoptosis was assessed by TUNEL fluorescence. Untreated controls showed low levels of TUNEL fluorescence, while mock-infected cells exposed to Staurosporine (STS) were TUNEL positive due to DNA fragmentation. Data are representative of at least three independent experiments.

stained using the TUNEL labeling kit, and displayed minimal basal levels of DNA fragmentation (Fig. 3.2, panel a, c, e, and g). MEF cells treated with STS exhibited an increase in TUNEL fluorescence characteristic of apoptosis (Fig. 3.2, panel b). Infection with either VACVCop or ECTV significantly inhibited STS-induced DNA fragmentation in MEF cells (Fig. 3.2).

UV-light potently induces the intrinsic apoptotic cascade and readily induces Bax activation [190,191]. Infections were carried out as previously mentioned in both human and mouse cell lines with VACV, or ECTV. Six hrs post infection the cells were subjected to 200 mJ/cm^2 of UV-C in PBS to induced apoptosis. The cells were allowed to recover for 5 hrs, and the cells were stained with the TUNEL kit. These experiments followed a similar trend as what was observed in cases of STS induced apoptosis. Uninfected Jurkat cells (Fig 3.3) and uninfected J774 (Fig. 3.4) cells were susceptible to UV induced apoptosis. VACV and ECTV infected Jurkat cells (Fig 3.3) and J774 (Fig. 3.4) were protected against UV induced apoptosis.

Intrinsic apoptosis is associated with the activation and cleavage of caspase-3 and poly-ADP ribose polymerase (PARP)[192]. Caspase-3 is an initiator caspase, while PARP is a nuclear protein that is cleaved upon caspase activation [192,193]. To confirm that ECTV can inhibit the intrinsic apoptotic cascade, we monitored caspase-3 and PARP activation following treatment with STS. Jurkat cells were mock infected, or were infected with VACVCop or ECTV at an MOI of 5. Six hrs post-infection, cells were treated with 2μM STS for 2, 4 or 6 hrs to trigger apoptosis. Activated caspase-3 and cleaved PARP were detected in mock-infected Jurkat cells treated with STS two hrs post-treatment, and PARP was completely processed into the cleaved form following four hrs of STS

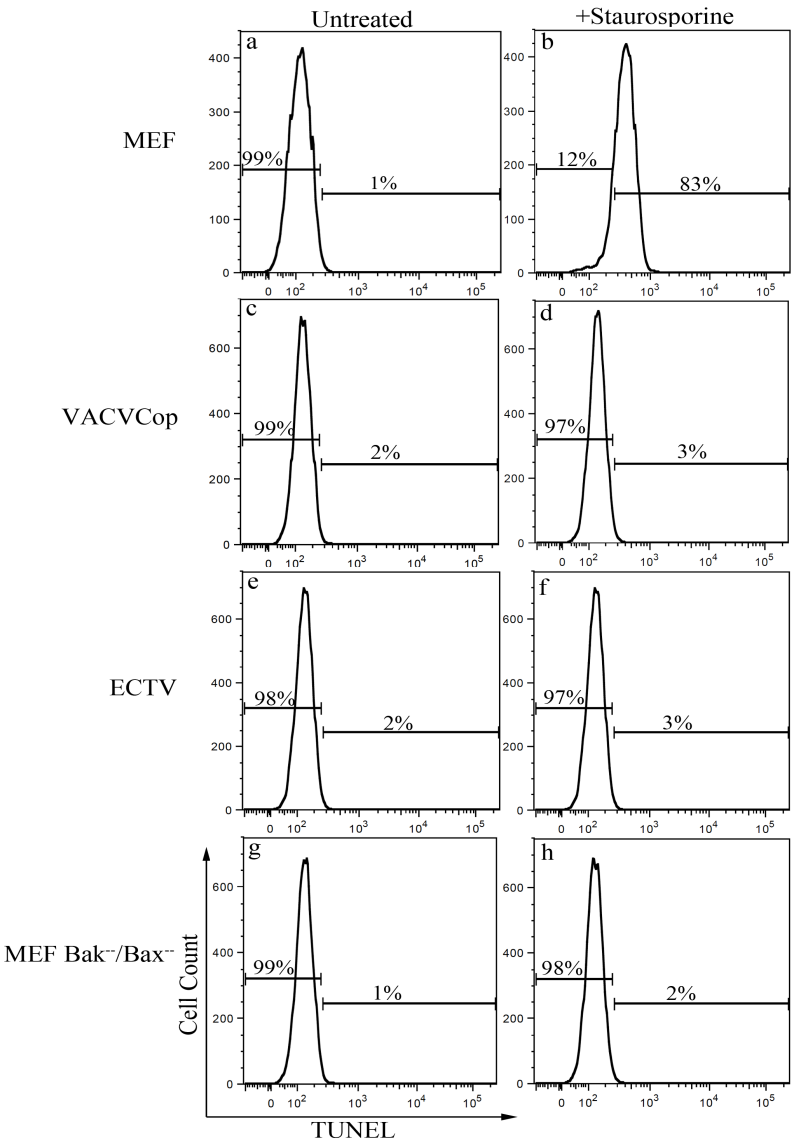

Figure 3.2- ECTV infection inhibits STS induced apoptosis in MEF cells. MEF cells were either mock-infected (a, b), infected with VACVCop (c, d) or ECTV (e, f) at an MOI of 5. MEFBak$^{-/-}$Bax$^{-/-}$ cells were mock-infected (g, h). Six hours post-infection cells were treated with 3μM STS for 120 min to induce apoptosis. Apoptosis was assessed by TUNEL fluorescence. Untreated controls showed low levels of TUNEL fluorescence, while mock-infected cells exposed to Staurosporine (STS) were TUNEL positive due to DNA fragmentation. Data are representative of at least three independent experiments.

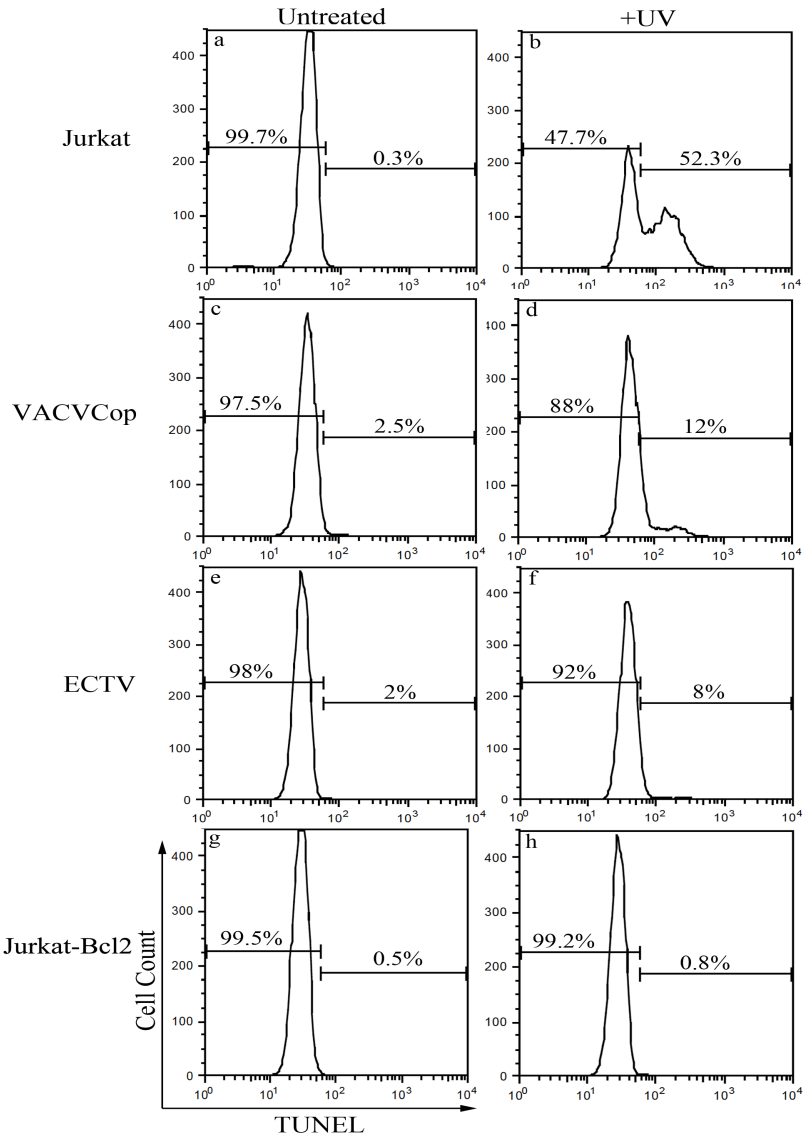

Figure 3.3- ECTV infection inhibits UV induced apoptosis in Jurkat cells. Jurkat cells were either mock-infected (a, b), infected with VACVcop (c, d) or infected with ECTV (e, f) at an MOI of 5. Jurkat cells overexpressing Bcl-2 were also mock-infected (g, h). After 6 hours of infection cells were either treated with 200 mJ/cm of UV to induce apoptosis. The cells were incubated for 5 hours. Apoptosis was assessed by TUNEL fluorescence. Untreated controls showed low levels of TUNEL fluorescence, while mock-infected cells exposed to Staurosporine (STS) were TUNEL positive due to DNA fragmentation. Data are representative of at least three independent experiments.

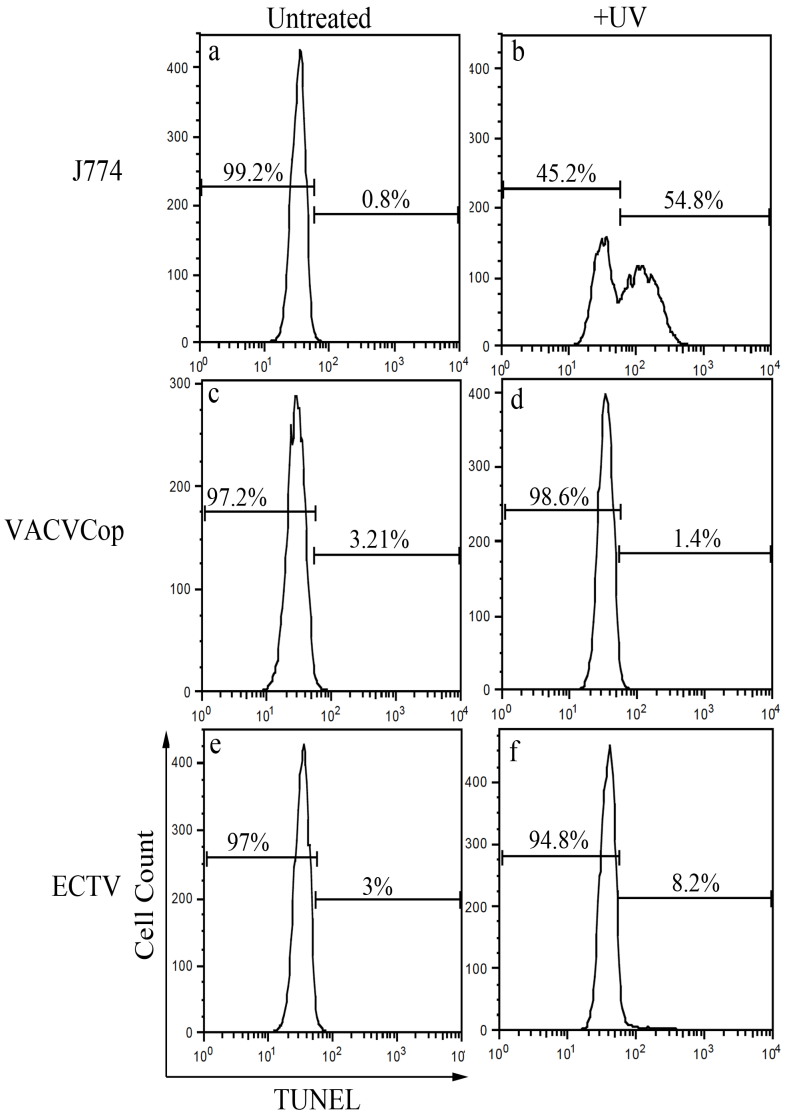

Figure 3.4 - ECTV infection inhibits UV induced apoptosis in J744. J744 were either mock-infected (a, b), infected with VACVcop (c, d) or infected with ECTV (e, f) at an MOI of 5. After 6 hours of infection cells were either treated with 200 mJ/cm of UV to induce apoptosis. The cells were incubated for 5 hours. Apoptosis was assessed by TUNEL fluorescence. Untreated controls showed low levels of TUNEL fluorescence, while mock-infected cells exposed to Staurosporine (STS) were TUNEL positive due to DNA fragmentation. Data are representative of at least three independent experiments.

treatment (Fig. 3.5). In contrast, infection of Jurkat cells, with either VACVCop or ECTV prevented the activation of caspase-3 and PARP following STS treatment.

These data would suggest that ECTV is capable of inhibiting apoptosis triggered by STS and UV; two stimuli that are specific to the intrinsic pathway in both human and murine cell lines.

3.2.2. ECTV encodes EVM025 a homologue of VACV F1

VACV encodes F1, an inhibitor of mitochondrial apoptosis [134,138,139,141], and orthologues of F1 are only found within members of the Orthopoxviridae (Fig. 3.6). EVM025, the ectromelia virus (ECTV Moscow) orthologue, is 95% identical to F1, but encodes a large N-terminal extension comprised of up to 30 copies of an eight amino acid motif, "Asp-Asn-Gly-Ile-Val-Gln-Asp-Ile" (DNGIVQDI). This eight amino acid motif is also present twenty-five times in EVM025 from ECTV strain Naval, and so far is unique to EVM025 of ectromelia virus as it is absent in other orthopoxvirus F1 orthologues, nor is it present in any other known cellular or viral proteins. Intriguingly, variola virus (VARV) Garcia orthologue of F1 also contains a large N-terminal extension, consisting of 36 aspartic acid-rich repeats (DDI) that are absent in VARV Bangladesh, and the function of these repeat regions is currently unknown.

The C-terminal half of EVM025 shares 95% sequence identity with VACV Cop F1, although there are multiple substitution mutations, as well as a single DI insertion mutation (Fig 3.6). Given the high degree of sequence identity between F1 and EVM025, we hypothesized that EVM025 might also act as an anti-apoptotic protein to facilitate ECTV pathogenesis.

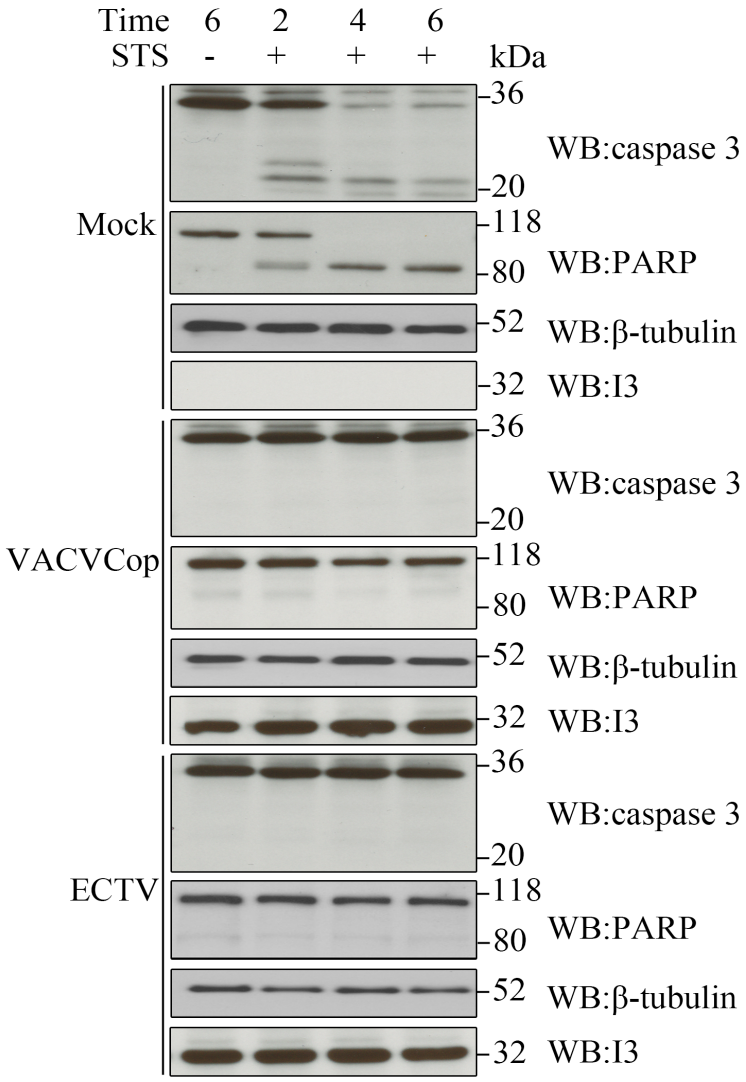

Figure 3.5 - ECTV protects cells from staurosporine-induced apoptosis. Jurkat cells were mock infected or infected with VACVcop and ECTV at an MOI of 5. Six hours post infection cells were treated with 2μM STS. Samples were collected 2, 4, and 6 post STS treatment. The cells were lysed in 1% NP40. Samples were subjected to SDS-PAGE and immunoblotted for PARP and Caspase 3 to determine the trigger of apoptosis; β-tubulin was used as a loading control and I3L as a control of infection.

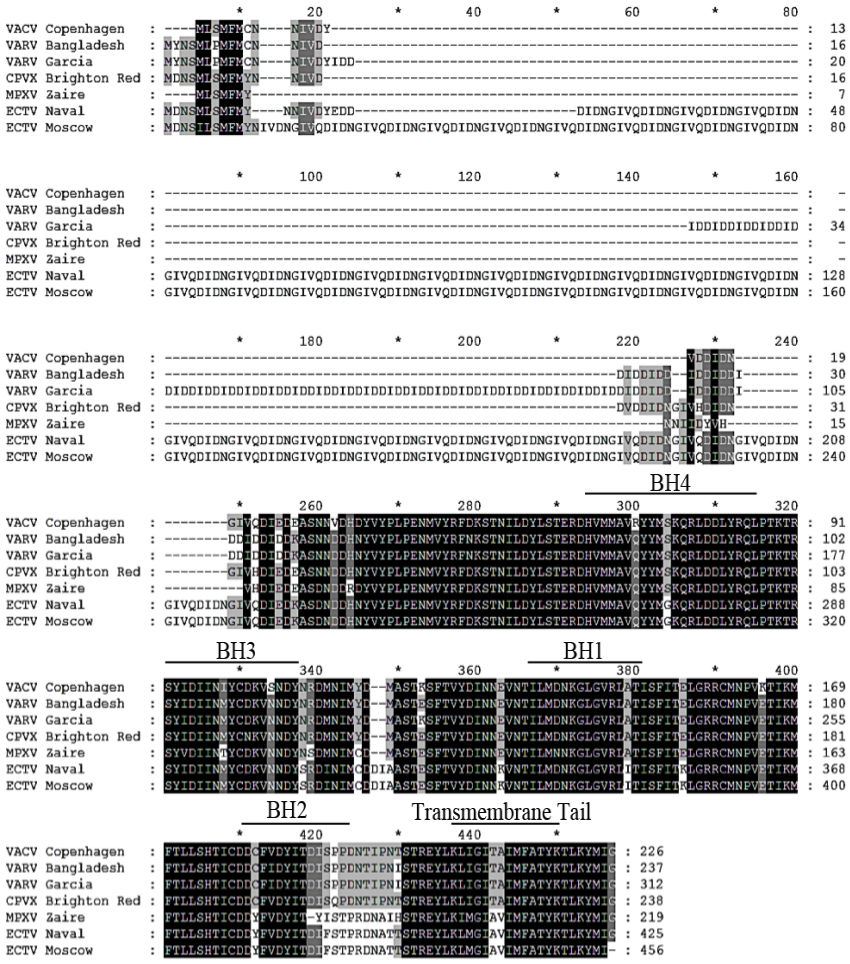

Figure 3.6 - Sequence alignment of EVM025 and its orthologs. Sequence alignment of the following orthologs: VACVCop F1L (AAA48014), VARV Bangladesh C5L (AAA60773), VARV Garcia E1L (CAB54625), CPXV Brighton Red CPXV048 (NP_619836.1), MPXV Zaire C7L (AAY97031), ECTV strain Naval EVM025 (VP0042282), and ECTV strain Moscow EVM025 (NP_671543). Sequence alignments were generated using the ClustalW program with a BLOSUM32 matrix. The conserved BH (BH homology) domains and transmembrane tail of the proteins are marked with the over-lines. The black shaded regions are amino acids conserved though all the proteins. The grey shaded regions are amino acids conserved among most proteins.

3.2.3. EVM025 expression protects cells against intrinsic apoptosis

To further elucidate the anti-apoptotic mechanism of EVM025 and its importance in modulating the cellular apoptotic response during virus infection, we generated two recombinant viruses; one virus that is devoid of EVM025 (ECTVΔ025), and a double deletion virus that is missing both EVM025 and CrmA (ECTVΔ025/ΔCrmA). The genetic profile and purity of the knockout and revertant (ECTVΔ025rev) virus were confirmed by PCR in MEF cells (Fig. 3.7b).

To determine the contribution of EVM025 during virus infection, MEF cells were mock-infected or infected with ECTV, ECTVΔ025, ECTVΔCrmA, ECTVΔ025/ΔCrmA and ECTVΔ025rev at a MOI of 5. After 6 hrs of infection the cells were treated with 2μM STS for an additional 2 hrs to trigger apoptosis, and the mitochondrial membrane potential was monitored using TMRE staining [194,195]. In the absence of STS treatment, mock-infected cells retained TMRE in healthy respiring mitochondria and demonstrated high levels of TMRE fluorescence (Fig. 3.8, panel a). In contrast, mock-infected cells treated with STS showed a clear loss of TMRE fluorescence, indicative of the loss of inner mitochondrial membrane potential and apoptosis (Fig. 3.8, panel a). MEF cells infected with ECTV were protected against the loss of inner mitochondrial membrane potential following STS treatment (Fig. 3.8, panel b). Interestingly, loss of TMRE fluorescence was observed in MEF cells infected with ECTVΔ025 and subsequently treated with STS (Fig. 3.8, panel c). Similar to ECTV, MEF cells infected with ECTVΔCrmA and ECTVΔ025rev were protected against loss of mitochondrial respiration upon STS treatment. However, MEF cells infected with

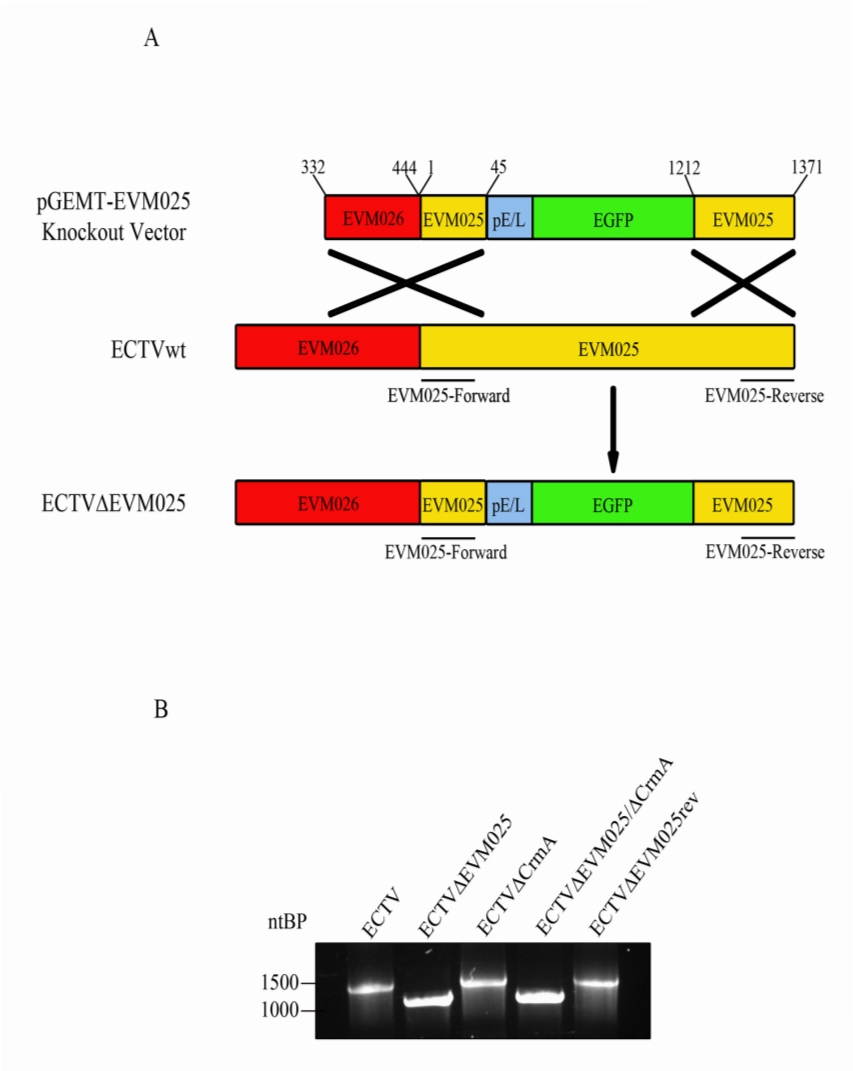

Figure 3.7 - Characterization of the recombinant ECTV devoid of EVM025. (A) Schematic Diagram of the strategy employed for the generation of ECTVΔ025 virus. The binding site of the EVM025 sequencing primers is also indicated in the figure. (B)Viral DNA was extracted from BGMK cells infected with ECTV, ECTVΔ EVM025, ECTVΔCrmA, ECTVΔEVM025/ΔCrmA, and ECTVΔEVM025rev. Successful deletion of EVM025 was confirmed by PCR using EVM025-Forward primer and EVM025-reverse primer.

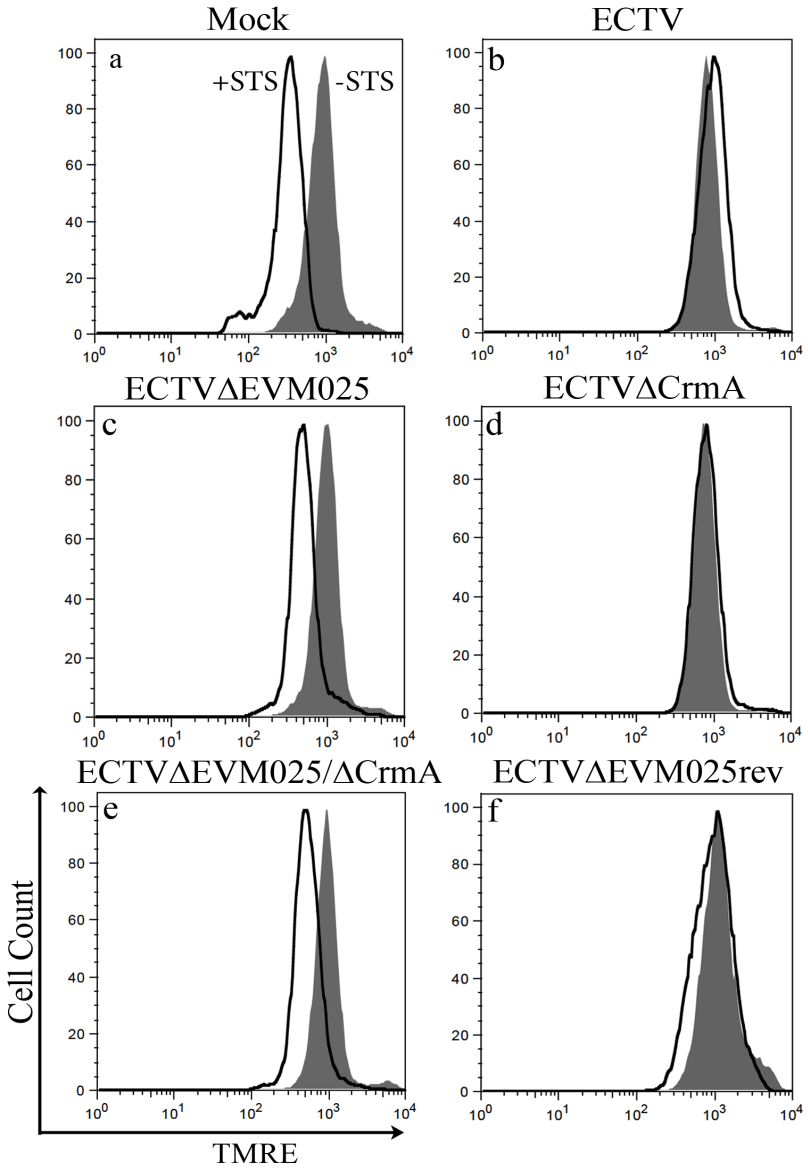

Figure 3.8 - EVM025 ORF is required to prevent STS induced loss of mitochorial membrane potential during infection. EVM025 protects cells from STS-induced loss of the outer mitochondrial membrane potential. Jurkat cells were mock-infected (a), infected with ECTV (b), ECTVΔ025 (c), ECTVΔCrmA (d), ECTVΔ025/ΔCrmA (e), or ECTVΔ025rev (f) at an MOI of 5. Six hours post-infection cells were treated with 2μM staurosporine for 90 mins or mock-treated and stained with 2μM of TMRE. Untreated cells, (shaded histogram); staurosporine treated cells, open histogram. Data are representative of three independent experiments. Apoptosis was assessed by TMRE fluorescence, which measures loss of the inner mitochondrial membrane potential.

ECTVΔ025/ΔCrmA were unable to maintain the inner mitochondrial membrane potential. These data indicate that EVM025, and not CrmA, is required for ECTV to inhibit STS-induced apoptosis.

Following loss of mitochondrial membrane potential, cytochrome c is released which triggers the activation of the apoptosome leading to intrinsic apoptosis [99]. We next assessed the role of EVM025 in preventing cytochrome c release during virus infection. Jurkat cells were infected with ECTV, ECTVΔ025, ECTVΔCrmA, and ECTVΔ025/ΔCrmA, treated with 2μM STS and analyzed at 2, 4, and 6 hrs post-stimulation (Fig. 3.9) for cytochrome c release analysis by western blot. While cytochrome c was rapidly released from mitochondria into the cytosol in mock-infected cells treated with STS (data not shown), Cytochrome c was retained in the mitochondria of ECTV-infected Jurkat cells, indicating that ECTV protected cells from STS-induced cytochrome c release. Similar protection was also observed in Jurkat cells infected with ECTVΔCrmA. In contrast, cells infected with ECTVΔ025 or ECTVΔ025/ΔCrmA and treated with STS demonstrated abundant cytosolic cytochrome c. Together these data suggest that EVM025 is important in preserving the mitochondrial membrane integrity to block apoptosis.

Jurkat cells were analyzed for STS-induced PARP cleavage after infection with ECTV, ECTVΔ025, ECTVΔCrmA, and ECTVΔ025/ΔCrmA. Mock-infected Jurkat cells rapidly processed full length PARP into the cleaved form upon STS treatment. Four hrs post-STS treatment full-length PARP was completely converted into the 89kDa cleaved form (Fig. 3.10). Infection was confirmed using an antibody to the early ECTV protein I3L, and β-tubulin was used as a loading control (Fig. 3.10). As expected, ECTV and

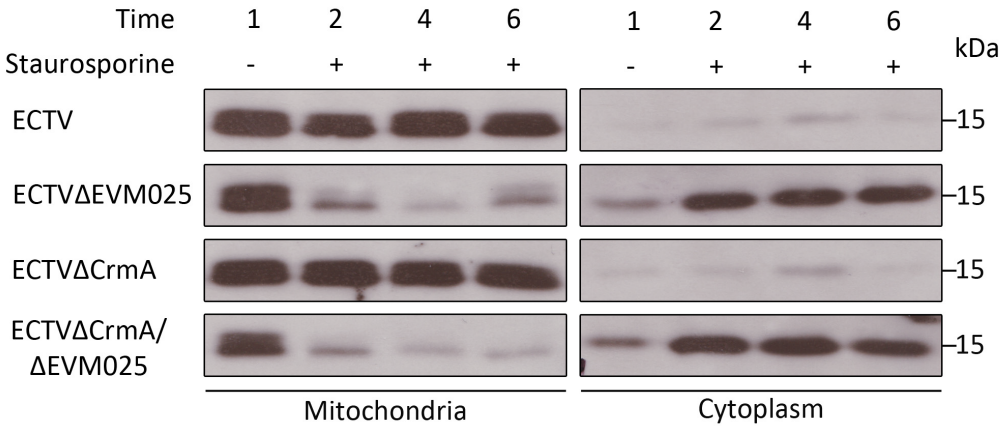

Figure 3.9 - EVM025 ORF is required to prevent STS induced Cyto-c release during ECTV infection. EVM025 expression inhibits STS induced cytochrome c release. Jurkat cells were infected with ECTV, ECTVΔ 025, ECTVΔCrmA, and ECTVΔ025ΔCrmA at an MOI of 5 for 6 hours. Six hours post-infection, the samples were treated with 2μM STS. Cells were collected at 2, 4, and 6 hours post-STS treatment. The cytosolic fraction was obtained by permeabilization using digitonin. The pellet fraction was resuspended in 0.1% Triton lysis buffer. Both the pellet and the supernatant fraction were immunoblotted with anti-cytochrome c.

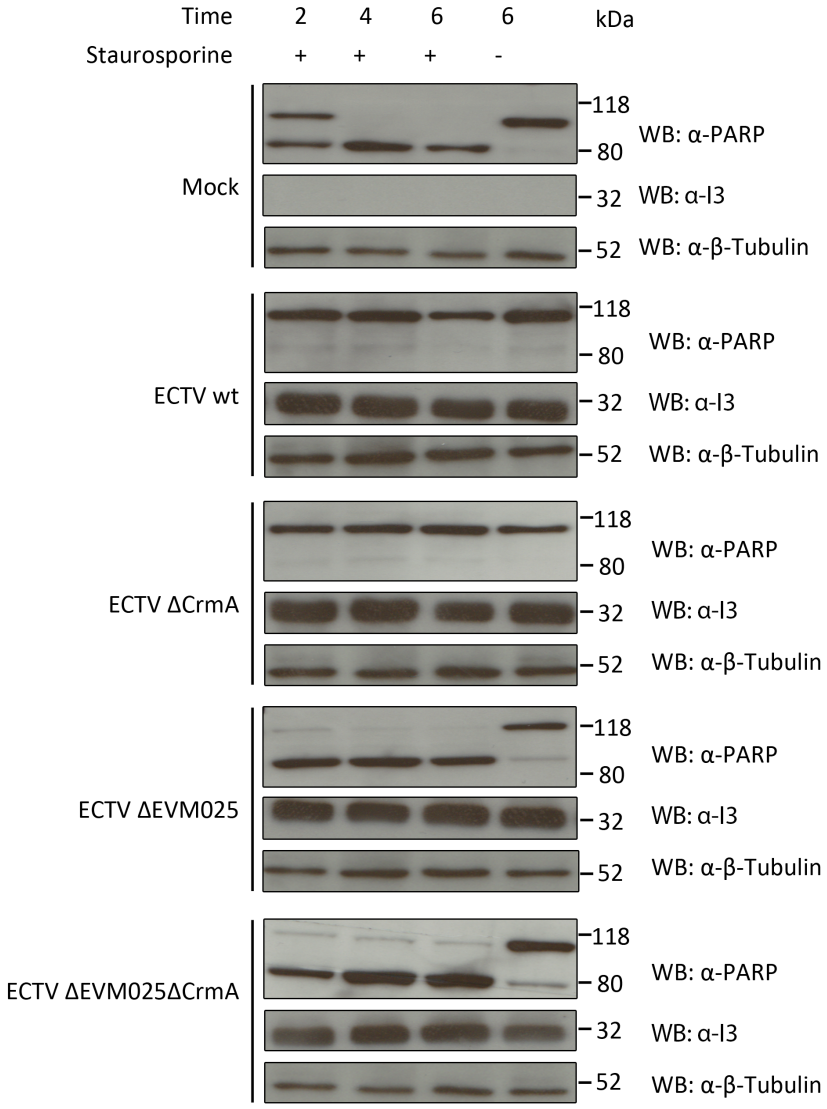

Figure 3.10 - EVM025 ORF is required to prevent STS induced PARP cleavage during infection. Jurkat cells were mock-infected, infected with ECTV, ECTVΔCrmA, ECTVΔ025, or ECTVΔ025/ΔCrmA at an MOI of 5. Six hours post-infection, samples were treated with 2μM STS. Cells were collected at 2, 4, and 6 hours post STS treatment, and cells were lysed in RIPA buffer and reduced in SDS sample buffer containing 8 M urea. Samples were subjected to SDS-PAGE and immunoblotted for PARP. β-tubulin was used as a loading control and I3L as a control of infection.

a ECTVΔCrmA protected against STS-induced PARP cleavage. However, infection with ECTVΔ025 and ECTVΔ025/ΔCrmA was unable to protect against STS-induced PARP cleavage.

In addition to assessing the ability of ECTV to block STS-induced apoptosis, we also asked whether EVM025 was sufficient to protect against infection-induced cell death, as virus infection can induce apoptosis. MEF cells were either mock-infected or infected with ECTV, ECTVΔ025, ECTVΔCrmA, or ECTVΔ025/ΔCrmA. MEF cells infected with ECTV and ECTVΔCrmA showed no change in the amounts of full length PARP for 48 hrs post-infection. In contrast, MEF cells infected with ECTVΔ025 or ECTVΔ025/ΔCrmA induced PARP cleavage as early as 12 hrs post-infection, and by 36 hrs post-infection, no full length PARP was detected in these infected cells (Fig 3.11). These data indicate that EVM025 prevents the induction of apoptosis during ECTV infection. This experiment highlights the importance of EVM025 during in-vitro infection.

3.2.4. EVM025 is a tail-anchored protein that localizes to the mitochondria

The anti-apoptotic protein Bcl-2 possesses a C-terminal tail anchor that targets proteins to the mitochondrial membrane [98,108]. Sequence analysis of EVM025 confirmed the presence of a thirteen amino acid hydrophobic domain flanked by positively charged lysines at positions 436 and 450 in EVM025, suggesting that EVM025 localizes to the mitochondria. To evaluate whether EVM025 localizes to the mitochondria, HeLa cells were transfected with either pEGFP, pEGFP-EVM025, or pEGFP-EVM025(Δ438-453), a mutant construct that lacked the predicted transmembrane domain. Sixteen hrs post-

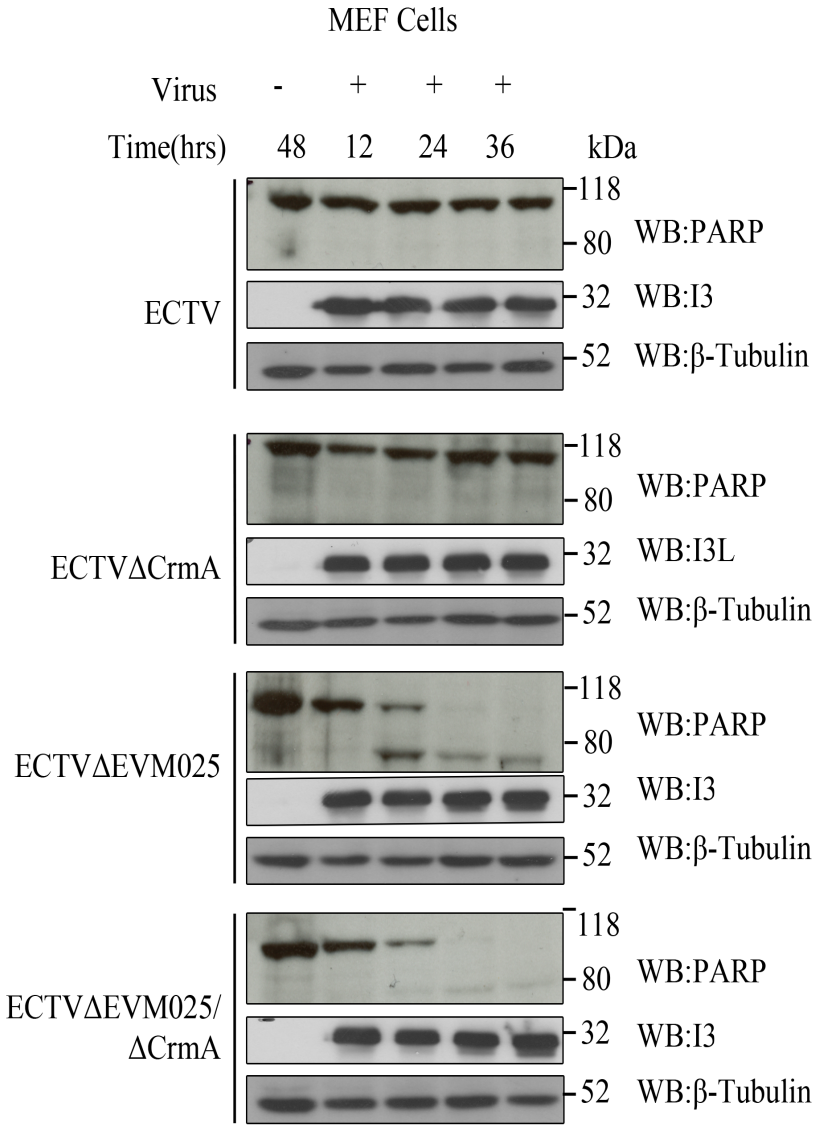

Figure 3.11 - EVM025 ORF is required to prevent apoptosis in MEF cells during infection. MEF cells were mock-infected or infected with ECTV, ECTVΔCrmA, ECTVΔ025, or ECTVΔ025/ΔCrmA at an MOI of 5. Cells were collected 12, 24, 36 and 48 hours post-infection, and lysed in SDS-PAGE sample buffer containing 8 M urea. Samples were subjected to SDS-PAGE and immunoblotted for PARP to determine virus induced apoptosis. β-tubulin was used as a loading control and I3L as a control for infection.

transfection cells were stained with MitoTracker to visualize the mitochondria (Fig. 3.12). Cells transfected with the control vector pEGFP showed a diffuse pattern of GFP expression (Fig. 3.12, panel e.). In contrast, cells transfected with pEGFP-EVM025 displayed a reticular fluorescence pattern that co-localized with mitochondrial staining (Fig. 312, panel g.). When the predicted transmembrane domain was removed (EVM025(Δ438-453)), a diffuse pattern similar to the empty vector was observed (Fig. 3.12, panel j). These data suggest that like Bcl-2, EVM025 is a mitochondria-localized protein, and this localization is dependent on the C-terminal transmembrane domain.

3.2.5. EVM025 interacts with Bak to prevent Bak activation

The activation of Bak is an essential step in the intrinsic apoptotic pathway that precedes the release of cytochrome c from the mitochondria [196,197]. Following an apoptotic stimulus, Bak undergoes a conformational change that results in the exposure of the N-terminus, resulting in destabilization of the outer mitochondrial membrane potential, loss of mitochondrial membrane integrity, and the release of molecules like cytochrome c and SMAC/Diablo [98]. To determine whether EVM025 could prevent the conformational change of Bak, we assessed Bak activation following apoptotic stimulation. Jurkat cells were either mock-infected or infected with ECTV, ECTVΔCrmA, ECTVΔ025, or ECTVΔ025/ΔCrmA, and activation of Bak and exposure of the Bak N-terminus was induced by STS treatment (Fig. 3.13). Exposure of the Bak N-terminus during Bak activation was detected with a conformation-specific anti-Bak AB-1 antibody and analyzed by flow cytometry. The Bak AB-1 is able to detect the

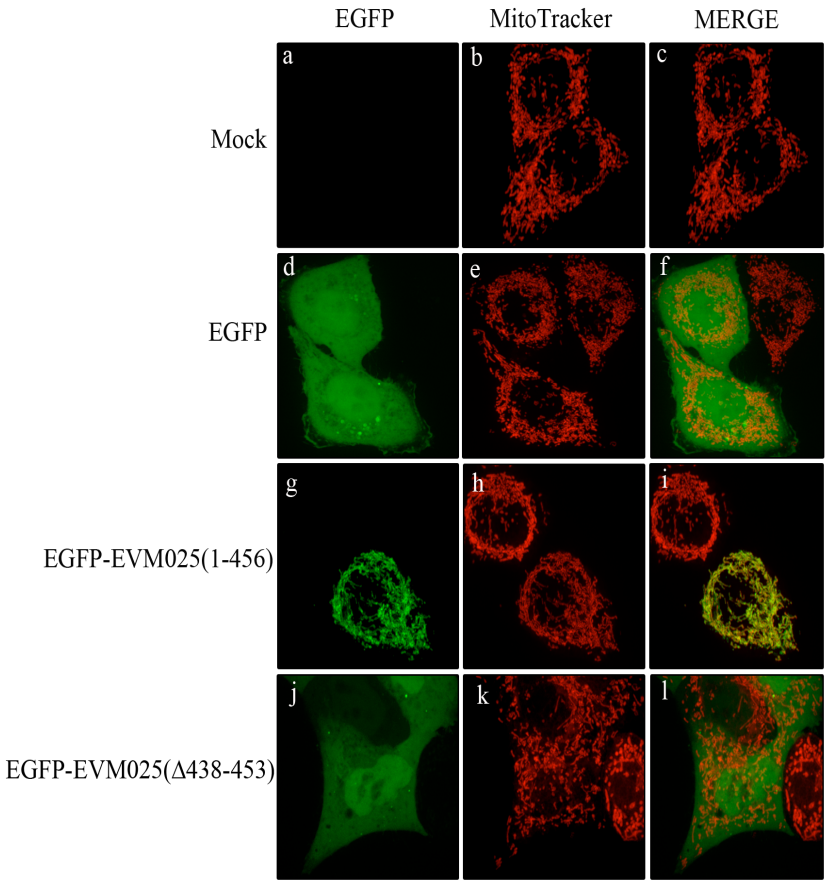

Figure 3.12 - EVM025 localizes to the mitochondria. HeLa cells were mock-infected transiently transfected with pEGFP, pEGFP-EVM025(1-456) or pEGFP-EVM025(Δ438-453). Fourteen hours post-transfection the mitochondria were stained with 15ng/ml of MitoTracker Red CMXRos (Invitrogen Corp.). The cells were observed under a spinning disc confocal microscope.

conformation change in the N-termius of Bak when it is activated. As expected, uninfected cells treated with STS exhibited a significant increase in fluorescence intensity (Fig. 3.13 panel a), indicating the conformational change and activation of Bak. Infection of Jurkat cells with ECTV or ECTVΔCrmA, on the other hand, inhibited the exposure of the Bak N-terminus following STS treatment (Fig. 3.13 A panel b). Infection with ECTVΔ025 and ECTVΔ025/ΔCrmA did not inhibit STS-induced Bak activation (Fig. 3.13, panels c and d), suggesting that EVM025 is necessary to inhibit the activation of Bak in infected Jurkat cells. We next determined if EVM025 could interact with the pro-apoptotic molecule Bak. BMK cells were transfected with pEGFP, pEGFP-Bcl-2, or pEGFP-EVM025. Cells were lysed in 2% CHAPS, a detergent known to preserve the conformational integrity of the Bcl-2 family members [198]. Immuno-complexes were precipitated using a GFP antibody and detected using anti-Bak antibody (Fig. 3.14). Interestingly, EGFP-EVM025 associated with endogenous Bak, while no Bak co-immunoprecipitation was seen with GFP alone. pEGFP-Bcl-2 also co-precipitated Bak, as has been demonstrated previously. Overall, our data suggests that EVM025 can associate with endogenous Bak.

Next, we asked whether EVM025 could inhibit the induction of apoptosis following Bak over-expression. Ectopic expression of Bak saturates the mitochondrial membrane resulting in the activation of the apoptotic cascade [102]. HeLa cells were co-transfected with HA tagged Bak, along with pEGFP, pEGFP-EVM025, or pEGFP-Bcl-2. Cells transfected with empty EGFP underwent a loss of TMRE fluorescence following over expression of HA-Bak (Fig. 3.15). Cells transfected with EGFP-EVM025, on the other hand, were protected from Bak-induced apoptosis (Fig. 3.15). Similar results were

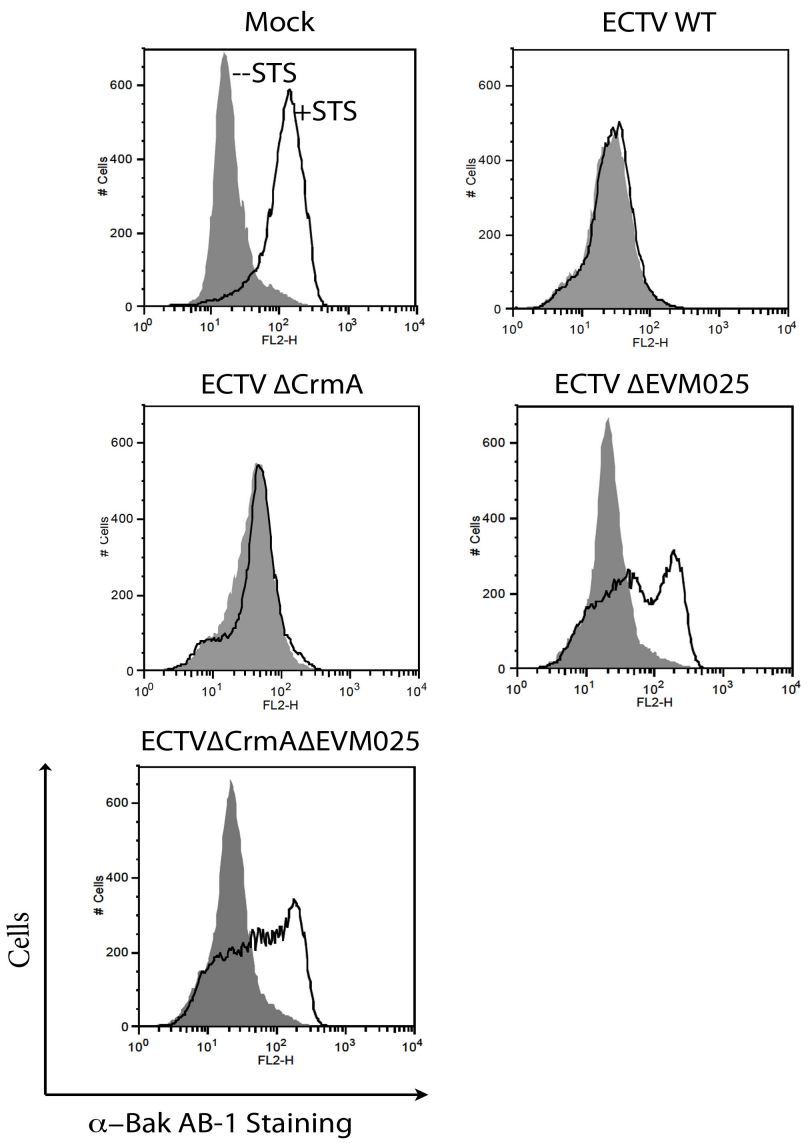

Figure 3.13 - EVM025 expression inhibits Bak activation. Jurkat cells were mock-infected (a), infected with ECTV (b), ECTVΔCrmA (c), ECTVΔ025 (e) or ECTVΔ025/ΔCrmA (f) at an MOI of 5 for 4 hours, followed by treatment with 0.25μM STS for 2 hours to induce apoptosis. Exposure of the N-terminus of Bak was monitored by flow cytometry using a conformation-specific N-terminal Bak Ab-1 antibody. Untreated cells, (shaded histogram); STS treated cells (open histogram). Data are representative of at least three independent experiments.

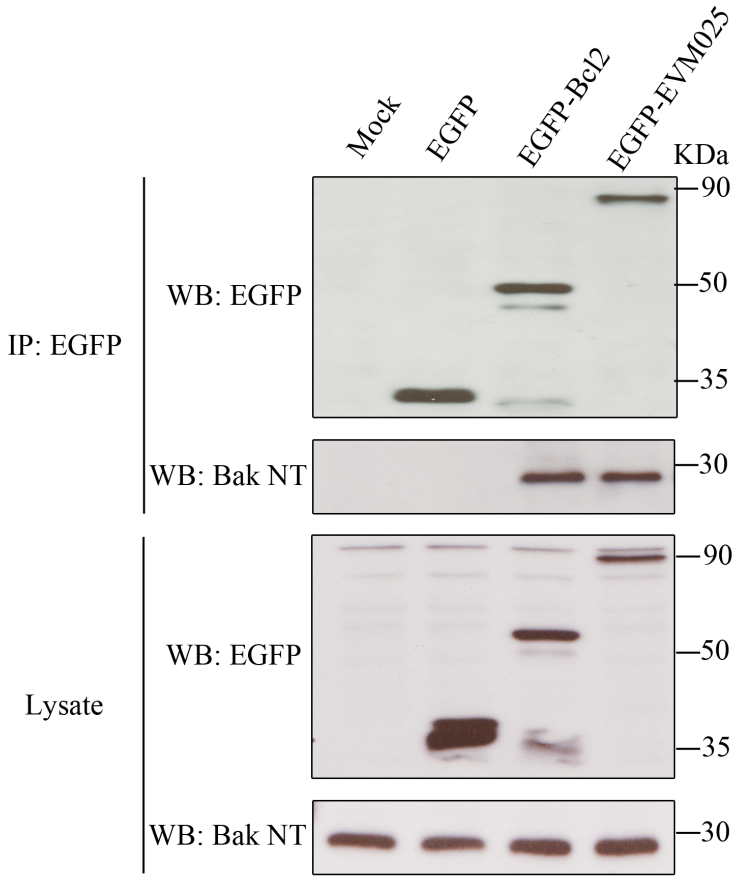

Figure 3.14 -EVM025 interacts with endogenous Bak. BMK cells were transfected with pEGFP, pEGFP-Bcl-2, or pEGFP-EVM025. Cells were lysed in CHAPs buffer and cellular lysates were immunoprecipitated (IP) with anti-GFP. The immuno-precipitates were immunoblotted with anti-Bak NT or anti-GFP antibody. Cell lysates were immunoblotted with anti-EGFP to check the expression of the EGFP constructs, and anti-Bak NT to determine the levels of endogenous Bak.

observed in cells transfected with EGFP-Bcl-2 (Fig. 3.15), a protein known to inhibit Bak-induced apoptosis. Overall, these data indicate that EVM025 directly interacts with Bak during the overexpression of these proteins and this interaction prevents the activation of Bak-induced apoptosis.

3.2.6 EVM025 prevents apoptosis induced by Bax

The other key pro-apoptotic mitochondrial regulator, Bax, exists in an inactive form in the cytoplasm and undergoes a conformational change in response to an apoptotic stimulus, resulting in the exposure of its N-terminus and localization to the mitochondria [199]. Activated Bax undergoes homo-oligomerization facilitating mitochondrial damage and ultimately results in the release of cytochrome c [200]. To determine if EVM025 could inhibit Bax activation, we used flow cytometry to monitor the conformational change of activated Bax. Jurkat cells were either mock-infected, or infected with ECTV, ECTVΔCrmA, ECTVΔ025, or ECTVΔ025/ΔCrmA. Six hrs post-infection, the activation of Bax was induced by STS treatment, and the conformational change in Bax was detected by staining with anti-Bax6A7, an antibody that recognizes the Bax N-terminus, a domain only exposed during apoptosis. Upon STS treatment of uninfected Jurkat cells, a significant increase in anti-Bax 6A7 fluorescence was seen as compared to untreated cells, indicating that Bax was activated and underwent a conformational change exposing its N-terminus (Fig. 3.16, panel a). Conversely, cells infected with ECTV (Fig. 3.16, panel b) or ECTVΔCrmA (Fig. 3.16, panel c) completely inhibited the activation of Bax upon STS treatment. In contrast, cells infected with ECTVΔ025 (Fig. 3.16, panel d) or ECTVΔ025/ΔCrmA (Fig. 3.16, panel e) were not protected from STS-induced Bax activation, suggesting that EVM025 can inhibit Bax activation.

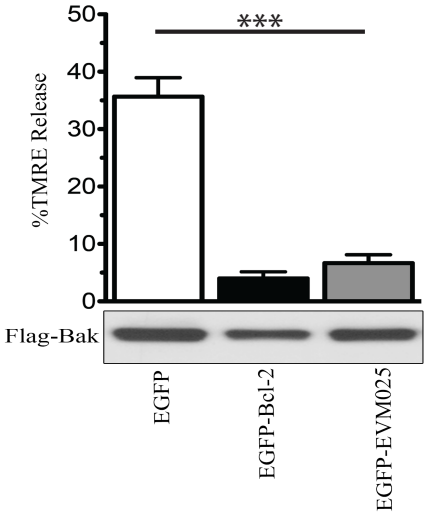

Figure 3.15 - EVM025 expression inhibits Bak induced apoptosis. HeLa cells were co-transfected with pEGFP, pEGFP-Bcl-2, and pEGFP-EVM025 and pcDNA-Flag-Bak for 16 hours and stained with 50nM TMRE to label mitochondria, and apoptosis was analyzed in EGFP-positive cells using two-color flow cytometry. Assays were performed in triplicate and were quantified as the mean percentage of EGFP-positive cells (±S.D.) demonstrating a loss of TMRE. Flag-Bak expression levels from transfected cells were analyzed by Western blotting with an anti-Flag antibody. ***, $P < 0.001$.

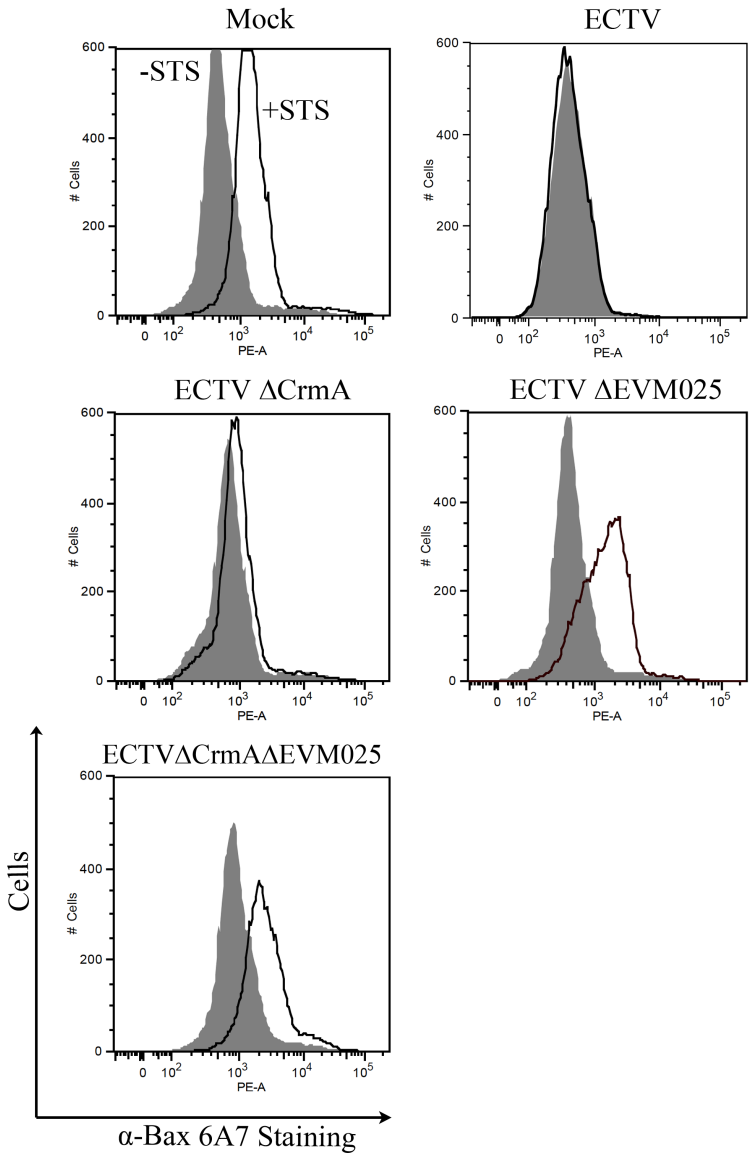

Figure 3.16 - EVM025 expression inhibits Bax activation. Jurkat cells were mock-infected (a), infected with ECTV (b), ECTVΔCrmA (c), ECTVΔ025 (d) or ECTVΔ025/ΔCrmA (e) at an MOI of 5 for 4 hours, followed by treatment with 0.25μM STS for 2 hours to induce apoptosis. Exposure of the N-terminus of Bax was monitored by flow cytometry using a conformation-specific N-terminal Bax 6A7 antibody. Untreated cells, (shaded histogram); STS treated cells (open histogram). Data is the representative of at least three independent experiments.

Next we determined if EVM025 could inhibit apoptosis induced by Bax over-expression. HeLa cells were co-transfected with HA-Bax, and pEGFP, pEGFP-Bcl-2, or pEGFP-EVM025, and apoptosis was quantified in transfected cells by measuring mitochondrial membrane potantial TMRE (Fig. 3.17 A). Overexpression of Bax resulted in the artificial activation of Bax and subsequent loss of the mitochondrial membrane potential in 45% of EGFP-transfected cells. Interestingly, transfection of EGFP-EVM025 protected the cells against Bax-induced apoptosis. Similarly, transfection of EGFP-Bcl-2 significantly inhibited apoptosis induced by Bax over-expression, as expected. We failed to detect any interaction between EVM025 and Bax (Fig 3.17 B). The lack of interaction between Bax and EVM025 suggests that EVM025 functions by interacting with a BH3-only protein upstream of Bax to prevent its activation.

3.2.7. EVM025 inhibits Bim-induced apoptosis

EVM025 expression inhibited Bax activation, but no direct interaction between EVM025 and Bax was detected, suggesting that EVM025 may function upstream of Bax. The BH3-only protein Bim acts as a direct upstream activator of Bax, and is activated during cellular stress such as virus infection [100,201]. To examine the possible interaction between EVM025 and BimL, HeLa cells were co-transfected with FLAG-BimL and either EGFP, EGFP-Bcl2, or EGFP-EVM025, and immunoprecipitated with anti-GFP (Fig. 3.18). Western blotting with anti-Bim demonstrated that both EGFP-EVM025 and EGFP-Bcl-2 co-precipitated with BimL, whereas no interaction was observed with EGFP. These data indicate that EVM025 can associate with BimL.

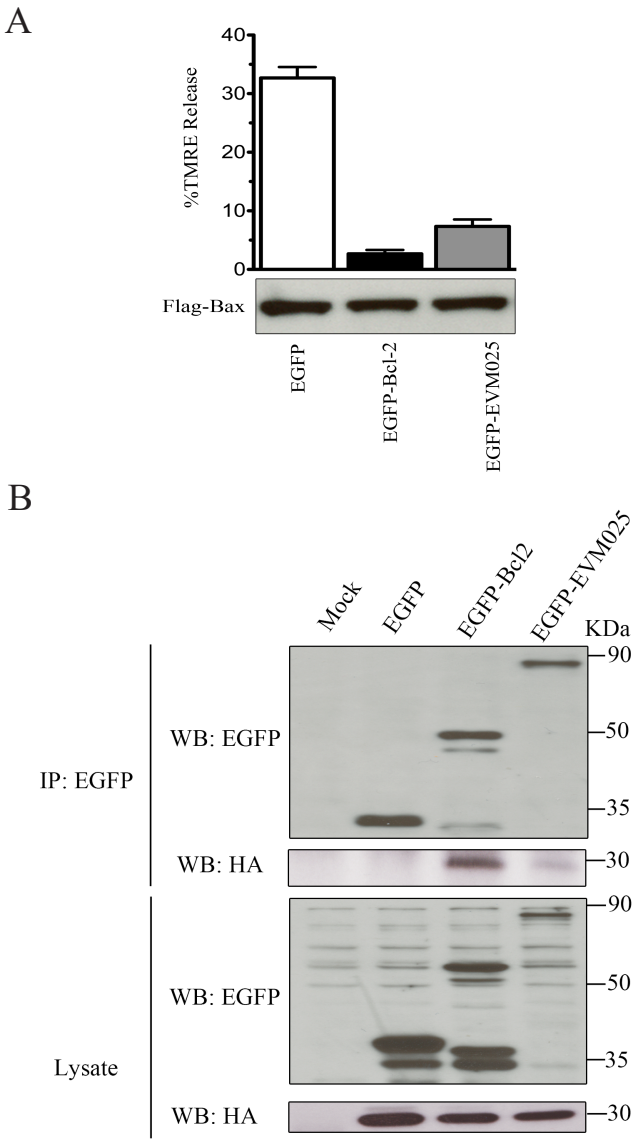

Figure 3.17 - EVM025 expression inhibits Bax activation. HeLa cells were co-transfected with pEGFP, pEGFP-Bcl-2, and pEGFP-EVM025 and pcDNA-Flag-Bak for 16 hours and stained with 50nM TMRE to label mitochondria, and apoptosis was analyzed in EGFP-positive cells using two-color flow cytometry. Assays were performed in triplicate and were quantified as the mean percentage of EGFP-positive cells (±S.D.) demonstrating a loss of TMRE. Flag-Bax expression levels from transfected cells were analyzed by Western blotting with an anti-Flag antibody. (B) EVM025 interacts with does not transfected Bax. HeLa cells were transfected with pEGFP, pEGFP-Bcl-2, and pEGFP-EVM025 and pcDNA-Ha-Bax for 12 hours. The cells were lysed in 2% CHAPS buffer, lysates were immunoprecipitated (IP) with anti-GFP (goat) antibody and subjected to western blotting with anti-GFP or anti-HA antibody to detect the interaction. Whole cell lysates were subjected to western blotting with the anti-GFP or anti-HA antibody to detect the expression levels of the transfected protiens.

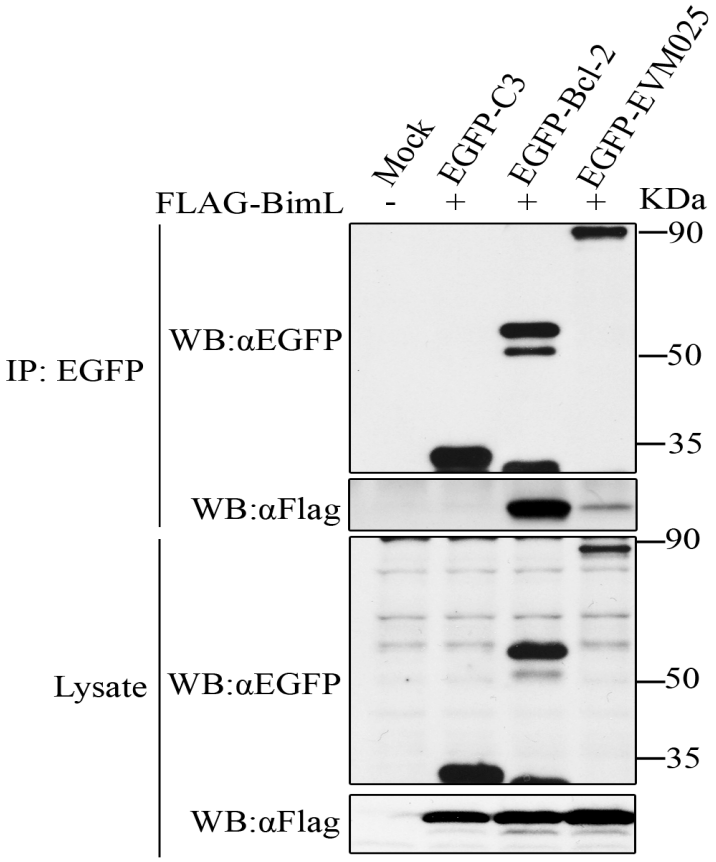

Figure 3.18 - EVM025 interacts with BimL. HeLa cells were transfected with pEGFP, pEGFP-Bcl-2, and pEGFP-EVM025 and pcDNA-Flag-BimL for 14 hours. The cells were lysed in 2% CHAPS buffer, lysates were immunoprecipitated (IP) with anti-GFP (goat) antibody and subjected to western blotting with anti-GFP or anti-Flag antibody to detect the interaction. Whole cell lysates were subjected to western blotting with the anti-GFP or anti-Flag antibody to detect the expression levels of the transfected protiens.

We next sought to determine if EVM025 could prevent apoptosis induced by BimL over-expression. HeLa cells were co-transfected with Flag-BimL and pEGFP, pEGFP-Bcl-2 or pEGFP-EVM025 for 12 hrs, and apoptosis was assessed by staining with TMRE and flow cytometry (Fig. 3.19). In cells transfected with pEGFP, and Flag-BimL, approximately 40% of the cells showed a loss of TMRE staining. Conversely, only 3% of cells showed a loss of TMRE when Flag-BimL was co-expressed with EGFP-Bcl-2, a cellular antagonist of BimL protein. Similar results were observed in cells transfected with BimL and EVM025, in which only 7% of the transfected population showed a loss of TMRE staining. These results indicate that EVM025 interacts with the BH3 only protein BimL and prevents BimL-induced apoptosis. Thus it is likely that EVM025 inhibits the activation of the pro-apoptotic protein Bax by interacting and inhibiting the activity of its upstream regulator Bim.

3.2.8. Deletion of N-terminus of EVM025 improves EVM025's interaction with Bim

ECTV EVM025 consists of a N-terminal repeat region that is not present in other orthologues of the protein. The function of this N-terminal region is currently unknown. We thus sought to determine the importance of this region. To test whether the N-terminus had any impact on interaction with Bim, we used constructs that had deletions at the N-terminus of the protein. We used two new constructs for the experiments, one which lacked the entire repeat, EVM025 (E255), and a second construct which contained two copies of the 'DNGIVQDI' repeat, EVM025 (D237) (Fig. 3.20). HeLa cells were either mock transfected or transfected with pEGFP, pEGFP-Bcl-2, pEGFP-F1L, pEGFP-EVM025, pEGFP-EVM025(E255), and pEGFP-EVM025(D237) or pcDNA-flag-BimL

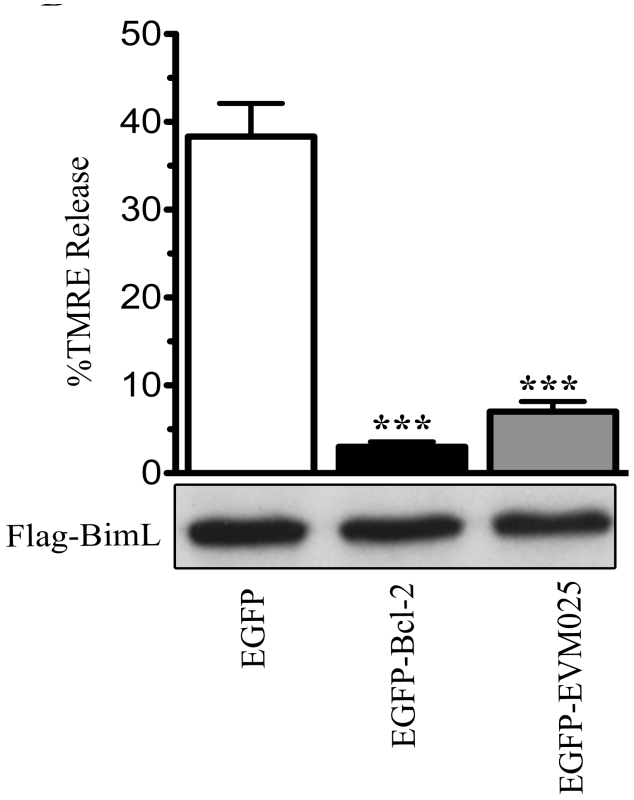

Figure 3.19 - EVM025 expression inhibits BimL overexpression induced apoptosis. HeLa cells were co-transfected with pEGFP, pEGFP-Bcl-2, and pEGFP-EVM025 and pcDNA-Flag-BimL for 16 hours. Transfected cells were stained with 50nM TMRE to label mitochondria, and apoptosis was analyzed in EGFP-positive cells using two-color flow cytometry. Assays were performed in triplicate and were quantified as the mean percentage of EGFP-positive cells (±S.D.) demonstrating a loss of TMRE uptake. Flag-Bax expression levels from transfected cells were analyzed by Western blotting with anti-Flag antibody. ***, $P < 0.001$.

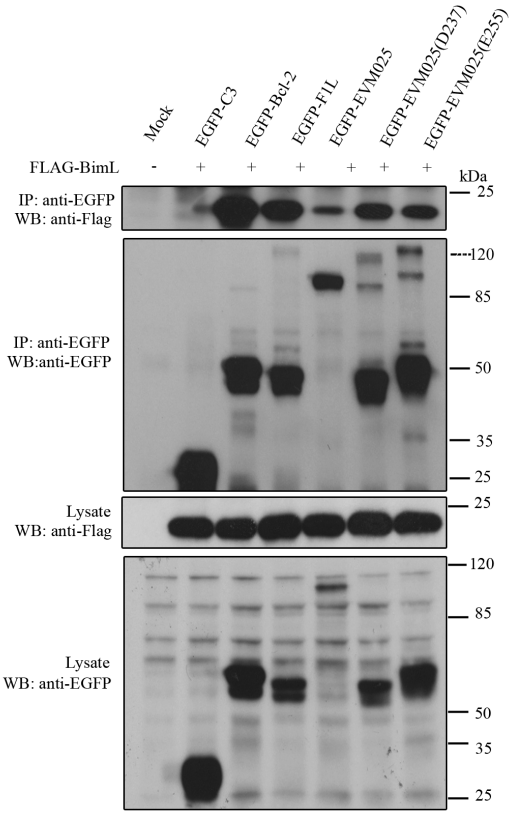

Figure 3.20 - EVM025 interacts with BimL. HeLa cells were transfected with pEGFP, pEGFP-Bcl-2, pEGFP-F1L pEGFP-EVM025 pEGFP-EVM025(E255), or pEGFP-EVM025(D237) and pcDNA-Flag-BimL for 14 hours. The cells were lysed in 2% CHAPS buffer, lysates were immunoprecipitated (IP) with anti-GFP (goat) antibody and subjected to western blotting with anti-GFP or anti-Flag antibody to detect the interaction. Whole cell lysates were subjected to western blotting with the anti-GFP or anti-Flag antibody to detect the expression levels of the transfected protiens

for 16 h. The cells were subsequently lysed using 2% CHAPS detergent, and the immuno-complexes were precipitated using a GFP antibody and anti-Flag antibody was used to detect BimL. As expected, EGFP-Bcl-2 interacts with BimL and so does EGFP-F1L. As previously discussed, EGFP-EVM025 interacts weakly with BimL. In contrast to full length EVM025, the two deletion mutants, pEGFP-EVM025(E255) and pEGFP-EVM025(D237) interact relatively strongly with Flag-BimL especially when compared to full length EVM025. This experimental data essentially showed that the interaction with BimL was somehow hindered by the presence of the long N-terminal repeat region.

Based on this observation, we sought to determine if the N-terminus of EVM025 had any effect on protection against the apoptosis induced by BimL over-expression. HeLa cells were co-transfected with Flag-BimL and pEGFP, pEGFP-Bcl-2, pEGFP-EVM025, pEGFP-EVM025(E255), or pEGFP-EVM025(D237) for 12 hrs, and apoptosis was assessed by staining with TMRE by flow-cytometery (Fig. 3.21). In cells transfected with pEGFP, and Flag-BimL, approximately 40% of the cells showed a loss of TMRE staining. Conversely, only 3% of cells showed a loss of TMRE when Flag-BimL was co-expressed with EGFP-Bcl-2, a cellular antagonist of BimL protein. Similar results were observed in cells transfected with BimL and EVM025 and all of the N-terminus mutants, in which only about 10% of the transfected population showed a loss of TMRE staining. These results indicate that though the N-terminus of EVM025 has some effect on the binding of BimL to EVM025, it has no effect on the ability of EVM025 to protect against BimL induced apoptosis.

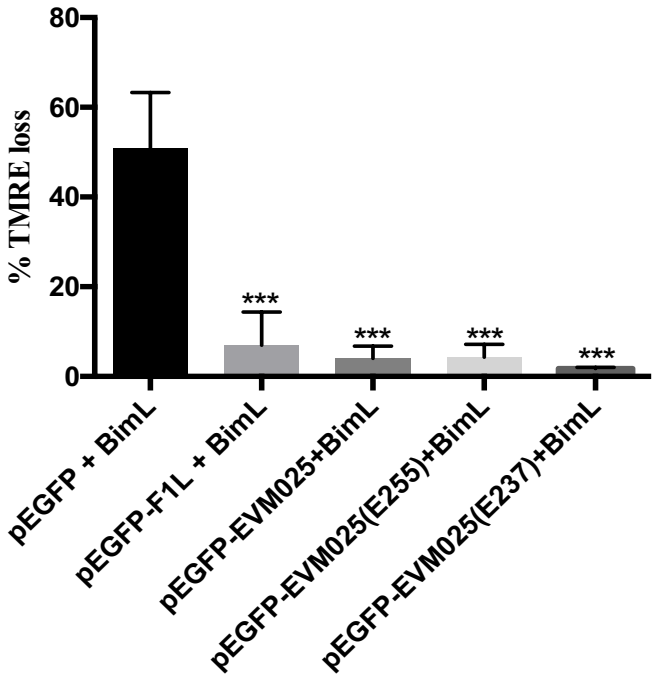

Figure 3.21 - EVM025 expression inhibits BimL overexpression induced apoptosis. HeLa cells were co-transfected with pEGFP, pEGFP-F1L, pEGFP-EVM025, pEGFP-EVM025(E255), or pEGFP-EVM025(D237) and pcDNA-Flag-BimL for 16 hours. Transfected cells were stained with 50nM TMRE to label mitochondria, and apoptosis was analyzed in EGFP-positive cells using two-color flow cytometry. Assays were performed in triplicate and were quantified as the mean percentage of EGFP-positive cells (±S.D.) demonstrating a loss of TMRE uptake. Flag-Bax expression levels from transfected cells were analyzed by Western blotting with anti-Flag antibody. ***, $P < 0.001$.

3.4. Summary

Here we show that like VACV, ECTV infection was able to inhibit STS and UV induced apoptosis. ECTV was capable of inhibiting apoptosis in both mouse and human cells. ECTV infection protected human and mouse cell lines against STS induced activation of caspases-3 and caspase-mediated cleavage of PARP. Genome analysis of ECTV revealed that EVM025 has a long N-terminal repeat region consisting of an eight amino acid motif 'DNGIVQDI' repeated 30 times. The functional importance of these repeated regions remains unknown, the repeat regions are absent in VACV Copenhagen, VARV Bangladesh, MPXV Zaire, and CPVX Brighton Red. Despite the variability present at the N-terminal region of the F1 orthologues, F1 and EVM025 share 95% sequence homology at the C-termini. We were able to establish that the expression of EVM025 prevents the triggering of the intrinsic apoptotic pathway. EVM025 was crucial in preventing the loss of mitochondrial membrane potential and loss of Cytochrome-c during an ECTV infection. Our experiments also suggest that EVM025 is crucial in preventing virus-induced apoptosis in MEF cells. The data would insinuate that EVM025 is necessary to prevent apoptosis during virus infection. Like VACV F1, EVM025 is a tail anchored protein that localizes to the mitochondria, where it inhibits the activity of Bak by direct interaction. In addition, EVM025 is also able to inhibit Bax activation, and this is likely achieved by interactions with other BH3-domain proteins such as BimL. The deletion of N-terminus of EVM025 improved its ability to interact with BimL, but had no measureable effect on EVM025s ability to protect against BimL induced apoptosis.

Chapter-4- Ectromelia Virus EVM025 acts as a Virulence Factor

Experiments in this chapters are unpublished
The experiments were performed under the supervision of Dr. Mark Buller, Dr. Jim Smiley and Dr. Michele Barry.
The experiments were performed at Molecular Microbiology & Immunology, Saint Louis University (SLU), School of Medicine.
Dr. Scott Parker, Kristin Burles, and Ryan Crump helped with the experiments in this section.
Dr. Scott Parker was responsible for helping me with infections and organ collections.
Ryan Crump performed the footpad infections and the LD-50 infection.
Kristin Burles helped weigh the mice post infection, and performed the titration in section 4.2.4.
SLU animal facility staff helped in housing, and care of the animals. They also performed the blood collection from the infected and mock infected mice.
All experiments in this chapter were performed by Ninad Mehta with the help of the above-mentioned people with the exception of Section 4.2.2. This experiment was planned by Ninad Mehta but executed by Ryan Crump from Dr. Buller's laboratory.

4.1. Introduction

In the previous chapter, we have demonstrated that EVM025 acts as an anti-apoptotic protein during ECTV infection. The data also show that the protein is analogous to VACV F1 in function. Previous work has shown that VACV missing the F1 ORF displays reduced virulence in mice [143]. The study provided no information on the spread of the virus, and the immune response against the virus in the absence of the anti-apoptotic gene. The natural host for VACV virus is currently unknown, and infection of mice with VACV requires a relatively high dose. We sought to study the importance of the orthopoxvirus anti-apoptotic protein in a poxvirus with its natural host. In this chapter, we attempted to understand the importance of EVM025 during a ECTV infection, and how the absence of this gene affects the spread of the virus and the immune response.

4.2. Results

4.2.1. Deletion of EVM025 does not compromise virus growth *in vitro*

We have previously demonstrated that EVM025 acts as an inhibitor of apoptosis in a tissue culture system[202], but the effect of the EVM025 ORF on growth and virulence of the virus is yet to be understood. To determine whether EVM025 is required for efficient replication *in vitro,* a single step growth curve was performed in mouse cell lines. MEF cells were infected with ECTV, ECTVΔ025, and ECTVΔ025rev at an MOI of 5. In MEF cells we observed that ECTV, ECTVΔ025 and ECTVΔ025rev all exhibited a

similar growth pattern (Fig. 4.1 A). These results would suggest that the EVM025ORF is not crucial for the growth of the virus *in vitro*.

In addition to the single step growth curve, we performed a multi-step growth curve. The multi-step growth curve was performed using ECTV, ECTVΔ025 and ECTVΔ025rev on MEF cells. This experiment was performed to help us determine the role of EVM025 in the spread of the virus in tissue culture. We did not observe any difference in the growth between ECTV or the EVM025 deletion mutant (Fig. 4.1. B). This data would suggest that the absence of EVM025 has no negative effect on the growth and spread of the virus *in vitro.*

4.2.2. BALB/c mice are highly susceptible to ECTV infection

It is known that BALB/c mice are highly susceptible to ECTV infection[38,44,45,48]. The LD_{50} for BALB/c varies between 2 PFU/mouse to 20 PFU/mouse; this variation was based on the source of BALB/c mice, handling conditions and route of infection. We wanted to determine the LD_{50} of ECTV in our experimental conditions. Disease signs, such as disheveled coat, foot swelling, movement impairment, and mortality were recorded daily and scored. Mice that demonstrated a drop in body weight to 70% of their original mass, or signs of severe morbidity were euthanized. BALB/c mice were infected with 0, 1, 10, 100, 1000, and 10,000 PFU of ECTV subcutaneously (s.c.) in both hind leg foot pads in a total volume of 30 µl phosphate-buffered saline (PBS) (15 µl per leg). At 1000 and 10,000 PFU, animals infected with ECTV exhibited a sudden loss of weight. At lower dose the mice experienced a drop of body weight as well, but the surviving mice regained their body weight (Fig. 4.2. A). At higher infectious dose of 10,000, 1000 and

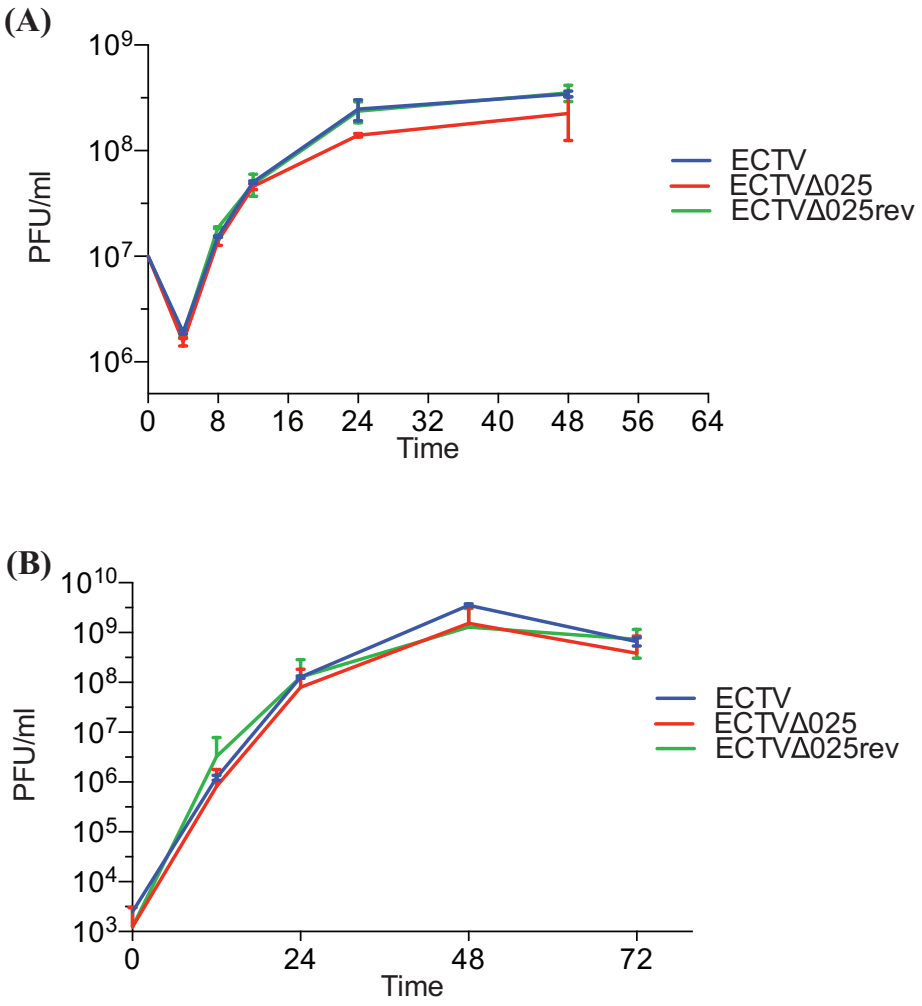

Figure 4.1. EVM025 deletion has no effect on growth or spread of the virus. (A) MEF cells were infected at an MOI of 5 with ECTV, ECTVΔ025, or ECTVΔ025rev for a single-step growth analysis. The infected cells were harvested at 4, 8,12, 24 and 48 hours post-infection and lysaed to release infectious particles. Serial dilutions of infectious virus were plated on Bsc-40 cells. The infected monolyer was fixed and stained with crystal violet and plaques were counted. (B) MEF cells were infected at an MOI of 0.01 with ECTV, ECTVΔ 025, or ECTVΔ025rev for a multi-step growth analysis. The infected cells were harvested at 0, 12, 24 and 48 hours post-infection and lysed to release infectious particles. Serial dilutions of infectious virus were plated on Bsc-40 cells. Infected monolyer was fixed and stained with crystal violet and plaques were counted.

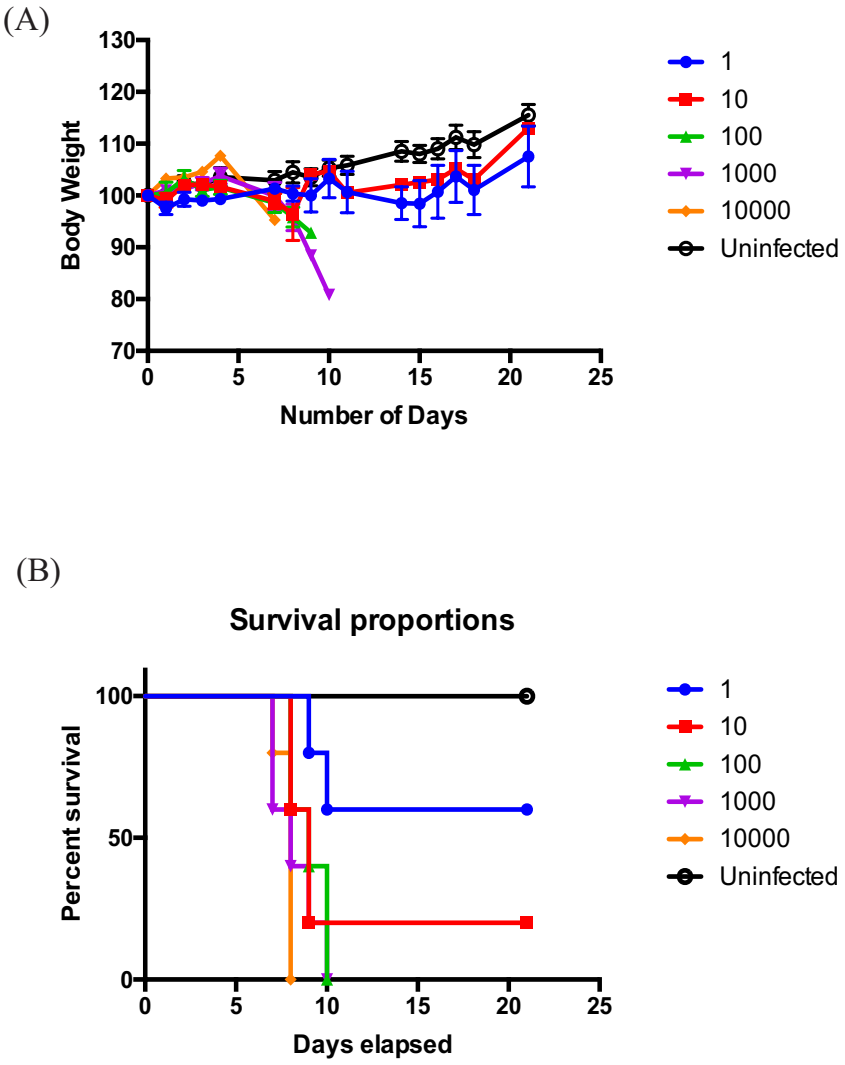

Figure 4.2. Survival of BALB/c mice in response to ECTV infection. Female BALB/c mice were mock-infected or infected with 1, 10, 100, 1000, 10000 pfu of ECTV via the foot-pad. Mice were monitored daily for body weight (A) and mortality (B).

100 all the infected mice succumbed to the infection. Only 20 % of the infected mice survived at an infectious dose of 10 PFU per mouse (Fig. 4.2 B). At a PFU dose of 1, 60% of the infected mice survived. Mortality of mice was then used to calculate the LD_{50} for each strain of ECTV using the Reed-Muench analysis[203]. The LD_{50} was 5.7 PFU per mouse.

Based on the observations in this pilot study, we decided to use an infectious dose of 600 PFU per mouse. We determined this dose was appropriate as it was 100 times higher than the calculated LD_{50}, and we would expect 100 percent mortality during an ECTV infection and a detectable immune response.

4.2.3. ECTVΔ025 is avirulent

We have previously shown that EVM025 acts as an inhibitor of apoptosis. Previous results have shown that this gene is dispensable during the replication of the virus in tissue culture. Next we wanted to determine if EVM025 acts as a virulence factor, or is dispensable during an animal infection. We mock infected BALB/c mice or infected with ECTV, ECTVΔ025 or ECTVΔ025rev virus. We used two different doses of the virus: 600 PFU and 6000 PFU. The weight and mortality of infected and mock infected mice were recorded every day. All mock infected mice survived until the experimental end-point. Mice infected with 600 PFU ECTV survived a maximum of 9 days. Similar results were observed in the case of mice infected with ECTVΔ025rev virus (Fig. 4.3 A). In contrast, ECTVΔ025 infected mice all survived the infection. In addition, we also observed that mice infected with ECTVΔ025 showed a lower magnitude of

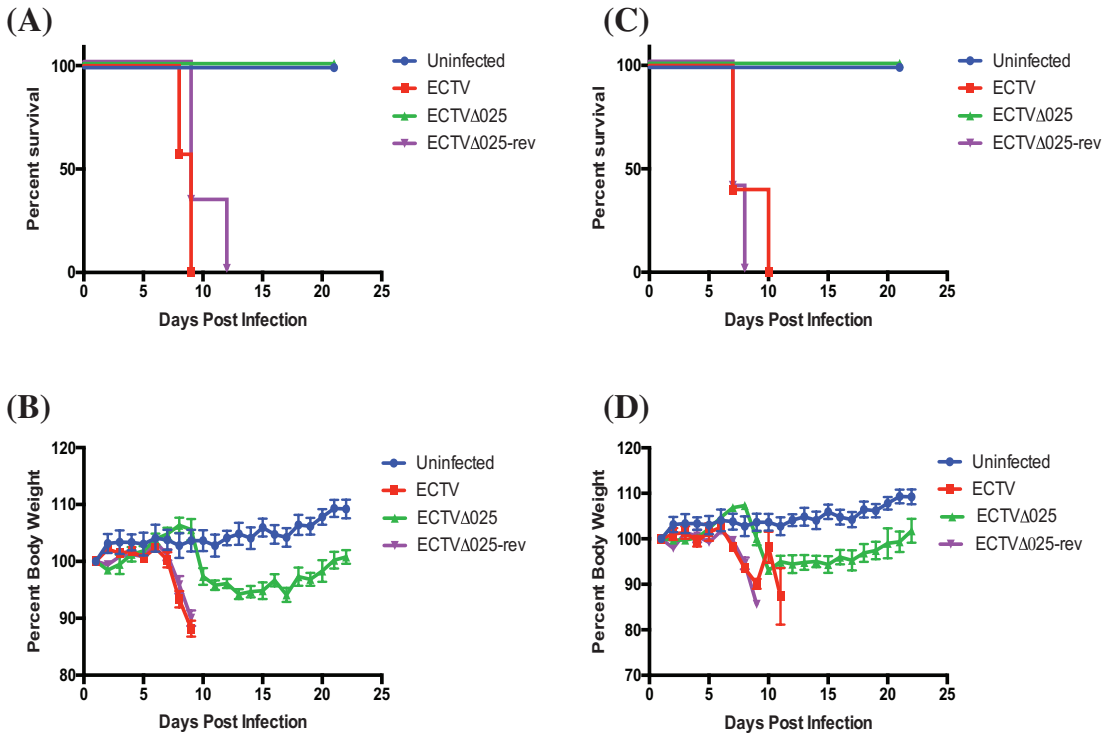

Figure 4.3. BALB/c mice survive a ECTVΔ025 infecton. Female BALB/c mice were mock-infected or infected with ECTV, ECTVΔ025 or ECTVΔ025-rev at 600 pfu (A and B) or 6000 pfu (C and D) via the foot-pad. Each group consists of five age and sex matched mice. Mice were monitored daily for mortality (A and C), and body weight (B and D). Weight loss for individual animals was normalized to their starting weight, and mean SEM is shown.

weight loss when compared to mice infected with ECTV or ECTVΔ025rev. The weight loss of mice infected with ECTVΔ025 stabilized at day 10 post infection. A recovery in body weight was observed in ECTVΔ025 infected mice. The weight gain is a sign of recovery, as the mice returned to their normal feeding pattern (Fig. 4.3 B). Similar results were observed in the case of mice infected with 6000 PFU of ECTV, ECTVΔ025, ECTV025rev (Fig. 4.3 C and D). Mice infected with ECTV survived a maximum of 10 days, and mice infected with a similar PFU of ECTVΔ025rev succumbed to the infection by day 9. But all mice infected with ECTVΔ025 survived the 6000 PFU infection (Fig. 4.3 C). With respect to weight, we again observed a trend that was similar to the mice infected with 600 PFU of the wild type and mutant viruses (Fig. 4.3 D). In addition, BALB/c mice survived $1x10^5$ PFU of the ECTVΔ025. All mice infected with this high dose survived (Fig. 4.4 A). The mice infected with $1x10^5$ PFU lost the same amount of body weight as mice infected with lower infectious doses. The weight of the mice dropped drastically at day 8 post infection, and started stabilizing at day 10 (Fig. 4.4 B).

These data suggest that EVM025 plays a crucial role during virus infection. The results show that though EVM025 was unnecessary during ECTV infection of tissue culture cells, it is indispensable during mouse infections. Hundred percent of mice infected with EVM025-deficient viruses survived the infection, although some signs of illness, including disheveled coat, conjunctivitis, and limb swelling were observed throughout the course of infection. As the time post infection progressed, the mice started recovery and the signs of infection subsided. The absence of EVM025 renders the virus severely attenuated.

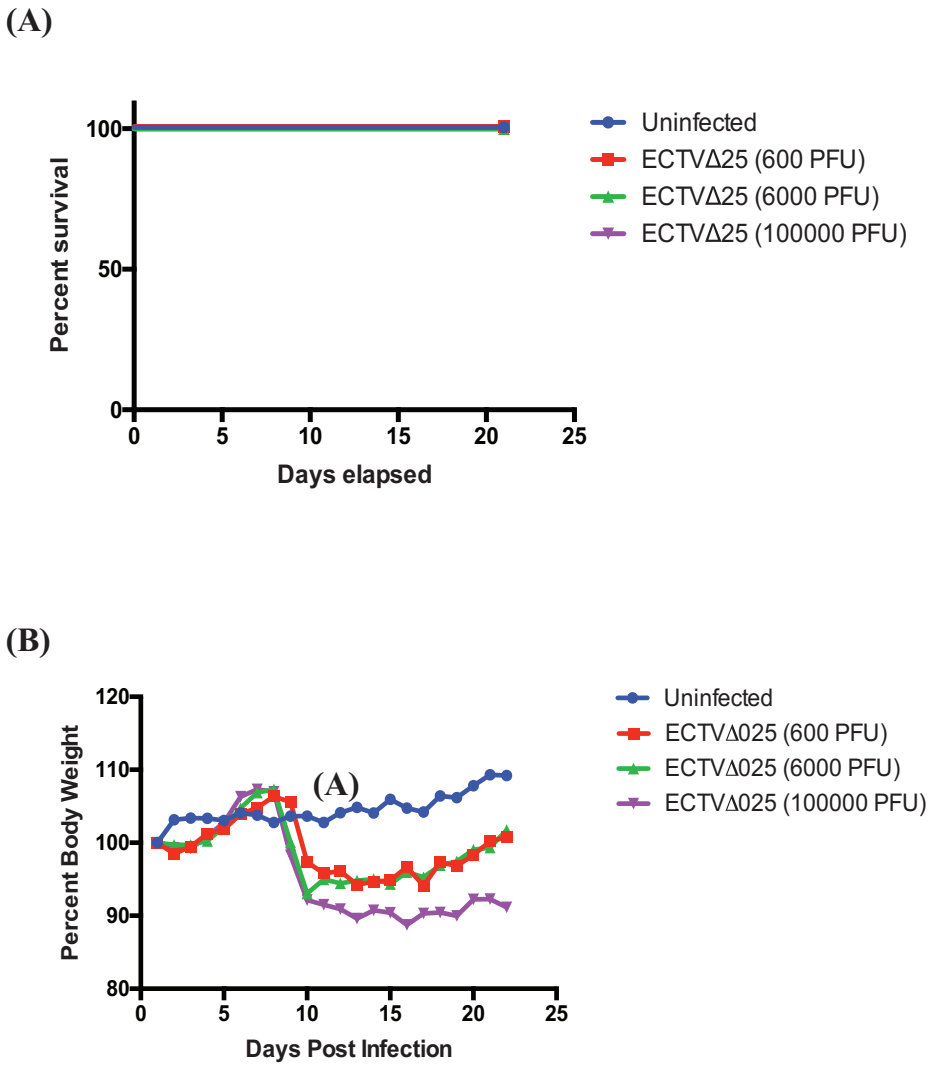

Figure 4.4. BALB/c mice can survive a high dose ECTVΔ025 infecton. Female BALB/c mice were mock-infected or infected with ECTVΔ025 at 600, 6000 or 100000 pfu via the foot-pad. Each group consists of 5 age and sex matched mice. Mice were monitored daily for mortality (A), and body weight (B). Weight loss for individual animals was normalized to their starting weight

4.2.4. ECTVΔ025 spread is restricted to the P-LN

Mice infected with ECTV succumb to the disease due to multiple organ failure as a result of virus infiltration[38]. The virus replicates uninhibited in infected tissues causing necrosis. It was thus of interest to understand the effect of EVM025 on the spread of the virus. To determine virus spread we infected BALB/c mice with 600 PFU of the ECTV, ECTVΔ025 and ECTVΔ025rev viruses. Popliteal lymph node (P-LN), spleen, liver, kidney, and lung were collected from the infected mice at day 2, 4 and 7 post infection. At day two post infection, we did not detect any virus in the harvested tissue. This result would indicate that ECTV, ECTVΔ025, ECTVΔ025rev were unable to make it to the P-LN during the first 2 days of infection. At day 4 post infection, all the viruses were detectable in the P-LN. ECTV and ECTVΔ025rev were detected at around 10^6 PFU/g. In contrast to ECTV and ECTVΔ025rev, ECTVΔ025 was detected at 10^5 PFU/g. We also detected ECTV and ECTVΔ025rev in the spleens at about 10^6 PFU/g. At day four, we did not detect any ECTVΔ025 in the spleens of infected mice. This result would suggest that ECTVΔ025 is unable to make it to the spleen within the first four days of infection. In addition, ECTV and ECTVΔ025rev were detected at low levels in the lung and kidney of infected mice (Fig. 4.5 B). At day seven, we detected increased levels of ECTV and ECTVΔ025rev virus in the P-LN and the spleen. The level of virus in the spleen increased to 10^8 PFU/g. By day seven the wild type ECTV and revertant had spread to the liver, lung and kidneys of the infected mice. In contrast, the level of ECTVΔ025 was reduced by half a log in the draining lymph node. ECTVΔ025 remained below detectable limit in spleen, liver and kidney. Low levels of ECTVΔ025 were detected in the lungs in 3 of 5 mice (Fig. 4.5 C). We think that the infection of the lungs was due to a reinfection

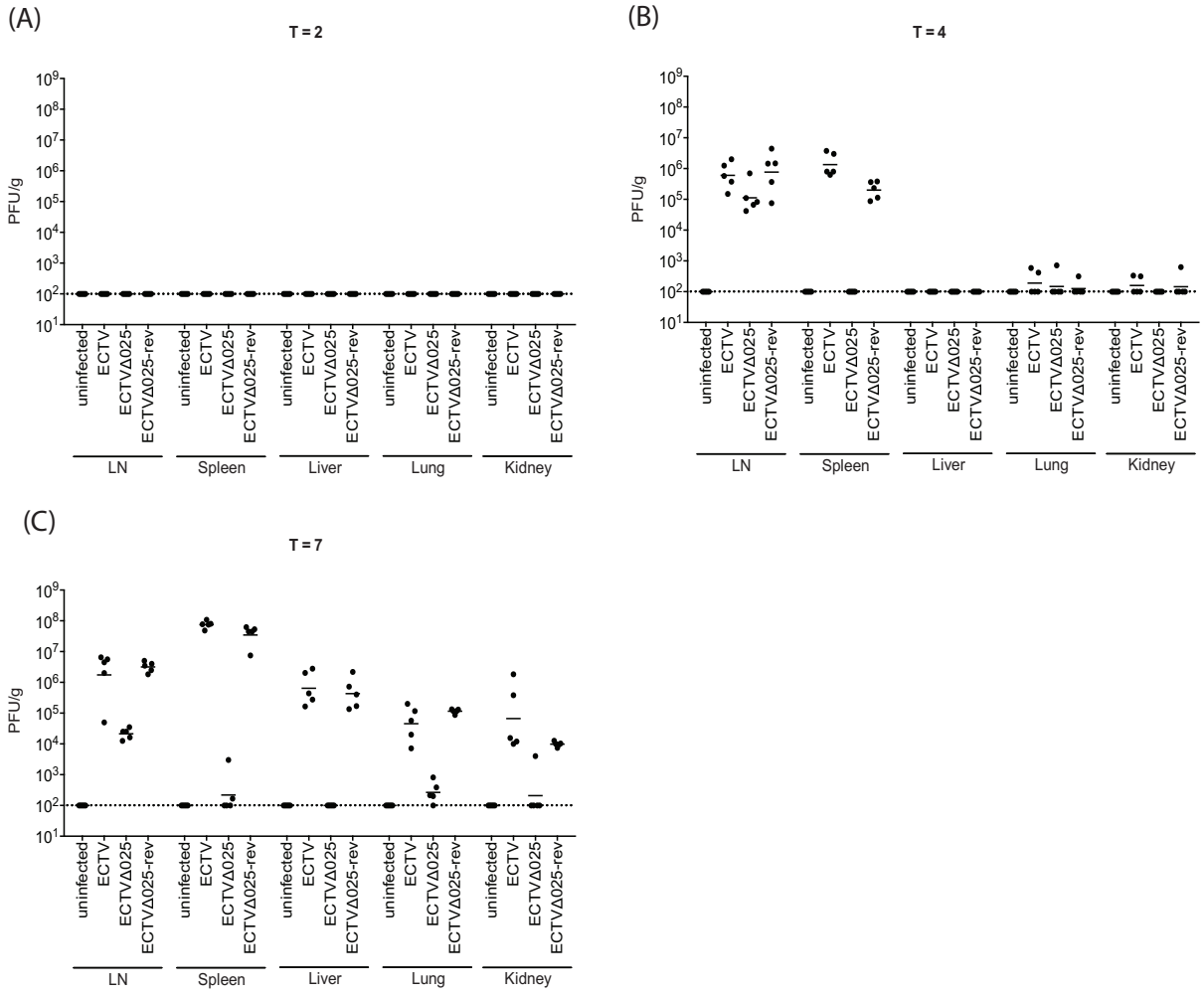

Figure 4.5. ECTVΔ025 spread is limited to the P-LN. BALB/c mice were mock-infected or infected with 600 pfu of ECTV, ECTVΔ025, ECTVΔ025-rev via the foot-pad. Each group consists of 5 age and sex matched mice. Indicated tissues were collected at 2 , 4 and 7 days post infection. Harvested tissues were homogenized and plated onto BSC-1 cells to measure viral titers at day 2 (A), day 4 (B) and 7 (C) post infection. This data represents the mean of the five samples.

of mice through the nasal route. The data would suggest that unlike the wild type virus and the revertant, ECTVΔ025 was unable to efficiently spread to organs beyond the draining lymph node. As mentioned earlier, death caused by ECTV is due to multiple organ failure due to virus infiltration. ECTVΔ025 does not spread beyond P-LNs, an observation that can explain the inability of ECTVΔ025 to kill infected mice.

4.2.5. Deletion of EVM025 causes a lower level of viremia in infected mice

After a foot pad infection, ECTV replicates at the site of inoculation and in the primary draining lymph node, giving rise to primary viremia that seeds the spleen and liver with the virus. Virus released from these target organs causes a secondary viremia[38]. The secondary viremia seeds other tissues. Avirulent ECTV strains show decreased levels of viremia. Thus, we wanted to determine if the absence of EVM025 had any effect on the viremia caused by the virus. To study this, whole blood was collected from mice at days 2, 4 and 7 post infection. Whole blood was used for detection of virus as it provides an unbiased method to detect viral genomic DNA in the plasma or in infected cells. Quantitative PCR was employed to detect viral DNA in whole blood. At day 2 post infection, the levels of ECTV, ECTVΔ025 and ECTVΔ025rev remained below the detection limit of the assay. In contrast, by day 4 post infection, we detected all three viruses in the blood. ECTVΔ025 was detected at levels 10% lower than the levels of ECTV and ECTVΔ025rev (Fig. 4.6 A). At day 7 post infection, the difference between levels of ECTV, ECTVΔ025rev and ECTVΔ025 was more pronounced. The levels of

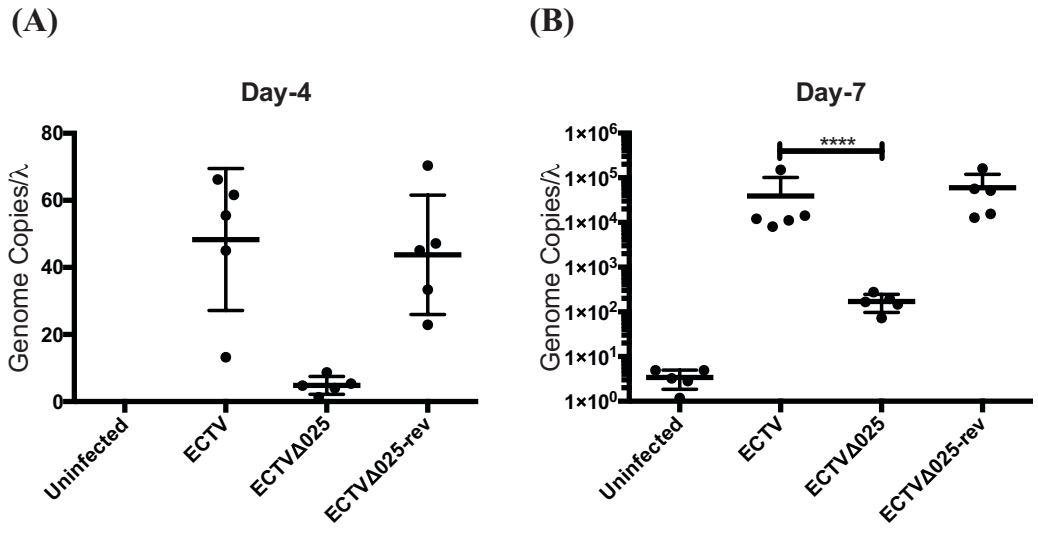

Figure 4.6. ECTVΔ025 infection results in a lower virema. BALB/c mice were mock-infected or infected with 600 pfu of ECTV or ECTVΔ025 via the foot-pad. Each group consists of 5 age and sex matched mice. Blood was collected 4 and 7 days post infection. The levels of viral DNAin the blood were measured using qPCR using ECTV specific primers at day 4 (A) and 7 (B) post infection. These data respresents the mean of the five samples. **** $p<0.0001$

ECTV and ECTVΔ025rev were found to be approximately 3 log higher than the mutant ECTVΔ025 (Fig. 4.6 B). The increased viremia correlates with the ability of ECTV and ECTVΔ025rev to spread to the secondary organs. The lower levels of ECTVΔ025 detected in the blood likely accounts for its inability to spread effectively to secondary organs.

4.2.6. Early spread of ECTVΔ025

Our previous results demonstrate that ECTVΔ025 is unable to spread beyond the P-LN. Thus, we next sought to determine the dynamics of spread at the site of infection and the draining lymph node. BALB/c mice were either mock infected or infected with ECTV or ECTVΔ025. The footpad and the P-LN of the mice were harvested at days 1, 2, 3 and 4 post infection. A qPCR-based approach was used to determine the level of viral DNA present in the footpad and the P-LN. On days 1 and 2, ECTV was below the detection threshold in the foot pad of infected mice. At days 3 and 4 post infection we detected increasing amounts of viral genomic DNA in the footpad of ECTV infected mice. In contrast, we detected lower amounts ECTVΔ025 in the footpad at day 3 and 4 post infection. The difference in the levels of ECTV and ECTVΔ025 levels in the footpad were statistically significant at day 4. This result would indicate that ECTVΔ025 cannot replicate efficiently in the footpad (Fig. 4.7 A). Next we looked at the kinetics of virus spread to the P-LN. In mice infected with ECTV, the number of ECTV genome copies per μg of DNA remained below detectable limit at days 1 and 2 post infection, and become detectable at day 3 and 4 post infection. The levels continued to rise between the

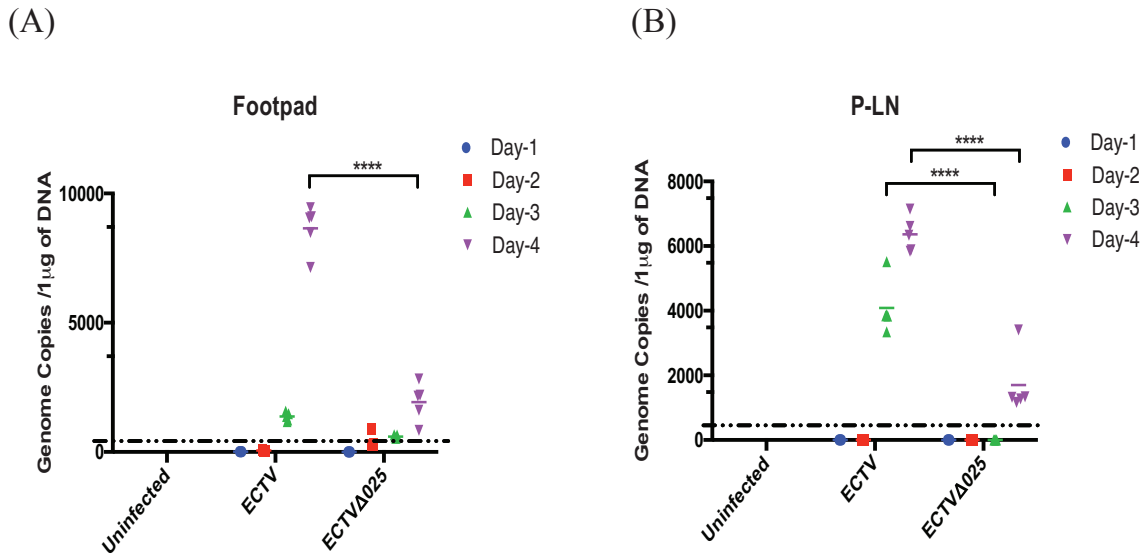

Figure 4.7. The early spread of ECTVΔ025 is slower. BALB/c mice were mock-infected or infected with 600 pfu of ECTV or ECTVΔ025 via the foot-pad. Each group consists of 5 age and sex matched mice. Foot pad (A) and P-LN (B) were collected at 1, 2, 3 and 4 days post infection. Total DNA was isolated from the isolated tissues. Viral genome number was quantified though qPCR using ECTV specific primers. This data represent the mean of the five samples. **** $p<0.0001$

two time points. In contrast, ECTVΔ025 remained below detection at day 3 post infection. ECTVΔ025 was detected at significantly lower levels than ECTV at day 4 post infection (Fig. 4.7 B). This difference between ECTV and ECTVΔ025 was statistically significant. The results would suggest that ECTVΔ025 takes longer to make it into the P-LN when compared to the wild-type ECTV. The stark difference between the number of ECTV and ECTVΔ025 genomes detected by day 4 of infection suggests that there is a defect in virus growth that starts at the site of initial infection. This defect in the footpad accounts for the failure of ECTVΔ025 to effectively spread to the P-LN. The replication in the P-LN also is negatively affected in the absence of the EVM025 ORF.

4.2.7. EVM025 infections are lethal in the absence of T-cells.

The previous experiments show that the spread of ECTVΔ025 is restricted to the lymph nodes of the infected mice. Previous work has shown that $CD8^+$ are crucial in preventing lethality caused by ECTV infection[204]. Cell mediated immunity is crucial in keeping the virus in check in the lymph node and limiting the spread of the virus[38]. Next we questioned whether cell mediated immunity is necessary to control the spread of ECTVΔ025. BALB/c-SCID mice lack both T and B cells, while BALB/c-Nude mice lack functional T-cells. Using the SCID and Nude mouse would help us determine the importance of B or T cells during an ECTVΔ025 infection. BALB/c, BALB/c-Nude and BALB/c-SCID mice were mock infected or infected with ECTV or ECTVΔ025. The mice were monitored for weight change and morbidity. As previously observed, BALB/c mice infected with ECTV succumbed to the infection by day 9. In contrast, the mice infected with ECTVΔ025 survived the 21 day experiment end point (Fig. 4.8 A).

BALB/c-SCID mice infected with ECTV succumbed to ECTV infection with in the first 10 days post infection. BALB/c-SCID mice infected with EVM025 survived until day 13 (Fig. 4.8 B). A similar trend was observed in BALB/c-Nude mice infected with ECTV or ECTVΔ025. This increase in survival is statistically significant (Fig. 4.8 C). Thus the data would suggest that innate immunity or cell intrinsic immunity is able to slow the early spread of the ECTVΔ025. But, in the absence of a cell mediated immune response, the virus eventually causes mortality in infected mice. This result suggests that T-cells are important in the protecting cells against ECTVΔ025 infected mice. B-cells in the absence of T-cells are not sufficient to protect mice infected with ECTVΔ025. The current experiments are not sufficient to discern the role or importance of NK cells during an ECTVΔ025 infection.

4.2.8. ECTVΔ025 infection results in elevated number of splenocytes

The preceding data suggest that cell mediated immunity is crucial in preventing the mortality caused by ECTVΔ025 infection. A large body of evidence supports the role of a strong cellular response in controlling the spread of virus. Resistant strains of mice are able to produce a rapid, stronger and more sustained NK and cytotoxic T-lymphocyte response[38,46,56]. To examine the effect of the EVM025 deletion on the splenocytes of BALB/c mice, we collected spleens from mock, ECTV and ECTVΔ025 infected mice at day 7 post infection. The spleens from ECTV infected mice are smaller in size and show clear signs of tissue necrosis. The tissue necrosis is likely due to the high virus titers detected in the spleen at day seven post infection. Other studies have also associated tissue necrosis with the presence of high ECTV titers[38,41,45]. In contrast, in mice infected with ECTVΔ025, we did not observe any necrosis of the spleen. The spleens in

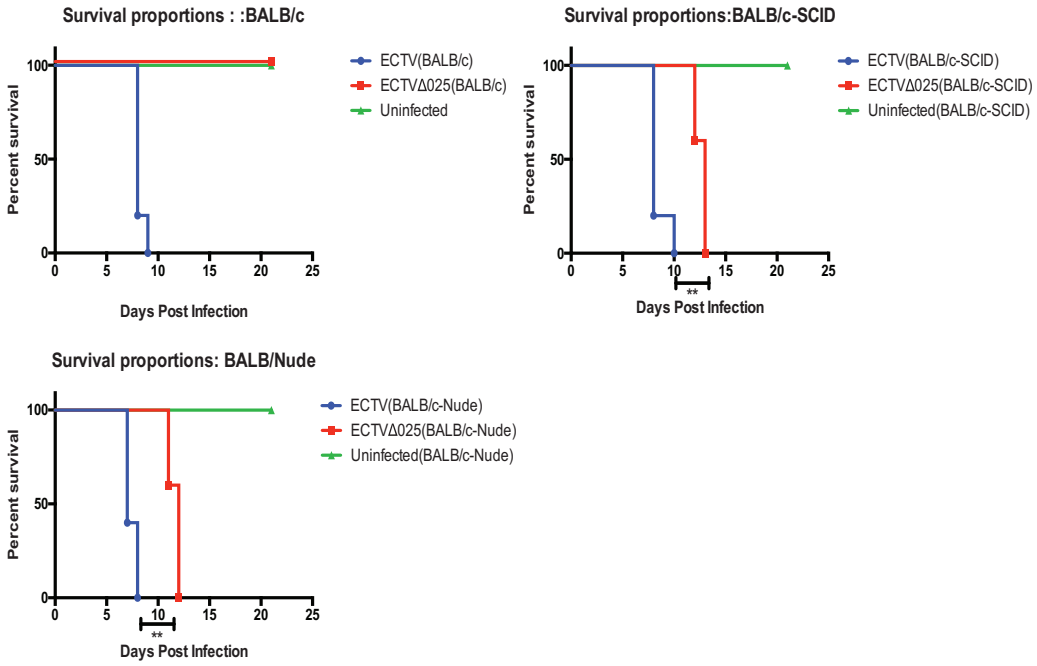

Figure 4.8. ECTVΔ025 is lethal in the absence of cell mediated immunity. Female BALB/c mice, (A) BALB/c-SCID (B), BALB/c-Nude and were mock-infected or infected with ECTV, or ECTVΔ025 at 600 pfu pfu via the foot-pad. Each group consists of five age and sex matched mice. Mice were monitored daily for mortality. $p<0.0023$

ECTVΔ025 infected mice were approximately twice as large as those of uninfected mice (Fig. 4.9 A), which is indicative of splenocyte proliferation. Next we counted the number of splenocytes present in mock, ECTV or ECTVΔ025 infected mice. The number of splenocytes in ECTV infected mice was similar to uninfected mice. The total number of splenocytes was at least 2-fold higher in mice infected with ECTVΔ025 (Fig. 4.9 B). The data would suggest that there is cell proliferation or infiltration in the spleen during a VACVΔ025 infection.

4.2.9. CD8 T-cell and NK cells response is enhanced in the absence of EVM025

As mentioned earlier, $CD8^+$ T-cells and NK cells are crucial in conferring resistance to ECTV infection. It has been demonstrated that the depletion of $CD8^+$ T-cells and NK cells results in greatly increased mortality in the ECTV resistant C57BL/6 mouse strain[204,205]. In addition, $CD4^+$ T-cells are required for cytolysis-independent clearance of the virus[204]. We wanted to establish the significance of these populations of cells in the control of the spread of ECTVΔ025. Next we assessed the relative proportion of $CD4^+$, $CD8^+$ T-cells and NK cells in the spleens and blood of infected mice. We gated on the CD3 marker, a T cell co-receptor, to differentiate the T-cells from the rest of the splenocytes. The $CD3^+$ cells were then sub-gated to determine the $CD8^+$ and $CD4^+$ T- cell populations in the spleen and blood samples. We observed elevated percentages of $CD3^+CD8^+$ T-cells in ECTVΔ025 infected compared to that in ECTV infected mice (Fig 4.10 A). In addition, we also stained cells for the presence of intracellular IFN-γ. We did not observe elevated levels of IFN-γ in the $CD3^+CD8^+$ T-cells in ECTVΔ025 infected mice. Higher levels of IFN-γ were detected in mice infected with ECTV or ECTVΔ025

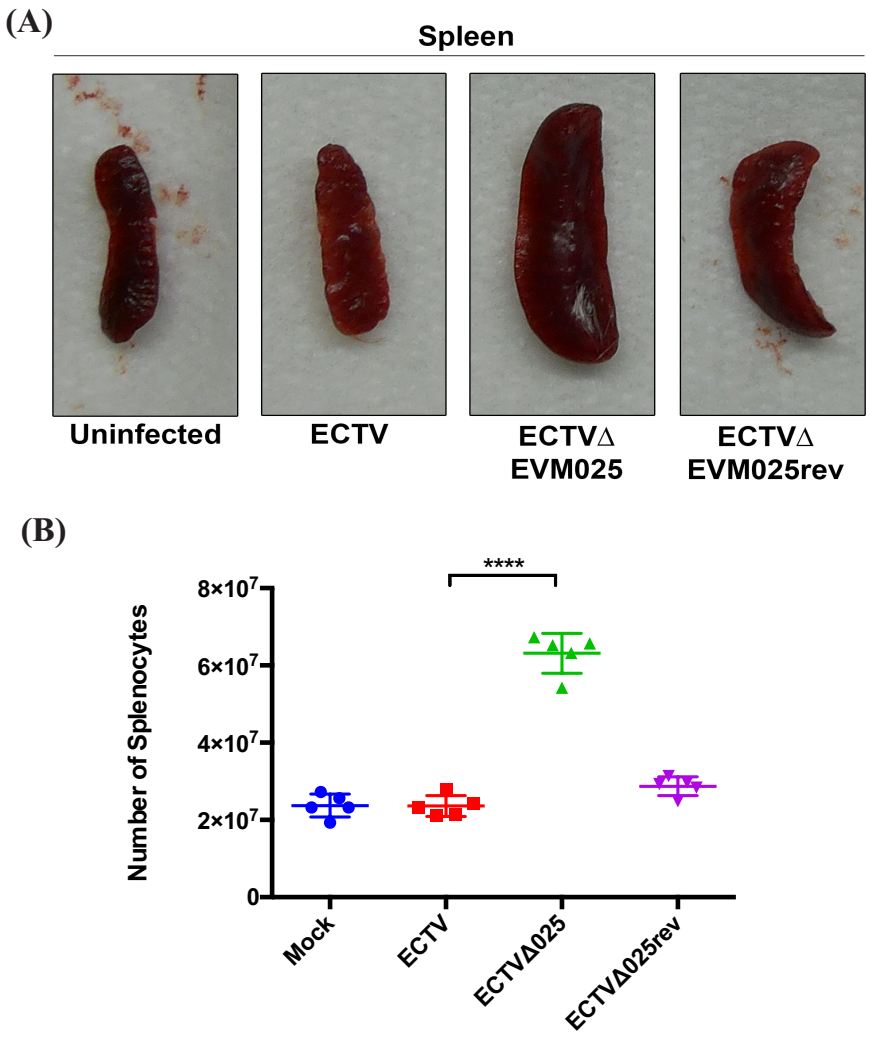

Figure 4.9. ECTVΔ025 infection leads to increased number of splenocytes. BALB/c mice were mock-infected or infected with 600 pfu of ECTV, ECTVΔ025 or ECTVΔ025rev via the foot-pad. Each group consists of 5 age and sex matched mice. Spleens were harvested at day 7 post infection. The harvested spleen are photographed to document the change in size and morphogology (A). Subsequently the spleens were homogenized and the number of splenocytes counted using a hemocytometer. **** $p<0.0001$

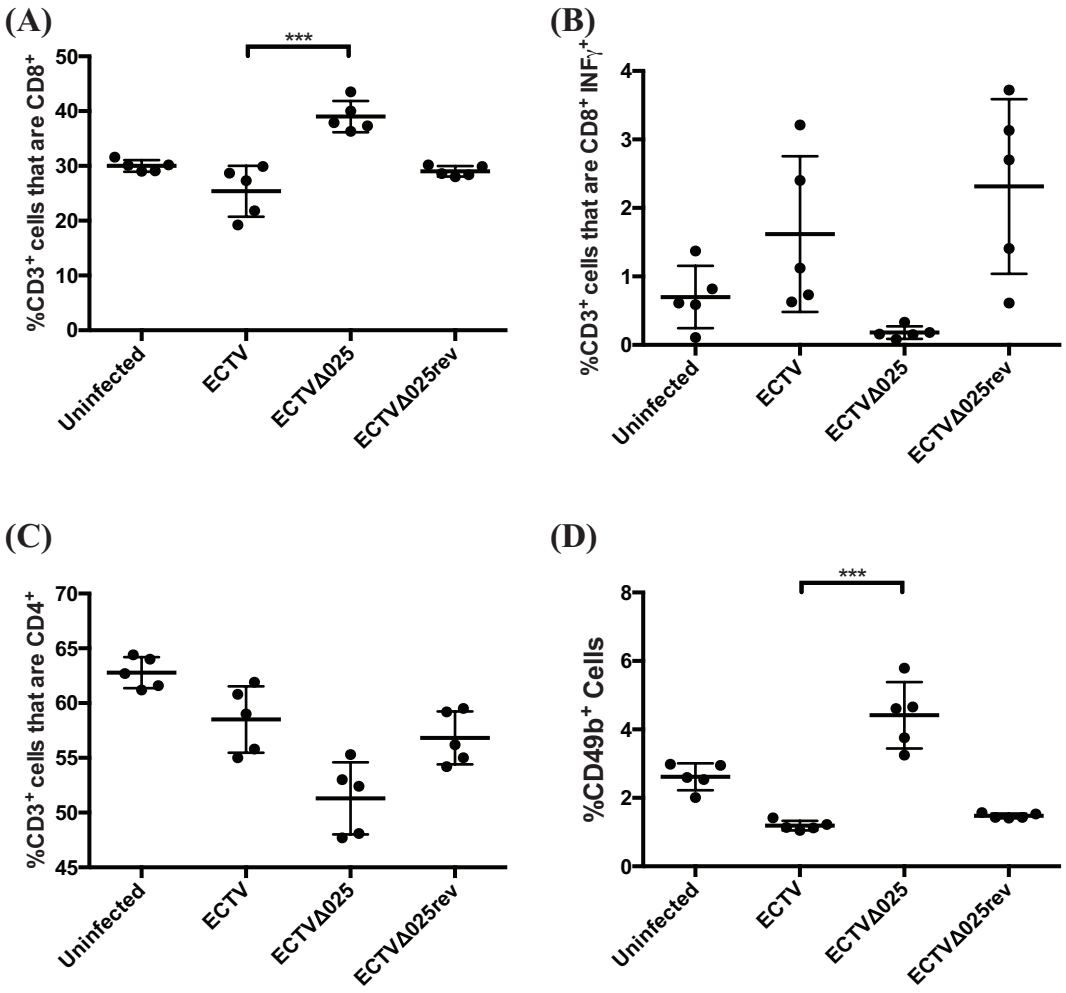

Figure 4.10. CD8 and NK cells are elevated in the spleen during ECTVΔ025 infection. BALB/c mice were mock-infected or infected with 600 pfu of ECTV, ECTVΔ025, ECTVΔ025rev via the foot-pad. Each group consists of 5 age and sex matched mice. Spleens where harvested at 7 days post infection. The organs were homogenized and the RBC were lysed. Subsequently cells were stained with CD4, CD8, CD3, CD49b (NK) for 1 hour at 4 C. Post staining the cells were fixed and permeabilized and stained for IFN-γ. The cells were analyzed using a flow-cytometer. The data analysis was done using FlowJo. Live cells were gated for the precence of CD45 marker. The $CD45^+$ cells were gated on the CD3 marker, to differentiate the T-cells from the rest of the splenocytes. The $CD3^+$ cells were then sub-gated to determine the $CD8^+$ and $CD4^+$ T- cell populations in the spleen.The NK cell population was determined by gating on $CD45^+$ and $CD49b^+$ cells. This data represents the mean of the five mice.

Infected mice (Fig. 4.10 B). This increased levels did not correlate with survival. The level of $CD3^+CD4^+$ T-cells were slightly lower in ECTVΔ025 infected mice, when compared to the ECTV and ECTVΔ025rev infected mice (Fig 4.10 C). Next we looked at the NK cell population in the spleen of infected mice. We found elevated levels of NK cells in ECTVΔ025 mice, then the levels observed in ECTV or ECTVΔ025rev infected mice (Fig 4.10 D). A similar trend was observed in case of the white blood cells of the infected mice (Fig. 4.11). In the blood, we also observed elevated levels of $CD3^+CD8^+$ T-cells (Fig. 4.11 A) and NK (Fig. 4.11 D) cells in ECTVΔ025 infected mice. The elevated levels of $CD8^+$ T-cells and NK cells may contribute to limiting the spread of the ECTVΔ025 virus.

Further work is required to understand the role of CD8 T-cells and NK cells in the control of ECTVΔ025 infection. It would also be interesting to understand the ECTV specific response in the mice. In addition, the current experiment does not rule out the importance of CD4 T cells in controlling the spread of ECTVΔ025 infection.

4.2.10. Elevated chemokine and cytokine responses to ECTVΔ025 infection

Our previous experiment suggests that CD8 T-cells are important in limiting the spread of ECTVΔ025 in infected mice. This finding would suggest a role for chemokine and chemokine receptor-mediated recruitment of CD8 T-cells following a ECTVΔ025 infection. Therefore, we examined the levels of cytokines and chemokines using the ThermoFisher Scientific Cytokine Mouse 20-Plex Panel for the Luminex™ platform

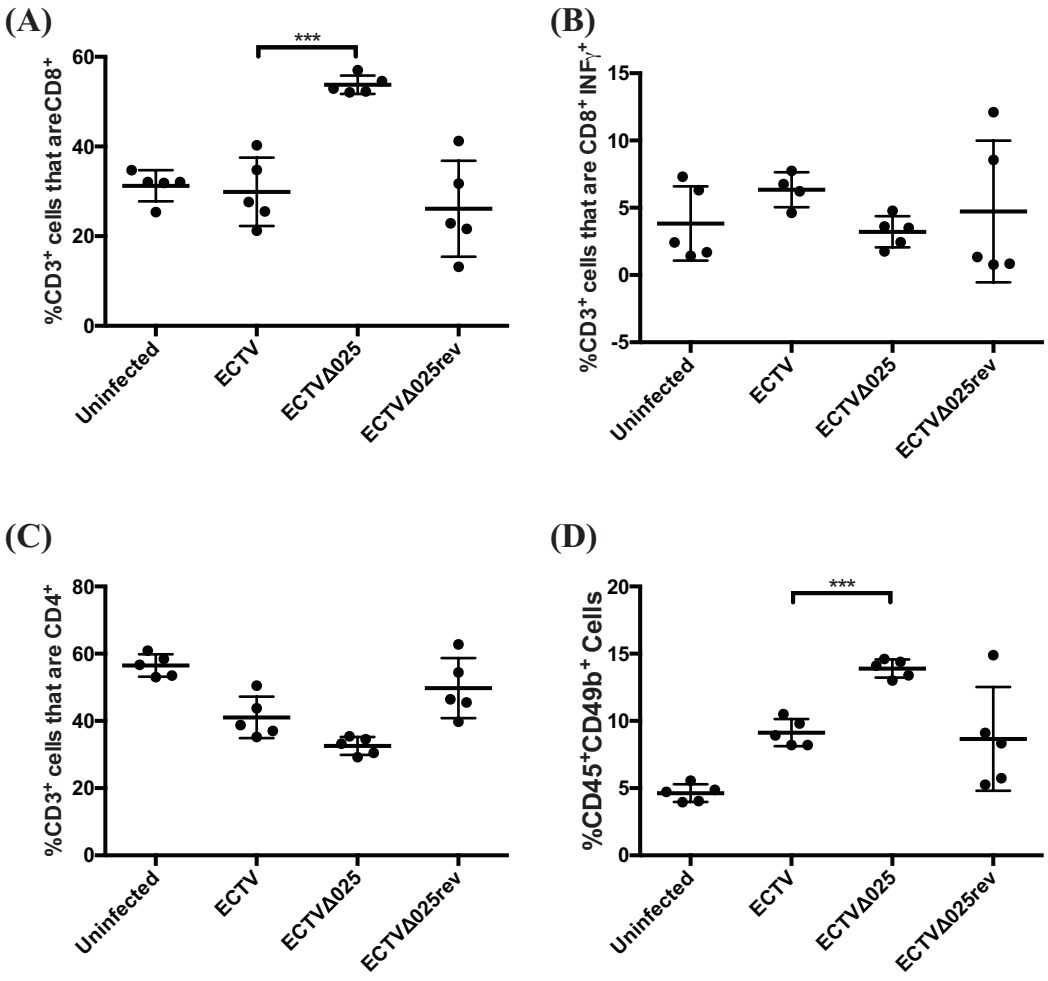

Figure 4.11. CD8 and NK cells are elevated in the blood during ECTVΔ025 infection. BALB/c mice were mock-infected or infected with 600 pfu of ECTV, ECTVΔ025, ECTVΔ025rev via the foot-pad. Each group consists of 5 age and sex matched mice. Spleens where harvested at 7 days post infection. The blood was collected in EDTA tubes and the RBC were lysed. Subsequently cells were stained with CD4, CD8, CD3, CD49b (NK) for 1 hour at 4 C. Post staining the cells were fixed and permeabilized and stained for IFN-γ. The cells were analyzed using a flowcytometer. The data analysis was done using FlowJo. Live cells were gated for the precence of CD45 marker. The $CD45^+$ cells gated on the CD3 marker, to differentiate the T-cells from the rest of the splenocytes. The $CD3^+$ cells were then sub-gated to determine the $CD8^+$ and $CD4^+$ T- cell populations in the spleen.The NK cell population was determined by gating on $CD45^+$ and $CD49b^+$ cells. This data represents the mean of the five mice.

(GM-CSF, TNF-α, IL-2, IL-1β, IL-4, FGF-Basic, IL-1α, IFN-γ, IL-13, MCP-1, IP-10 (CXCL10), MIG (CXCL9), KC, VEGF, IL-17, MIP-1α, IL-12, IL-10, IL-6, IL-5). The Luminex analysis was performed on serum collected from mice infected with ECTV or ECTVΔ025 at day 2, 4 and 7 post infection. The levels of GM-CSF, TNF-α, IL-2, IL-1β, IL-4, FGF-Basic, IL-1α, MCP-1, KC, VEGF, IL-17, MIP-1α, IL-12, IL-6, IL-5 were not markedly changed in ECTV or ECTVΔ025 infected mice when compared to uninfected mice or remained below detectable levels.

ECTVΔ025 infected mice presented higher levels of CXCL9 and CXCL10 at day 2 post infection. CXCL9 and CXCL10 cytokines remained undetectable at this time point in mice infected with ECTV. The levels of CXCL9 and CXCL10 peaked at day 4 and then declined in mice infected with ECTVΔ025 by day 7. In contrast, mice infected with ECTV showed an increase in CXCL9 and CXCL10 production at day 4 and maintained the level of production at day 7 (Fig. 4.12 A and B). In addition, the blood of mice infected with ECTVΔ025 showed elevated levels of IFN-γ at day 2 and 4 post infection as compared to uninfected mice or ECTV infected mice. In addition to the elevated levels of IFN-γ, we also observed elevated levels of IL-10. Mice infected with ECTVΔ025 showed elevated levels of IL-10 at day 2 and 4 post infection. In contrast, by day 7 the levels of IFN-γ and IL-10 were comparable between ECTV and ECTVΔ025 infected mice (Fig. 4.12 C and D). CXCL9 and CXCL10 are involved in the recruitment of CD8 T cells and NK cells at the site of an intra-cellular infection. These results and the previous experiment suggest that the earlier increases in CXCL9 and CXCL10 might lead to an earlier and increased recruitment of CD8 cells, which would limit the spread of ECTVΔ025 in infected mice. The elevated levels of IFN-γ and IL-10 early post infection

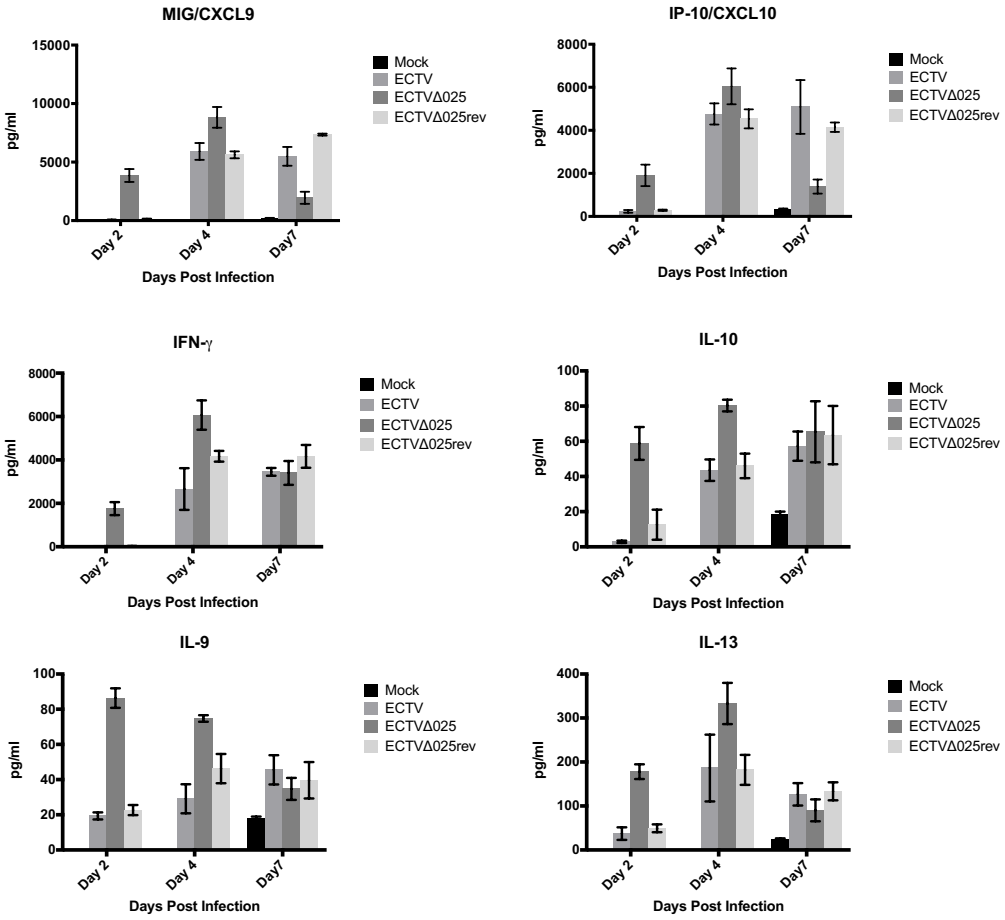

Figure 4.12. ECTVΔ025 infected mice show altered cytokine levels. BALB/c mice were mock-infected or infected with 600 pfu of ECTV, ECTVΔ025, or ECTVΔ025rev via the foot-pad. Each group consists of 5 age and sex matched mice. Blood was collected at days 2, 4 and 7 post infection. Blood from uninfected mice was collected at day 7. The ThermoFisher Scientific Cytokine Mouse 20-Plex Panel for the Luminex™ was used for the analysis of the blood for the presence of cytokine. The samples represent the mean of the 5 different samples.

might help in mounting a Th-1 type cytotoxic T-cell response, which in turn may help prevent the spread of ECTVΔ025. We also detected elevated levels of IL-9 and IL-13 in infected cells, but we are unable to explain the role of these cytokine during infection (Fig. 4.12 E and F).

4.3. Summary

The data in the previous chapter show that EVM025 is involved in the inhibition of apoptosis. In this chapter, we show that although EVM025 ORF is dispensable for *in-vitro* growth of the virus, it is critical in the *in-vivo* replication of the virus. We could establish that ECTVΔ025 is severely attenuated, and typically susceptible BALB/c mice can survive high doses of ECTVΔ025. We were also able to establish that the mutant ECTVΔ025 is unable to spread beyond the draining lymph-node. In addition, we demonstrated that cell mediated immunity was crucial in controlling the spread of ECTVΔ025 and is required to prevent the lethality caused by the mutant virus. Additional work is needed to understand the spread of the virus in the Nude and SCID BALB/c mice. Our data also shows that there is a Th-1 type cytokine response, and CD8 T cells and NK cells are elevated in ECTVΔ025 infected mice. Additional work needs to be done to study the effect of changes in the levels of ECTV specific CD8 T-cells.

Chapter-5- Expression of the vaccinia virus anti-apoptotic F1 protein is blocked by PKR in the absence of the viral E3 protein.

Experiments in this chapters are unpublished
The experiments were performed under the supervision of Dr. Jim Smiley.
All experiments in this chapter were performed by Ninad Mehta with the help of Theodor Dos Santos. Theodor Dos Santos, helped with performing repeats and helped generating all the plasmids used in this chapter.
Dr. Emeka Enwere helped develop the initial idea of the project.
Dr. Bart Hazes helped with the initial analysis of the RNAseq results.
Megan Desaulniers generated the VACVΔF2L virus used in this study.
The members of Dr. David Evans' laboratory have been extremely helpful during this project.

5.1. Introduction

A variety of functions have been assigned to the VACV innate immunity modulator E3. These functions include the ability to modulate the cellular dsRNA response, inhibition of the NF-κB and IRF3 pathways and inhibition of apoptosis. Previously work done by Ficher S F *et al.* and Zhang *et al.* has demonstrated that vaccinia virus missing the E3 protein triggers apoptosis during infection[136,142]. In addition, published research by Kwon J *et al.* presented data suggesting that E3 is an active inhibitor of hygromycin B induced apoptosis[180]. Ficher S F *et al.* demonstrated MVAΔE3L infected cells undergoes apoptosis through the intrinsic pathway, which is similar to cells infected with MVA missing the F1 ORF[142]. Intriguingly, F1 is an early protein and thus should be present during VACVΔE3L infection. It has previously been demonstrated that F1 is an apoptosis inhibitor, and can inhibit apoptosis in the absence of other viral proteins. Thus, we wanted to understand why F1 was is unable to inhibit VACVΔE3L or MVAΔE3L induced apoptosis. Thus, we sought to understand the mechanism underlying the apoptosis triggered by VACVΔE3L infection and its dependency on the VACV protein F1.

5.2. Results

5.2.1 Infection of HeLa cells with VACVΔE3L triggers the intrinsic apoptotic pathway

Previous work on the highly attenuated vaccinia virus MVA strain and the MVA mutant devoid of E3L (MVAΔE3L) has shown that MVAΔE3L triggers apoptosis through the intrinsic pathway[136]. In addition, earlier work on VACV strain Copenhagen has demonstrated that infection of HeLa cells with VACVΔE3L triggers apoptotic cell death[207]. As a prelude to our study we wanted to confirm the aforementioned studies. To this end, HeLa cells were either mock infected or infected with VACV or VACVΔE3L for 24 hrs, and then stained with Alamar Blue, a dye that measures cellular health. Ninety-eight percent of HeLa cells infected with VACV survived, but only 50% of the VACVΔE3L-infected cells survived (Fig. 5.1). Treatment of VACVΔE3L infected HeLa cells with zVAD.FMK blocked cell death, suggesting that the mechanism of death was apoptotic (Fig. 5.1). Since Alamar Blue staining is a non-specific assay, we decided to characterize mitochondrial cell death by evaluating mitochondrial potential and PARP cleavage in infected cells[73,78]. PARP is a nuclear protein that is cleaved upon activation of cellular caspases, a characteristic event that occurs during apoptotic cell death. HeLa cells were infected with VACV or VACVΔE3L. The cells were stained with 0.3μM TMRE, a dye retained in healthy mitochondria, after 12 and 24 hrs of infection. At the 12-hour time point, most of the VACV-infected cells retained TMRE; in contrast, circa 30% of the VACVΔE3L infected cells lost their TMRE staining. A similar trend was observed in

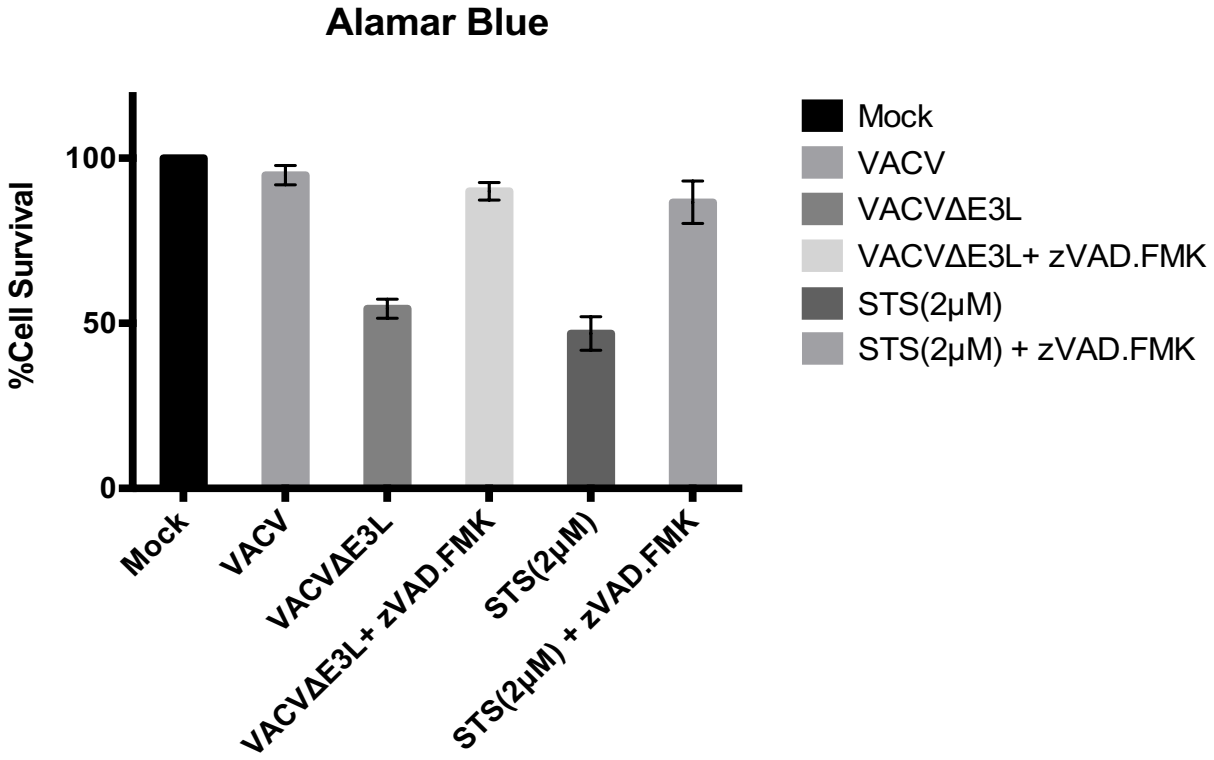

Figure 5.1- VACVΔE3L infection induces cell death. HeLa cells were mock infected, infected with VACV, infected with VACVΔE3L, or infected with VACVΔE3L with 100 μM zVAD.fmk for 24 hours. As a control, HeLa cells were treeated with 2μM STS or 2μM STS+100 μM zVAD.fmk for 6 hours. Post the infection and treatment, the HeLa cells were stained with Alamar Blue for 1 hour at 37 °C in a humidified incubator with 5% CO_2. The conversion of Alamar Blue dye to a reduced product was measured using a fluorecent platereader.

HeLa cells infected for 24 hrs, in that about 24% of VACV-infected cells showed loss of mitochondrial potential, while approximately 51% of VACVΔE3L-infected cells showed a loss of TMRE straining (Fig. 5.2). This result suggests that the mitochondria of HeLa cells infected with VACVΔE3L undergo loss of TMRE staining. The depolarization of the mitochondria can be associated with apoptosis. Next we directly assessed apoptosis by measuring PARP cleavage. HeLa cells were infected with VACV or VACVΔE3L for 2, 4, 6, 12 and 24 hrs and then were analyzed by western blot for PARP cleavage. VACV-infected cells did not process full-length PARP into its 89kDa cleaved form. However, HeLa cells infected with VACVΔE3L did process the full-length PARP into its cleaved form 12 hrs after infection. Since PARP is a substrate for activated caspases, our data suggest that cells infected with VACVΔE3L have activated caspases and are undergoing apoptotic cell death. These results are in accordance with previously published studies [136,207]. In addition to virus induced cell death, we wanted to test whether VACVΔE3L could prevent STS induced apoptosis (Fig. 5.3). Previous studies have demonstrated that VACV is capable of resisting cell death triggered by STS[129]. To test if VACVΔE3L can inhibit STS induced apoptosis, HeLa cells were mock infected or infected with VACV or VACVΔE3L for six hrs. Post infection the cells were treated with 2μM STS for a further six hrs. STS treatment of uninfected cells resulted in increased levels of apoptosis as determined by TUNEL assay. Similar results were observed in the case of VACVΔE3L-infected cells. In contrast, VACV-infected cells were protected against STS induced apoptosis (Fig. 5.4). Thus, our data suggests that VACVΔE3L is capable of triggering virus induced cell death and is unable to prevent

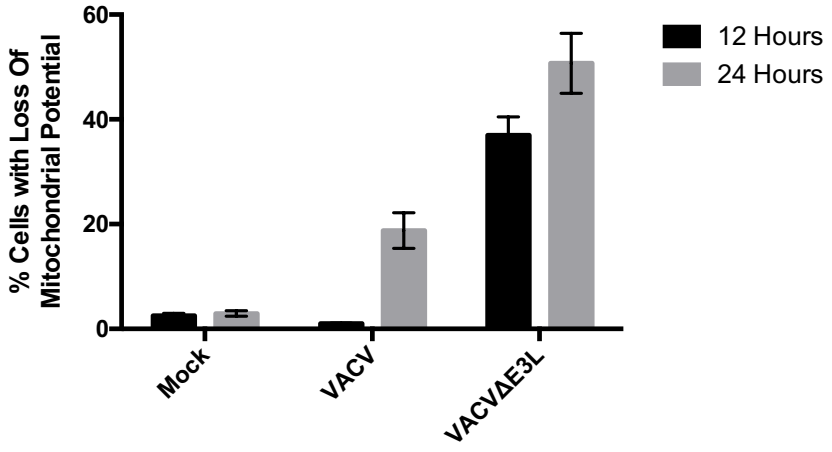

Figure 5.2- VACVΔE3L induces loss of mitochondrial membrane potential. HeLa cells were either mock infected or infected with VACV or VACVΔE3L at an MOI of 5. The HeLa cells were stained with 50nM TMRE, to label mitochondria 12 and 24 hours post infection. Apoptosis was analyzed using flow cytometry. The mean percentage of cells demonstrating a loss of TMRE uptake is displayed. n=3

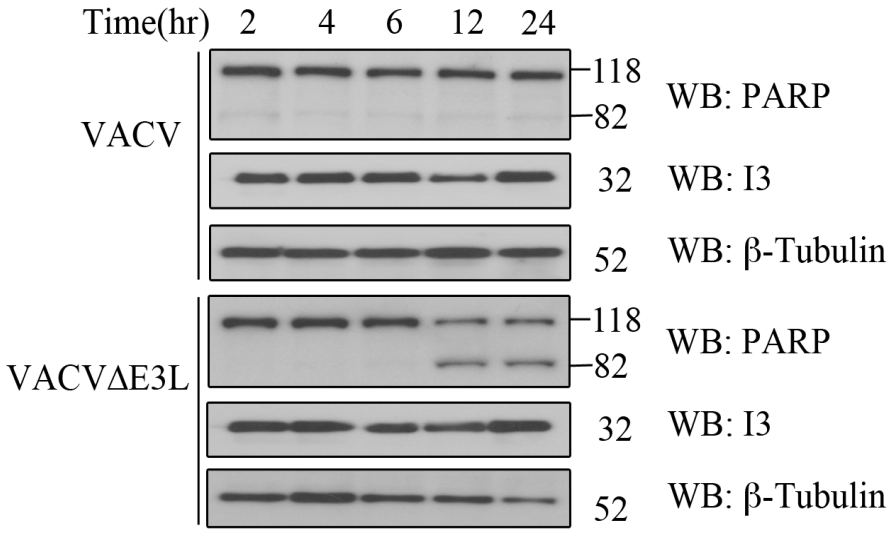

Figure 5.3- VACVΔE3L induces PARP cleavage. HeLa cells were infected with VACV or VACVΔE3L at an MOI of 5. Infected cells were collected 2, 4, 6, 12 and 24 hours post-infection, and lysed in SDS-PAGE sample buffer containing 8 M urea. Samples were subjected to SDS-PAGE and immunoblotted for PARP to determine virus induced apoptosis. β-tubulin was used as a loading control and I3L as a control for infection.

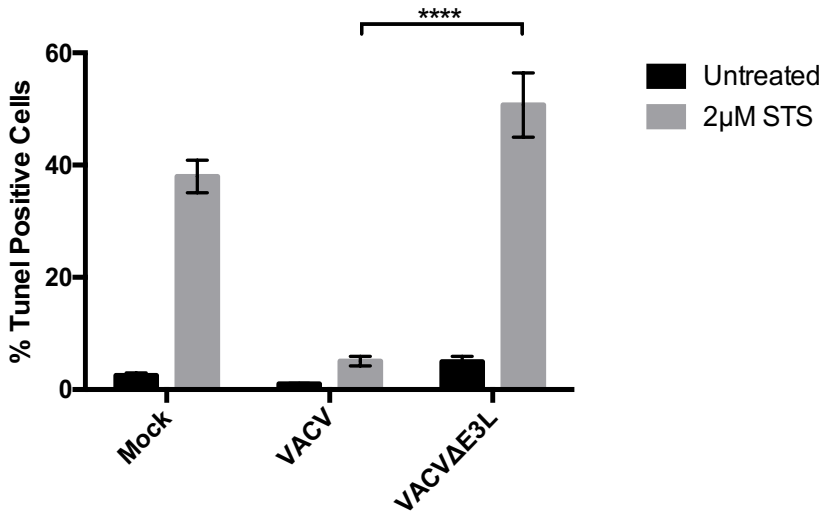

Figure 5.4- VACVΔE3L does not inhibit STS induced apoptosis. HeLa cells were mock infected or infected with VACV or VACVΔE3L at an MOI of 5 for six hours. Six hours post infection, the cells were treated with either DMSO (untreated) or treated with 2μM STS for 6 hours. Six hours post treatment apoptotsis was assessed using the TUNEL assay. The percentage of apoptotic cells was determined using flow-cytometry. n=3, *** $p \leq 0.001$

STS induced apoptosis. These results are consistent with what was observed by P Zhang *et al.* and S F Fischer *et al.* in their studies [136,207].

5.2.2. Ectopically expressed VACV virus E3 does not inhibit induced apoptosis in HeLa cells

A previous report suggested that E3 could protect transfected HeLa cells against hygromycin B induced apoptosis[180]. This observation implies that E3 can act as an apoptosis inhibitor. We were unable to reproduce the previously published results. Thus we asked if E3 expressed on its own could inhibit apoptosis triggered by STS and TNF-α. Previous work on VACV has demonstrated that VACV can protect against apoptosis triggered by STS and TNF- α[138,139]. HeLa cells were transfected with pEGFP, pEGFP-Bcl2, pEGFP-F1L and pEGFG-E3L. Fourteen hours after transfection the cells were treated with 1μM STS for 6 hrs. Apoptosis was assessed by TUNEL staining. In this experiment pEGFP-Bcl2 and p-EGFP-F1L were used as positive controls[102,138,139,208]. GFP positive cells were gated during the flow cytometry. In HeLa cells transfected with pEGFP, approximately 55% of the GPF positive cells were TUNEL positive following STS treatment. A similar percentage of TUNEL positive cells was observed in the case of GFP positive HeLa cells transfected with pEGFP-E3L. In contrast, cells transfected with the cellular anti-apoptotic protein Bcl2 and vaccinia virus anti-apoptotic protein F1 were protected against STS induced apoptosis with less than 7% of the GFP positive cells TUNEL positive (Fig.5.5). Next we tested another apoptotic stimulus TNF- α. A similar trend was observed in HeLa cells that were treated with 10 ng/ml TNF-α

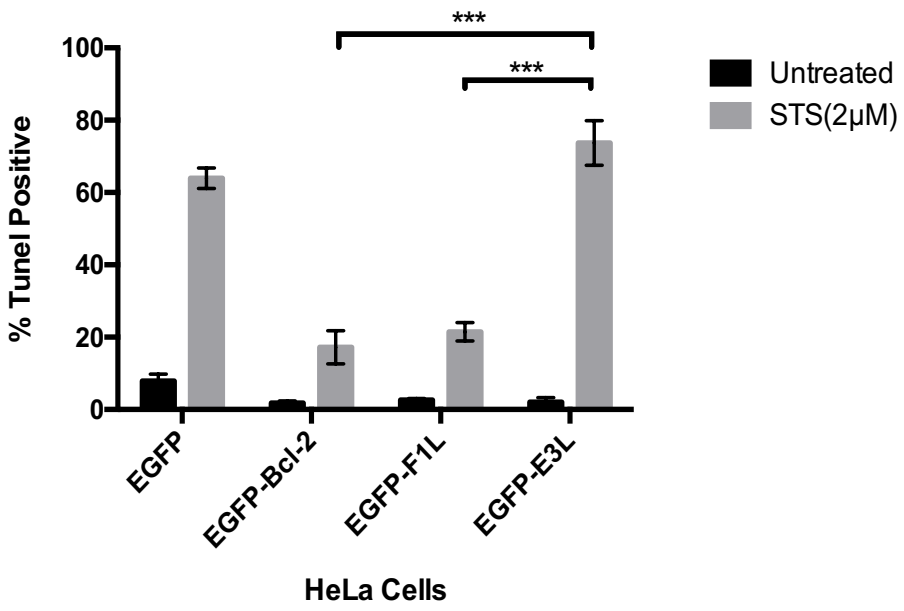

Figure 5.5- E3 does not inhibit STS induced apoptosis. HeLa cells were transfected with pEGFP, pEGFP-Bcl2, pEGFP-F1L and pEGFP-E3L for 16 hours. Post transfection, the cells were treated with either DMSO (untreated) or treated with 2.5μM STS for 6 hours. Six hours post treatment apoptotsis was assessed using the TUNEL assay. The percentage of apoptotic cells were determined using flow-cytometry. n=4, *** $p \leq 0.001$

and 5 μg/ml of cycloheximide/ml for 16 hrs to trigger apoptosis. Cells that were mock transfected or transfected with pEGFP or pEGFP-E3L were not protected against TNF-α induced apoptosis. GFP positive cells were gated during the flow cytometry. Approximately 40% of the cells were TUNEL positive in this case. In contrast, less than 4% of the cells that has been transfected with pEGFP-Bcl2 and pEGFP-F1L were apoptotic (Fig.5.6). Thus our data would suggest that E3 fails to protect the cells against STS or TNF-α induced intrinsic apoptotic stimuli. These data suggest that E3 is unable to act as direct inhibitor of STS and TNF-α induced apoptosis.

5.2.3. F1L is not expressed during VACVΔE3L infection

Our finding that E3 does not serve as a direct inhibitor of apoptosis raised interesting questions about the mechanisms underlying the pro-apoptotic phenotype of VACVΔE3L. One possibility, suggested previously by S F Fischer *et al.*, is that E3 acts together in the same pathway as the VACV anti-apoptotic F1 protein, a direct inhibitor of apoptosis. VACV F1 can inhibit mitochondrial apoptosis in HeLa cells by inhibiting the activation of cellular apoptotic proteins Bak and Bax[134,139,140,209]. However, this suggestion is difficult to reconcile with the ability of F1 to prevent apoptosis in the absence of any other VACV proteins. An alternate possibility is that E3 is required for the synthesis of F1. This possibility seemed improbable because F1 has been reported to be an early protein. Previous work with the E3L deletion mutant virus suggested that early proteins are expressed during infection with this virus[210]. However, this theory has never been tested in the case of F1 expression.

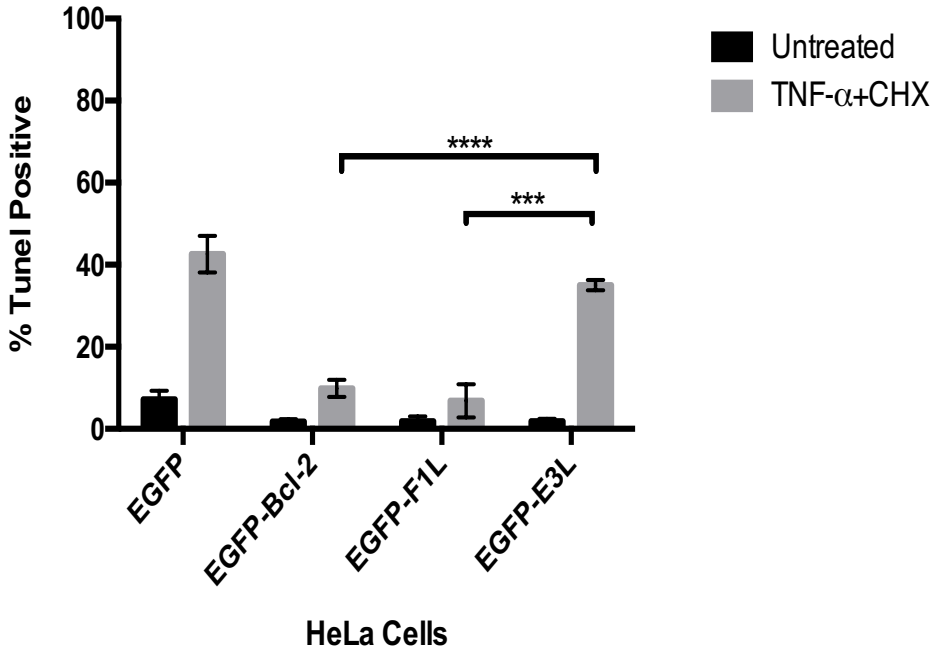

Figure 5.6 - E3 does not inhibit TNF-α induced apoptosis. HeLa cells were transfected with pEGFP, pEGFP-Bcl2, pEGFP-F1L and pEGFP-E3L for 16 hours. Post transfection, the cells were treated with either PBS(untreated) or 10 ng/ml TNF-α and 5 μg/ml of cycloheximide/ml for 16 hours . Sixteen hours post treatment apoptotsis was assessed using the TUNEL assay. The percentage of apoptotic cells was determined using flow-cytometry. n=3, *** $p \leq 0.001$, **** $p \leq 0.0001$

We therefore examined the effect of deleting E3 on the expression of the F1 protein. HeLa, RAW, Jurkat and 293T cells were either mock infected, or infected with VACV or VACVΔE3L for 6 hrs. The cell lysates were probed for the expression of F1 protein by western blot analysis. We observed that F1 was present in a VACV-infected cell. To our surprise however, F1 was not detected in cells infected with VACVΔE3L. This observation remained consistent between HeLa, Jurkat, RAW and 293T cells. Antibody against I3L was used as an infection control. Previous publications have demonstrated that I3L is present during VACVΔE3L infections[207]. β-tubulin was used as the loading control (Fig. 5.7). Together these data suggest that F1L remains undetectable during VACVΔE3L infection in a wide variety of infected cell lines.

The previous observations suggest that the presence of E3 is required for the expression of F1. To test this possibility, we asked whether ectopic expression of E3 was sufficient to restore the expression of F1 during VACVΔE3L infection. To this end, HeLa cells were transfected with pEGFP or pEGFP-E3L for 18 hrs. The transfected cells were infected with either VACV or VACVΔE3L virus for 6 hrs. The infected cells were then subjected to western-blot analysis. In HeLa cells expressing pEGPF and infected with VACVΔE3L, F1 was not detected by western blotting. In contrast, in HeLa cells transfected with pEGFP-E3L and infected with VACVΔE3L virus, the expression of F1 was restored. This result suggests that the ectopic expression of E3 during VACVΔE3L infection is sufficient to restore the expression of F1 (Fig. 5.8). These sets of experiments help us understand the relationship between E3 and F1 and suggest E3 is required for the expression of F1.

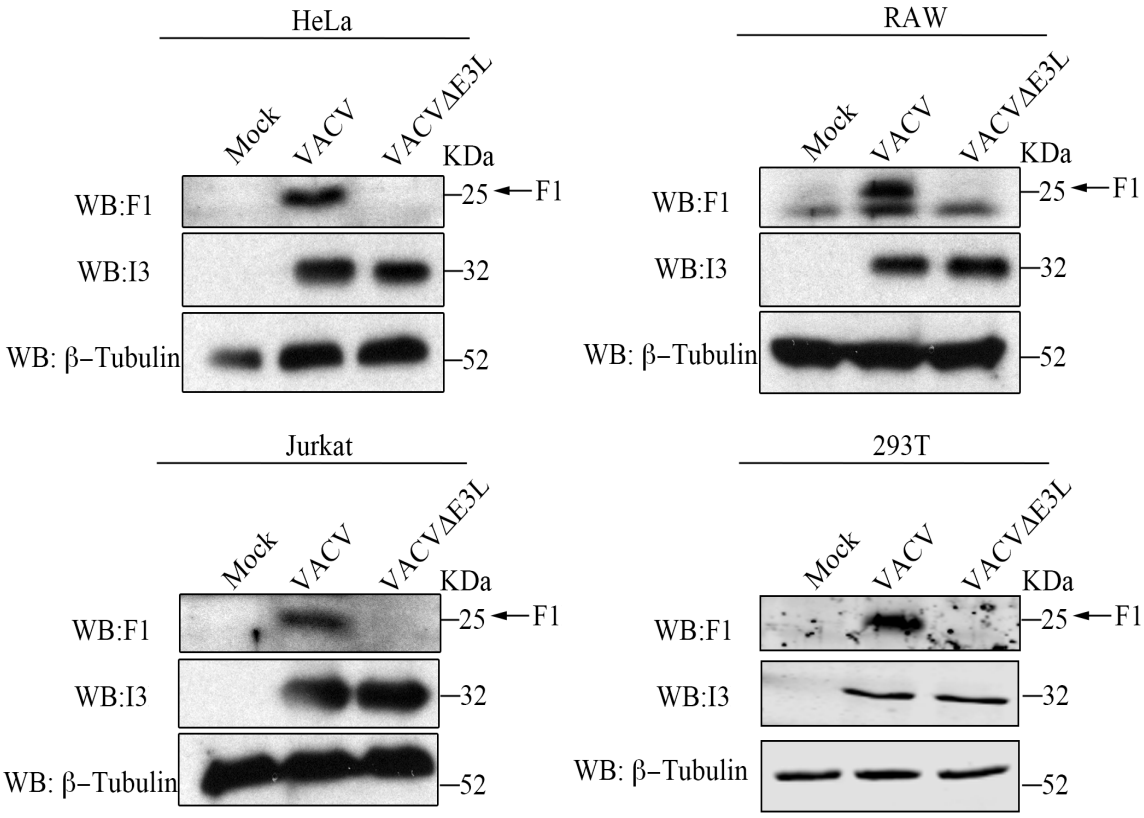

Figure 5.7 - F1 is not detected during VACVΔE3L infection. The indicated cells were either mock infected, infected with VACV, or infected with VACVΔE3L at an MOI-5. Six hours post infection the cells were lysed in RIPA buffer and cell lysates were immunoblotted with anti-F1 antibody to analyse the expression of the F1, and anti-I3 to determine the levels of infection. β-tubulin was used as a loading control.

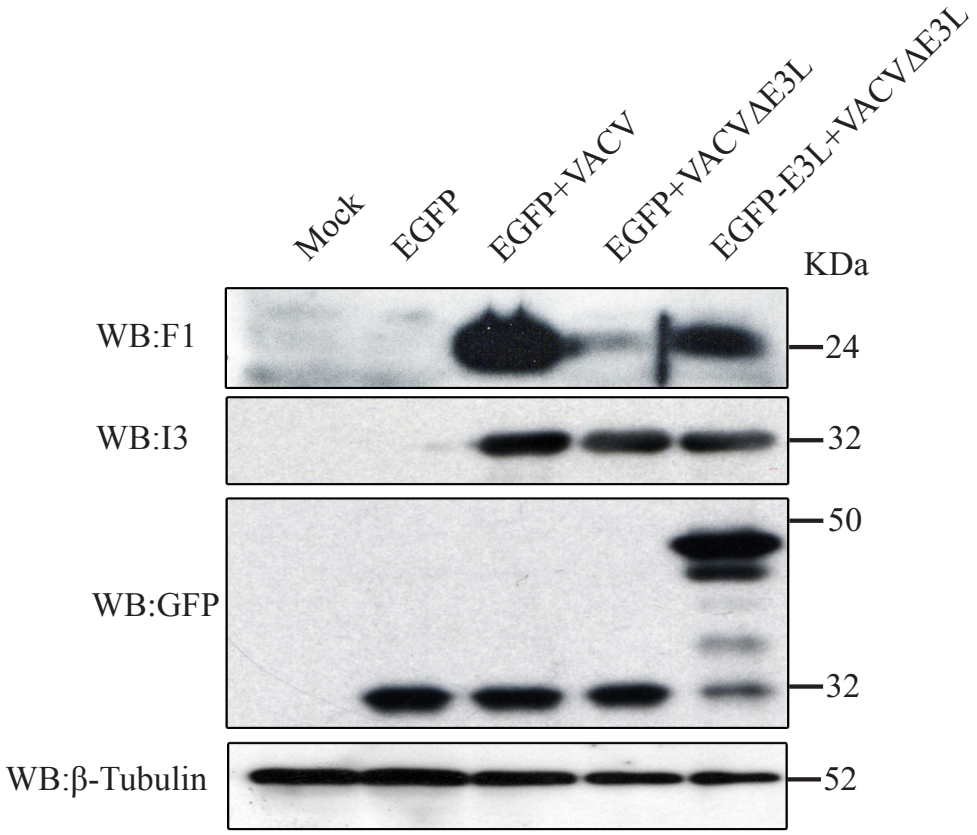

Figure 5.8 - Ectopic expression of E3 rescues the expression of F1. HeLa cells were either transfected with pEGFP (vector) or EGFP-E3L. Eighteen hours post transfection, the cells were infected with VACV or VACVΔ E3L at an MOI of 5. Six hours post infection the cells were lysed in RIPA buffer and subjected to immunoblotting. The samples were subjected to anti-F1 antibody. Anti-I3 to determine the levels of infection, anti-GFP antibody was used to check expression levels of the transfected plasmid, β-tublin was used as a loading control.

5.2.4. The ectopic expression of F1 is sufficient to prevent apoptosis triggered by VACVΔE3L

The results from the previous experiment suggest that E3 is required for the expression of F1 during a VACV infection. Since F1 is an anti-apoptotic protein, we next wanted to determine if the absence of F1 was the reason behind VACVΔE3L's inability to inhibit apoptosis. We transfected HeLa cells with an empty pEGFP-C3 vector, or with pEGFP-F1L. Sixteen hrs post transfection, the cells were either mock infected, or infected with VACV or VACVΔE3L. Twenty-four hrs post infection apoptosis was measured by TUNEL staining (Fig. 5.9). Low numbers of TUNEL positive cells were observed in HeLa cells that had been transfected with pEGFP or pEGFP-F1L and subsequently mock infected. Similar results were obtained for HeLa cells transfected with pEGFP or pEGFP-F1L and infected with VACV. In contrast, 55% of HeLa cells that had been transfected with pEGFP-C3 and infected with VACVΔE3L stained TUNEL positive. However, in HeLa cells transfected with pEGFP-F1L and infected with VACVΔE3L the number TUNEL positive cells fell to 25% of the total screened cells (Fig. 5.9). This result suggests that the ectopic expression of F1 is sufficient to reduce the apoptosis triggered by VACVΔE3L infection. Thus, we infer that the underlying reason for the apoptosis triggered by VACVΔE3L infection is the absence of F1 protein.

5.2.5. The C-terminus of E3 is required for the expression of F1 in VACV-infected cells

As reviewed in Chapter 1, E3 is a 190-amino-acid protein with N-terminal DNA-binding and C-terminal RNA-binding domains. Previous work on E3 has shown that the

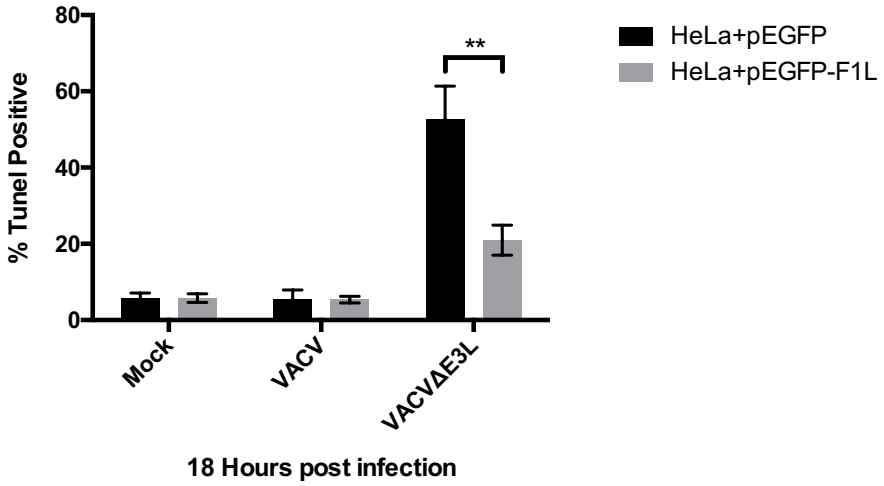

Figure 5.9 - Ectopic expression of F1L is sufficient to prevent the apoptosis triggered by VACVΔE3L. HeLa cells were transfected with pEGFP or pEGFP-F1L. Sixteen hours post transfection, the transfected HeLa cells were either mock infected, infected with VACV or with VACVΔE3L at an MOI of 5. The level of apoptosis was assessed by TUNEL assay. The percentage of apoptotic cells (TUNEL positive) was deteremined by flowcytometry. n=3,
$p \leq 0.05$

C-terminal RNA-binding domain is necessary and sufficient for PKR inhibition and virus replication, and the N-terminus of the protein has a Z-DNA binding motif [163,174,175]. VACV-E3LΔ26C is a mutant virus that is unable to inhibit the PKR pathway, while VACV-E3LΔ83N virus still inhibits the PKR pathway. In addition, VACV-E3LΔ26C infected HeLa cells undergo apoptosis[207]. A study by P Zhang *et al.* has shown that an E3-N-terminal deletion mutant (VACV-E3LΔ83N) has no apoptotic activity, and this virus is able to replicate to a titer similar to that of wild type VACV[207]. In addition, their data shows that this is not the case with an E3-C-terminal deletion mutant (VACV-E3LΔ26C). Infection of HeLa with VACV-E3LΔ026C triggers apoptosis[207]. However, their data fails to ascertain the reason underlying the apoptosis during a VACVΔE3L or VACV-E3LΔ26C infection. We initially reproduced the above mentioned results. Previous work has also demonstrated that VACV is capable of inhibiting STS induced apoptosis. Thus, we tested the ability the mutants to inhibit both virus and STS induced apoptosis. In addition, we wanted to determine the status of F1 protein during VACV-E3LΔ85N and VACV-E3LΔ26C. We hypothesize that the apoptosis triggered by VACV-E3LΔ26C was due to the absence of F1 protein during infection.

We mock infected HeLa cells or infected them with VACV, VACVΔE3L, VACV-E3LΔ26C, or VACV-E3LΔ85N. The infected cells were stained with TMRE at 12 and 24 hrs post infection. The cells were then analyzed by flow-cytometry (Fig. 5.10). As shown previously in Fig 5.2, at both 12 and 24-hour post-infection cells infected with VACVΔE3L displayed substantially lower levels of TMRE staining than those infected with wild-type virus, indicating that E3L is required to protect cells from virus-induced cell death. VACV-E3LΔ23C infected HeLa cells displayed a similar phenotype to HeLa

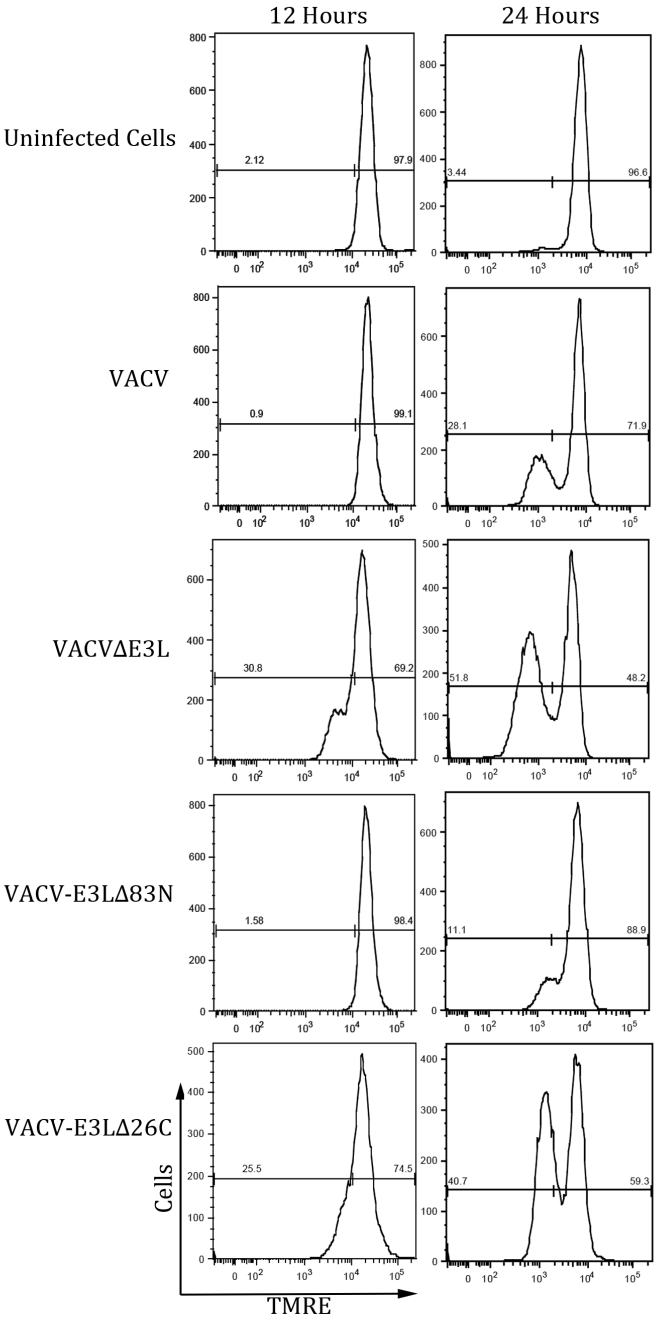

Figure 5.10 - The C-terminus of E3L is required to maintain membrane potential during virus infection. HeLa cells were infected mock infected, infected with VACV, VACVΔE3L, VACV-E3LΔ83N or VACV-E3LΔ26C at an MOI of 5 for 12 or 24 hours. Post infection the infected cells were stained with 50nM TMRE to label mitochondria, and apoptosis was analyzed in the infected cells using two-color flow cytometry. These data are representative of at least three independent experiments

cells infected with VACVΔE3L. In contrast, VACV-E3LΔ85N failed to trigger any loss of mitochondrial potential, just like the wild type VACV. Next we assessed the capacity of the E3L mutants to prevent STS induced apoptosis. HeLa cells were infected with the same virus as previously described and treated with 2μM STS for 6 hrs. The level of apoptosis was assayed using the TUNEL assay (Fig. 5.11). As previously observed in Fig 5.4, VACV infected HeLa cells were protected against STS induced apoptosis, while VACVΔE3L infection did not offer the same protection. VACV-E3LΔ23C was also unable to protect against STS induced cell death. In contrast, like VACV-infected cells, VACV-E3LΔ83N-infected cells were protected against STS induced apoptosis (Fig. 5.11). In summary, the results displayed in Fig. 5.10 and Fig. 5.11 confirm the findings of Zhang et al, namely that the C-terminal region of E3L is required to block cell death while the N-terminal region is dispensable [207].

The afore-mentioned results raised the question of the status of the F1 protein during VACV-E3LΔ83N and VACV-E3LΔ26C infection. To answer this question, we mock infected HeLa cells or infected them with VACV, VACVΔE3L, VACV-E3LΔ83N and VACV-E3LΔ26C. F1 was detected in VACV-infected cells but was not detected in VACVΔE3L-infected cells. This result was consistent with our previous observation (Fig 5.7). F1 was present in VACV-E3LΔ83N-infected cells but always in lower amounts than in VACV-infected cells. This observation was consistent for multiple repeats of the experiment. However, no F1 protein was detected in of HeLa cells infected with VACV-E3LΔ26C (Fig. 5.12). These results would suggest that the ability of VACV-E3LΔ83N to inhibit apoptosis is due to its ability to express F1 during infection. In addition, the data

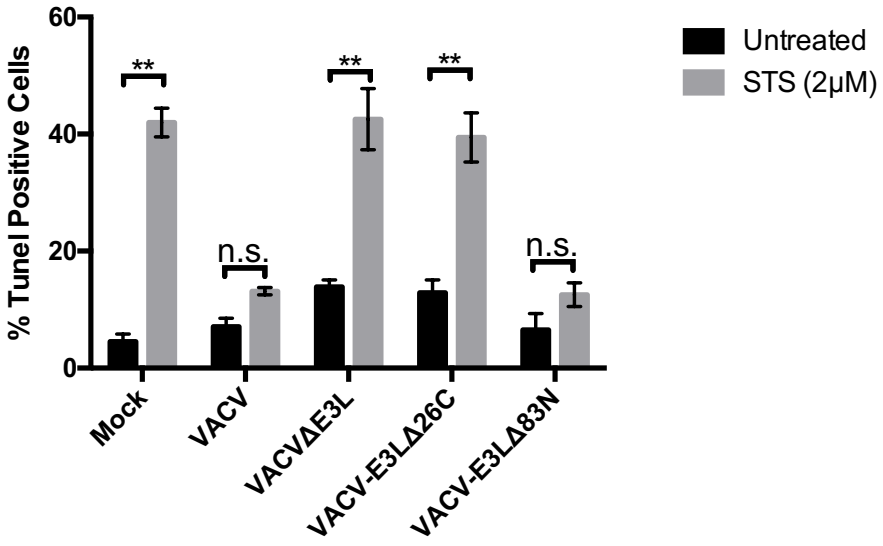

Figure 5.11- VACV-E3LΔ26C does not protected against STS induced apoptosis. HeLa cells were either mock infected, or infected with VACV, VACVΔE3L, VACV-E3LΔ26C, or VACV-E3LΔ83N at an MOI of 5. Six hours post infection, the cells were either treated with 2μl of DMSO or 2μM STS for six hours. The cells were TUNEL stained to access the level of apoptosis. The percentage of TUNEL positive cells was determined using Flow cytometry. n=3, $p<0.05$.

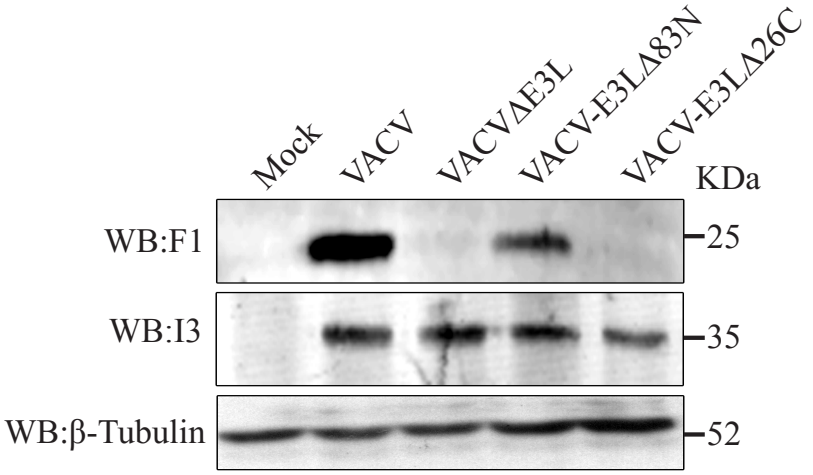

Figure 5.12- F1 is absent duing VACV-E3L26C. HeLa cells were either mock infected, infected with VACV, VACVΔE3L, VACV-E3L83N, VACV-E3L26C at an MOI of 5. Six hours post infection, the cells were harversted and lysed using the RIPA buffer. The cell lysates were subjected to immunoblotting using the anti-F1L antibody to detect F1L expression, anti-I3L antibody to detect virus infection and anti-b-Tubulin was used as a loading control.

also suggest that low levels of F1 are sufficient to inhibit apoptosis. VACV-E3L83N can inhibit the PKR pathway, which led us to infer that inhibition of the PKR pathway is responsible mediating F1 expression in infected HeLa cells.

5.2.6. Activated PKR inhibits the expression of F1 in the VACVΔE3L mutant

Zhang *et al.* have shown that knocking down PKR eliminates the pro-apoptotic phenotype induced by VACVΔE3 infection [207]. Their data also shows that knocking down PKR corrects the growth defect and restores late gene expression in VACVΔE3L infected cells. This led us to inquire about the role of PKR in the expression of F1 during a VACVΔE3L infection. HeLa and HeLa-PKR KO cells were mock infected or infected VACV or VACVΔE3L. As observed in Fig. 5.7, in HeLa cells infected with VACV, F1 was detected. Conversely in HeLa cells infected with VACVΔE3L, F1 was not detected. F1 was detected in HeLa PKR-KO cells infected with VACV. F1 was also detected in cell lysates of HeLa-PKR KO infected with VACVΔE3L (Fig 15.13). These results indicate that the absence of F1 in VACVΔE3L-infected cells could be correlated to a functional cellular PKR pathway. This was surprising as F1 is an early protein, and literature would suggest that early proteins should be present during a VACVΔE3L infection.

5.2.7. Intermediate Summary

The experimental results suggest that, contrary to previously published data, E3 cannot act as an anti-apoptotic protein under the conditions of our experiments. Our western blot data show that F1 is not detectable during a VACVΔE3L infection.

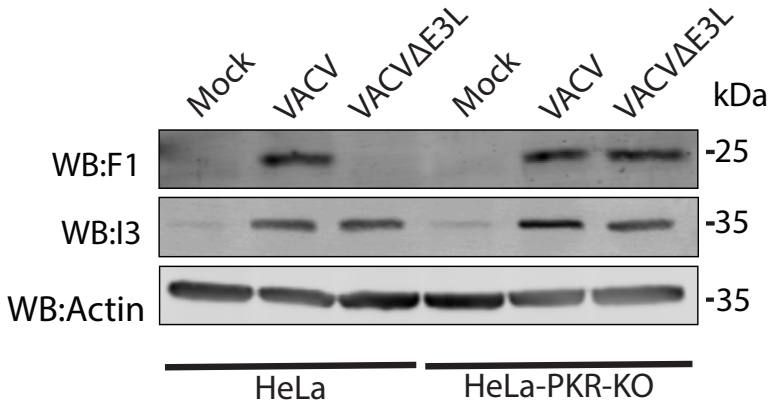

Figure 5.13 - Activated PKR inhibits the expression of F1 in the VACVΔE3L mutant. HeLa and HeLa-PKR-KO cells were either mock infected or infected with VACV or VACVΔE3L virus at an MOI of 5. Six hours post infection, the infcted cells were lysed in RIPA buffer. The cell lysates were subjected to western blot anlysis using the anti-F1 , anti-I3 and anti-β-actin antibody.

Moreover, we could establish that the absence of F1 is responsible for the apoptosis induced during VACVΔE3L infection. Previous work has demonstrated that knocking down the PKR pathway alleviated the apoptosis triggered by VACVΔE3L infection. Our experiments have demonstrated that the expression of F1 during a VACV infection is dependent on the ability of E3 to inhibit the PKR pathway. VACV transcripts are classified into three different temporal classes: early, intermediate post-replicative and late post-replicative. The classification of the VACV transcripts is based on Northern Blot analysis[178], microarray experiments, and RNA-seq analysis[26]. The classification of the proteins is based on the time of the appearance of the transcripts. The literature suggests that intermediate post-replicative and late post-replicative proteins are absent during VACVΔE3L infection [163,178,207,210]. Previous northern blot analysis on the F1 transcript from MVA strain [136] and RNA-seq data from VACVwr [26] would suggest that F1 is an early protein. In addition, Postigo *et al.* were able to demonstrate that F1 was detected by western blot as early as 2 hrs post infection [140]. Thus, the literature would suggest that early proteins are present during VACVΔE3L infection, so the absence of F1 is unexpected. We next wanted to try to determine the reason for the absence of F1 during a VACVΔE3L infection.

5.2.8. F1 transcript is present during VACVΔE3L infection

As mentioned earlier, Fisher *et al.* showed that the F1 transcript is present early during a MVAΔE3L infection, but the levels of F1 transcript diminished quickly after infection [136]. No experimental data is available about the F1 transcript during the VACVΔE3L infection. We wanted to determine the fate of the F1 transcript during a

VACVΔE3L infection. We performed an RNA-seq experiment to determine the presence and kinetics of the F1 transcript during a VACVΔE3L infection. HeLa cells were infected with VACV and VACVΔE3L for 0.5, 1.5, 2, 3, 5 and 12 hrs. The poly(A) RNA from these samples was used for RNA-seq. The number of sequenced reads obtained at each point is tabulated in Table 5.1. All the obtained reads were aligned against the VACV genome to construct a high-resolution map of the VACV transcriptome. The number and percentage of the reads mapped to the VACV genome can also be found in Table 5.1. We observed a high variability in the number of reads sequenced in each sample, but the percentage of reads mapped to the VACV genome was similar between the experimental repeats (Table 5.1.). The results demonstrate that F1 transcript was present during a VACVΔE3L infection. The F1 transcript in VACV and VACVΔE3L infected HeLa cells were detected in comparable quantities for the first 5 time points (Fig. 15.14). At 12 hrs, we detected lower numbers of F1 transcripts in VACV-infected cells. Thus, the F1 transcript is present during VACVΔE3L infection, and the transcript persists in VACVΔE3L-infected cells. This result was different from what was previously reported by Fisher *et al*., where they observed a drop in F1 transcript within the first two hrs of a MVAΔE3L infection[207]. Conventionally it is assumed that if the transcript for the protein is present then that protein is present during a poxvirus infection. Thus the absence of F1 is especially surprising during a VACVΔE3L infection.

Next we asked if any other early protein is absent during a VACVΔE3L infection, or is F1 unique in this matter. Since a limited number VACV antibodies were available for this experiment, we looked at the expression of I3, N2, F4, F1, B5, A36, A34 and I5 during VACVΔE3L infection. Our RNA-seq data would suggest that I3, N2, F4 and F1

Table 5.1- Summary of RNAseq reads in VACV infected HeLa cells

Samples	Time Post Infection	Total Number Of Reads	No of Reads Mapped to VACV Genome	Percentage of Mapped reads
Experiment-1				
VACV	0.5	4770090	3586	0.075
VACV	1.5	6520244	16613	0.25
VACV	2	3770368	14804	0.39
VACV	3	1976210	16479	0.83
VACV	5	3616381	101308	2.80
VACV	12	4735453	1877160	39.64
VACVΔE3L	0.5	2849818	15734	0.55
VACVΔE3L	1.5	10228508	85174	0.83
VACVΔE3L	2	5009717	66268	1.32
VACVΔE3L	3	10677165	308978	2.89
VACVΔE3L	5	2045295	81723	3.99
VACVΔE3L	12	13950672	517101	3.70
Experiment-2				
VACV	0.5	6371966	4933	0.077
VACV	1.5	20667487	57058	0.27
VACV	2	18381580	61110	0.33
VACV	3	30450578	221291	0.72
VACV	5	5152132	130837	2.53
VACV	12	6520543	2405997	36.89
VACVΔE3L	0.5	18559427	81862	0.44
VACVΔE3L	1.5	4332395	38797	0.89
VACVΔE3L	2	7925871	122223	1.54
VACVΔE3L	3	6786536	199355	2.93
VACVΔE3L	5	33761314	1802666	3.33
VACVΔE3L	12	6253168	254888	4.07

are early genes (Fig. 5. 14). B5, A36 are post replicative intermediate genes. A34 and I5 are post replicative late genes (Fig. 5.15). To determine the status of the above mentioned proteins during VACVΔE3L infection, we infected HeLa cells with VACV or VACVΔE3L. We observed that I3, N2 and F4 protein were detected in both VACV and VACVΔE3L-infected cells (Fig. 5. 16). In contrast, F1 was detected at 4 hrs post VACV infection, however F1 was undetectable in VACVΔE3L infected HeLa cells (Fig. 5. 16). These observations would suggest that during a VACVΔE3L infection the F1 protein is not detected with an altered timeline. VACV protein B5 was detected during a VACV infection, but B5 was not detected during VACVΔE3L infection. This observation is consistent with the previously published data about B5R during a VACVΔE3L infection [207]. A similar pattern was observed in the case of the VACV protein A36, in that the protein was detected at 6-hour post infection but was absent in HeLa cells infected with VACVΔE3L (Fig. 5. 16). This experiment would suggest that F1 is an early protein that is absent during a VACVΔE3L infection. F1 expression is highly sensitive to the activation of PKR. One possible reason for the higher sensitivity of F1 to the activation of the PKR pathway, is the time at which we detect the F1 protein. Though Postigo *et al.* were able to demonstrate that F1 was detected by western blot as early as 2 hrs post infection, we do not detect the protein till 4 hrs post infection. The late appearance of F1 could be the reason behind the higher sensitivity to the translational block imposed by the activation of the PKR pathway.

In addition, the RNA-seq experiment also led to another unexpected observation. While analyzing the RNA-seq data and the fluctuating coverage depths of the mapped reads on the VACV genome, we noticed that the coverage depth remained similar

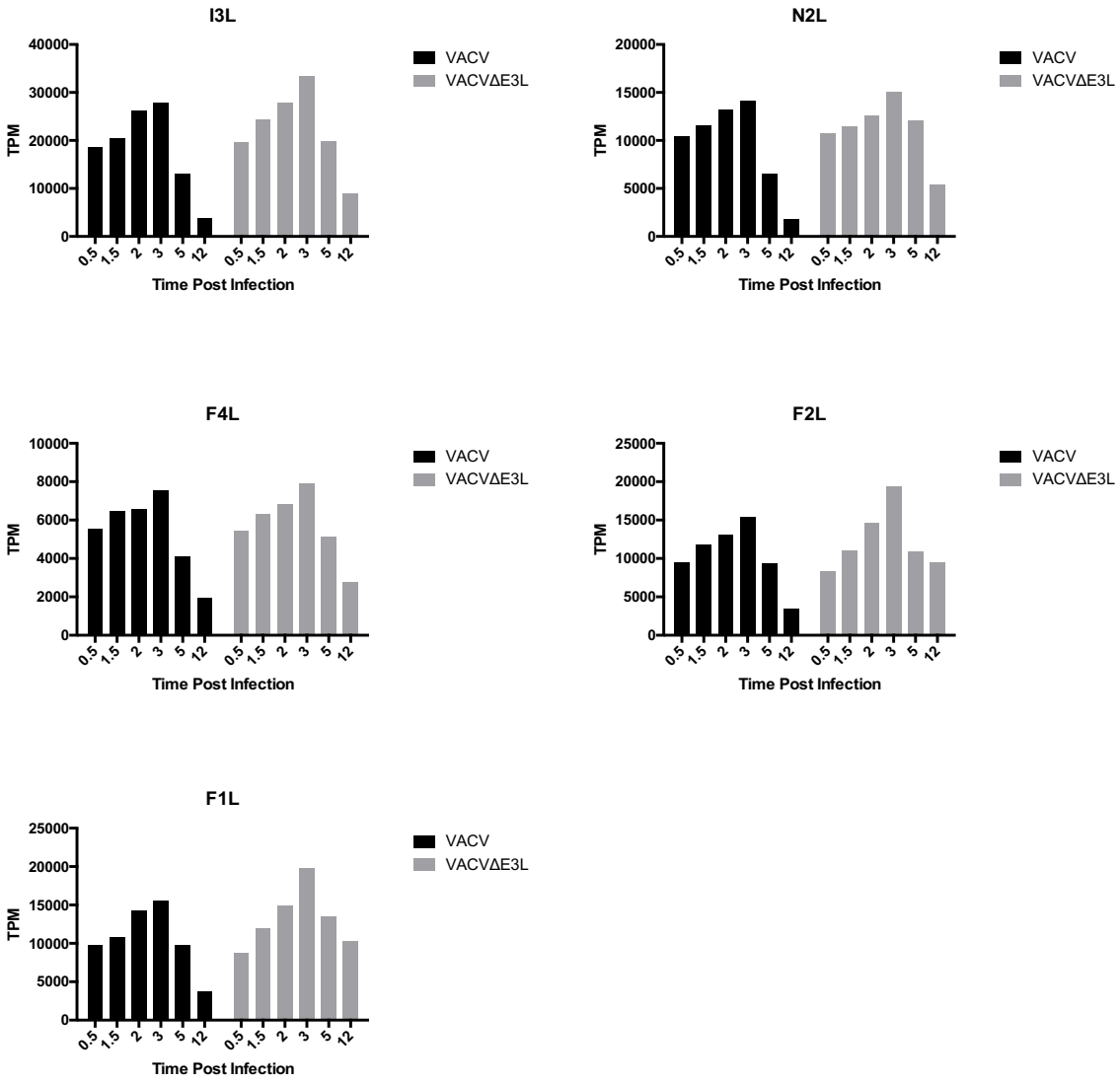

Figure 5.14- F1L transcript is present during a VACVΔE3L infection. Transcripts per Million (TPM mapped sequence reads) of selected early transcripts on the VACV genome. n=2

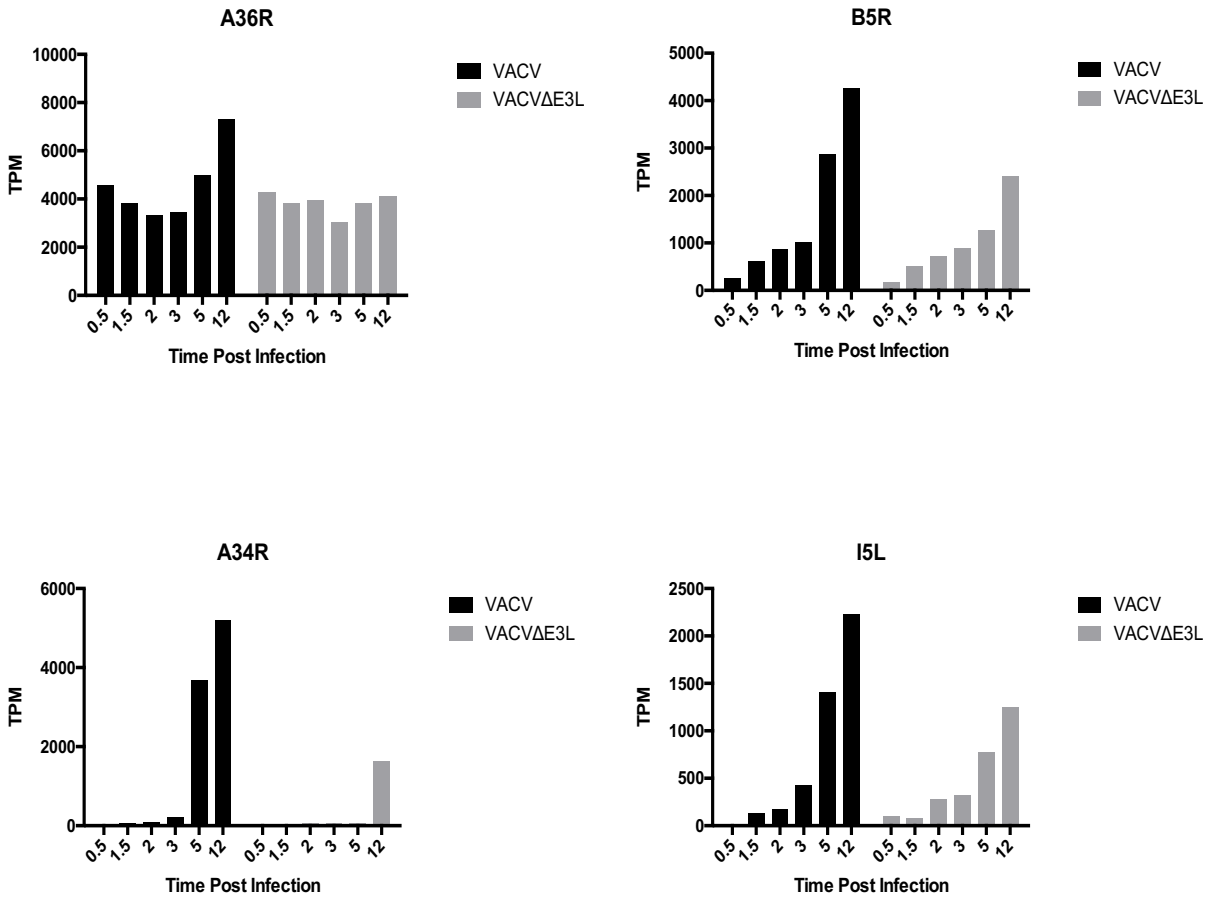

Figure 5.15- intermediate and late transcripts during a VACVΔE3L infection. Transcripts per Million (TPM) mapped sequence reads of the post replicative intermediate genes A36R and B5R, and late genes A36R and I5R. n=2

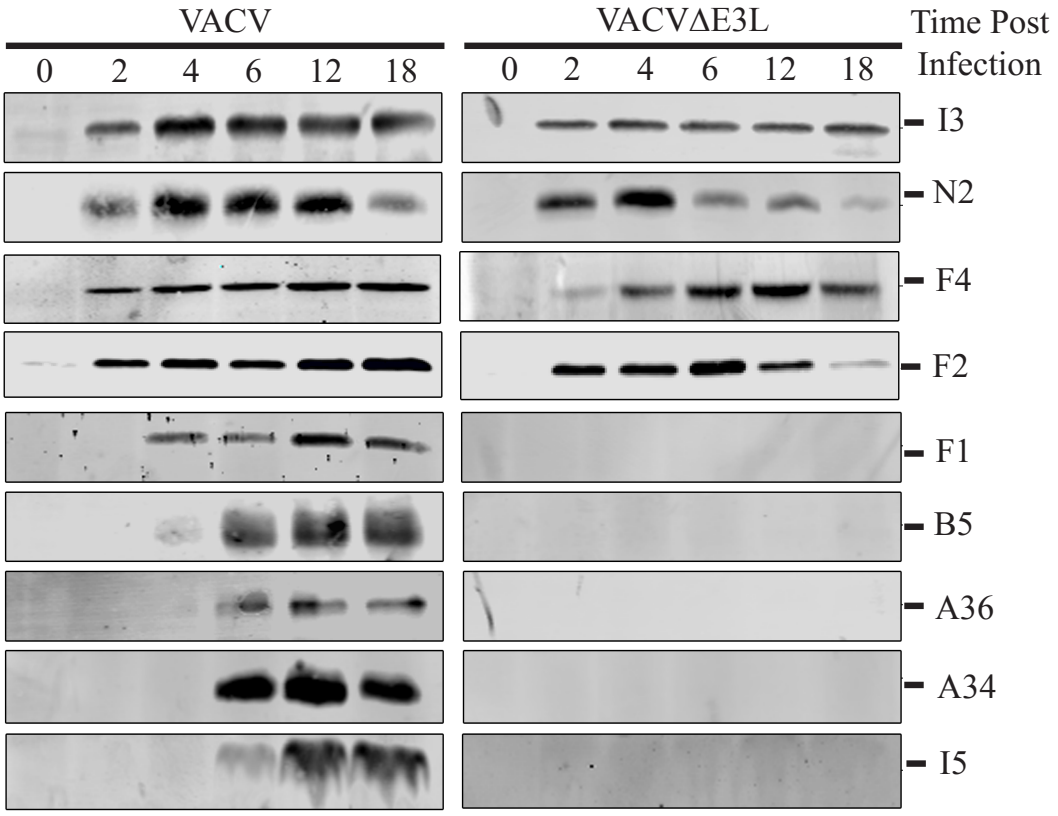

Figure 5.16- F1 expression pattern was not altered during VACVΔE3L infection. HeLa cells were infected with VACV or VACVΔE3L infection at an MOI of 5. The cells were harvest at 0, 2, 4, 6, 12 and 18 hours post infection and the samples were lysed in RIPA buffer. The cell lysates were subjected to immunoblotting using the anti-I3 antibody, anti-N2 antibody, anti-F4 antibody, anti-F2 antibody, anti-F1 antibody, anti-B5 antibody, anti-A36 antibody, anti-A34 antibody, anti-I5 antibody.

between the *F1L* and *F2L* orf. There were no fluctuations in coverage depth of RNA-seq reads that mapped to the F1L and F2L regions of the VACV genome (Fig 5.17 A). In contrast, when we look at the neighboring region of F3L and F4L, we detect fluctuations in the coverage depth of the RNAseq reads between this region (Fig. 5. 17 B). Also we can detect regions which distinctly mark the start site and the end site of the transcripts for the F3L and F4L genes (Fig 5.17 B black arrow). It was also surprising that no such region was detected between the F1L and F2L orf (Fig. 5. 17 A). The absence of clear start and stop sites between the reads that map to the F1L and F2L regions suggests that there is one message that spans the F1L and F2L orf. Thus, it is possible that F1 and F2 are encoded from the same bicistronic mRNA.

5.2.9. Two distinct mRNAs are detected by an *F1L-probe*

The data from the previous section suggests that there is a possibility of a bicistronic mRNA for F1 and F2 proteins. These observations were confirmed using northern blotting. HeLa cells were mock infected, or infected with VACV or VACVΔE3L at an MOI of 5 for 3 hrs, and the RNA from infected cells was harvested. For the northern blot analysis, we used a ^{32}P labelled probe generated by random priming against the full-length F1L gene (Fig. 5.19 A). We detected F1 transcript 3 hrs post infection in VACV and VACVΔE3L-infected cells. We observed that the F1 probe hybridized to two distinct bands of approximately 1.7 kb and 900 kb (band-A and band-B) (Fig. 5.18). The annotated gene size for F1L is 682 bp and for F2L is 444 bp in size. Thus, the 1.7 kb message (band-A) can be explained as a sum of the two genes plus a poly A tail on the mRNA. The binding of the F1L-*probe* to a larger mRNA was expected

(A)

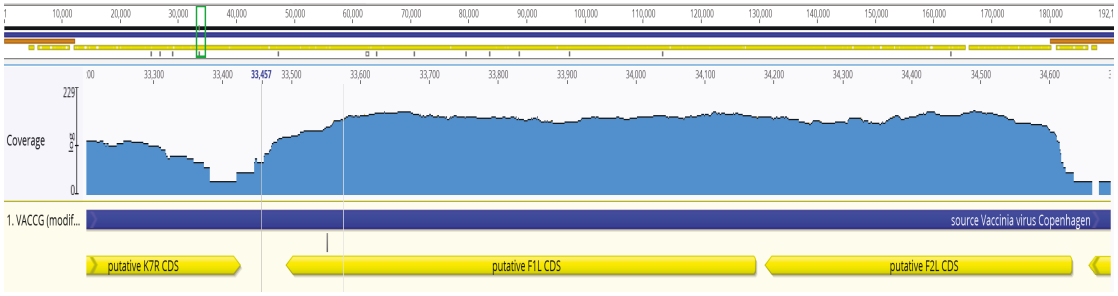

(B)

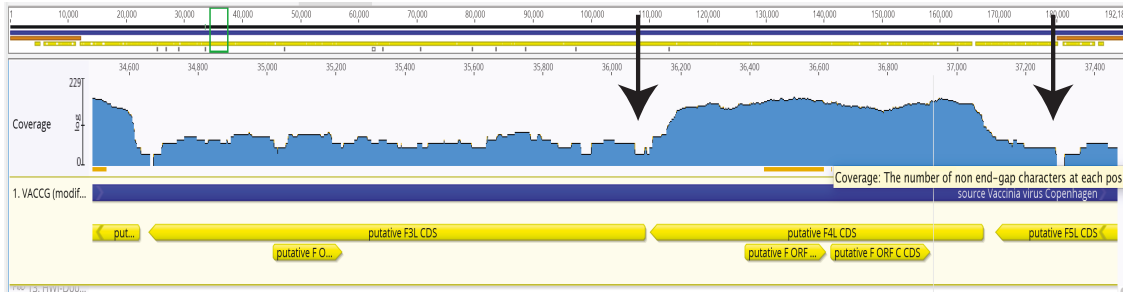

Figure 5.17 - RNAseq Coverage over the F1 and F2 CDS. The figure shows RNA-seq read coverage plots. (A) Shows the reads that mapped back to the F1 and F2 CDS. (B) Shows the reads that mapped back to the neighbouring region of F3 and F4 CDS.

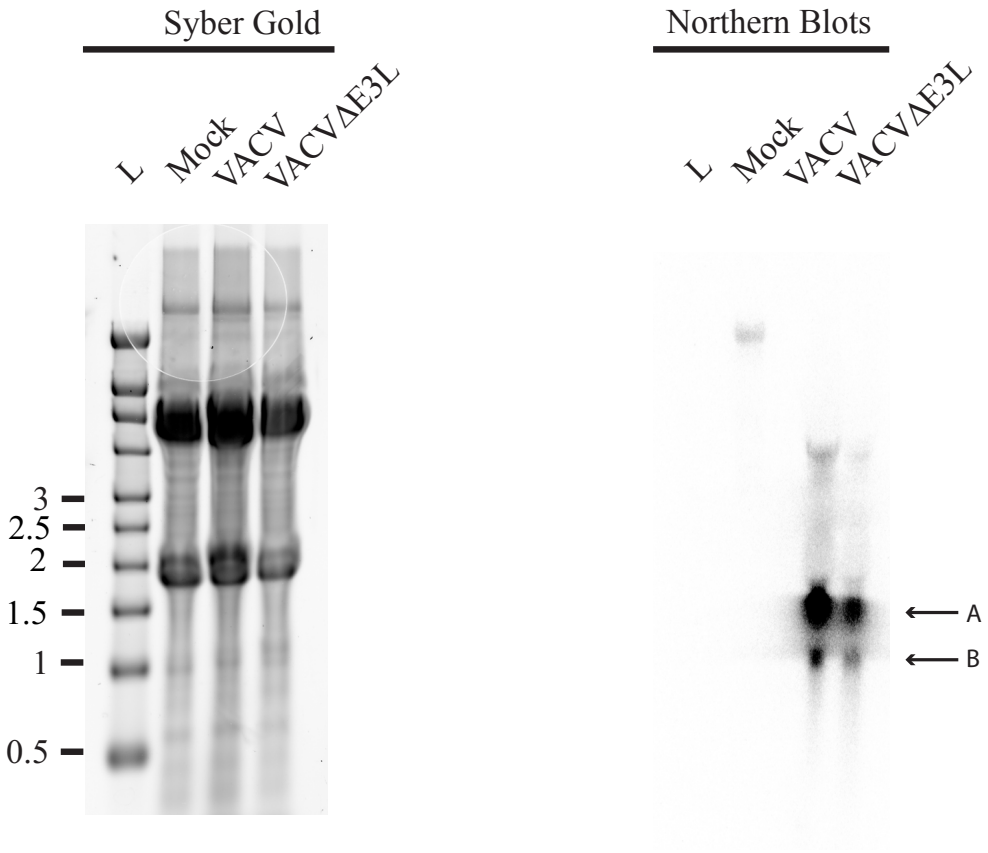

Figure 5.18 -F1L probe detects a larger then expected message. HeLa cells were mock infected or infected with either VACV or VACVΔE3L at a MOI of 5. Total RNA was isolated 3 hours postinfection and electrophoretically separated in 1% agarose formaldehyde gels applying 10 µg of total RNA per lane. In Lane L 2µL of Millennium RNA Markers ladder was also loaded. For loading control RNAs were stained with Syber Gold. Subsequently, RNA was transferred onto a positively charged nylon membrane via vacuum blot and hybridised to P^{32}-probes specific for F1L that were generated using the F1 gene PCR amplicon.

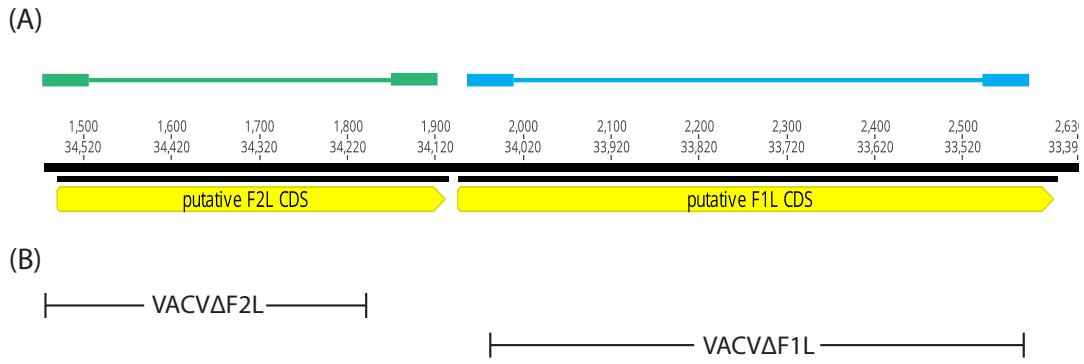

Figure 5.19. Schematic diagram of the probe biding region and VACV mutants. (A) The green bars represent the f2l gene product that extracted from the pcDNA3.1-F2L plasmid. The blue bars represent the f1l gene product that extracted from the pcDNA3-F1L plasmid. These gene products were used to generate the f2l- and f1l -probe respectively. These probes were used in the northern blot experiment. (B) The schematic diagram represents the the regions of the gene that have been deleted in the VACVΔF2L and VACVΔF1L mutants.

based on the RNA-seq results. But the appearance of the smaller (band-B) mRNA was surprising. This band likely consist of only the F1L open reading frame. The results from this experiment indicates that there are two mRNA that potentially contain the F1L orf.

5.2.10. *F2L-probe* binds only to the large mRNA

The previous experiments suggests that there are two distinct mRNAs that contain the *f1l orf*. The RNA-seq results would suggest that a F2L-*probe* would also bind to this larger mRNA (Fig. 5.19 A). We performed a northern blot to determine if F1L and F2L-*probe* bind to the same mRNA. In addition, we also wanted determine if the *F2L-probe* detects more than one mRNA. HeLa cells were infected with VACV, VACVwr, VACVΔE3L, VACVΔF1L and VACVΔF2L virus for 3 hrs. The VACVΔF2L mutant used in this study has 119 bp upstream of F1 ORF intact and was in the VACVwr background (Fig. 5.19 B). As previously observed in Fig. 15.18, the F1L-probe detected two distinct bands in mRNA from VACV, VACVwr, and VACVΔE3L infected HeLa cells. The F1L-probe did not detect any message in the RNA from the VACVΔF1L-infected cells. A similar result was observed in the case of RNA extracted from VACVΔF2L-infected cells. This result was especially surprising because the VACVΔF2L mutant virus has an intact F1L gene, and the promoter was also assumed to be intact. When using the F2L gene probe we detected a band that was approximately 1.5kb in size in lanes with VACV, VACVwr or VACVΔE3L (Fig. 15.20). The F2L-probe only detected one distinct band which corresponded in size to the large band detected by F1L-probe. In the lane with the RNA from VACVΔF1L mutant, the F2L-probe hybridized to a mRNA that

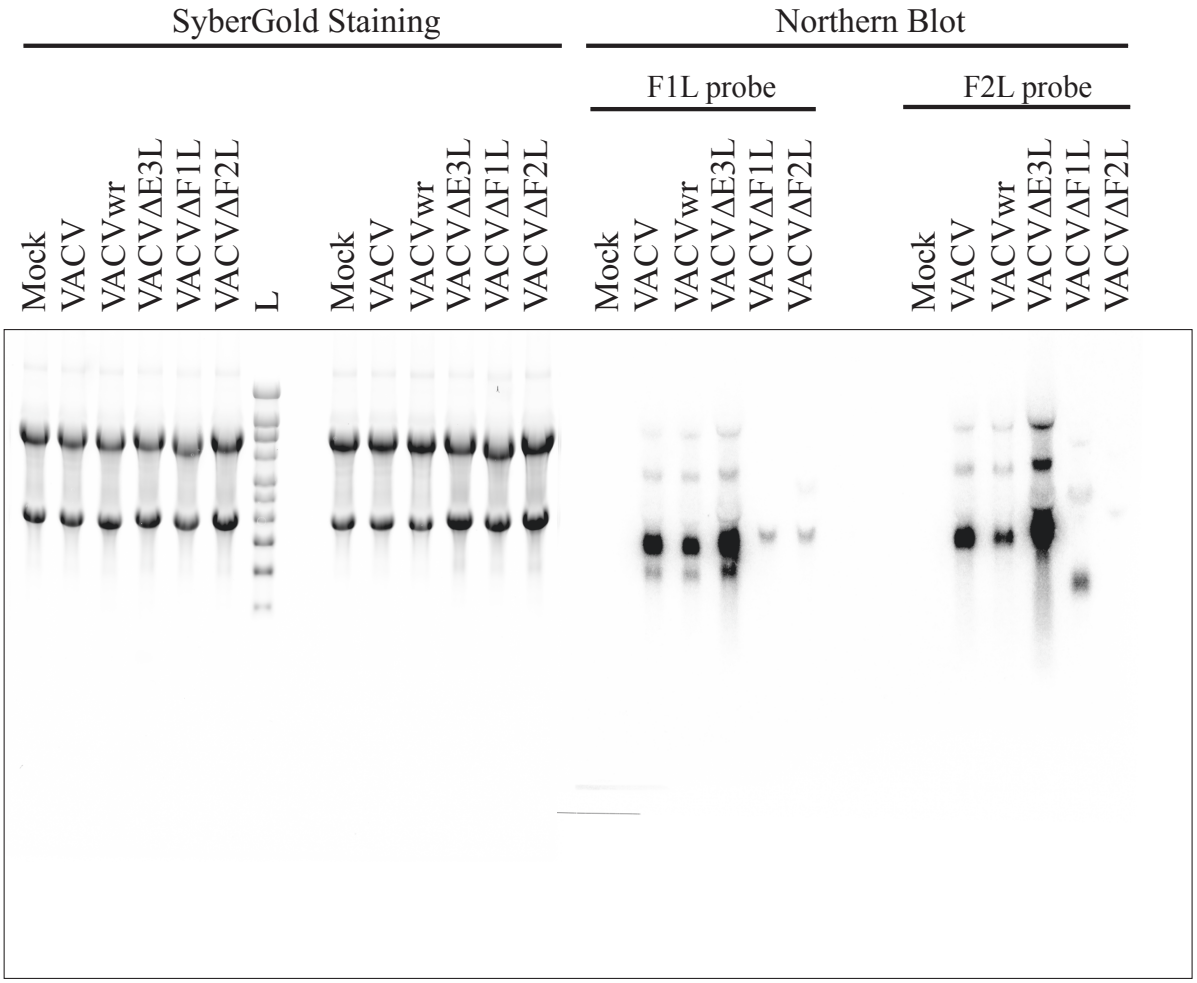

Figure 5.20 - F1L and F2L probes detect the same transcript. HeLa cells were mock infected or infected with either VACV (VACV Cop), VACVwr, VACVΔE3L, VACVΔF1L, VACVΔF2L at a MOI of 5. Total RNA was isolated 3 hours postinfection and electrophoretically separated in 1% agarose formaldehyde gels applying 10 µg of total RNA per lane. In Lane L 2µL of Millennium RNA Markers ladder was also loaded. For loading control RNAs were stained with Syber Gold. Subsequently, RNA was transferred onto a positively charged nylon membrane via vacuum blot and hybridised to ia vacuum blot and hybridised to P^{32}-probes specific for F1L and F2L that were generated against the cloned F1L gene and F2L gene respectivly.

was smaller in size. This drop in size is likely due to the deletion of a majority of the F1L orf in the mutant. The F2L-probe failed to detect any message (Fig. 5.20). These results would suggest that there is a F2L-F1L bicistronic mRNA. In addition to this bicistronic mRNA, there is a smaller mRNA that is a monocistronic and hybridizes to the F1L-probe (Fig. 5.21). This observation of a bicistronic mRNA is unique, as no other evidence of bicistronic mRNA has been reported in VACV virus.

The western blot results support the results that were observed in the northern blots. HeLa cells were infected with VACV, VACVwr, VACVΔE3L, VACVΔF2L, and VACVΔF1L virus. In the cell lysates, F1 was detected in HeLa cells that were infected with VACV and VACVwr. The protein was absent in the cell lysates of HeLa cells infected with VACVΔE3L and VACVΔF1L mutants. In addition, we were unable to detect F1 in the lysates from HeLa cells infected with VACVΔF2L (Fig. 5.22). This observation along with the absence of the small monocistronic mRNA in the VACVΔF2L infected HeLa cells (Fig. 5.20) indicates that the promotor is not present directly upstream of the predicted F1 start site.

5.2.11. The bicistronic and monocistronic *F1L* transcripts have similar kinetics

Having observed two distinct bands, we wanted to explore the possibility of difference in kinetics between the two mRNAs. To deduce the kinetics, total RNA from VACV or VACVΔE3L infected HeLa cells was extracted at 1, 2, 3, 4, and 5 hrs post infection. The F1L transcripts were detected as early as 2 hrs post infection. In VACV or VACVΔE3L-infected cells, both bands appear at 2 hrs and remain detectable until 5 hrs post infection (Fig. 5.23). Thus, the data indicates that there is no difference in the

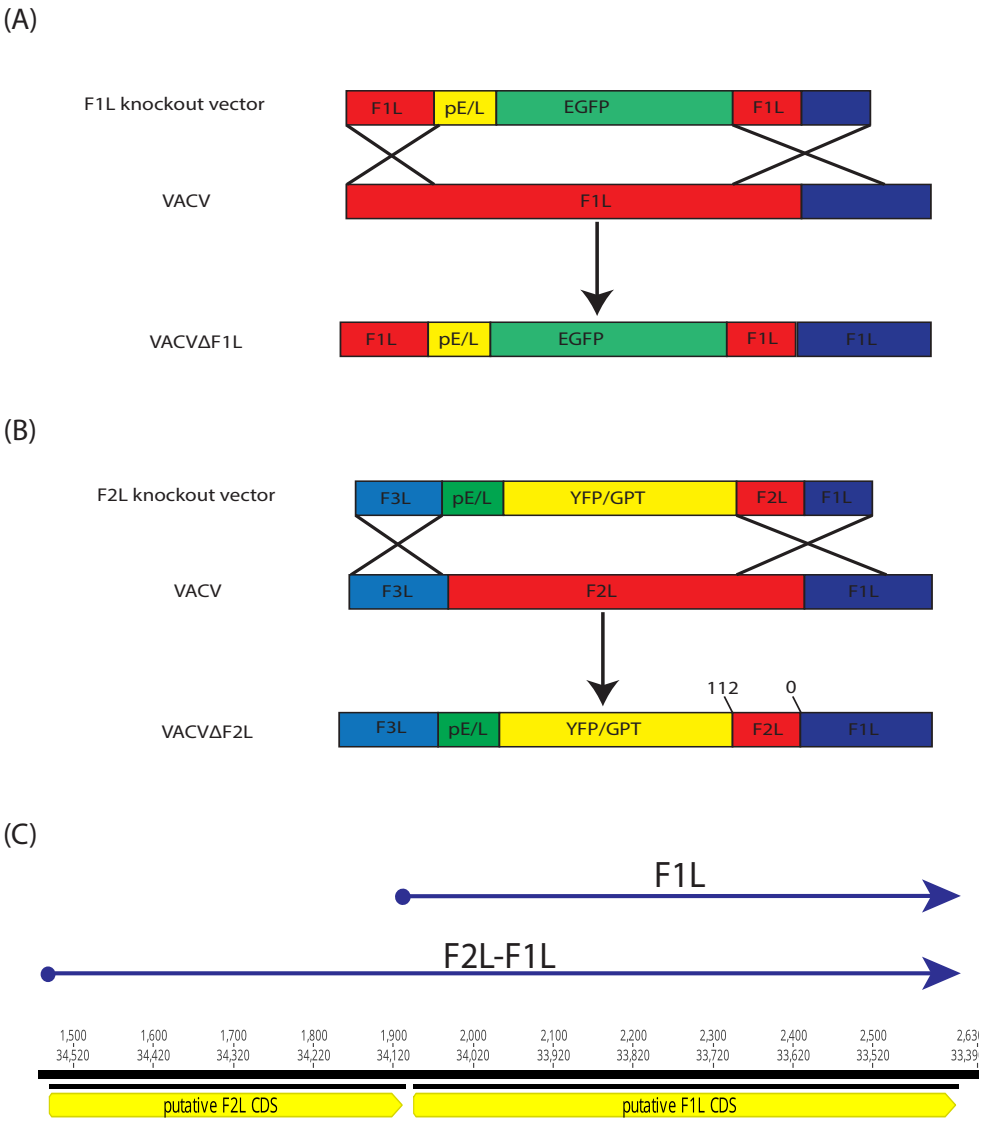

Figure 5.21. Schematic diagrams (A) The schematic diagram of the VACVΔF1L mutant. (B) The schematic diagram of the VACVΔF2L mutant. (C)The figure represents the schematic diagram of the possible mRNA detected by the F1 probe bases on our previous ovservations.

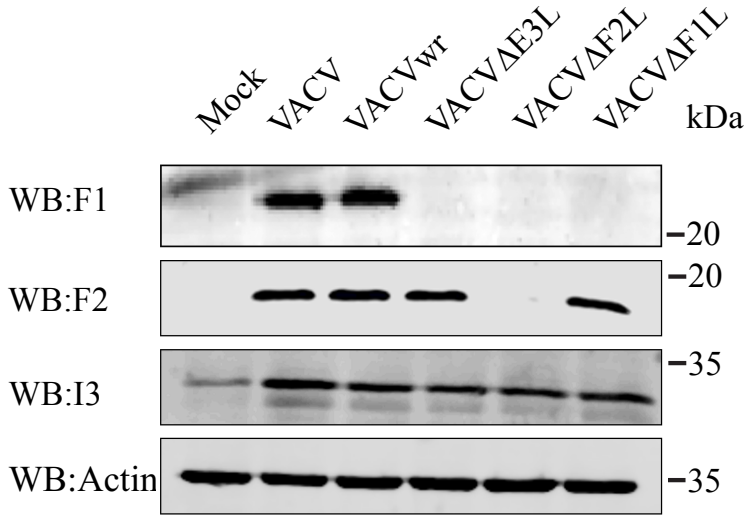

Figure 5.22 - F1L is absent during VACVΔF2L infection. HeLa cells were mock infected, infected with VACV, VACVwr, VACVΔE3L, VACVΔF1L, and VACVΔF2L at an MOI of 5. Six hours post infection the cells were lysted in RIPA lysis buffer with a protease inhibitor. The cell lysates were subjected to western blot analysis using the anti-F1L, anti-F2L, anti-I3L and anti-Actin antibody.

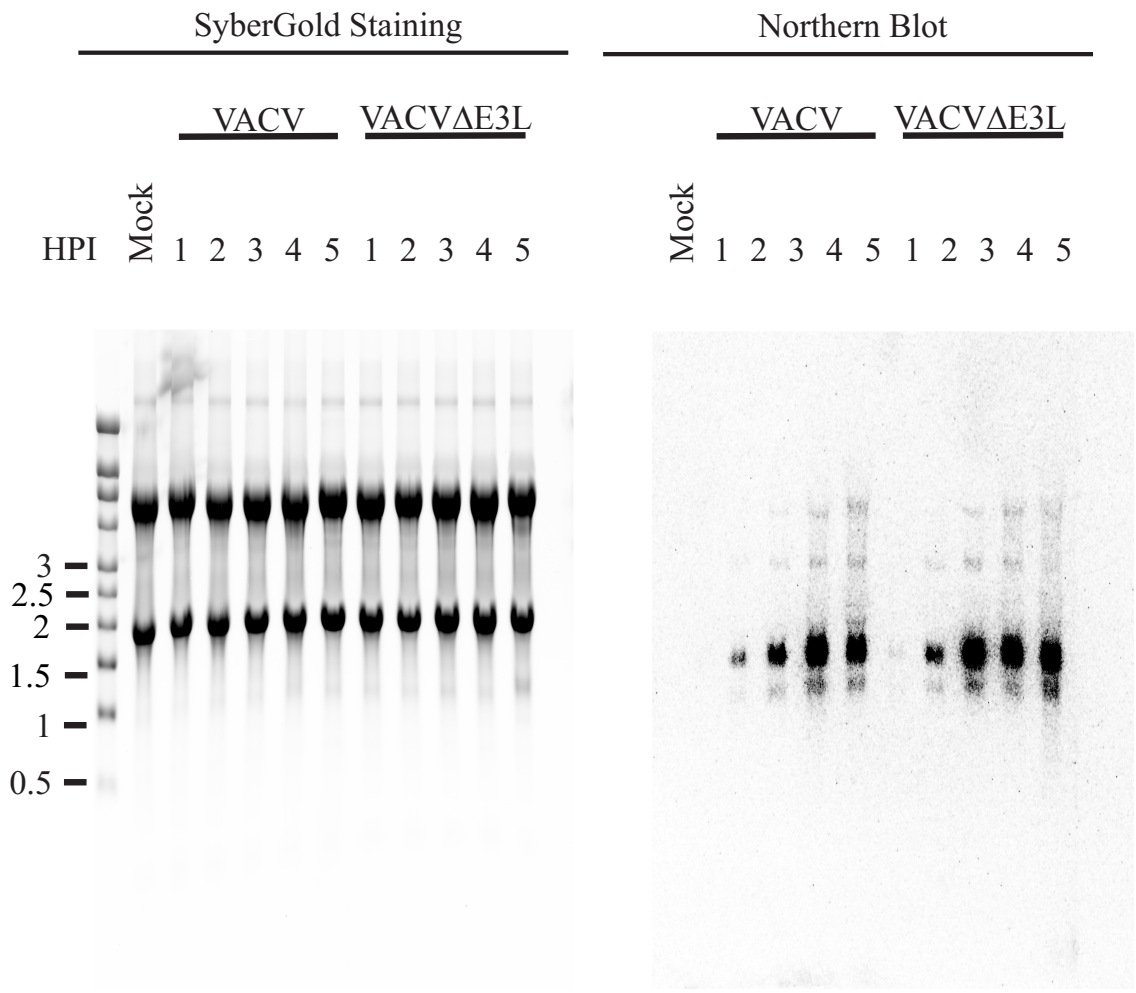

Figure 5.23 - F1L transcript time course during VACV and VACVΔE3L infection. HeLa cells were mock infected or infected with either VACV or VACVΔE3L at a MOI of 5. Total RNA was isolated 1, 2, 3, 4 and 5 hours post infection (h.p.i) and electrophoretically separated in 1% agarose formaldehyde gels applying 10 µg of total RNA per lane. In Lane L, 2µL of Millennium RNA Markers ladder was also loaded. For loading control RNAs were stained with Syber Gold. Subsequently, RNA was transferred onto a positively charged nylon membrane via vacuum blot and hybridised to P^{32}-probes specific for F1L generated against a F1L PCR product.

kinetics of the two mRNAs detected by the F1L-probe. In addition, the relative intensity between the two bands also remained consistent at any given time point.

5.2.12. F1 protein is translated from the small mRNA

Next we wanted to determine the mRNA that was used for the translation of F1. To answer this question, we designed siRNAs against two distinct regions of the bicistronic mRNA. One set of siRNA (F2L-siRNA) would target the 5'-end of the bicistronic mRNA. This siRNA would only target the big bicistronic mRNA. The second set of siRNA (F1L-siRNA) would target the 3'-end of the bicistronic mRNA. This siRNA set would be able to target both the bicistronic and monocistronic mRNA (Fig 5.24). HeLa cells were transfected with the F2L-siRNAs, control scramble F2L-siRNAs, F1L-siRNAs, control scramble F1L-siRNAs. The transfected cells were infected with VACV. Post infection the cell lysates were subjected to a western blot analysis. In cells that were transfected with F2L-siRNA and infected with VACV we detected less F2 protein. Thus the knock-down was successful. F1 was present in the lysates of the F2L knock-down cells (Fig 5.25). This result suggests that the bicistronic mRNA is not the source of the F1 protein. Next we knocked-down the F1 protein in VACV-infected cells using the F1L-siRNA. We could knock-down the expression of F1 protein effectively in VACV-infected cells. In cells with the F1 knock-down, the F2 protein was not detected (Fig. 5.26). The scramble siRNAs had no effect on the expression of the F1 or F2 protein. In addition, the siRNAs and the scrambled siRNA did not influence the VACV I3 protein. These data would suggest that when we target the small mRNA and the big

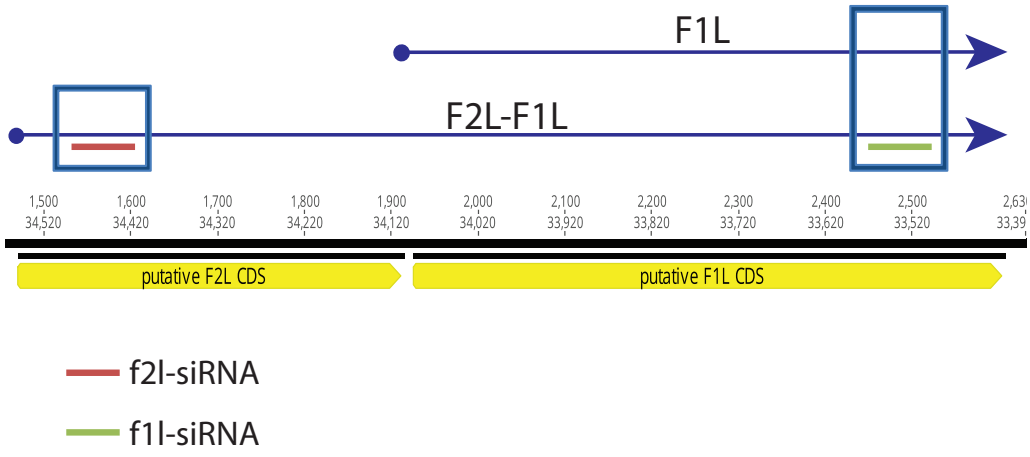

Figure 5.24. Schematic diagram showing siRNA targets. The figure represents the schematic diagram the mRNAs that would be targetted by the two f2l-siRNAs and f1l-siRNAs.

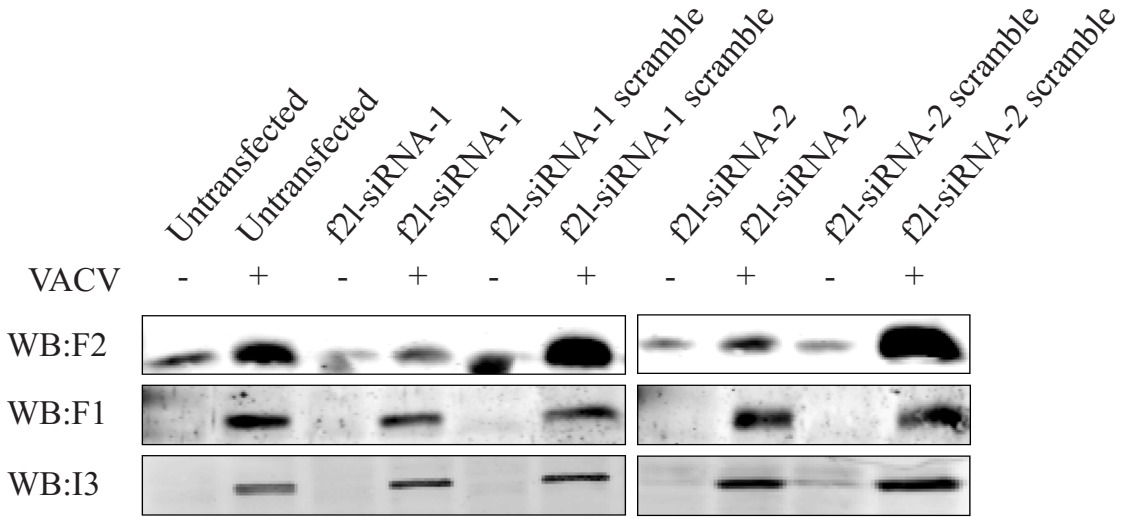

Figure 5.25. f2l-siRNA targets the expression of F2 and not F1. HeLa cells were transfected with two distinct f2l-siRNA or the scramble siRNA for 12 hours. Post transfection, the HeLa cells were either mock infected or infected with VACV at an MOI of 5. Six hours post transfection the cells where harvested and lysed in RIPA buffer. The cell lysates were subjected to immunoblotting using the anti-F1L antibody, anti-F2L antibody, and anti-I3L antibody.

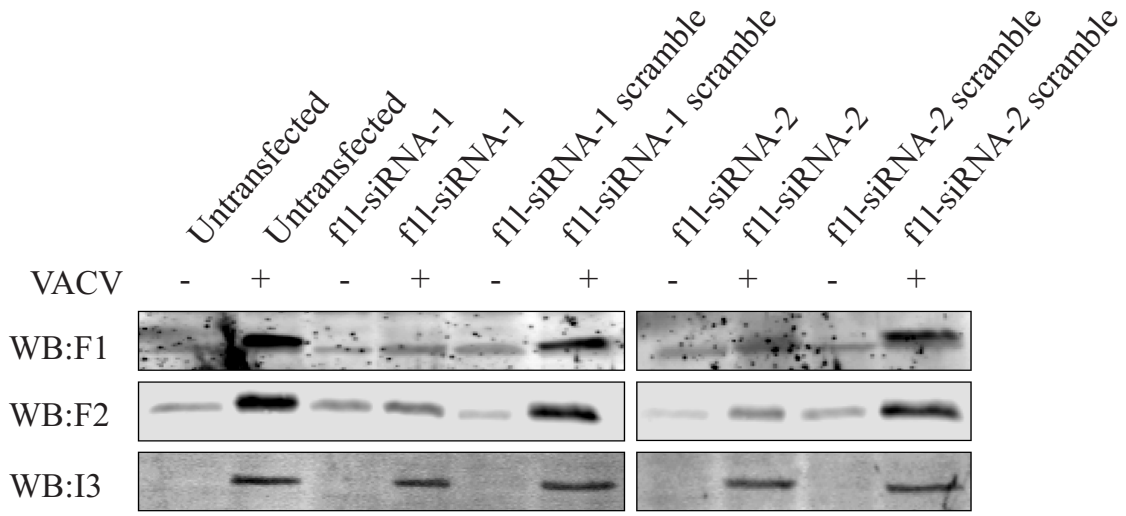

Figure 5.26. f1l-siRNA targets the expression of F1 and F2. HeLa cells were transfected with two distinct f1l-siRNA or the scramble siRNA for 12 hours. Post transfection, the HeLa cells were either mock infected or infected with VACV at an MOI of 5. Six hours post transfection the cells where harvested and lysed in RIPA buffer. The cell lysates were subjected to immunoblotting using the anti-F1L antibody, anti-F2L antibody, and anti-I3L antibody.

mRNA we can eliminate the expression of F1 and F2 together. Thus, the small mRNA is responsible for the expression of F1 protein.

5.3. Summary

Altogether our data confirmed that infection of HeLa cells with VACVΔE3L triggered apoptotic cell death. We show that the apoptosis triggered by a VACVΔE3L infection was a result of the absence of F1 in infected cells. It was observed that the expression of VACV F1 is blocked by PKR in the absence of E3 protein. Our RNA-seq results showed mapped reads that spanned the entire region F1 and F2 ORFs. These results were confirmed using northern blot analysis. The northern blot analysis using the f1 probe revealed two distinct mRNAs, a bicistronic and a monocistronic mRNA. Our siRNA experiment suggests that the majority of the F1 protein is encoded by the smaller mRNA. We have yet to determine the start site of the second smaller mRNA and the reason behind the higher sensitivity of F1 to the activation of PKR pathway in HeLa cells.

Chapter-6-Discussion

6.1. EVM025 inhibits the intrinsic apoptotic pathway

Apoptosis is a critical tool used by the cell to block virus replication, so it is not surprising that many viruses have evolved strategies to overcome or delay cell death [114,129,211]. Human and murine cytomegaloviruses inhibit the apoptotic pathway through a unique apoptosis inhibitor, vMIA [126]. The gammaherpesviruses Kaposi's sarcoma-associated herpesvirus (KSHV), Epstein Barr virus (EBV), and murine gammaherpesvirus-68 (MHV-68) encode viral homologues of the cellular anti-apoptotic protein Bcl-2 (v-Bcl-2) to inhibit the intrinsic apoptosis pathway [114,123,126,128,129,211-213]. Other viruses such as African swine fever virus (ASFV) and Adenovirus also encode vBcl-2 homologues that inhibit apoptosis. Poxviruses are renowned for their ability to manipulate the apoptotic pathway, and they encode a variety of distinct proteins that interfere with the Bcl-2 family of proteins [123,214]. Avipoxviruses encode obvious cellular Bcl-2 homologues, while several other members of the poxvirus family encode anti-apoptotic proteins that lack sequence similarity to cellular Bcl-2 proteins [130,215]. Previous work performed in our laboratory led to the identification of *F1L* in vaccinia virus [137]. VACV F1 consists of divergent Bcl-2 homology domains and replaces cellular anti-apoptotic proteins, Mcl-1 and Bcl-2, during infection to prevent apoptosis [141].

Ectromelia virus (ECTV), more commonly known as mousepox, is a member of the Orthopoxviridae that was first described in 1930 [38]. A majority of our understanding regarding orthopoxviruses has come through the use of VACV, whose natural host is unknown. ECTV, however, is a natural pathogen of mice. Understanding the virulence of ECTV will help improve our understanding of poxvirus infection. To date, no work has investigated the role of EVM025 in apoptotic inhibition during ectromelia virus infection.

Our data confirm that ECTV encodes a functional mitochondrial inhibitor of apoptosis, EVM025, which inhibits cell death induced at the mitochondria via the intrinsic pathway. Both human and murine cells infected with wild-type ECTV, but not ECTVΔ025 viruses, were resistant to apoptosis induced by multiple stimuli. We also found that EVM025 blocks apoptosis at the mitochondria, much like VACV F1 poxviral inhibitors of apoptosis, including M11L and F1, are localized at the mitochondria [127,134]. We were able to establish that similar to F1, EVM025 also localizes to the mitochondria via a C-terminal hydrophobic tail.

Many of the poxviral mitochondrial anti-apoptotic proteins, such as M11L, F1, FPV039 and DPV022, are believed to function primarily by inhibiting the activation of Bak and Bax [130-132,138,139,216]. Our data suggest that the expression of EVM025 was similarly sufficient to prevent the activation of Bak and Bax. EVM025 was able to interact directly with endogenous Bak, but not with Bax. This is similar to results previously observed with F1. In contrast, M11L, DPV022, and FPV039 are able to interact with both Bak and Bax to prevent their activation during virus infection. Since EVM025 inhibits the activation of Bax in the absence of detectable interaction, we hypothesized that EVM025 may function by interacting with and inhibiting BH3-only proteins that act upstream of Bax activation. One such upstream activator of Bax is the BH3-only protein Bim. Bim exists as three isoforms, BimS, BimL and BimEL, and is able to trigger apoptosis in response to various stimuli. EVM025 expression significantly inhibited BimL-induced loss of mitochondria membrane potential, a hallmark of apoptotic cells, and EVM025 was also seen to weakly interact with ectopically expressed BimL. It is interesting to note that previous work done on F1 demonstrates that F1 is able

to bind to BimL strongly. This is not the case with EVM025. Addition, work needs to be done to determine the ability of EVM025 to interfere with the function of other BH3-only proteins. The orthopoxviral proteins F1 and EVM025 appear to function differently from the other poxviral proteins (M11L, FPV039) despite their similar anti-apoptotic phenotype suggesting a different biochemical mechanism [130,131].

Sequence analysis of genomes of orthopoxviridae revealed that orthologues of F1L were found in multiple members of the family. Our analysis showed that F1L orthologs from VARV Garcia, ECTV Moscow, and ECTV Naval have a distinct repetitive sequence at the amino terminus of the protein. The repetitive sequence is absent in other members of the Orthopoxviridae family. EVM025 consists of a long N-terminal repeat region consisting of an eight amino acid motif 'DNGIVQDI' repeated 30 times. VARV Garcia contains multiple 'DDI' repeats at the N-terminus. These repeat regions share no sequence homology with any known cellular or viral proteins. Although the functional importance of these repeated regions remains unknown, the repeat regions are absent in VACV Copenhagen, VARV Bangladesh, MPXV Zaire, and CPVX Brighton Red. Additional studies are required to improve our understanding of the functional and evolutionary importance of these regions. Despite the variability present at the N-terminal region of the F1 orthologues, F1L and EVM025 share 95% sequence homology at the C-termini. Based on the C-terminal similarity it is likely that ECTV EVM025 will fold in a manner similar to F1. Previous work has shown that F1L, despite lacking obvious sequence similarity with cellular Bcl-2, folds in a manner similar to cellular Bcl-2 protein [135,141]. The predicted divergent BH domains of F1 are highly conserved between EVM025 and other orthologues of the orthopoxviridae family. Poxviruses have

recently been shown to encode a variety of proteins that adopt a Bcl-2-like conformation [217,218]. A52R and B14R both share limited sequence similarity with cellular Bcl-2 proteins but fold like the Bcl-2 proteins. Despite their secondary structure, A52R and B14R are involved in inhibiting the NF-κB pathway but not apoptosis [218]. Several other vaccinia viral proteins, such as A46, K7, N1 and C1, have all been reported to possess Bcl-2-like folds, and thus could be grouped within the same protein family [217-219]. Of these proteins, however, only N1 has been shown to have any ability to inhibit apoptosis [220]. Other studies has shown that N1 is involved in the modulation of NF-κB pathway and not apoptosis [219]. The role of these or any other putative anti-apoptotic proteins remains to be seen. Our data, however, confirm the hypothesis that EVM025 is the predominant anti-apoptotic inhibitor, as EVM025 knock-out viruses are completely unable to block apoptosis induced by multiple intrinsic pro-apoptotic stimuli, thereby casting some doubt on the ability of other ectromelia virus proteins to also contribute to the inhibition of apoptosis.

EVM025 is a potent anti-apoptotic poxviral protein, similar to F1. EVM025 has a distinct N-terminal end with an unknown function. EVM025 shares little similarity to cellular Bcl-2 proteins, yet effectively inhibits apoptosis. It is evident from this study that EVM025 is evolutionarily related to F1. But the basic function of apoptosis inhibition still remains to achieve the final goal of keeping the infected cell alive.

6.2. EVM025 is a virulence factor

As a natural mouse pathogen, ECTV offers a distinct opportunity to study virus-host interactions. Orthopoxvirus gene function has been studied in VACV, but the natural host of the virus is unknown. Thus studying the importance of these genes in virulence is difficult in the VACV model. At genome level, ECTV is closer to VARV then VACV[7] and the similarity extends beyond the genome sequence. ECTV and VARV are highly pathogenic in their natural host, and cause systemic infection. In addition, like VARV, ECTV has a relatively narrow host range [10]. In chapter-3, we described EVM025 as an anti-apoptotic protein of ECTV[202]. A single study has shown that VACV F1, an orthologue of EVM025, is a virulence factor, but the mechanism underlying this phenotype is not completely understood[143]. In chapter 4 of this thesis, we analyzed EVM025's importance during *in vivo* infection.

Early work on ECTV has described a route of infection as through skin abrasions[38]. Thus, we infected BALB/c mice through the footpad with a low dose of the virus. As expected a low dose of wild type ECTV is lethal in susceptible BALB/c mice (Fig. 4.2), however ECTVΔ025 infection was not lethal (Fig. 4.3) at either an equivalent infectious dose or at 10 and 1000-fold higher doses (Fig. 4.4).Thus, ECTVΔ025 was avirulent at even higher infectious doses. Mice infected with the highest dose of virus showed initial weight loss but all recovered and survived until the experiment end-point. Work done on ECTV SPI-2, N1 and A36 has shown that, like EVM025, knocking out a single gene attenuates the pathogenicity of the virus[45,221,222]. ECTVΔN1L virus caused lethality at higher infectious doses[221], in contrast, dose dependent lethality was not observed in the ECTVΔ025 mutant. Interestingly, the degree of ECTVΔ025 attenuation

was greater than what was described for VACVwr lacking F1. In addition, the intranasal infection of mice with VACVΔF1L, showed a dose dependent response[143].

One of the most intriguing results was the inability of ECTVΔ025 to spread beyond the D-LN. We were unable to detect any mutant virus in internal organs such as the liver, spleen and lungs. Such a phenotype has been observed in ECTVΔN1L virus; but, that study was done using a resistant B6 mouse strain[221]. In contrast, ECTVΔ025's spread was limited in susceptible BALB/c model. The wild type ECTV spreads aggressively into the secondary organs. Thus, the limited spread of ECTVΔ025 illustrates the importance of EVM025 in the pathogenesis of ECTV. ECTVΔ025 was unable to spread from D-LN to secondary organs such as spleen, liver, kidney and lung. As previously mentioned, the spread of the virus from the D-LN to the secondary organs is a result of a viremia. We observed about 2 log lower viremia in mice infected with ECTVΔ025 (Fig. 4.6), which could be the result of reduced ECTVΔ025 replications at the primary site of infection. The lower viremia observed in ECTVΔ025 by day 7 could be a combination of lower replication in infected tissues, and an adaptive immune response that is better able to control the spread of the virus. A similar trend in viral loads was also observed at the site of infection and primary lymph-node very early after infection. At day three post infection, the ECTVΔ025 and ECTV virus was detected at comparable levels in the footpad. In contrast by day four, ECTV was able to establish itself in the footpad but ECTVΔ025 was detected in lower quantities (Fig. 4.7 A). A similar trend was also observed in the D-LN in that ECTVΔ025 was detected in the D-LN a day later than the wild-type virus (Fig. 4.7 B). The above mentioned experimental data suggests that ECTVΔ025 is limited in its spread from the onset of infection. Thus the

data would imply that ECTVΔ025 is unable to overcome the mouse cell-intrinsic anti-viral response or the mouse's innate immune response. This assumption would be in line with the previously published literature on EVM025 and its orthologue F1. We have shown in the previous chapter that like F1, EVM025 can inhibit apoptosis. In addition, previous research on F1 has shown that it can inhibit the activation of caspase-1 and the inflammasome[140,143]. Thus, F1 and its orthologue are directly involved in altering the cell-intrinsic and innate immune responses.

The previous data would suggest that a robust cell-intrinsic or innate immune response is sufficient to retard the initial spread of the ECTVΔ025. The experiments also show that ECTVΔ025 remains detectable at day 7 post infection, suggesting that an adaptive immune response might be required for the continued suppression of ECTVΔ025. SCID mice that were infected with ECTVΔ25 succumbed to the infection, unlike their wild type counterparts (Fig. 4.8). The SCID mice infected with ECTVΔ025 survived 33% longer than those infected with wild type virus. A similar trend was observed in ECTVΔ025 infected BALB/c Nude mice. The increased survival of mice infected with ECTVΔ025 supports our previous observation that the cell-intrinsic and innate immune response may help delay the spread of the virus, but those responses are not sufficient to prevent the spread of the virus and eventual lethality. The SCID mice are severely deficient in functional B and T lymphocytes[223]. Thus, the results observed in the SCID model implies that an adaptive immune response is critical in limiting the mortality caused by an ECTVΔ025 infection. Nude mice have functionally deficient T lymphocytes. Thus, the Nude mice experiment demonstrates that T-cells are crucial in limiting the spread of ECTVΔ025 virus. The Nude mouse model has reduced NK cell

functionality [224]. In addition, previous studies have emphasized the importance of T-cells and NK cells in survival and recovery from ECTV infection. In agreement with these studies, our analysis of ECTVΔ025 infection of Nude mice demonstrated a clear dependency on functional T-cell or NK cells in controlling the ECTVΔ025 infection. The BALB/c Nude experiments demonstrates that in the absence of T-cells, the B-cells and the antibody response against ECTV is not sufficient to limit the spread of the virus. These current experiments cannot distinguish between the importance of NK cell or T-cell in limiting the spread of the mutant virus; neither can they help determine which subset of T cells is important. Individually depleting each population is required to help determine the importance of these individual cell populations.

Virus attenuation has been observed in VACVΔF1L mutants, but this is the first time that we have been able to demonstrate an increased infiltration of lymphocytes in the spleens of mice infected with a virus missing the F1 orthologue. The spleens of ECTV and ECTVΔ025rev infected mice showed signs of necrosis, but these signs were not present in the ECTVΔ025 infected mice. This observation makes sense as the virus was unable to spread to the spleen in BALB/c mice when infected through the foot pad. We observed elevated levels of $CD3^+CD8^+$ T-cells and NK cells in the spleen. The elevated levels of these cells indicate that animals infected with the virus missing EVM025 are able to mount a stronger immune response, consisting of higher percentages of NK cells and $CD3^+CD8^+$ T-cells (Fig 4.10). As previously observed in the SCID mice experiment, a stronger adaptive immune response is most likely responsible for virus clearance and decreased mortality of mice, and the observed inability to spread beyond the D-LN. A similar trend was observed in the blood of mice infected with ECTVΔ025. Elevated

levels of NK cells and $CD8^+$ T-cells have been observed in multiple ECTV mutants [45,64,221]. In addition, as previously mentioned T-cells and NK cells play a crucial role in controlling an ECTV infection and recovery from infection[38,48,63].

We also observed elevated levels of CXCL9 and CXCL10 post ECTVΔ025 infection (Fig. 4.11). CXCL9 and CXCL10 elicit chemotactic functions by interacting with the CXCR3 receptor (CXCR3-R) ligands[225]. CXCL3R is expressed on activated T cells, NK cells, monocytes, dendritic cells, and microglia. It is preferentially expressed on activated Th1 T cells[226]. CXCL9 (also known as MIG) is induced by IFN-γ in macrophages[227]. Similarly, CXCL10 is induced by IFN-α, IFN-β, IFN-γ, or LPS[226,228]. CXCL9 and CXCL10 expression is associated with the recruitment of NK-cells and activated T-cells. Thus, the elevated levels of CXCL9 and CXCL10 can be correlated to the importance of activated T-cells and NK-cells in limiting the spread of ECTVΔ025. Previously published research has shown that CXCL9, CXCL10 and CXCL11 are important in the recruitment of NK cells by macrophages in CPXV infection of mice[229]. In addition, previous work on HSV-2 has demonstrated CXCL9 and CXCL10 expression is critical for control of HSV-2 by promoting a Th1 response[230,231]. Th1 responses are required for effective control or clearance of ECTV infection[56,66]. Thus, it is likely that the higher levels of these two chemokines during the early stages of the ECTVΔ025 infection help setup conditions that are required for the proper recruitment of NK and T-cells at the site of infection and D-LN to prevent the further spread of the virus. In contrast, ECTV infection does not elicit a similar early CXCL9 and CXCL10 response. The delayed recruitment of T-cell and NK cells may allow the virus to spread the secondary organs leading to the mortality observed during ECTV infection.

Interestingly, ECTVΔ025 infected mice presented with elevated levels of IFN-γ by day 2. IFN-γ is a crucial cytokine in the recovery from mousepox[232,233]. Previous work has shown that IFN-γ is crucial for the survival of C57BL/6 mice that were infected with through the foot pad[232]. It is likely that the elevation of IFN-γ in early post ECTVΔ025 infection helps triggers multiple innate immune responses like the NOS pathway, NF-κB pathway and activation of NK cells all of which are important in surviving an ECTV infection[38,233]. In addition, CXCL9 and CXCL10 are both upregulated in the presence of IFN-γ. Thus, it is likely that the IFN-γ produced early during ECTVΔ025 infection helps stimulate the chemokines that are required for the appropriate homing of activated NK cells and NK cells.

The serum of ECTVΔ025 infected BALB/c mice had elevated levels of IL-10 at day 2 and 4 post infection. This was a curious observation, as IL-10 has both immunostimulatory and immunosuppressive properties. However, its main function is to exert a potent immunosuppressive effect[234]. Multiple viruses have been shown to upregulate the expression of cellular IL-10 to suppress immune functions[235]. It has been previously observed that lymphocytic choriomeningitis virus (LCMV) modulates the expression of IL-10 to establish chronic infections[236]. Similarly, HIV also depends on modulating the expression of IL-10 to establish a latent infection[237]. It is very likely that in the absence of EVM025, ECTV triggers IL-10 expression in BALB/c mice and along with IFN-γ, T-cells and NK-cells it creates a balance that would allow a persistent ECTVΔ025 infection to be established. Work done by Sakala I G *et al.* demonstrates that ECTV is able to establish a persistent infection in C57BL/6 mice[238]. Thus it is possible that ECTVΔ025 might be able to establish a persistent infection in BALB/c mice.

However, the experiments presented in this thesis are not sufficient to address this issue. Additional experiments looking at ECTVΔ025 titers and its clearance beyond 21 days are required. We also observed elevated levels of IL-9 and IL-13 post ECTVΔ025 infection. These cytokines are typically associated with a Th2 response. Previous work on Th2 cytokines and orthopoxviruses has shown that a deficiency in the Th2 cytokine response aggravates an ECTV infection[239]. IL-9 and IL-13 both affect B-cell development. Research on respiratory syncytial virus (RSV) has shown that IL-9 has a negative effect on virus clearance[240]. There is limited literature on the role of this cytokine during a virus infection. Our current set of experiments are not sufficient to provide clues into the function of these cytokines during ECTVΔ025 infection. We also have not evaluated the role of B-cells during ECTVΔ025 infection. Additional experiments using IL-9 and IL-13 knockout mice might help better understand the role of these cytokines during ECTVΔ025 infection.

Previously published data on EVM025, and the work done on F1, has demonstrated the role of these proteins in the inhibition of apoptosis. Though most of the previous data would suggest that F1 is required in the inhibition of the cell-intrinsic defense mechanism, we observe a T-cell response and upregulated cytokines and chemokines during ECTVΔ025 infection. One probable reason for this could be an earlier and easier exposure of the immune system to ECTV antigens is possible in the absence of the EVM025 orf. Alternatively, EVM025 also affects other signaling pathways. One possibility is the absence of EVM025 allows the release of mitochondrial DNA (mt DNA) in a BAK and BAX mediated manner. This mt DNA may be responsible for the activation of the cGAS/STING-dependent trigger for IFN production[241]. Additional

experiments will be required to determine the role of EVM025 in preventing the activation of the cell mediated immune response. A study associates VACVΔF1L infection with the activation of the inflammasome and the production of IL-1β though the activation of caspases-1[143]. We were unable to detect the production of IL-1β in ECTVΔ025 infected mice. This could be due to the presence of SPI-2 in the ECTV. SPI-2 is capable of inhibiting caspase-1 during infection preventing the production of IL-1β. Improving our understanding about the immune response will help improving our understanding on how poxvirus interact with their host.

In conclusion, the data presented here demonstrate that the ECTV EVM025 protein is a virulence factor in the infection of susceptible BALB/c mice. The protein is crucial in the spread of the virus beyond the primary draining lymph node. Our experiment suggests that the spread of the virus is limited very early post infection. Our current data suggests that the mutant virus spread may be limited due to a combination of cell mediated immunity and innate immunity. These early host responses are not sufficient to prevent lethality caused by a mutant virus. Our data suggests a strong adaptive immune response involving T cells and NK cells help bottle neck the virus in the primary draining lymph node. The data presented here suggests that EVM025, either directly or indirectly interferes with the cell-mediated, innate and adaptive responses to enable virus spreading.

6.3. Expression of the vaccinia virus anti-apoptotic F1 protein is blocked by PKR in the absence of the viral E3 protein.

The VACV E3 protein has also been described as an IFN resistance protein and a dominant host range protein[1,2]. E3 is a 25 kDa protein that is produced early during the viral infection cycle, and viruses that are devoid of the E3 ORF have a very limited host range. VACV E3 protein consists of two distinct domains: the N-terminal Z-DNA binding motif and the C-terminal dsRNA binding domain[1,3]. The N-terminus of the protein is dispensable for growth of the virus in tissue culture, while deletion of the C-terminus of the protein severely impairs the ability of the virus to reproduce in multiple cell lines[4]. The dsRNA binding domain is directly involved in the inhibition of the PKR pathway. In addition to inhibiting the PKR pathway, E3 has previously been associated with the inhibition of apoptosis[3]. Infection of HeLa cells with MVAΔE3L triggers the intrinsic apoptotic pathway through Noxa activation[5]. The results from the previously published experiments led us to ask why F1 does not inhibit apoptosis. In chapter five we investigate the role of F1 during VACVΔE3L infection.

In previous work by Zhang *et al.,* they demonstrated that infection of HeLa cells with VACVΔE3L triggered apoptosis[6]. We were also able to demonstrate triggering of cell death during the infection of HeLa cells with VACVΔE3L (Fig 5.1-5.3). Work done on VACV anti-apoptotic proteins has demonstrated that infected cells are protected against STS induced apoptosis[7,8]. In this study, we could demonstrate VACVΔE3L was unable to protect infected cells against STS induced apoptosis. The observations made by Zhang *et al.* and Fisher *et al.* and our observation led us to question whether E3 is an anti-apoptotic protein. A single previous publication by Kwon J. *et al.* has associated the Z-DNA-binding domain of E3 with anti-apoptotic activity in HeLa cells[3]. In contrast to the data presented in this paper, we were unable to demonstrate an anti-apoptotic phenotype

for the E3 protein (Fig 5.5-5.6). A crucial difference between the Kwon J. *et al* study and our experiments was a difference in the stimuli provided as a trigger for apoptosis in the transfected HeLa cells. We chose to use STS in our experiments as previous work has demonstrated that wild type VACV can resist STS induced apoptosis. In contrast, the virus missing E3 was susceptible to STS induced apoptosis. In addition, the ectopic expression of E3 was not able to inhibit apoptosis in STS treated HeLa cells. Cellular Bcl-2 protein and VACV F1 protein can protect cells against STS induced apoptosis. These observations led us to question the validity of E3 as an anti-apoptotic protein, as well as the reason behind the apoptosis triggered by VACVΔE3L mutants.

In the study on MVAΔE3L, Fisher *et al.* suggested that E3 and F1 work together to prevent apoptosis. In their discussion, they allude to the possibility of diminished F1 levels during a MVAΔE3L infection of HeLa cells[5]. Our experiments show that F1 is not detectable in HeLa cells infected with VACVΔE3L. A similar trend was observed in multiple cell lines (Fig. 5.8). In addition, in VACVΔE3L infected HeLa cells that ectopically express E3, the expression of F1 is restored (Fig. 5.8). These results show that unlike the previous assumption by Fisher *et al.*, the F1 protein is absent during a VACVΔE3L infection. The expression of E3 is sufficient to restore the expression of F1 during a VACVΔE3L infection. Another important observation is that the ectopic expression of F1 was sufficient to alleviate the apoptosis triggered by VACVΔE3L infection of HeLa cells. These results would suggest that the VACV anti-apoptotic protein was absent during a VACVΔE3L infection, and the absence of the protein might be the underlying reason behind the apoptosis triggered during infection. Zhang *et al.* previously described that VACV mutant of E3 with a deleted C-terminus is capable of

triggering apoptosis in HeLa cells during infection[6]. We were able to demonstrate a similar trend in that VACV-E3LΔ26C-infected cells triggered mitochondrial membrane depolarization upon infection, and this mutant virus was unable to protect cells against STS induced apoptosis. VACV-E3LΔ83N infection protects against STS induced apoptosis. This observation would suggest that VACV-E3LΔ26C behaves like a VACVΔE3L mutant, and VACV-E3LΔ83N mimics the wild type virus. The C-terminus of the protein is responsible for the inhibition of the dsRNA PKR response. F1 was not detectable in HeLa cells infected with VACV-E3LΔ26C while F1 was detected in VACV-E3LΔ83N. The level of F1 detected in the VACV-E3LΔ83N mutant was always lower than that detected in HeLa cells infected with VACV. It is important to note that this lower amount of F1 is sufficient to prevent the apoptosis triggered by virus infection. From the above mentioned results we can infer that the ability of VACVΔE3L and VACV-E3LΔ26C to trigger apoptosis is directly related to the failure of these mutant virus to inhibit the PKR pathway. Zhang *et al.* had previously demonstrated that PKR-deficient cells are resistant to VACVΔE3L infection triggered apoptosis[6]. To add to this observation, we were able to demonstrate that F1 expression is restored during VACVΔE3L infection of a PKR-deficient HeLa cells (Fig. 5.13).

The observation that F1 was absent during a VACVΔE3L infection was quite surprising. Previous RNAseq and microarray experiments on VACV have demonstrated that F1 is an early protein[9,10]. Yang Z. *et al.* demonstrated that in VACVwr infected HeLa cells, the F1 transcript is detectable as early as 0.5 hours post the addition of the virus[6]. We were also able to confirm the presence of F1 within the first 0.5 hours of virus addition. Our RNAseq experiments confirmed the previously published results, we were

also able to demonstrate that the F1 transcript is present during a VACVΔE3L infection. The level of F1 transcript remain comparable between HeLa cells infected with VACV or VACVΔE3L (Fig 5.14). Our RNAseq data showed early mRNA (I3, N2, F4, and F2) were present in comparable amounts during a VACV and VACVΔE3L infection. In contrast, intermediate (A36, and B5) and late gene (A34 and I5) transcript levels were altered during VACVΔE3L infection (Fig 5.15). The observation that early transcripts are present during a VACVΔE3L infection, while intermediate and late transcripts are altered or absent is in agreement with previously described observations[11]. The western blot analysis demonstrated that all early gene products except F1 were present during a VACVΔE3L infection. One crucial point to consider is that though F1 has previously been classified as an early gene, in our western blot analysis we didn't detect the protein till 4 hours post infection. In contrast, other early proteins that we tested where detectable by 2 hours post infection. This delay in the accumulation of F1 may be responsible for the higher sensitivity of the F1 translation to PKR. The above mentioned data clearly demonstrates that the F1 protein is absent during VACVΔE3L infection of HeLa cells, but the transcript is present. This observation would indicate that there is a translation block that is preventing the formation of the F1 protein. This observation also reconciles the function of E3 during VACV infection, which is to inhibit the function of PKR. The presence of F1 mRNA but the absence of the F1 protein is a classic sign of a translation block that is a result of the phosphorylation of eIF-2α. The phosphorylation of eIF-2α is a critical step in the in cellular defense PKR pathway.

During the analysis of the RNAseq reads we observed that the reads mapped to the F1 region were continuous to the reads that mapped to the F2 region (Fig. 5.17). This

observation suggested that F1 and F2 may be encoded from a bicistronic mRNA. This observation was unique because poxviruses have no reported bicistronic mRNAs. To confirm the RNAseq results, we performed northern blot analysis. In our northern blot analysis, the probe against F1 the gene hybridized to two distinct bands (Fig. 5.18). As mentioned in the results section, our northern blot data (Fig. 5.18 and 5.20) would suggest that are two distinct transcripts that each encodes the F1 orf. The larger transcript that is approximately 1.8 kb hybridizes with both the *F2L* and the *F1L* probe while the smaller transcript that is under 1 kb hybridizes only to the *F1L* probe. The data shows that the larger transcript comprises of the *F2L* and *F1L* orf, while the smaller transcript encodes only the *F1L* orf. The northern blots also show a similar timeline for the appearances of the smaller and the larger transcripts during infection of HeLa cells with VACV and VACVΔE3L. This result was different from what was previously reported by Fisher *el al*.[5]. The difference could be attributed to the difference in strains used in the two studies. The northern blots on mRNA extracted from HeLa cells infected with VACVΔF2L virus demonstrated that the *F1L* probe failed to detect any F1 mRNA (Fig. 5.20). This would suggest that in the VACVΔF2L mutant used in this study does not produce the F1 mRNA. Our western blot data supported the northern blot where F1 protein was absent during the infection of HeLa cells with VACVΔF2L mutant (Fig. 5.22). These observations suggest that there is a possible bicistronic mRNA that encodes *F2L* and *F1L* orfs. Alternatively, it is likely that in the VACVΔF2L mutant, the actual *F1L* promoter might have been deleted.

To address the possibility of F2 and F1 being translated from a bicistronic mRNA, we performed a siRNA experiment. The experiments demonstrated that an siRNA

targeting the F2 mRNA was able to diminish the expression of F2, but had no effect on the expression of F1. In contrast, the siRNA targeting F1 mRNA diminished the expression of both F1 and F2. The results from these two experiments demonstrate that F1 is translated from the smaller monocistronic mRNA. The surprising observation was that F2 was translated from a bicistronic mRNA. An important result to note is that though F2 is translated from a bicistronic mRNA that consists of the F2 and F1 orfs, a majority of F1 is translated from the smaller monocistronic mRNA and not the bicistronic mRNA. The results from the siRNA experiment would suggest that the promoter of F1 was deleted in the VACVΔF2L mutant. This would suggest that promoter of the *F1L* is significantly upstream of the F1 start codon, and is located somewhere inside the *F2L* orf. Additional experiments will be required to determine the location of the promotor. The extended distance between the expected start site and the promoter might suggest a long 5' untranslated region (5' UTR) is present in the F1 mRNA. This longer 5'-UTR may be responsible for the increased sensitivity of the F1 message to the activation of PKR. Additional experiments will be required to understand why the F1 protein is more sensitive to the activation of PKR. Another important observation from this study is the lack of a transcriptional terminator between F2 and F1 orfs. This is a unique situation that exists between these two adjacent genes, and has not previously observed in *Orthopoxvirus.* We currently don't know the reason behind absence of a transcriptional terminator, and the presence of the bicistronic mRNA that is responsible for encoding one protein. It would be interesting to understand the evolutionary process behind this unique gene arrangement. The current study put F1 into a unique category of VACV early transcripts where the protein is absent during VACVΔE3L infection. VACV D9 is the

only other protein that has previously been demonstrated to be an early protein that is absent during VACVΔE3L infection[12].

In conclusion, we were able to establish that absence of F1 during a VACVΔE3L infection of HeLa cells was responsible for the activation of apoptotic pathway. Better understanding the sensitivity of the F1 protein to the activation of the PKR pathway will help improve our understanding how the VACV interacts with the innate immune responses.

References

1 Rivas, C., Gil, J., Melkova, Z., Esteban, M. & Diaz-Guerra, M. Vaccinia virus E3L protein is an inhibitor of the interferon (i.f.n.)-induced 2-5A synthetase enzyme. *Virology* **243**, 406-414 (1998).

2 Chang, H. W., Watson, J. C. & Jacobs, B. L. The E3L gene of vaccinia virus encodes an inhibitor of the interferon-induced, double-stranded RNA-dependent protein kinase. *Proc Natl Acad Sci U S A* **89**, 4825-4829 (1992).

3 Kwon, J. A. & Rich, A. Biological function of the vaccinia virus Z-DNA-binding protein E3L: gene transactivation and antiapoptotic activity in HeLa cells. *Proc Natl Acad Sci U S A* **102**, 12759-12764, doi:10.1073/pnas.0506011102 (2005).

4 Shors, T. *et al.* Complementation of vaccinia virus deleted of the E3L gene by mutants of E3L. *Virology* **239**, 269-276, doi:10.1006/viro.1997.8881 (1997).

5 Fischer, S. F. *et al.* Modified vaccinia virus Ankara protein F1L is a novel BH3-domain-binding protein and acts together with the early viral protein E3L to block virus-associated apoptosis. *Cell Death Differ* **13**, 109-118, doi:10.1038/sj.cdd.4401718 (2006).

6 Zhang, P., Jacobs, B. L. & Samuel, C. E. Loss of protein kinase PKR expression in human HeLa cells complements the vaccinia virus E3L deletion mutant phenotype by restoration of viral protein synthesis. *J Virol* **82**, 840-848, doi:10.1128/JVI.01891-07 (2008).

7 Wasilenko, S. T., Stewart, T. L., Meyers, A. F. & Barry, M. Vaccinia virus encodes a previously uncharacterized mitochondrial-associated inhibitor of apoptosis. *Proc Natl Acad Sci U S A* **100**, 14345-14350, doi:10.1073/pnas.2235583100 (2003).

8 Wasilenko, S. T., Banadyga, L., Bond, D. & Barry, M. The vaccinia virus F1L protein interacts with the proapoptotic protein Bak and inhibits Bak activation. *J Virol* **79**, 14031-14043, doi:10.1128/JVI.79.22.14031-14043.2005 (2005).

9 Yang, Z., Bruno, D. P., Martens, C. A., Porcella, S. F. & Moss, B. Simultaneous high-resolution analysis of vaccinia virus and host cell transcriptomes by deep RNA sequencing. *Proc Natl Acad Sci U S A* **107**, 11513-11518, doi:10.1073/pnas.1006594107 (2010).

10 Assarsson, E. *et al.* Kinetic analysis of a complete poxvirus transcriptome reveals an immediate-early class of genes. *Proc Natl Acad Sci U S A* **105**, 2140-2145, doi:10.1073/pnas.0711573105 (2008).

11 Ludwig, H. *et al.* Role of viral factor E3L in modified vaccinia virus ankara infection of human HeLa Cells: regulation of the virus life cycle and identification of differentially expressed host genes. *J Virol* **79**, 2584-2596, doi:10.1128/JVI.79.4.2584-2596.2005 (2005).

12 Liu, R. & Moss, B. Opposing Roles of Double-Stranded RNA Effector Pathways and Viral Defense Proteins Revealed with CRISPR-Cas9 Knockout Cell Lines

and Vaccinia Virus Mutants. *J Virol* **90**, 7864-7879, doi:10.1128/JVI.00869-16 (2016).

1 N Fields, B., Mahan Knipe, D., M Howley, P. & E Griffin, D. *Fields Virology, Volume 1*. (2006).
2 Behbehani, A. M. The smallpox story: life and death of an old disease. *Microbiol Rev* **47**, 455-509 (1983).
3 Eyler, J. M. Smallpox in history: the birth, death, and impact of a dread disease. *The Journal of laboratory and clinical medicine* **142**, 216-220, doi:10.1016/S0022-2143(03)00102-1 (2003).
4 Lofquist, J. M., Weimert, N. A. & Hayney, M. S. Smallpox: a review of clinical disease and vaccination. *American journal of health-system pharmacy : AJHP : official journal of the American Society of Health-System Pharmacists* **60**, 749-756; quiz 757-748 (2003).
5 Moore, Z. S., Seward, J. F. & Lane, J. M. Smallpox. *Lancet* **367**, 425-435, doi:10.1016/S0140-6736(06)68143-9 (2006).
6 Bray, M. & Buller, M. Looking back at smallpox. **38**, 882-889, doi:10.1086/381976 (2004).
7 Gubser, C., Hue, S., Kellam, P. & Smith, G. L. Poxvirus genomes: a phylogenetic analysis. *J Gen Virol* **85**, 105-117 (2004).
8 Haller, S. L., Peng, C., McFadden, G. & Rothenburg, S. Poxviruses and the evolution of host range and virulence. *Infect Genet Evol* **21**, 15-40, doi:10.1016/j.meegid.2013.10.014 (2014).
9 Lefkowitz, E. J., Wang, C. & Upton, C. Poxviruses: past, present and future. *Virus Res* **117**, 105-118, doi:10.1016/j.virusres.2006.01.016 (2006).
10 McFadden, G. Poxvirus tropism. *Nat Rev Microbiol* **3**, 201-213, doi:10.1038/nrmicro1099 (2005).
11 Werden, S. J., Rahman, M. M. & McFadden, G. Poxvirus host range genes. *Advances in virus research* **71**, 135-171, doi:10.1016/S0065-3527(08)00003-1 (2008).
12 Johnson, G. P., Goebel, S. J. & Paoletti, E. An update on the vaccinia virus genome. *Virology* **196**, 381-401, doi:10.1006/viro.1993.1494 (1993).
13 Kennedy, R. B., Ovsyannikova, I. G., Jacobson, R. M. & Poland, G. A. The immunology of smallpox vaccines. *Curr Opin Immunol* **21**, 314-320, doi:10.1016/j.coi.2009.04.004 (2009).
14 Condit, R. C., Moussatche, N. & Traktman, P. In a nutshell: structure and assembly of the vaccinia virion. *Advances in virus research* **66**, 31-124, doi:10.1016/S0065-3527(06)66002-8 (2006).
15 Smith, G. L. & Vanderplasschen, A. Extracellular enveloped vaccinia virus. Entry, egress, and evasion. *Advances in experimental medicine and biology* **440**, 395-414 (1998).
16 Smith, G. L., Vanderplasschen, A. & Law, M. The formation and function of extracellular enveloped vaccinia virus. *J Gen Virol* **83**, 2915-2931 (2002).
17 Moss, B. Poxvirus entry and membrane fusion. *Virology* **344**, 48-54, doi:10.1016/j.virol.2005.09.037 (2006).

18 Roberts, K. L. & Smith, G. L. Vaccinia virus morphogenesis and dissemination. *Trends Microbiol* **16**, 472-479, doi:10.1016/j.tim.2008.07.009 (2008).
19 Boyle, D. B. & Heine, H. G. Recombinant fowlpox virus vaccines for poultry. *Immunol Cell Biol* **71 (Pt 5)**, 391-397, doi:10.1038/icb.1993.45 (1993).
20 Shchelkunov, S. N. Functional organization of variola major and vaccinia virus genomes. *Virus genes* **10**, 53-71 (1995).
21 Wittek, R. Organization and expression of the poxvirus genome. *Experientia* **38**, 285-297 (1982).
22 Upton, C., Slack, S., Hunter, A. L., Ehlers, A. & Roper, R. L. Poxvirus orthologous clusters: toward defining the minimum essential poxvirus genome. *J Virol* **77**, 7590-7600 (2003).
23 Bengali, Z., Townsley, A. C. & Moss, B. Vaccinia virus strain differences in cell attachment and entry. *Virology* **389**, 132-140, doi:10.1016/j.virol.2009.04.012 (2009).
24 Carter, G. C., Law, M., Hollinshead, M. & Smith, G. L. Entry of the vaccinia virus intracellular mature virion and its interactions with glycosaminoglycans. *J Gen Virol* **86**, 1279-1290, doi:10.1099/vir.0.80831-0 (2005).
25 Schmidt, F. I., Bleck, C. K. & Mercer, J. Poxvirus host cell entry. *Curr Opin Virol* **2**, 20-27, doi:10.1016/j.coviro.2011.11.007 (2012).
26 Yang, Z., Bruno, D. P., Martens, C. A., Porcella, S. F. & Moss, B. Simultaneous high-resolution analysis of vaccinia virus and host cell transcriptomes by deep RNA sequencing. *Proc Natl Acad Sci U S A* **107**, 11513-11518, doi:10.1073/pnas.1006594107 (2010).
27 Yang, Z., Maruri-Avidal, L., Sisler, J., Stuart, C. A. & Moss, B. Cascade regulation of vaccinia virus gene expression is modulated by multistage promoters. *Virology* **447**, 213-220, doi:10.1016/j.virol.2013.09.007 (2013).
28 Condit, R. C. & Niles, E. G. Regulation of viral transcription elongation and termination during vaccinia virus infection. *Biochim Biophys Acta* **1577**, 325-336 (2002).
29 Leite, F. & Way, M. The role of signalling and the cytoskeleton during Vaccinia Virus egress. *Virus Res* **209**, 87-99, doi:10.1016/j.virusres.2015.01.024 (2015).
30 van Eijl, H., Hollinshead, M., Rodger, G., Zhang, W. H. & Smith, G. L. The vaccinia virus F12L protein is associated with intracellular enveloped virus particles and is required for their egress to the cell surface. *J Gen Virol* **83**, 195-207, doi:10.1099/0022-1317-83-1-195 (2002).
31 Chang, T. H. *et al.* Crystal structure of vaccinia viral A27 protein reveals a novel structure critical for its function and complex formation with A26 protein. *PLoS Pathog* **9**, e1003563, doi:10.1371/journal.ppat.1003563 (2013).
32 Carter, G. C. *et al.* Vaccinia virus cores are transported on microtubules. *J Gen Virol* **84**, 2443-2458 (2003).
33 Boukhebza, H., Bellon, N., Limacher, J. M. & Inchauspe, G. Therapeutic vaccination to treat chronic infectious diseases: current clinical developments using MVA-based vaccines. *Human vaccines & immunotherapeutics* **8**, 1746-1757, doi:10.4161/hv.21689 (2012).

34 Guse, K., Cerullo, V. & Hemminki, A. Oncolytic vaccinia virus for the treatment of cancer. *Expert Opin Biol Ther* **11**, 595-608, doi:10.1517/14712598.2011.558838 (2011).
35 Thorne, S. H. Immunotherapeutic potential of oncolytic vaccinia virus. *Frontiers in oncology* **4**, 155, doi:10.3389/fonc.2014.00155 (2014).
36 Fenner, F. Studies in infectious ectromelia in mice; natural transmission; the portal of entry of the virus. *Aust J Exp Biol Med Sci* **25**, 275-282 (1947).
37 Buller, R. M. & Wallace, G. D. Reexamination of the efficacy of vaccination against mousepox. *Lab Anim Sci* **35**, 473-476 (1985).
38 Esteban, D. J. & Buller, R. M. L. Ectromelia virus: the causative agent of mousepox. *The Journal of general virology* **86**, 2645-2659, doi:10.1099/vir.0.81090-0 (2005).
39 Roberts, J. A. Histopathogenesis of mousepox. II. Cutaneous infection. *Br J Exp Pathol* **43**, 462-468 (1962).
40 Wallace, G. D., Buller, R. M. & Morse, H. C., 3rd. Genetic determinants of resistance to ectromelia (mousepox) virus-induced mortality. *J Virol* **55**, 890-891 (1985).
41 Wallace, G. D. & Buller, R. M. Kinetics of ectromelia virus (mousepox) transmission and clinical response in C57BL/6j, BALB/cByj and AKR/J inbred mice. *Lab Anim Sci* **35**, 41-46 (1985).
42 Buller, R. M. & Palumbo, G. J. Poxvirus pathogenesis. *Microbiological reviews* **55**, 80-122 (1991).
43 Chen, N. *et al.* The genomic sequence of ectromelia virus, the causative agent of mousepox. *Virology* **317**, 165-186 (2003).
44 Buller, R. M. The BALB/c mouse as a model to study orthopoxviruses. *Curr Top Microbiol Immunol* **122**, 148-153 (1985).
45 Melo-Silva, C. R. *et al.* The Ectromelia Virus SPI-2 Protein Causes Lethal Mousepox by Preventing NK Cell Responses. **85**, 11170-11182, doi:10.1128/JVI.00256-11 (2011).
46 Parker, S. *et al.* Mousepox in the C57BL/6 strain provides an improved model for evaluating anti-poxvirus therapies. *Virology* **385**, 11-21, doi:10.1016/j.virol.2008.11.015 (2009).
47 Brownstein, D. G., Bhatt, P. N., Gras, L. & Budris, T. Serial backcross analysis of genetic resistance to mousepox, using marker loci for Rmp-2 and Rmp-3. *J Virol* **66**, 7073-7079 (1992).
48 Delano, M. L. & Brownstein, D. G. Innate resistance to lethal mousepox is genetically linked to the NK gene complex on chromosome 6 and correlates with early restriction of virus replication by cells with an NK phenotype. *J Virol* **69**, 5875-5877 (1995).
49 Karupiah, G., Panchanathan, V., Sakala, I. G. & Chaudhri, G. Genetic resistance to smallpox: lessons from mousepox. *Novartis Foundation symposium* **281**, 129-136; discussion 136-140, 208-129 (2007).
50 Karupiah, G., Chen, J. H., Nathan, C. F., Mahalingam, S. & MacMicking, J. D. Identification of nitric oxide synthase 2 as an innate resistance locus against ectromelia virus infection. *J Virol* **72**, 7703-7706 (1998).

51 Chapman, J. L., Nichols, D. K., Martinez, M. J. & Raymond, J. W. Animal models of orthopoxvirus infection. *Veterinary pathology* **47**, 852-870, doi:10.1177/0300985810378649 (2010).
52 McCollum, A. M. & Damon, I. K. Human monkeypox. *Clin Infect Dis* **58**, 260-267, doi:10.1093/cid/cit703 (2014).
53 Fang, M. & Sigal, L. J. Antibodies and CD8+ T cells are complementary and essential for natural resistance to a highly lethal cytopathic virus. *J Immunol* **175**, 6829-6836 (2005).
54 Amanna, I. J., Slifka, M. K. & Crotty, S. Immunity and immunological memory following smallpox vaccination. *Immunol Rev* **211**, 320-337, doi:10.1111/j.0105-2896.2006.00392.x (2006).
55 Jung, Y. W., Rutishauser, R. L., Joshi, N. S., Haberman, A. M. & Kaech, S. M. Differential localization of effector and memory CD8 T cell subsets in lymphoid organs during acute viral infection. *J Immunol* **185**, 5315-5325, doi:10.4049/jimmunol.1001948 (2010).
56 Szulc, L. *et al.* T cell cytokine synthesis at the single-cell level in BALB/c and C57BL/6 mice infected with ectromelia virus. **66**, 222-230 (2012).
57 Haga, I. R. & Bowie, A. G. Evasion of innate immunity by vaccinia virus. *Parasitology* **130 Suppl**, S11-25, doi:10.1017/S0031182005008127 (2004).
58 Guerra, S., Caceres, A., Knobeloch, K. P., Horak, I. & Esteban, M. Vaccinia virus E3 protein prevents the antiviral action of ISG15. *PLoS Pathog* **4**, e1000096, doi:10.1371/journal.ppat.1000096 (2008).
59 Myskiw, C., Arsenio, J., van Bruggen, R., Deschambault, Y. & Cao, J. Vaccinia virus E3 suppresses expression of diverse cytokines through inhibition of the PKR, NF-kappaB, and IRF3 pathways. *J Virol* **83**, 6757-6768, doi:10.1128/JVI.02570-08 (2009).
60 Kampfer, H. *et al.* Lack of interferon-gamma production despite the presence of interleukin-18 during cutaneous wound healing. *Mol Med* **6**, 1016-1027 (2000).
61 Karupiah, G., Fredrickson, T. N., Holmes, K. L., Khairallah, L. H. & Buller, R. M. Importance of interferons in recovery from mousepox. *J Virol* **67**, 4214-4226 (1993).
62 Rubio, D. *et al.* Crosstalk between the type 1 interferon and nuclear factor kappa B pathways confers resistance to a lethal virus infection. *Cell Host Microbe* **13**, 701-710, doi:10.1016/j.chom.2013.04.015 (2013).
63 Chaudhri, G. *et al.* Polarized type 1 cytokine response and cell-mediated immunity determine genetic resistance to mousepox. *Proc Natl Acad Sci U S A* **101**, 9057-9062, doi:10.1073/pnas.0402949101 (2004).
64 van Buuren, N. *et al.* EVM005: an ectromelia-encoded protein with dual roles in NF-kappaB inhibition and virulence. *PLoS Pathog* **10**, e1004326, doi:10.1371/journal.ppat.1004326 (2014).
65 Di Pilato, M. *et al.* NFkappaB activation by modified vaccinia virus as a novel strategy to enhance neutrophil migration and HIV-specific T-cell responses. *Proc Natl Acad Sci U S A* **112**, E1333-1342, doi:10.1073/pnas.1424341112 (2015).

66 Parker, A. K., Parker, S., Yokoyama, W. M., Corbett, J. A. & Buller, R. M. Induction of natural killer cell responses by ectromelia virus controls infection. *J Virol* **81**, 4070-4079, doi:10.1128/JVI.02061-06 (2007).
67 Parker, S., Nuara, A., Buller, R. M. & Schultz, D. A. Human monkeypox: an emerging zoonotic disease. *Future microbiology* **2**, 17-34, doi:10.2217/17460913.2.1.17 (2007).
68 Moulton, E. A., Atkinson, J. P. & Buller, R. M. Surviving mousepox infection requires the complement system. *PLoS Pathogens* **4**, e1000249, doi:10.1371/journal.ppat.1000249 (2008).
69 Mullbacher, A. *et al.* Granzyme A is critical for recovery of mice from infection with the natural cytopathic viral pathogen, ectromelia. *Proc Natl Acad Sci U S A* **93**, 5783-5787 (1996).
70 Wang, Y. Q. *et al.* Defective antiviral CD8 T-cell response and viral clearance in the absence of c-Jun N-terminal kinases. *Immunology* **142**, 603-613, doi:10.1111/imm.12270 (2014).
71 McIlwain, D. R., Berger, T. & Mak, T. W. Caspase functions in cell death and disease. *Cold Spring Harbor perspectives in biology* **5**, a008656, doi:10.1101/cshperspect.a008656 (2013).
72 Kiraz, Y., Adan, A., Kartal Yandim, M. & Baran, Y. Major apoptotic mechanisms and genes involved in apoptosis. *Tumour Biol* **37**, 8471-8486, doi:10.1007/s13277-016-5035-9 (2016).
73 Wang, X. The expanding role of mitochondria in apoptosis. *Genes Dev* **15**, 2922-2933 (2001).
74 Green, D. R. Apoptotic pathways: ten minutes to dead. *Cell* **121**, 671-674, doi:10.1016/j.cell.2005.05.019 (2005).
75 Parnaik, R., Raff, M. C. & Scholes, J. Differences between the clearance of apoptotic cells by professional and non-professional phagocytes. *Curr Biol* **10**, 857-860 (2000).
76 Erwig, L. P. & Henson, P. M. Clearance of apoptotic cells by phagocytes. *Cell Death Differ* **15**, 243-250, doi:10.1038/sj.cdd.4402184 (2008).
77 Nicholson, D. W. & Thornberry, N. A. Caspases: killer proteases. *Trends in biochemical sciences* **22**, 299-306 (1997).
78 Hengartner, M. O. The biochemistry of apoptosis. *Nature* **407**, 770-776, doi:10.1038/35037710 (2000).
79 Nicholson, D. W. Caspase structure, proteolytic substrates, and function during apoptotic cell death. *Cell Death Differ* **6**, 1028-1042, doi:10.1038/sj.cdd.4400598 (1999).
80 Cullen, S. P. & Martin, S. J. Caspase activation pathways: some recent progress. *Cell Death Differ* **16**, 935-938, doi:10.1038/cdd.2009.59 (2009).
81 Gil, J. & Esteban, M. The interferon-induced protein kinase (PKR), triggers apoptosis through FADD-mediated activation of caspase 8 in a manner independent of Fas and TNF-alpha receptors. *Oncogene* **19**, 3665-3674, doi:10.1038/sj.onc.1203710 (2000).
82 Gerschenson, L. E. & Rotello, R. J. Apoptosis: a different type of cell death. *Faseb J* **6**, 2450-2455 (1992).

83 Hao, Z. & Mak, T. W. Type I and type II pathways of Fas-mediated apoptosis are differentially controlled by XIAP. *J Mol Cell Biol* **2**, 63-64, doi:10.1093/jmcb/mjp034 (2010).
84 Wajant, H. The Fas signaling pathway: more than a paradigm. *Science* **296**, 1635-1636, doi:10.1126/science.1071553 (2002).
85 Larrick, J. W. & Wright, S. C. Cytotoxic mechanism of tumor necrosis factor-alpha. *Faseb J* **4**, 3215-3223 (1990).
86 Yuan, J. Molecular control of life and death. *Current opinion in cell biology* **7**, 211-214 (1995).
87 Liu, X., Kim, C. N., Yang, J., Jemmerson, R. & Wang, X. Induction of apoptotic program in cell-free extracts: requirement for dATP and cytochrome c. *Cell* **86**, 147-157 (1996).
88 Chai, J. *et al.* Structural and biochemical basis of apoptotic activation by Smac/DIABLO. *Nature* **406**, 855-862, doi:10.1038/35022514 (2000).
89 Kuida, K. *et al.* Altered cytokine export and apoptosis in mice deficient in interleukin-1 beta converting enzyme. *Science* **267**, 2000-2003 (1995).
90 Vayssiere, J. L., Petit, P. X., Risler, Y. & Mignotte, B. Commitment to apoptosis is associated with changes in mitochondrial biogenesis and activity in cell lines conditionally immortalized with simian virus 40. *Proc Natl Acad Sci U S A* **91**, 11752-11756 (1994).
91 Hu, Q. *et al.* Molecular determinants of caspase-9 activation by the Apaf-1 apoptosome. *Proc Natl Acad Sci U S A* **111**, 16254-16261, doi:10.1073/pnas.1418000111 (2014).
92 Bratton, S. B. *et al.* Recruitment, activation and retention of caspases-9 and -3 by Apaf-1 apoptosome and associated XIAP complexes. *EMBO J* **20**, 998-1009, doi:10.1093/emboj/20.5.998 (2001).
93 Purring-Koch, C. & McLendon, G. Cytochrome c binding to Apaf-1: the effects of dATP and ionic strength. *Proc Natl Acad Sci U S A* **97**, 11928-11931, doi:10.1073/pnas.220416197 (2000).
94 Zou, H., Henzel, W. J., Liu, X., Lutschg, A. & Wang, X. Apaf-1, a human protein homologous to C. elegans CED-4, participates in cytochrome c-dependent activation of caspase-3. *Cell* **90**, 405-413 (1997).
95 Wu, G. *et al.* Structural basis of IAP recognition by Smac/DIABLO. *Nature* **408**, 1008-1012, doi:10.1038/35050012 (2000).
96 Du, C., Fang, M., Li, Y., Li, L. & Wang, X. Smac, a mitochondrial protein that promotes cytochrome c-dependent caspase activation by eliminating IAP inhibition. *Cell* **102**, 33-42 (2000).
97 James, D. *et al.* Mechanisms of mitochondrial outer membrane permeabilization. *Novartis Foundation symposium* **287**, 170-176; discussion 176-182 (2007).
98 Chipuk, J. E., Moldoveanu, T., Llambi, F., Parsons, M. J. & Green, D. R. The BCL-2 Family Reunion. *Molecular Cell* **37**, 299-310, doi:10.1016/j.molcel.2010.01.025 (2010).
99 Willis, S. & Adams, J. Life in the balance: how BH3-only proteins induce apoptosis. *Current opinion in cell biology* **17**, 617-625 (2005).

100 Connor, L. *et al.* Bim: a novel member of the Bcl-2 family that promotes apoptosis. *Embo J* **17**, 384-395 (1998).
101 Wei, M. C. *et al.* Proapoptotic BAX and BAK: a requisite gateway to mitochondrial dysfunction and death. *Science* **292**, 727-730, doi:10.1126/science.1059108 (2001).
102 Chittenden, T. *et al.* A conserved domain in Bak, distinct from BH1 and BH2, mediates cell death and protein binding functions. *EMBO J* **14**, 5589-5596 (1995).
103 Karbowski, M., Norris, K. L., Cleland, M. M., Jeong, S.-Y. & Youle, R. J. Role of Bax and Bak in mitochondrial morphogenesis. *Nature* **443**, 658-662, doi:10.1038/nature05111 (2006).
104 Kim, H. *et al.* Stepwise Activation of BAX and BAK by tBID, BIM, and PUMA Initiates Mitochondrial Apoptosis. **36**, 487-499, doi:10.1016/j.molcel.2009.09.030 (2009).
105 Hutcheson, J. *et al.* Combined loss of proapoptotic genes Bak or Bax with Bim synergizes to cause defects in hematopoiesis and in thymocyte apoptosis. *J Exp Med* **201**, 1949-1960, doi:10.1084/jem.20041484 (2005).
106 Kuwana, T. *et al.* BH3 Domains of BH3-Only Proteins Differentially Regulate Bax-Mediated Mitochondrial Membrane Permeabilization Both Directly and Indirectly. *Molecular Cell* **17**, 525-535, doi:10.1016/j.molcel.2005.02.003 (2005).
107 Kim, H. *et al.* Hierarchical regulation of mitochondrion-dependent apoptosis by BCL-2 subfamilies. *Nat Cell Biol* **8**, 1348-1358, doi:http://www.nature.com/ncb/journal/v8/n12/suppinfo/ncb1499_S1.html (2006).
108 Youle, R. J. & Strasser, A. The BCL-2 protein family: opposing activities that mediate cell death. *Nature Reviews Molecular Cell Biology* **9**, 47-59, doi:10.1038/nrm2308 (2008).
109 Kantari, C. & Walczak, H. Caspase-8 and bid: caught in the act between death receptors and mitochondria. *Biochim Biophys Acta* **1813**, 558-563, doi:10.1016/j.bbamcr.2011.01.026 (2011).
110 Billen, L. P., Shamas-Din, A. & Andrews, D. W. Bid: a Bax-like BH3 protein. *Oncogene* **27 Suppl 1**, S93-104, doi:10.1038/onc.2009.47 (2008).
111 Billen, L. P., Shamas-Din, A. & Andrews, D. W. Bid: a Bax-like BH3 protein. **27**, S93-S104, doi:10.1038/onc.2009.47 (2009).
112 White, E. *et al.* The 19-kilodalton adenovirus E1B transforming protein inhibits programmed cell death and prevents cytolysis by tumor necrosis factor alpha. *Mol Cell Biol* **12**, 2570-2580 (1992).
113 Bennett, M. *et al.* Cell surface trafficking of Fas: a rapid mechanism of p53-mediated apoptosis. *Science* **282**, 290-293 (1998).
114 Benedict, C., Norris, P. & Ware, C. To kill or be killed: viral evasion of apoptosis. *Nature Immunology* **3**, 1013-1018 (2002).
115 Scheffner, M., Werness, B. A., Huibregtse, J. M., Levine, A. J. & Howley, P. M. The E6 oncoprotein encoded by human papillomavirus types 16 and 18 promotes the degradation of p53. *Cell* **63**, 1129-1136 (1990).

116 Yew, P. R. & Berk, A. J. Inhibition of p53 transactivation required for transformation by adenovirus early 1B protein. *Nature* **357**, 82-85, doi:10.1038/357082a0 (1992).
117 Schultz, D. R. & Harrington, W. J., Jr. Apoptosis: programmed cell death at a molecular level. *Semin Arthritis Rheum* **32**, 345-369, doi:10.1053/sarh.2003.50005 (2003).
118 Miura, M., Friedlander, R. M. & Yuan, J. Tumor necrosis factor-induced apoptosis is mediated by a CrmA-sensitive cell death pathway. *Proc Natl Acad Sci U S A* **92**, 8318-8322 (1995).
119 Dbaibo, G. S. *et al.* Cytokine response modifier A (CrmA) inhibits ceramide formation in response to tumor necrosis factor (TNF)-alpha: CrmA and Bcl-2 target distinct components in the apoptotic pathway. *J Exp Med* **185**, 481-490 (1997).
120 Seet, B. T. *et al.* Poxviruses and immune evasion. *Annual Review of Immunology* **21**, 377-423, doi:10.1146/annurev.immunol.21.120601.141049 (2002).
121 Benedict, C. A. *et al.* Cutting edge: a novel viral TNF receptor superfamily member in virulent strains of human cytomegalovirus. *J Immunol* **162**, 6967-6970 (1999).
122 Sundararajan, R., Cuconati, A., Nelson, D. & White, E. Tumor necrosis factor-alpha induces Bax-Bak interaction and apoptosis, which is inhibited by adenovirus E1B 19K. *J Biol Chem* **276**, 45120-45127, doi:10.1074/jbc.M106386200 (2001).
123 Cuconati, A. & White, E. Viral homologs of BCL-2: role of apoptosis in the regulation of virus infection. *Genes Dev* **16**, 2465-2478, doi:10.1101/gad.1012702 (2002).
124 Goldmacher, V. S. *et al.* A cytomegalovirus-encoded mitochondria-localized inhibitor of apoptosis structurally unrelated to Bcl-2. *Proc Natl Acad Sci U S A* **96**, 12536-12541 (1999).
125 Arnoult, D. *et al.* Cytomegalovirus cell death suppressor vMIA blocks Bax- but not Bak-mediated apoptosis by binding and sequestering Bax at mitochondria. *Proc Natl Acad Sci U S A* **101**, 7988-7993, doi:10.1073/pnas.0401897101 (2004).
126 Norris, K. L. & Youle, R. J. Cytomegalovirus proteins vMIA and m38.5 link mitochondrial morphogenesis to Bcl-2 family proteins. *J Virol* **82**, 6232-6243, doi:10.1128/JVI.02710-07 (2008).
127 Everett, H. *et al.* M11L: a novel mitochondria-localized protein of myxoma virus that blocks apoptosis of infected leukocytes. *J Exp Med* **191**, 1487-1498 (2000).
128 Pogo, B. G.-T., Melana, S. M. & Blaho, J. Poxvirus infection and apoptosis. *International reviews of immunology* **23**, 61-74 (2003).
129 Barry, M., Wasilenko, S. T., Stewart, T. L. & Taylor, J. M. Apoptosis regulator genes encoded by poxviruses. *Prog Mol Subcell Biol* **36**, 19-37 (2004).
130 Banadyga, L., Gerig, J., Stewart, T. & Barry, M. Fowlpox virus encodes a Bcl-2 homologue that protects cells from apoptotic death through interaction with

the proapoptotic protein Bak. *J Virol* **81**, 11032-11045, doi:10.1128/JVI.00734-07 (2007).
131 Banadyga, L., Veugelers, K., Campbell, S. & Barry, M. The fowlpox virus BCL-2 homologue, FPV039, interacts with activated Bax and a discrete subset of BH3-only proteins to inhibit apoptosis. *J Virol* **83**, 7085-7098, doi:10.1128/JVI.00437-09 (2009).
132 Banadyga, L. *et al.* Deerpox virus encodes an inhibitor of apoptosis that regulates Bak and Bax. **85**, 1922-1934, doi:10.1128/JVI.01959-10 (2011).
133 Okamoto, T. *et al.* Sheeppox virus SPPV14 encodes a Bcl-2-like cell death inhibitor that counters a distinct set of mammalian proapoptotic proteins. *J Virol* **86**, 11501-11511, doi:10.1128/JVI.01115-12 (2012).
134 Stewart, T. L., Wasilenko, S. T. & Barry, M. Vaccinia virus F1L protein is a tail-anchored protein that functions at the mitochondria to inhibit apoptosis. *J Virol* **79**, 1084-1098, doi:10.1128/JVI.79.2.1084-1098.2005 (2005).
135 Kvansakul, M. *et al.* Vaccinia virus anti-apoptotic F1L is a novel Bcl-2-like domain-swapped dimer that binds a highly selective subset of BH3-containing death ligands. *Cell Death Differ* **15**, 1564-1571, doi:10.1038/cdd.2008.83 (2008).
136 Fischer, S. F. *et al.* Modified vaccinia virus Ankara protein F1L is a novel BH3-domain-binding protein and acts together with the early viral protein E3L to block virus-associated apoptosis. *Cell Death Differ* **13**, 109-118, doi:10.1038/sj.cdd.4401718 (2006).
137 Wasilenko, S. T., Stewart, T. L., Meyers, A. F. & Barry, M. Vaccinia virus encodes a previously uncharacterized mitochondrial-associated inhibitor of apoptosis. *Proc Natl Acad Sci U S A* **100**, 14345-14350, doi:10.1073/pnas.2235583100 (2003).
138 Wasilenko, S. T., Banadyga, L., Bond, D. & Barry, M. The vaccinia virus F1L protein interacts with the proapoptotic protein Bak and inhibits Bak activation. *J Virol* **79**, 14031-14043, doi:10.1128/JVI.79.22.14031-14043.2005 (2005).
139 Taylor, J. M., Quilty, D., Banadyga, L. & Barry, M. The vaccinia virus protein F1L interacts with Bim and inhibits activation of the pro-apoptotic protein Bax. *J Biol Chem* **281**, 39728-39739, doi:10.1074/jbc.M607465200 (2006).
140 Postigo, A., Cross, J. R., Downward, J. & Way, M. Interaction of F1L with the BH3 domain of Bak is responsible for inhibiting vaccinia-induced apoptosis. *Cell Death Differ* **13**, 1651-1662, doi:10.1038/sj.cdd.4401853 (2006).
141 Campbell, S., Hazes, B., Kvansakul, M., Colman, P. & Barry, M. Vaccinia virus F1L interacts with Bak using highly divergent Bcl-2 homology domains and replaces the function of Mcl-1. *J Biol Chem* **285**, 4695-4708, doi:10.1074/jbc.M109.053769 (2010).
142 Eitz Ferrer, P. *et al.* Induction of Noxa-mediated apoptosis by modified vaccinia virus Ankara depends on viral recognition by cytosolic helicases, leading to IRF-3/IFN-beta-dependent induction of pro-apoptotic Noxa. *PLoS Pathog* **7**, e1002083, doi:10.1371/journal.ppat.1002083 (2011).

143 Gerlic, M. *et al.* Vaccinia virus F1L protein promotes virulence by inhibiting inflammasome activation. *Proc Natl Acad Sci U S A* **110**, 7808-7813, doi:10.1073/pnas.1215995110 (2013).
144 Duesberg, P. H. & Colby, C. On the biosynthesis and structure of double-stranded RNA in vaccinia virus-infected cells. *Proc Natl Acad Sci U S A* **64**, 396-403 (1969).
145 Colby, C. & Duesberg, P. H. Double-stranded RNA in vaccinia virus infected cells. *Nature* **222**, 940-944 (1969).
146 Willis, K. L., Langland, J. O. & Shisler, J. L. Viral double-stranded RNAs from vaccinia virus early or intermediate gene transcripts possess PKR activating function, resulting in NF-kappaB activation, when the K1 protein is absent or mutated. *J Biol Chem* **286**, 7765-7778, doi:10.1074/jbc.M110.194704 (2011).
147 Williams, B. R. Signal integration via PKR. *Sci STKE* **2001**, re2, doi:10.1126/stke.2001.89.re2 (2001).
148 Lemaire, P. A., Anderson, E., Lary, J. & Cole, J. L. Mechanism of PKR Activation by dsRNA. *J Mol Biol* **381**, 351-360, doi:10.1016/j.jmb.2008.05.056 (2008).
149 Clemens, M. J. *et al.* PKR: proposed nomenclature for the RNA-dependent protein kinase induced by interferon. *J Interferon Res* **13**, 241, doi:10.1089/jir.1993.13.241 (1993).
150 Husain, B., Mukerji, I. & Cole, J. L. Analysis of high-affinity binding of protein kinase R to double-stranded RNA. *Biochemistry* **51**, 8764-8770, doi:10.1021/bi301226h (2012).
151 Taylor, D. R. *et al.* Autophosphorylation sites participate in the activation of the double-stranded-RNA-activated protein kinase PKR. *Mol Cell Biol* **16**, 6295-6302 (1996).
152 Donze, O., Jagus, R., Koromilas, A. E., Hershey, J. W. & Sonenberg, N. Abrogation of translation initiation factor eIF-2 phosphorylation causes malignant transformation of NIH 3T3 cells. *EMBO J* **14**, 3828-3834 (1995).
153 Williams, B. R. PKR; a sentinel kinase for cellular stress. *Oncogene* **18**, 6112-6120, doi:10.1038/sj.onc.1203127 (1999).
154 Gil, J. *et al.* TRAF family proteins link PKR with NF-kappa B activation. *Mol Cell Biol* **24**, 4502-4512 (2004).
155 Desai, S. Y. & Sen, G. C. Effects of varying lengths of double-stranded RNA on binding and activation of 2'-5'-oligoadenylate synthetase. *J Interferon Cytokine Res* **17**, 531-536, doi:10.1089/jir.1997.17.531 (1997).
156 Sadler, A. J. & Williams, B. R. Interferon-inducible antiviral effectors. *Nat Rev Immunol* **8**, 559-568, doi:10.1038/nri2314 (2008).
157 Hovanessian, A. G. Interferon-induced and double-stranded RNA-activated enzymes: a specific protein kinase and 2',5'-oligoadenylate synthetases. *J Interferon Res* **11**, 199-205 (1991).
158 Gantier, M. P. & Williams, B. R. The response of mammalian cells to double-stranded RNA. *Cytokine Growth Factor Rev* **18**, 363-371, doi:10.1016/j.cytogfr.2007.06.016 (2007).
159 Matsumoto, M., Oshiumi, H. & Seya, T. Antiviral responses induced by the TLR3 pathway. *Rev Med Virol* **21**, 67-77, doi:10.1002/rmv.680 (2011).

160 Seth, R. B., Sun, L. & Chen, Z. J. Antiviral innate immunity pathways. *Cell research* **16**, 141-147, doi:10.1038/sj.cr.7310019 (2006).
161 Melkamu, T., Kita, H. & O'Grady, S. M. TLR3 activation evokes IL-6 secretion, autocrine regulation of Stat3 signaling and TLR2 expression in human bronchial epithelial cells. *J Cell Commun Signal* **7**, 109-118, doi:10.1007/s12079-012-0185-z (2013).
162 Cassady, K. A., Gross, M. & Roizman, B. The herpes simplex virus US11 protein effectively compensates for the gamma1(34.5) gene if present before activation of protein kinase R by precluding its phosphorylation and that of the alpha subunit of eukaryotic translation initiation factor 2. *J Virol* **72**, 8620-8626 (1998).
163 Chang, H. W., Watson, J. C. & Jacobs, B. L. The E3L gene of vaccinia virus encodes an inhibitor of the interferon-induced, double-stranded RNA-dependent protein kinase. *Proc Natl Acad Sci U S A* **89**, 4825-4829 (1992).
164 Min, J. Y. & Krug, R. M. The primary function of RNA binding by the influenza A virus NS1 protein in infected cells: Inhibiting the 2'-5' oligo (A) synthetase/RNase L pathway. *Proc Natl Acad Sci U S A* **103**, 7100-7105, doi:10.1073/pnas.0602184103 (2006).
165 Haasnoot, J. *et al.* The Ebola virus VP35 protein is a suppressor of RNA silencing. *PLoS Pathog* **3**, e86, doi:10.1371/journal.ppat.0030086 (2007).
166 Yue, Z. & Shatkin, A. J. Double-stranded RNA-dependent protein kinase (PKR) is regulated by reovirus structural proteins. *Virology* **234**, 364-371, doi:10.1006/viro.1997.8664 (1997).
167 Sharp, T. V., Witzel, J. E. & Jagus, R. Homologous regions of the alpha subunit of eukaryotic translational initiation factor 2 (eIF2alpha) and the vaccinia virus K3L gene product interact with the same domain within the dsRNA-activated protein kinase (PKR). *Eur J Biochem* **250**, 85-91 (1997).
168 Fang, Z. Y. *et al.* Expression of vaccinia E3L and K3L genes by a novel recombinant canarypox HIV vaccine vector enhances HIV-1 pseudovirion production and inhibits apoptosis in human cells. *Virology* **291**, 272-284, doi:10.1006/viro.2001.1209 (2001).
169 Ward, S. L. *et al.* In vivo replication of an ICP34.5 second-site suppressor mutant following corneal infection correlates with in vitro regulation of eIF2 alpha phosphorylation. *J Virol* **77**, 4626-4634 (2003).
170 Wylie, K. M., Schrimpf, J. E. & Morrison, L. A. Increased eIF2alpha phosphorylation attenuates replication of herpes simplex virus 2 vhs mutants in mouse embryonic fibroblasts and correlates with reduced accumulation of the PKR antagonist ICP34.5. *J Virol* **83**, 9151-9162, doi:10.1128/JVI.00886-09 (2009).
171 Kazemi, S. *et al.* Control of alpha subunit of eukaryotic translation initiation factor 2 (eIF2 alpha) phosphorylation by the human papillomavirus type 18 E6 oncoprotein: implications for eIF2 alpha-dependent gene expression and cell death. *Mol Cell Biol* **24**, 3415-3429 (2004).
172 Clemens, M. J. *et al.* Regulation of the interferon-inducible eIF-2 alpha protein kinase by small RNAs. *Biochimie* **76**, 770-778 (1994).

173 Langland, J. O., Cameron, J. M., Heck, M. C., Jancovich, J. K. & Jacobs, B. L. Inhibition of PKR by RNA and DNA viruses. *Virus research* **119**, 100-110, doi:10.3201/eid1204.051181 (2006).
174 Davies, M. V., Chang, H. W., Jacobs, B. L. & Kaufman, R. J. The E3L and K3L vaccinia virus gene products stimulate translation through inhibition of the double-stranded RNA-dependent protein kinase by different mechanisms. *Journal of virology* **67**, 1688-1692 (1993).
175 Chang, H. W. & Jacobs, B. L. Identification of a conserved motif that is necessary for binding of the vaccinia virus E3L gene products to double-stranded RNA. *Virology* **194**, 537-547, doi:10.1006/viro.1993.1292 (1993).
176 Vijaysri, S. *et al.* The Orf virus E3L homologue is able to complement deletion of the vaccinia virus E3L gene in vitro but not in vivo. *Virology* **314**, 305-314 (2003).
177 Brandt, T. *et al.* The N-terminal domain of the vaccinia virus E3L-protein is required for neurovirulence, but not induction of a protective immune response. *Virology* **333**, 263-270, doi:10.1016/j.virol.2005.01.006 (2005).
178 Ludwig, H. *et al.* Role of viral factor E3L in modified vaccinia virus ankara infection of human HeLa Cells: regulation of the virus life cycle and identification of differentially expressed host genes. *J Virol* **79**, 2584-2596, doi:10.1128/JVI.79.4.2584-2596.2005 (2005).
179 Seet, B. T. *et al.* Poxviruses and immune evasion. *Annu Rev Immunol* **21**, 377-423, doi:10.1146/annurev.immunol.21.120601.141049 (2003).
180 Kwon, J. A. & Rich, A. Biological function of the vaccinia virus Z-DNA-binding protein E3L: gene transactivation and antiapoptotic activity in HeLa cells. *Proc Natl Acad Sci U S A* **102**, 12759-12764, doi:10.1073/pnas.0506011102 (2005).
181 Sambrook, J., Russell, D. W. & Sambrook, J. *The condensed protocols from Molecular cloning : a laboratory manual*. (Cold Spring Harbor Laboratory Press, 2006).
182 Larkin, M. A. *et al.* Clustal W and Clustal X version 2.0. *Bioinformatics* **23**, 2947-2948, doi:10.1093/bioinformatics/btm404 (2007).
183 Dauber, B. *et al.* The Herpes Simplex Virus Virion Host Shutoff Protein Enhances Translation of Viral True Late mRNAs Independently of Suppressing Protein Kinase R and Stress Granule Formation. *J Virol* **90**, 6049-6057, doi:10.1128/JVI.03180-15 (2016).
184 Heibein, J. A. *et al.* Granzyme B-mediated cytochrome c release is regulated by the Bcl-2 family members bid and Bax. *J Exp Med* **192**, 1391-1402 (2000).
185 Beattie, E. *et al.* Reversal of the interferon-sensitive phenotype of a vaccinia virus lacking E3L by expression of the reovirus S4 gene. *J Virol* **69**, 499-505 (1995).
186 Stuart, D., Graham, K., Schreiber, M., Macaulay, C. & McFadden, G. The target DNA sequence for resolution of poxvirus replicative intermediates is an active late promoter. *J Virol* **65**, 61-70 (1991).
187 Parker, S. *et al.* Efficacy of therapeutic intervention with an oral ether-lipid analogue of cidofovir (CMX001) in a lethal mousepox model. *Antiviral Res* **77**, 39-49, doi:10.1016/j.antiviral.2007.08.003 (2008).

188 Ruegg, U. T. & Burgess, G. M. Staurosporine, K-252 and UCN-01: potent but nonspecific inhibitors of protein kinases. *Trends Pharmacol Sci* **10**, 218-220 (1989).
189 Lindsten, T. *et al.* The combined functions of proapoptotic Bcl-2 family members bak and bax are essential for normal development of multiple tissues. *Molecular Cell* **6**, 1389-1399 (2000).
190 Antonsson, B., Montessuit, S., Sanchez, B. & Martinou, J. C. Bax is present as a high molecular weight oligomer/complex in the mitochondrial membrane of apoptotic cells. *J Biol Chem* **276**, 11615-11623 (2001).
191 Kashkar, H., Wiegmann, K., Yazdanpanah, B., Haubert, D. & Kronke, M. Acid sphingomyelinase is indispensable for UV light-induced Bax conformational change at the mitochondrial membrane. *J Biol Chem* **280**, 20804-20813 (2005).
192 Duriez, P. J. & Shah, G. M. Cleavage of poly(ADP-ribose) polymerase: a sensitive parameter to study cell death. *Biochemistry and cell biology = Biochimie et biologie cellulaire* **75**, 337-349 (1997).
193 Gobeil, S., Boucher, C. C., Nadeau, D. & Poirier, G. G. Characterization of the necrotic cleavage of poly(ADP-ribose) polymerase (PARP-1): implication of lysosomal proteases. *Cell Death Differ* **8**, 588-594, doi:10.1038/sj.cdd.4400851 (2001).
194 Ehrenberg, B., Montana, V., Wei, M. D., Wuskell, J. P. & Loew, L. M. Membrane potential can be determined in individual cells from the nernstian distribution of cationic dyes. *Biophysical journal* **53**, 785-794, doi:10.1016/S0006-3495(88)83158-8 (1988).
195 Farkas, D. L., Wei, M. D., Febbroriello, P., Carson, J. H. & Loew, L. M. Simultaneous imaging of cell and mitochondrial membrane potentials. *Biophysical journal* **56**, 1053-1069, doi:10.1016/S0006-3495(89)82754-7 (1989).
196 Antignani, A. & Youle, R. J. How do Bax and Bak lead to permeabilization of the outer mitochondrial membraneΔ **18**, 685-689, doi:10.1016/j.ceb.2006.10.004 (2006).
197 Westphal, D., Dewson, G., Czabotar, P. E. & Kluck, R. M. Molecular biology of Bax and Bak activation and action. *Biochim Biophys Acta* **1813**, 521-531, doi:10.1016/j.bbamcr.2010.12.019 (2011).
198 Yao, S. *et al.* NMR studies of interactions between Bax and BH3 domain-containing peptides in the absence and presence of CHAPS. *Archives of biochemistry and biophysics* **545**, 33-43, doi:10.1016/j.abb.2014.01.003 (2014).
199 Oltvai, Z. N., Milliman, C. L. & Korsmeyer, S. J. Bcl-2 heterodimerizes in vivo with a conserved homolog, Bax, that accelerates programmed cell death. *Cell* **74**, 609-619 (1993).
200 Annis, M. G. *et al.* Bax forms multispanning monomers that oligomerize to permeabilize membranes during apoptosis. *EMBO J* **24**, 2096-2103, doi:10.1038/sj.emboj.7600675 (2005).

201 Bouillet, P. *et al.* Proapoptotic Bcl-2 relative Bim required for certain apoptotic responses, leukocyte homeostasis, and to preclude autoimmunity. *Science* **286**, 1735-1738 (1999).
202 Mehta, N., Taylor, J., Quilty, D. & Barry, M. Ectromelia virus encodes an anti-apoptotic protein that regulates cell death. *Virology* **475**, 74-87, doi:10.1016/j.virol.2014.10.023 (2015).
203 Ozanne, G. Estimation of endpoints in biological systems. *Comput Biol Med* **14**, 377-384 (1984).
204 Karupiah, G., Buller, R. M., Van Rooijen, N., Duarte, C. J. & Chen, J. Different roles for CD4+ and CD8+ T lymphocytes and macrophage subsets in the control of a generalized virus infection. *J Virol* **70**, 8301-8309 (1996).
205 Fang, M. *et al.* CD94 is essential for NK cell-mediated resistance to a lethal viral disease. *Immunity* **34**, 579-589, doi:10.1016/j.immuni.2011.02.015 (2011).
206 Sakala, I. G. *et al.* Poxvirus-encoded gamma interferon binding protein dampens the host immune response to infection. *J Virol* **81**, 3346-3353, doi:10.1128/JVI.01927-06 (2007).
207 Zhang, P., Jacobs, B. L. & Samuel, C. E. Loss of protein kinase PKR expression in human HeLa cells complements the vaccinia virus E3L deletion mutant phenotype by restoration of viral protein synthesis. *J Virol* **82**, 840-848, doi:10.1128/JVI.01891-07 (2008).
208 Adams, J. M. *et al.* Subversion of the Bcl-2 life/death switch in cancer development and therapy. *Cold Spring Harbor symposia on quantitative biology* **70**, 469-477, doi:10.1101/sqb.2005.70.009 (2005).
209 Campbell, S. *et al.* Structural Insight Into BH3-Domain Binding of Vaccinia Virus Anti-Apoptotic F1L. *J Virol*, doi:10.1128/JVI.01092-14 (2014).
210 Ludwig, H. *et al.* Double-stranded RNA-binding protein E3 controls translation of viral intermediate RNA, marking an essential step in the life cycle of modified vaccinia virus Ankara. *J Gen Virol* **87**, 1145-1155, doi:10.1099/vir.0.81623-0 (2006).
211 Galluzzi, L., Brenner, C., Morselli, E., Touat, Z. & Kroemer, G. Viral control of mitochondrial apoptosis. *PLoS Pathogens* **4**, e1000018, doi:10.1371/journal.ppat.1000018 (2008).
212 Teodoro, J. & Branton, P. Regulation of apoptosis by viral gene products. *J Virol* **71**, 1739 (1997).
213 Kepp, O. *et al.* Viral subversion of immunogenic cell death. *Cell Cycle* **8**, 860-869 (2009).
214 Taylor, J. M. & Barry, M. Near death experiences: poxvirus regulation of apoptotic death. *Virology* **344**, 139-150, doi:10.1016/j.virol.2005.09.032 (2006).
215 Tulman, E. R. *et al.* The genome of canarypox virus. *J Virol* **78**, 353-366 (2004).
216 Everett, H. *et al.* The myxoma poxvirus protein, M11L, prevents apoptosis by direct interaction with the mitochondrial permeability transition pore. *J Exp Med* **196**, 1127-1139 (2002).

217 Gonzalez, J. M. & Esteban, M. A poxvirus Bcl-2-like gene family involved in regulation of host immune response: sequence similarity and evolutionary history. *Virology journal* **7**, 59, doi:10.1186/1743-422X-7-59 (2010).
218 Graham, S. C. *et al.* Vaccinia virus proteins A52 and B14 Share a Bcl-2-like fold but have evolved to inhibit NF-kappaB rather than apoptosis. *PLoS Pathog* **4**, e1000128, doi:10.1371/journal.ppat.1000128 (2008).
219 DiPerna, G. *et al.* Poxvirus protein N1L targets the I-kappaB kinase complex, inhibits signaling to NF-kappaB by the tumor necrosis factor superfamily of receptors, and inhibits NF-kappaB and IRF3 signaling by toll-like receptors. *J Biol Chem* **279**, 36570-36578, doi:10.1074/jbc.M400567200 (2004).
220 Cooray, S. *et al.* Functional and structural studies of the vaccinia virus virulence factor N1 reveal a Bcl-2-like anti-apoptotic protein. *J Gen Virol* **88**, 1656-1666, doi:10.1099/vir.0.82772-0 (2007).
221 Gratz, M. S. *et al.* N1L is an ectromelia virus virulence factor and essential for in vivo spread upon respiratory infection. *J Virol* **85**, 3557-3569, doi:10.1128/JVI.01191-10 (2011).
222 Xu, R. H. *et al.* The orthopoxvirus type I IFN binding protein is essential for virulence and an effective target for vaccination. *J Exp Med* **205**, 981-992, doi:10.1084/jem.20071854 (2008).
223 Bosma, M. J. & Carroll, A. M. The SCID mouse mutant: definition, characterization, and potential uses. *Annu Rev Immunol* **9**, 323-350, doi:10.1146/annurev.iy.09.040191.001543 (1991).
224 Habu, S. *et al.* In vivo effects of anti-asialo GM1. I. Reduction of NK activity and enhancement of transplanted tumor growth in nude mice. *J Immunol* **127**, 34-38 (1981).
225 Farber, J. M. Mig and IP-10: CXC chemokines that target lymphocytes. *J Leukoc Biol* **61**, 246-257 (1997).
226 Liu, L., Callahan, M. K., Huang, D. & Ransohoff, R. M. Chemokine receptor CXCR3: an unexpected enigma. *Curr Top Dev Biol* **68**, 149-181, doi:10.1016/S0070-2153(05)68006-4 (2005).
227 Farber, J. M. HuMig: a new human member of the chemokine family of cytokines. *Biochem Biophys Res Commun* **192**, 223-230, doi:10.1006/bbrc.1993.1403 (1993).
228 Groom, J. R. & Luster, A. D. CXCR3 ligands: redundant, collaborative and antagonistic functions. *Immunol Cell Biol* **89**, 207-215, doi:10.1038/icb.2010.158 (2011).
229 Pak-Wittel, M. A., Yang, L., Sojka, D. K., Rivenbark, J. G. & Yokoyama, W. M. Interferon-gamma mediates chemokine-dependent recruitment of natural killer cells during viral infection. *Proc Natl Acad Sci U S A* **110**, E50-59, doi:10.1073/pnas.1220456110 (2013).
230 Thapa, M., Welner, R. S., Pelayo, R. & Carr, D. J. CXCL9 and CXCL10 expression are critical for control of genital herpes simplex virus type 2 infection through mobilization of HSV-specific CTL and NK cells to the nervous system. *J Immunol* **180**, 1098-1106 (2008).

231 Buller, R. M., Smith, G. L., Cremer, K., Notkins, A. L. & Moss, B. Decreased virulence of recombinant vaccinia virus expression vectors is associated with a thymidine kinase-negative phenotype. *Nature* **317**, 813-815 (1985).
232 Karupiah, G., Fredrickson, T. N., Holmes, K. L., Khairallah, L. H. & Buller, R. M. Importance of interferons in recovery from mousepox. *J Virol* **67**, 4214-4226 (1993).
233 Karupiah, G. *et al.* Inhibition of viral replication by interferon-gamma-induced nitric oxide synthase. *Science* **261**, 1445-1448 (1993).
234 O'Garra, A. & Murphy, K. M. From IL-10 to IL-12: how pathogens and their products stimulate APCs to induce T(H)1 development. *Nat Immunol* **10**, 929-932, doi:10.1038/ni0909-929 (2009).
235 Ouyang, P. *et al.* IL-10 encoded by viruses: a remarkable example of independent acquisition of a cellular gene by viruses and its subsequent evolution in the viral genome. *J Gen Virol* **95**, 245-262, doi:10.1099/vir.0.058966-0 (2014).
236 Richter, K. *et al.* Macrophage and T cell produced IL-10 promotes viral chronicity. *PLoS Pathog* **9**, e1003735, doi:10.1371/journal.ppat.1003735 (2013).
237 Ng, C. T. & Oldstone, M. B. IL-10: achieving balance during persistent viral infection. *Curr Top Microbiol Immunol* **380**, 129-144, doi:10.1007/978-3-662-43492-5_6 (2014).
238 Sakala, I. G. *et al.* Evidence for Persistence of Ectromelia Virus in Inbred Mice, Recrudescence Following Immunosuppression and Transmission to Naive Mice. *PLoS Pathog* **11**, e1005342, doi:10.1371/journal.ppat.1005342 (2015).
239 Sakala, I. G., Chaudhri, G., Eldi, P., Buller, R. M. & Karupiah, G. Deficiency in Th2 cytokine responses exacerbate orthopoxvirus infection. *PLoS One* **10**, e0118685, doi:10.1371/journal.pone.0118685 (2015).
240 Dodd, J. S. *et al.* IL-9 regulates pathology during primary and memory responses to respiratory syncytial virus infection. *J Immunol* **183**, 7006-7013, doi:10.4049/jimmunol.0900085 (2009).
241 White, M. J. *et al.* Apoptotic caspases suppress mtDNA-induced STING-mediated type I IFN production. *Cell* **159**, 1549-1562, doi:10.1016/j.cell.2014.11.036 (2014).